

# UNIVERSIDAD NACIONAL DE COLOMBIA

**LEOPOLDO MÚNERA RUIZ**  
RECTOR

**MARY LUZ ALZATE ZULUAGA**  
VICERRECTORA · SEDE MEDELLÍN

**OSCAR DE JESÚS CÓRDOBA GAONA**  
DECANO · FACULTAD DE CIENCIAS AGRARIAS

## COMITÉ CIENTÍFICO INTERNACIONAL

<b>Rita M. Ávila de Hernández</b> , Ph.D. Universidad Centroccidental Lisandro Alvarado Barquisimeto, Lara, Venezuela. ritaavila@ucla.edu.ve	<b>Walter Motta Ferreira</b> , D.Sc. Universidade Federal de Minas Gerais. Belo Horizonte, Brasil. pereira3456@hotmail.com
<b>Felipe Bravo Oviedo</b> , D.Sc. Universidad de Valladolid. Valladolid, España. fbravo@pvs.uva.es	<b>Tomas Norton</b> , Ph.D. University of Leuven. Leuven, Flanders, Bélgica. tnorton@harper-adams.ac.uk
<b>José Rafael Córdova</b> , Ph.D. Universidad Simón Bolívar y Universidad Central de Venezuela. Baruta, Venezuela. jcordova45@yahoo.com	<b>Pepijn Prinsen</b> , Ph.D. University of Amsterdam. Holanda. pepijnprinsen33@hotmail.com
<b>José Luis Crossa</b> , Ph.D. Centro Internacional de Mejoramiento de Maíz y Trigo (CIMMYT). Texcoco, México. j.crossa@cgiar.org	<b>Aixa Ofelia Rivero Guerra</b> , Ph.D. Centro Europeo de Estadística Aplicada. Sevilla, España. rivero-guerra@hotmail.com
<b>Mateo Itzá Ortiz</b> , D.Sc. Universidad Autónoma de Ciudad Juárez Chihuahua, México. mateo.itz@uacj.mx	<b>Antonio Roldán Garrigos</b> , Ph.D. Consejo Superior de Investigaciones Científicas. Murcia, España. aroldan@cebas.csic.es
<b>Juan Pablo Damián</b> , Ph.D. Universidad de la República, Uruguay. jpablodamian@gmail.com	<b>Elhadi M. Yahia</b> , Ph.D. Universidad Autónoma de Querétaro. Querétaro, México. elhadiyahia@hotmail.com
<b>Moncef Chouaibi</b> , Ph.D. Higher School of Food Industries of Tunisia (ESIAT), Tunisia. moncef.chouaibi@yahoo.com.au	<b>Meisam Zargar</b> , Ph.D. RUDN University, Rusia. zargar_m@pfur.ru

## COMITÉ EDITORIAL

**Período 2022-2024**

<b>Albeiro López Herrera</b> , Ph.D. Editor en Jefe	Universidad Nacional de Colombia. Colombia alherrera@unal.edu.co
<b>Flavio Alves Damasceno</b> , Ph.D.	Universidade Federal de Lavras. Brasil flavioua@gmail.com
<b>Luz Estela González de Bashan</b> , Ph.D.	The Bashan Institute of Science, USA legonzal04@cibno.mx
<b>Juan Diego León Peláez</b> , Ph.D.	Universidad Nacional de Colombia. Colombia jdleon@unal.edu.co
<b>Deyanira Lobo Luján</b> , Ph.D.	Universidad Central de Venezuela. Venezuela lobo.deyanira@gmail.com
<b>Sara Márquez Girón</b> , Ph.D.	Universidad de Antioquia. Colombia saramariamarquezg@gmail.com
<b>Jousset Alexandre</b> , Ph.D.	Utrecht University. Países Bajos A.L.C.Jousset@uu.nl
<b>Juan Gonzalo Morales Osorio</b> , Ph.D.	Universidad Nacional de Colombia. Colombia jgmorealeso@unal.edu.co
<b>Jaime Parra Suescún</b> , Ph.D.	Universidad Nacional de Colombia. Colombia jeparrasu@unal.edu.co
<b>Camilo Ramírez Cuartas</b> , Ph.D.	Universidad de Antioquia. Colombia camilo.ramirez@udea.edu.co
<b>Iang Schroniltgen Rondon B.</b> M.Sc. Ph.D(c)	Universidad del Tolima. Colombia isrondon@ut.edu.co
<b>Paola Andrea Sotelo Cardona</b> , Ph.D.	World Vegetable Center (WorldVeg). Taiwan paola.sotelo@worldveg.org

## EDICIÓN TÉCNICA

Mario Alejandro Vallejos Jiménez - Ingeniero Biológico. M.Eng. Química-  
mavallejosi@unal.edu.co

**Periodicidad:** Cuatrimestral  
Vol. 78 No. 3 - 2025

**Admitida en las Bases**

**Bibliográficas:** Scopus  
Scielo (Scientific Electronic Library Online)  
ISI-Scielo Citation Index  
REDIB (Red Iberoamericana e innovación y conocimiento científico)  
Cabi (www.cabi.org)  
EBSCO Host  
Google Scholar  
DOAJ (Directory of Open Access Journals)  
Ulrich's Periodicals Directory (Global Serials Directory)  
Redalyc (Red de Revistas Científicas de América Latina,  
el Caribe, España y Portugal)  
Latindex (Sistema Regional de Información en Línea para Revistas  
Científicas de América Latina, el Caribe, España y Portugal)  
ProQuest  
Teal (The Essential Electronic Agricultural Library)  
WZB (Berlin Social Science Center)  
Cross ref  
Cornell University  
Field Crop Abstracts  
Forestry Abstracts  
Plant Breeding Abstracts  
Índice Agrícola de América Latina y el Caribe  
Índice Bibliográfico Nacional  
Minciencias - Pubindex  
AGRIS-FAO

**Portada:** Programa de ganado de carne, Estación Agraria Cotové. Fotografía de  
Diana María Bolívar, Facultad de Ciencias Agrarias, Universidad Nacional de  
Colombia, Sede Medellín, Colombia - audiovisualfca\_med@unal.edu.co

**Contraportada:** Klara Torres Restrepo

**Dirección postal:** Apartado Aéreo 568, Medellín, Colombia

**Dirección electrónica:** rfnagron\_med@unal.edu.co

**Página Web:** <http://www.revistas.unal.edu.co/index.php/refame>

**Teléfono:** (\*4) 430 90 06; Fax: (\* 4) 230 04 20

**Diagramación:** Miryam Ospina Ocampo

**Marcación:** LandSoft S.A.

**Diseño e Impresión:** Centro de Publicaciones UN, Medellín.

**Primera edición:** Año 1939

**ISSN:** 0304-2847

**ISSN formato web:** 2248-7026

**doi:** 10.15446/rfnam 

**Licencia Ministerio de Gobierno:** 275/64

- 11191 Multi-trait selection of bread wheat (*Triticum aestivum* L.) genotypes under semi-arid conditions in Algeria**  
 Selección de múltiples características de genotipos de trigo harinero (*Triticum aestivum* L.) bajo condiciones semiáridas en Argelia  
 Khaoula Khadidja Ladoui / Samia Yahiaoui / Mohammed Mefti / Abdelkader Benbelkacem / Ouakkal Meriem / Chafika Djenadi
- 11203 Tomato (*Solanum lycopersicum* L.) leaf disease detection using computer vision**  
 Detección de enfermedades en las hojas del tomate (*Solanum lycopersicum* L.) mediante visión por computadora  
 Sebastian Palacio Betancur / Freddy Bolaños Martínez
- 11213 Response of *Corchorus olitorius* L. to cocoa pod husk powder and urea fertilizer**  
 Respuesta de *Corchorus olitorius* L. al polvo de cáscara demazorca de cacao y al fertilizante químico de nitrógeno  
 Tajudeen Bamidele Akinrinola / Miracle Oluwaseyi Aponjolosun / Olajire Fagbola
- 11227 Efficacy of *Tithonia diversifolia* and NPK fertilizers on papaya seedling growth in marginal soils**  
 Eficacia de fertilizantes de *Tithonia diversifolia* y NPK en plántulas de papaya en suelos marginales  
 Indra Purnama / Rizki Nurmadani / Corilia Dawiteratika / Muhammad Rizal / Anisa Mutamima
- 11239 *In vitro* propagation of sweet cucumber (*Solanum muricatum* Ait): Effects of auxins and cytokinins**  
 Propagación *in vitro* de pepino dulce (*Solanum muricatum* Ait): Efectos de las auxinas y las citoquininas  
 Cecilia Lazaro-Rodriguez / Lia Loana Bendezu-Granda / Julio A. Olivera-Soto / Alvaro Tumpe-Jaquehua / Graciela Gomez-Fuentes / Maria Vicente-Vega / Luz Sanchez-Quispe
- 11247 Non-destructive estimation of leaf area in hairy leabane (*Conyza bonariensis*)**  
 Estimación no destructiva del área foliar en rama negra (*Conyza bonariensis*)  
 Mariana Macedo / Bruno Mussoi Cavichioi / Glauco Pacheco Leães / Lilian Osmari Uhlmann / Ary José Duarte Junior / Tilio Adan Lucas / André da Rosa Ulguim
- 11255 Hydrogen production by dark fermentation from by-products of coffee wet processing and other organic wastes**  
 Producción de hidrógeno por fermentación oscura a partir de subproductos del beneficio húmedo del café y otros residuos orgánicos  
 Iván Andrés Quiñones Navia / Víctor Manuel Martínez Castro / Edilson León Moreno Cárdenas
- 11267 Global trends in sustainable cocoa (*Theobroma cacao* L.) production: A bibliometric analysis (2019-2025)**  
 Tendencias globales en la producción sostenible de cacao (*Theobroma cacao* L.): un análisis bibliométrico (2019-2025)  
 Alfredo Enrique Sanabria Ospino / Alix Estela Yusara Contreras Gómez / Mary Yaneth Rodríguez Villamizar

- 11285 **Gluten-free cookies made with white carrot (*Arracacia xanthorrhiza* Bancr) and rice (*Oryza sativa*) flour**  
Galletas sin gluten elaboradas con zanahoria blanca (*Arracacia xanthorrhiza* Bancr) y arroz (*Oryza sativa*)  
Gina Mariuxi Guapi Álava / Vicente Alberto Guerrón Troya / Milena Mayerli Alvarado Moran / Jhonnatan Placido Aldas Morejon / Karol Yannela Revilla Escobar
- 11293 **Assessment of physical properties and biological activity of chitosan beads with *Citrus hystrix* essential oil**  
Evaluación de las propiedades físicas y la actividad biológica de las perlas de quitosano con aceite esencial de *Citrus hystrix*  
Do Minh Long / Le Pham Tan Quoc
- 11307 **Postharvest conditions of *Capsicum annuum* and their effect on hot sauce added *Ananas comosus***  
Condiciones postcosecha de *Capsicum annuum* y su efecto en la salsa picante añadida con *Ananas comosus*  
Andry Annabel Alvarez-Aspiazu/ Alicia Nicole Batallas-Terrero / Jaime Fabián Vera-Chang / Jorge Gustavo Díaz-Arreaga
- 11319 **Genetic variants of caseins and  $\beta$ -lactoglobulin in Lucerna cattle and their association with milk quality**  
Variantes genéticas de caseínas y  $\beta$ -lactoglobulina en el ganado Lucerna y su asociación con la calidad de la leche  
Darwin Yovanny Hernández-Herrera / Luis Gabriel González-Herrera / Juan Carlos Rincón-Flórez
- 11335 **Effect of antibiotic residues from subclinical mastitis on  $\beta$ -lactoglobulin concentration in bovine and goat milk**  
Efecto de los residuos de antibióticos por mastitis subclínica sobre la concentración de  $\beta$ -lactoglobulina en leche bovina y caprina  
Yamile Jiménez Alfonso / Luis Edgar Tarazona-Manrique
- 11345 **Root colonization of tamarind tree (*Tamarindus indica* L.) and occurrence of arbuscular mycorrhizal fungi in soils – Sopetrán, Antioquia**  
Colonización de raíces de tamarindo (*Tamarindus indica* L.) y ocurrencia de hongos micorrízicos arbusculares en los suelos – Sopetrán, Antioquia  
Sandra Muriel Ruiz / Valentina Restrepo-Cossio / Estefanía Martínez Olier / Marcelo Betancur Agudelo
- 11353 **Woody Plant Medium optimizes *in vitro* germination and development of *Calycophyllum spruceanum***  
Woody Plant Medium optimiza la germinación y el desarrollo de *Calycophyllum spruceanum in vitro*  
Antony Cristhian Gonzales-Alvarado / Nilda Hilario-Román / Jorge Manuel Revilla-Chávez / Cristian Richard Saico Ccope / Jorge Arturo Mori-Vásquez

The ideas expressed in the articles published in this volume are exclusively those of the authors and do not necessarily reflect the opinion of the Facultad de Ciencias Agrarias

Las ideas de los trabajos publicados en esta entrega, son de exclusiva responsabilidad de los autores y no reflejan necesariamente la opinión de la Facultad de Ciencias Agrarias



## EVALUADORES

El Comité Editorial dentro de sus políticas, envía los artículos a especialistas, con el fin de que sean revisados. Sus observaciones en adición a las que hacen los editores, contribuyen a la obtención de una publicación de reconocida calidad en el ámbito de las Ciencias Agrarias. Sus nombres son mencionados como una expresión de agradecimiento.

**Abderrezzak Kirouani.** University  
Yahia Fares of Medea, Algeria.  
kirouani.abderrezzak@univ-medea.dz

**Carla Susana Salto.** Instituto Nacional  
de Tecnología Agropecuaria INTA,  
Argentina. salto.carla@inta.gob.ar

**Abiola Toyin Ajay.** Department of Plant Science  
and Biotechnology, Adekunle Ajasin University,  
AkungbaAkoko, Nigeria. toyin.ajayi@aau.edu.ng

**Carlos Mario Muñoz Maya.** Universidad  
de La Salle, Colombia.  
carmunoz@unisalle.edu.co

**Adrián Chávez.** Instituto Zuliano de  
Investigaciones Tecnológicas (INZIT),  
Venezuela. ajchavez3000@gmail.com

**Carlos Vilcatoma-Medina.** Universidade  
Federal do Paraná, Paraná, Brasil.  
catomedina101@gmail.com

**Ahmet Fatih Demirel.** Department of Animal Husbandry,  
Faculty of Veterinary Medicine, Van Yuzuncu  
Yil University, Türkiye. afatihdemirel@yyu.edu.tr

**Cristhian John Macías-Holguín.** Universidad  
Técnica Estatal de Quevedo, Ecuador.  
cristhian.macias2016@uteq.edu.ec

**Aline Camila Caetano.** Universidad  
Nacional Toribio Rodríguez de Mendoza  
de Amazonas, Perú. aline.caetano@unrm.edu.pe

**Daniel Iván Ospina Salazar.** Universidad  
Nacional de Colombia, Sede Medellín,  
Colombia. diospinas@unal.edu.co

**Andrea María Peñaranda-Rolón.** Corporación  
Colombiana de Investigación Agropecuaria – AGROSAVIA.  
Cundinamarca, Colombia. apenarandarolon@gmail.com

**Debarati Datta.** ICAR-Central Research  
Institute for Jute and Allied Fibres, Barackpore,  
India. myselfdebarati@gmail.com

**Andrés Rodríguez-Serrano.**  
Universidad de Cartagena, Colombia.  
camilo.rodriguez.serrano@gmail.com

**Edith Marleny Cadena Chamorro.** Universidad  
Nacional de Colombia, Sede Medellín, Colombia.  
emcadenac@unal.edu.co

**Anouar Mouhoub.** Université  
Cadi Ayyad, Marrakech, Morocco.  
anouar.mouhoub@edu.uca.ac.ma

**Eduardo Rodríguez Sandoval.** Universidad  
Nacional de Colombia, Sede Medellín,  
Colombia. edrodriguez@unal.edu.co

**Benjamín Luna Benoso.** Escuela  
Superior de Cómputo, Instituto Politécnico  
Nacional, México. blunab@ipn.mx

**Ericka Porras.** Instituto Nacional de  
Investigaciones Agrícolas (INIA), Venezuela.  
erickaeporras@gmail.com

**Bruna Hortolani.** Instituto  
de Zootecnia, Brasil.  
hortolanib@gmail.com

**Ernesto Castañeda-Hidalgo.** Tecnológico  
Nacional de México, México.  
casta\_h50@hotmail.com

**Calogero Schillaci.** European  
Commission JRC, Italy. calogero.  
schillaci@ec.europa.eu

**Francisco Gutiérrez.** Universidad  
Central del Ecuador, Ecuador.  
fgutierrez@uce.edu.ec

**Heriberto Méndez-Cortés.** Universidad Autónoma de San Luis Potosí, México.  
heriberto.mendez@uaslp.mx

**Ilse Silvia Cayo-Colca.** Universidad Nacional Toribio Rodríguez de Mendoza de Amazonas, Perú. icayo.fizab@untrm.edu.pe

**Israr Hussain.** Institute of Computing, Muhammad Nawaz Sharif University of Agriculture, Pakistan. israr.hussain@mnsuam.edu.pk

**Ives Yoplac.** Universidad Nacional Toribio Rodríguez de Mendoza de Amazonas, Perú. ives.yoplac@untrm.edu.pe

**John Jairo Pinargote Alava.** Investigador Independiente, Ecuador.  
john.pinargote2013@gmail.com

**Jorge Fernando Navia Estrada.** Universidad de Nariño (UDENAR), Colombia. jornavia@yahoo.com

**Jorge Olave.** Universidad Arturo Prat, Centro de Investigación y Desarrollo en Recursos Hídricos, Chile. jorge.olave@ciderh.cl

**Joshua Thambura.** Meru University of Science and Technology, Kenya.  
jthambura@must.ac.ke

**Juan Carlos Silva-Jarquin.** Universidad Autónoma de Querétaro, México. jcarlos.silva@uaq.mx

**Juan Manuel Sánchez-Yáñez.** Universidad Michoacana de San Nicolás de Hidalgo México. syanez@umich.mx

**Juan Venancio Benítez Núñez.** Universidad Nacional de Asunción, Paraguay. jbenitez@rec.una.py

**Kaboneka Salvator.** University of Burundi, Burundi.  
salvator.kaboneka@gmail.com

**Leonardo Hernan Talero-Sarmiento.** Universidad Autónoma de Bucaramanga, Colombia. ltalero@unab.edu.co

**Lina Chaib.** Institute of Agronomic and Veterinary Sciences, University of Souk Ahras, Algeria. linatam2308@gmail.com

**Luan Ramos da Silva.** Universidade Estadual de Campinas, Brasil.  
luanramosea@gmail.com

**Marcela Daniela Mollericona Alfaro.** Universidad Mayor de San Andrés, Bolivia.  
marcela.mollericonaalfaro@yahoo.com

**Marcos Ahumada-Velasco.** Universidad de Cartagena, Colombia.  
ganaderiaguajira@unicartagena.edu.co

**Muhammad Iqbal Fauzan.** Universitas Diponegoro, Indonesia.  
muhammadiqbalfauzan@lecturer.undip.ac.id

**Nanik Setyowati.** University of Bengkulu, Indonesia.  
nsetyowati@unib.ac.id

**Obse Fikiru Etefa.** Department of Postharvest Management, Jimma University, Ethiopia.  
obsemaatii@yahoo.com

**Oscar Aguilar-Juárez.** Centro de Investigación y Asistencia en Tecnología y Diseño del Estado de Jalisco, Mexico. oaguilar@ciatej.mx

**Pedro Alfonso Lizarazo-Peña.** Universidad El Bosque, Colombia.  
plizarazop@unbosque.edu.co

**Rajendran Kumaran.** Department of Chemistry, University of Madras, India. Kumaranwau@rediffmail.com

**Rajinder Kumar Dhall.** Punjab Agricultural University, India.  
rajinderkumar@pau.edu

**Rapialdi, Jamilah.** Universitas Tamansiswa Padang, Indonesia.  
jamilah@unitas-pdg.ac.id

**Ricardo Andrés García-León.** Universidad Francisco de Paula Santander Ocaña, Colombia. ragarcial@ufpso.edu.co

**Saiqa Khan.** University of,  
Westminster United Kingdom.  
saiqa.comp@gmail.com

**Seneida Lopera.** Universidad  
de Antioquia, Colombia.  
seneida.lopera@udea.edu.co

**Sofiane Tamendjar.** Institute of Agronomic  
and Veterinary Sciences, University of Souk  
Ahras, Algeria. sofianetam06@gmail.com

**Solomon Oyekale.** Department of Crop  
Science, Landmark University, Nigeria.  
oyekale.solomon@lmu.edu.ng

**Tatiana Rodríguez Chaparro.** Universidad  
Militar Nueva Granada, Bogotá, Colombia.  
adela.rodriguez@unimilitar.edu.co

**Urley Adrian Pérez-Moncada.** Corporación  
Colombiana de Investigación Agropecuaria – AGROSAVIA,  
Cundinamarca, Colombia. uperez@agrosavia.co

**Zine El Abidine Fellahi.**  
University of BBA, Algeria.  
zinou.agro@gmail.com






### **Agricultural engineering and the CONCIA 2025 congress: 60 years in Colombia addressing the challenges toward a sustainable and competitive agri-food production**

### **La ingeniería agrícola y el congreso CONCIA 2025: 60 años en Colombia afrontando los retos para lograr una producción agroalimentaria sostenible y competitiva**

La Ingeniería Agrícola tuvo su origen con la creación de los primeros colegios de agricultura y artes mecánicas en los Estados Unidos de América apareciendo como programa académico en 1862. En el ámbito europeo, en el año de 1930, se fundó la “*Commission Internationale du Génie Rural*”, con el propósito de coordinar los trabajos y desarrollos de la Ingeniería Agrícola. En América Latina este programa se estableció en la década de 1950, paralelamente, con la modernización de la agricultura. La primera Escuela de Ingeniería Agrícola se creó en la Universidad Técnica de Manabí-Ecuador en el año de 1957. El origen del primer programa de Ingeniería Agrícola en nuestro país, se remonta a 1956, cuando la Universidad Nacional de Colombia firmó un convenio de cooperación académica con la Universidad de Michigan, proponiendo en 1962 la creación de un programa a nivel universitario de cinco años sugiriendo que la Facultad de Agronomía de la sede Medellín se encargará de promoverlo y establecerlo, dado que era una de las Escuelas de mayor experiencia académica en la enseñanza de las Ciencias Agrícolas en Latinoamérica. Con la colaboración la FAO, la OEA, la Universidad Agraria La Molina de Perú, la Universidad de Michigan, y profesores de la Universidad Nacional de las sedes Bogotá, Palmira y Medellín, se designó al profesor de nuestra Facultad, Ingeniero Agrónomo y M.Sc., Fabio Bustamante Betancur (QEPD) como jefe de la sección de Ingeniería Agrícola, con el propósito de coordinar las labores tendientes a crear y diseñar el plan de estudios de la nueva carrera. La creación del programa se justificó por la necesidad de presentar una oferta curricular que incorporara los enunciados de la Ingeniería al tratamiento de la problemática de infraestructura en el campo, en particular lo relacionado con la postcosecha de productos agropecuarios, que abordara los problemas de la preservación de los recursos naturales y de infraestructura del sector agropecuario, y que involucrara el enfoque ético direccionado a la sostenibilidad ambiental, social y económica de la producción agraria. El programa fue aprobado por el Consejo Superior Universitario de la Universidad Nacional de Colombia, mediante el Acuerdo 268 del 2 de diciembre de 1965, como el primer plan de estudios de Ingeniería Agrícola establecido en nuestro país, el cual inició los cursos formales en 1965 con 25 admitidos y tuvo la primera cohorte de 13 graduados en 1970. Desde ese año hasta la fecha son 716 (237 ingenieras y 488 ingenieros) que han egresado del programa curricular.

El plan curricular de Ingeniería Agrícola desde su creación ha sido enfocado en las áreas de ingeniería de agua y del suelo; la mecanización agrícola; las construcciones rurales; y la ingeniería de postcosecha de procesos agrícolas. El perfil del Ingeniero Agrícola es de un profesional con capacidad de correlacionar los fundamentos de la ingeniería para dar óptimas soluciones técnico económicas a las necesidades de la producción de alimentos, que posee la preparación teórico-práctica que le proporciona los principios técnicos y científicos para su desempeño acertado en la investigación, consultoría, interventoría, dirección y administración de las actividades y proyectos de la Ingeniería en el sector agrario, con criterios de sostenibilidad.

Varias actualizaciones se han realizado al plan de estudios del programa acordes con los procesos de globalización y los avances tecnológicos que permiten un mejor aprovechamiento de los recursos, en los que la función del ingeniero



es esencial para la construcción de los objetivos del crecimiento económico con equidad y justicia social, como metas de cualquier estrategia de desarrollo. Propendiendo el mejoramiento continuo, el programa de Ingeniería Agrícola de la Universidad Nacional sede Medellín obtuvo la acreditación de alta calidad en el año 2007 (Resolución 540 del Ministerio de Educación Nacional-MEN) y, posteriormente, dos renovaciones de su acreditación, la más reciente en el 2022 por un período de 8 años (Resolución 002324 del MEN). De estos procesos, se han derivado análisis sobre la pertinencia del programa (debilidades y fortalezas) y planes de mejoramiento propuestos para mantener la calidad integral del programa curricular que han sido el resultado del trabajo colaborativo entre las directivas académicas, los estamentos universitarios, y la comunidad en general (estudiantes, profesores, y egresados). El Proyecto Educativo del Programa (PEP) mantiene una coherencia con los principios de formación del Proyecto Educativo Institucional (PEI) de la Universidad Nacional: excelencia académica, formación integral, contextualización, internacionalización, formación investigativa, interdisciplinariedad, flexibilidad y gestión para el mejoramiento académico.

Diversas instituciones en nuestro país han identificado como demandas de formación en los profesionales la incorporación de nuevas tecnologías para el mejoramiento de la productividad agraria y la necesidad de hacer de Colombia una despensa mundial de alimentos (con visión a 2050), así como la seguridad alimentaria de la población campesina, el posconflicto, la adaptación al cambio climático y la sostenibilidad ambiental. Por lo cual, en la preparación académica de los futuros profesionales de la ingeniería agrícola deben considerarse las necesidades sociales, del mercado, de las prácticas profesionales y de la preservación del medio ambiente (sostenibilidad económica, social y ambiental), incorporando los conocimientos en agricultura de precisión (digitalización, automatización y mecanización de la agricultura); agroindustria y generación de valor; modernización de los sistemas de extensión y transferencia; biotecnología; emprendimiento; estrategias de comercialización; mitigación y adaptación al cambio climático; producción sostenible; trazabilidad y control de calidad e inocuidad; y uso de los sistemas de información con el fin de optimizar los recursos y mejorar la toma de decisiones.

El programa de ingeniería agrícola deberá fortalecer en los próximos años las áreas de desempeño tradicionales: ingeniería de los recursos agua y suelo; ingeniería de procesos agroindustriales; mecanización agrícola; construcciones rurales, bioclimática y medio ambiente, con otras demandas científicas y tecnológicas del medio, en áreas como bioprocesos y biotecnología; seguridad y soberanía alimentaria; aprovechamiento de materias primas y coproductos; energías renovables y sostenibles; ciencias económicas y administrativas; tecnologías de la información y comunicación (TIC); y formación humana, integral y multidisciplinar. En síntesis, se buscará formar un profesional íntegro, no solo con capacidad técnico-científica, sino también con profunda vocación y sensibilidad socioambiental y con una visión específica de la problemática agropecuaria y rural.

La realización del XIII Congreso Colombiano de Ingeniería Agrícola y Áreas Afines - CONCIA 2025 organizado por el Departamento de Ingeniería Agrícola y Alimentos y la Facultad de Ciencias Agrarias de la Universidad Nacional de Colombia, Sede Medellín, con motivo del aniversario No. 60 de la creación del programa curricular de Ingeniería Agrícola, será una nueva oportunidad para la divulgación de resultados de investigación y discusión académica, presentando a la comunidad universitaria, a los diferentes actores del sector agropecuario, y a la sociedad en general, los logros y aportes que la ingeniería agrícola ha realizado, y los nuevos retos académicos y tecnológicos que la profesión, en sus diferentes áreas de desempeño, está afrontando y deberá solucionar en el corto, mediano y largo plazo para contribuir a una producción agro-alimentaria sostenible y competitiva.

---

Por todo lo anterior, el Congreso CONCIA 2025 será un trascendental encuentro académico de estudiantes, egresados, profesores, y profesionales de la ingeniería agrícola y de otras áreas afines que permitirá, sin lugar a duda, continuar fortaleciendo la interacción del programa de ingeniería agrícola con las organizaciones del Estado y con los diversos gremios de la producción, instituciones de educación, centros de investigación y desarrollo tecnológico, y entidades públicas y privadas del sector agrario y del ámbito agroindustrial, no solo para la consolidación del programa curricular, sino además para continuar aportando al desarrollo sostenible del agro colombiano y al fortalecimiento del sector agroalimentario nacional en las próximas décadas.

IVÁN DARÍO ARISTIZÁBAL TORRES

Profesor Asociado, Director Área Curricular Agroingeniería y Alimentos  
Departamento de Ingeniería Agrícola y Alimentos, Facultad de Ciencias Agrarias  
Universidad Nacional de Colombia, Sede Medellín  
idaristi@unal.edu.co





# Multi-trait selection of bread wheat (*Triticum aestivum* L.) genotypes under semi-arid conditions in Algeria

Selección de múltiples características de genotipos de trigo harinero (*Triticum aestivum* L.) bajo condiciones semiáridas en Argelia

<https://doi.org/10.15446/rfnam.v78n3.117143>

Khaoula Khadidja Ladoui<sup>1,2\*</sup>, Samia Yahiaoui<sup>2</sup>, Mohammed Mefti<sup>1</sup>, Abdelkader Benbelkacem<sup>3</sup>, Ouakkal Meriem<sup>2</sup> and Chafika Djenadi<sup>2</sup>

## ABSTRACT

### Keywords:

Agronomic traits  
ANOVA  
Correlation  
LSI  
MGIDI  
Wheat



The selection of high-yielding bread wheat (*Triticum aestivum* L.) genotypes with superior agronomic traits is critical for improving productivity in semi-arid regions like Algeria. To address national reliance on wheat imports and enhance local production, a preliminary yield trial was conducted in Constantine (36°16' N, 6°40' E) during the 2018–2019 cropping season. A total of 112 bread wheat genotypes, including local and international entries and five local checks, were evaluated using an augmented design with four blocks. Significant variability was detected among genotypes and checks for most traits, confirming the presence of exploitable genetic diversity. Phenotypic correlations showed that grain yield was positively associated with spike density ( $r=0.463$ ) and thousand-kernel weight ( $r=0.557$ ), while it was negatively correlated with days to heading ( $r=-0.293$ ), indicating the advantage of early heading under drought conditions. Using the Least Significant Increase (LSI) method, genotypes G29, G38, and G9 were found to be significantly earlier than several local checks, while G65 outperformed at least one check across all traits. In parallel, the Multi-Trait Genotype-Ideotype Distance Index (MGIDI) enabled the identification of 17 high-performing genotypes such as G60, G41, G65, and G111 alongside two superior local checks (C3 and C4). These genotypes combine favorable traits and are promising candidates for inclusion in breeding programs targeting yield stability and stress resilience. Overall, the study provides valuable insights into trait associations and highlights elite genetic materials suitable for advancing wheat improvement efforts in challenging semi-arid environments.


## RESUMEN


### Palabras clave:

Características agronómicas  
ANOVA  
Correlación  
LSI  
MGIDI  
Trigo

La selección de genotipos de trigo harinero (*Triticum aestivum* L.) de alto rendimiento con rasgos agronómicos superiores es fundamental para mejorar la productividad en regiones semiáridas como Argelia. Para reducir la dependencia nacional de las importaciones de trigo y aumentar la producción local, se llevó a cabo un ensayo preliminar de rendimiento en Constantina (36°16' N, 6°40' E) durante la temporada agrícola 2018–2019. Se evaluaron un total de 112 genotipos de trigo harinero, incluidos materiales locales e internacionales y cinco testigos locales, utilizando un diseño aumentado con cuatro bloques. Se detectó una variabilidad significativa entre genotipos y testigos para la mayoría de los rasgos, lo que confirma la presencia de diversidad genética aprovechable. Las correlaciones fenotípicas mostraron que el rendimiento en grano se asoció positivamente con la densidad de espigas ( $r=0,463$ ) y el peso de mil granos ( $r=0,557$ ), mientras que se correlacionó negativamente con los días hasta el espigado ( $r=-0,293$ ), lo que indica la ventaja de un espigado temprano en condiciones de sequía. Utilizando el método de Least Significant Increase (LSI), se encontró que los genotipos G29, G38 y G9 fueron significativamente más precoces que varios testigos locales, mientras que G65 superó al menos a un testigo en todos los rasgos. Paralelamente, Multi-trait genotype-ideotype distance index (MGIDI) permitió la identificación de 17 genotipos de alto rendimiento tales como G60, G41, G65 y G111, junto con dos testigos locales superiores (C3 y C4). Estos genotipos combinan características favorables y son candidatos prometedores para ser incluidos en programas de mejora enfocados a la estabilidad del rendimiento y la resiliencia al estrés. En general, el estudio proporciona información valiosa sobre las asociaciones entre rasgos y destaca materiales genéticos elite adecuados para avanzar en los esfuerzos de mejora del trigo en entornos semiáridos desafiantes.

<sup>1</sup>National Higher School of Agronomy (ENSA), Department of Plant Productions, Genetic Resources and Biotechnology Laboratory El Harrach, Algiers, Algeria. k.ladoui@edu.ensa.dz , mohammed.mefti@edu.ensa.dz 

<sup>2</sup>National Agronomic Research Institute of Algeria (INRAA), Biotechnology and Plant Breeding Division, Baraki, Algiers, Algeria. yahiaouisamia@hotmail.com , meriemouakkal@yahoo.com , cdjenadi@gmail.com 

<sup>3</sup>National Agronomic Research Institute of Algeria (INRAA), Biotechnology and Plant Breeding Division, El Khroub Station, Constantine, Algeria. Abdelkader. benbelkacem@inraa.dz 

\*Corresponding author

**B**read wheat (*Triticum aestivum* L.) stands as one of the most important staple crops worldwide, owing to its exceptional adaptability across a wide range of temperate agro-climatic zones and its diverse applications as a source of food, animal feed, seed, and raw material for various industrial uses (Venske et al. 2019; Sivakumar and Kumar 2023). Its dominance in global agriculture is further underscored by its central role in food security, providing approximately 20% of the calories and proteins consumed by the global population. In Algeria, despite favorable agro-ecological conditions in certain regions, the country remains highly dependent on cereal imports, particularly bread wheat to meet its growing consumption needs. This dependency is largely driven by the persistent mismatch between domestic wheat production and increasing national demand, which continues to exert pressure on food security and public finances (Bekkis et al. 2023). Illustratively, national cereal output fell from 4.39 million tons in the 2019–2020 growing season to 2.76 million tons in 2020–2021, while wheat import expenditures reached 6 billion dollars in 2022 (ONS 2023a, 2023b). Addressing this imbalance necessitates a profound transformation, with a particular focus on increasing local wheat productivity and resilience through strategic breeding and germplasm enhancement.

In this context, the identification and evaluation of high-potential genotypes and genetically enriched germplasm constitute a critical foundation for achieving durable improvements in yield and resilience to environmental stressors. The enhancement of genetic resources through the incorporation of diverse materials such as landraces and wild relatives enables the introduction of novel alleles into elite pools, thereby expanding genetic diversity and mitigating the limitations resulting from historical selection pressures and genetic erosion. This strategy is particularly relevant for selection programs in marginal and semi-arid environments, where crop performance is frequently constrained by abiotic challenges including drought, heat, and erratic precipitation. The implementation of these strategies is grounded in the detailed characterization and assessment of available germplasm, which provides a rich pool of adaptive traits. Detailed agro-morphological, physiological, and molecular analyses allow for the identification of accessions with beneficial features such as early vigor, robust root systems, efficient nutrient

uptake, or resistance to foliar diseases that may otherwise remain unexploited. This critical step transforms raw genetic variability into materials suitable for integration into selection pipelines. Incorporating such diversity facilitates the alleviation of genetic bottlenecks, enhances resilience to stress, and supports the development of improved genotypes tailored to the demands of semi-arid agro-ecosystems.

Current wheat selection strategies increasingly emphasize the integration of traits associated with adaptation, such as early flowering, drought avoidance, heat tolerance, and optimized root architecture, while simultaneously maintaining or enhancing yield-related attributes. Due to the complex genetic architecture of grain yield and its strong interaction with environmental factors, indirect selection based on correlated traits like plant height, spike density, and thousand-kernel weight is often preferred. These traits, typically characterized by higher heritability, serve as effective proxies for identifying superior genotypes under variable and stress-prone field conditions (Ullah et al. 2021; Khodarahmi et al. 2023).

The challenge lies in efficiently integrating multiple traits with varying levels of heritability and agronomic relevance into a single selection index. Traditional linear selection indices often fall short due to their reliance on arbitrarily assigned weights and assumptions of trait independence. To address this limitation, multivariate selection tools such as the Multi-Trait Genotype–Ideotype Distance Index (MGIDI) have been developed. MGIDI offers a holistic approach by quantifying the distance between a genotype's standardized multi-trait profile and that of an "ideotype". This approach enables the simultaneous consideration of multiple agronomic criteria without the need for predetermined economic weights, making it highly adaptable across breeding contexts (Olivoto and Nardino 2021; Olivoto et al. 2022).

The efficacy of MGIDI has been validated in numerous studies across diverse crops and agro-climatic environments. In wheat, it has been successfully applied to identify genotypes with balanced performance across yield components, stress tolerance traits, and phenological attributes (Pour-Aboughadareh and Poczaï 2021; Mamun et al. 2022; Romena et al. 2022). When integrated into early-stage field trials, MGIDI enhances the efficiency

of genotype ranking and supports data-driven decision-making in breeding pipelines.

The aim of the present study are threefold: (i) to assess the agro-morphological variability within a diverse panel of bread wheat genotypes cultivated under semi-arid conditions in Algeria, (ii) to investigate the phenotypic relationships between grain yield and key agronomic traits, and (iii) to identify superior genotypes outperforming local checks. Genotype selection was based on two complementary approaches: The Least Significant Increase (LSI) method and the Multi-Trait Genotype–Ideotype Distance Index (MGDI). Together, these tools enable the efficient identification of high-performing lines, thereby supporting the development of bread wheat cultivars with improved yield potential, enhanced adaptability, and greater resilience to stress in the context of challenging agro-climatic environments.

MATERIALS AND METHODS

**Genetic materials, location, and experimental design**  
The germplasm evaluated in this study comprised 107 bread

wheat (*Triticum aestivum* L.) genotypes sourced from diverse origins, including the International Center for Agricultural Research in the Dry Areas (ICARDA), the International Maize and Wheat Improvement Center (CIMMYT), as well as locally adapted varieties. Additionally, five local check cultivars were included for comparative assessment (Table 1). The field trial was conducted during the 2018–2019 cropping season at the El Baraouia experimental farm, located in the Constantine region (36°16'N, 6°40'E), a site characterized by cold, wet winters and hot, dry summers (Table 2).

The experimental soil was classified as a clayey–loamy soil with moderately alkaline pH (8.32), high phosphorus content (338.33 ppm), elevated lime content (28.63%), moderate organic matter (1.96%), and low nitrogen levels (0.098%). The soil texture was predominantly clay (69.25%), with a smaller fraction of loam (19.5%). Overall, the soil was classified as moderately alkaline, clayey–loam with a relatively low organic matter content.

Table 1. Code, pedigrees, and origin of local checks.

Code	Name	Pedigrees	Origin
C1	Anza	Lr/N10B//3*Ane II8739-4R-1M-1R	USA
C2	Arz	Mayo 54 ILR64/ "TAC S".	Cimmyt-Mexico
C3	Tidis	BUCKBUCK/FLICKER/MYNA/VULTURE	Cimmyt-Mexico
C4	Hidhab	HD1220/3*Kal/Nac	Cimmyt-Mexico
C5	Massine	PFAU/SERI-82//((SIB)BOBWHITE	Cimmyt-Mexico

Table 2. Climatic data of Constantine region during the 2018-2019 cropping season.

Month	Temperature (°C)	Precipitation (mm)
September	22.50	7.61
October	15.80	143.01
November	11.40	5.59
December	8.30	20.08
January	5.60	101.1
February	6.90	48.01
March	9.80	48.76
April	12.90	40.13
May	15.00	60.19
June	25.30	0.25
July	27.60	0.25
Mean	14.60	43.20

(Tutiempo 2024).

An augmented block design, following the methodology outlined by Federer (1956), was implemented to evaluate the agro-morphological performance of the bread wheat (*Triticum aestivum* L.) germplasm. The experimental layout consisted of four blocks, each containing five local check varieties sown in two replications to facilitate intra-block adjustment, while the test genotypes were evaluated without replication. The first three blocks included 27 genotypes each, whereas the fourth block comprised 26 genotypes, resulting in a total of 107 unique entries. Each entry sown in two rows of 1 m in length, spaced 25 cm apart, and planted at a soil depth of 2 to 3 cm. A total of 147 experimental plots were established following a standardized technical itinerary suitable for wheat cultivation under semi-arid conditions. The trial was conducted under rainfed conditions.

The agro-morphological traits assessed in the bread wheat germplasm under rainfed conditions were selected for their agronomic relevance to yield potential and adaptability in semi-arid environments. These traits included days to heading (DTH, days), recorded as the number of days from sowing to the emergence of the spike in 50% of the plants, and plant height (HGT, cm), measured from the base of the stem to the base of the spike, excluding the awns. The number of kernels per spike (NKS) was calculated as the average grain count from three representative spikes. In addition, the number of spikes per square meter (NS m<sup>2</sup>), the thousand-kernel weight (TKW, g), and grain yield (YLD, t ha<sup>-1</sup>) were also estimated. Together, these traits provided a comprehensive framework for evaluating genotypic performance under water-limited conditions.

### Statistical analysis

An analysis of variance was conducted on the quantitative data following the method described by Federer (1961). The analysis was carried out using the “*augmentedRCBD*” package (Aravind et al. 2023) within the R statistical software environment (R Core Team 2024). Adjusted means were estimated for the unreplicated treatments.

The error mean square obtained from this analysis was used to calculate different standard errors of differences for various comparisons, including: the means of two check varieties ( $SE_c$ ), the adjusted means of two new selections within the same block ( $SE_d$ ), the adjusted means of two new selections in different blocks ( $SE_v$ ), and the adjusted

mean of a new selection and a check variety ( $SE_{vc}$ ), as described by Federer (1961) (Equations 1–4).

$$SE_c = \sqrt{2MSE / r} \quad (1)$$

$$SE_d = \sqrt{2MSE} \quad (2)$$

$$SE_v = \sqrt{2(C + 1) MSE / c} \quad (3)$$

$$SE_{vc} = \sqrt{2(r + 1)(c + 1)MSE / rc} \quad (4)$$

Since the aim was to identify new selections that outperformed the checks, the Least Significant Increase (LSI) was computed using the formula (Equation 5):

$$LSI = SE_{vc} \times t_{\alpha} \quad (\text{at error df}) \quad (5)$$

In this case, a one-sided *t*-test was performed at a 5% level of significance, using the degrees of freedom associated with the error term. Where *t* is the one-tailed *t*-test at  $\alpha$  probability level at error degree of freedom (df) (Equation 6) and  $S_{vc}$  from Equation 4.

$$df \ t(\alpha = 0.05) = 1.694 \quad (6)$$

To describe the variability among genotypes, several basic univariate statistics were calculated, including the minimum, maximum, range, mean, and standard deviation.

Correlation analysis between the studied traits was carried out using the “*metan*” package in R (Olivoto and Lúcio 2020). Pearson correlation coefficients were calculated to examine the relationships between variables. A heatmap was used to visualize the results, making it easier to identify strong positive or negative correlations among the traits, as well as their statistical significance.

The Multi-trait Genotype–Ideotype Distance Index (MGIDI) was applied to identify the most promising genotypes based on their overall performance across multiple traits. This index estimates the weighted Euclidean distance of each genotype from an ideotype that represents the ideal combination of trait values, using scores derived from factor analysis to account for multicollinearity among traits.

The MGIDI value for each genotype was calculated using the following equation (Equation 7):

$$MGIDI = \left[ \sum_{i=1}^f (i\gamma_{ij} - \gamma_j)^2 \right]^{0.5} \quad (7)$$

Where  $i$ , is for the genotype,  $\gamma_{ij}$  is the  $j^{\text{th}}$  score of the  $i^{\text{th}}$  genotype, and  $\gamma_i$  is the  $j^{\text{th}}$  score of ideotype ( $i = 1, 2, \dots, t$ ;  $j = 1, 2, \dots, f$ ).  $t$  and  $f$  the number of genotypes and traits.

Genotypes with lower MGIDI values were considered closer to the ideotype and thus more desirable. A selection intensity of 15% was applied, enabling differential selection for each trait and the identification of superior genotypes combining multiple desirable characteristics.

The calculation of the strengths and weaknesses of genotypes is based on the proportion of the MGIDI value of the  $i^{\text{th}}$  genotype that is explained by the  $j^{\text{th}}$  factor, denoted as  $\omega_{ij}$  (Equation 8):

$$\omega_{ij} = \frac{\sqrt{D_{ij}^2}}{\sum_{j=1}^f \sqrt{D_{ij}^2}} \quad (8)$$

Where  $D_{ij}$  represents the distance between the  $i^{\text{th}}$  genotype and the ideal genotype for the  $j^{\text{th}}$  trait.

A low contribution of a given factor suggests that the traits associated with it are close to the ideotype, indicating the strength of the genotype.

## RESULTS AND DISCUSSION

### Genotypic performance across traits

The analysis of variance (ANOVA) presented in Table 3 showed significant differences among genotypes and local checks for all traits studied. The comparison between genotypes and checks was also significant ( $P \leq 0.001$ ) for most traits, except for NKS and TKW, for which no significant difference was observed. Table 3 also includes a summary of basic statistics for each trait.

**Table 3.** Analysis of variance for the studied agronomic traits.

Source of variation	DF	MS					
		DTH	HGT	NKS	NS m <sup>2</sup>	TKW	YLD
Blocks (Eliminating treatments)	3	58.29**	4.09**	18.99	9706**	39.13	214.00
Treatments (Eliminating blocks)	111	31.22***	162.93**	104.54***	3465.00**	55.88*	280.20**
Genotypes	106	27.21***	165.70**	98.76***	3447.00*	57.46*	282.00**
Checks	4	83.84***	292.84**	285.01***	6869.00**	120.25**	402.00*
Genotypes vs Checks	1	154.32***	14.85***	101.33	28323.00***	75.27	5177.00***
Error	32	9.65	21.14	30.76	1603.00	29.52	131.20
CV%		2.55	5.09	9.66	17.18	15.66	31.15

DTH: Date to heading; HGT: Plant height; NKS: Number of kernels per spike; NS m<sup>2</sup>: Number of spikes per square meter; TKW: Thousand kernel weight; YLD: Grain yield; SD: Standard deviation; LSI: Least significant increase, CV%: Coefficient of variation; \*: Represents significance at ( $P < 0.05$ ) level; \*\*: Represents significance at ( $P < 0.01$ ) level; \*\*\*: Represents significance at ( $P < 0.001$ ) level.

The descriptive statistics (Table 4) of the evaluated agro-morphological traits reveal considerable phenotypic variability within the studied germplasm, emphasizing its potential for genetic enhancement under semi-arid conditions. The observed standard deviations across traits further illustrate the extent of this variability, indicating a wide range of expressions that can be exploited in breeding programs aimed at improving yield performance and adaptability in water-limited environments. DTH ranged from 103.9 to 136.7 days, with a mean of 122.3 days, reflecting a broad spectrum of earliness among genotypes, an essential adaptation

trait under terminal drought stress. Earliness to heading is a key criterion for improving cereal production in rainfed environments, as it enables genotypes to complete their cycle before the drought period. HGT exhibited variation, from 65.92 to 137.62 cm (mean = 90.31 cm), highlighting the coexistence of dwarf and tall genotypes. Genotypes with medium straw are more desirable in semi-arid regions, as they ensure structural robustness while maintaining harvestable yield. The NKS varied from 21.64 to 84.94, with an average of 58.2, suggesting significant differences in spike fertility, a major determinant of final grain number. NS m<sup>2</sup>



ranged from 57.15 to 319.15 spikes  $m^{-2}$  (mean = 226.6), indicating broad variability in tillering ability and grain filling capacity. TKW showed a wide distribution, from 8.62 to 51.12 g (mean = 35.3 g), pointing to genotypic differences in grain size and filling efficiency. YLD

exhibited variability, ranging from 0.63 to 7.33 t  $ha^{-1}$ , with a mean of 3.35 t  $ha^{-1}$ , reflecting differences in yield potential among genotypes. This variability emphasizes the opportunity to identify and promote high-performing lines specifically adapted to water-limited conditions.

**Table 4.** Univariate statistics of the studied agronomic traits.

Statistics	DTH	HGT	NKS	NS $m^{-2}$	TKW	YLD
Min	103.90	65.92	21.64	57.15	8.62	0.63
Max	136.70	137.62	84.94	319.15	51.12	7.32
Range	32.70	71.70	63.30	262.00	42.50	6.71
Mean	122.30	90.31	58.23	226.62	35.34	3.35
SD	2.57	4.59	5.54	40.03	5.43	11.45
LSI	6.45	9.54	11.51	83.09	11.28	23.77

DTH: Days to heading; HGT: Plant height; NKS: Number of kernels per spike; NS  $m^{-2}$ : Number of spikes per square meter; TKW: Thousand kernel weight; YLD: Grain yield; SD: Standard deviation; LSI: Least significant increase.

The univariate statistics including minimum, maximum, mean, range, and standard deviation as well as the analysis of variance, revealed significant differences among treatments for all assessed traits. These findings are essential for the efficient identification and selection of superior genotypes adapted to the agro-ecological conditions of Constantine. The results are in line with previous studies conducted under similar semi-arid conditions in Algeria, which have demonstrated comparable relationships between grain yield and associated agronomic traits (Fellahi et al. 2013; Frih et al. 2022; Lamara et al. 2022; Hannachi and Fellahi 2023; Djoudi et al. 2024). Overall, the observed phenotypic variability constitutes a

valuable resource for targeted selection and the design of crossing strategies in wheat breeding programs aimed at improving productivity, resilience to environmental stress, and resource use efficiency in semi-arid agro-ecosystems.

According to the Least Significant Increase (LSI) criterion, genotypes exhibiting earlier heading than the mean performance of the local check – LSI value are considered desirable for the DTH. In this regard, genotypes G29, G38, and G9 were significantly earlier than four local checks (C1, C2, C4, and C5), while genotypes G111, G28, G40, G60, G61, G62, G65, G71, G8, G83, and G99 exhibited earliness superior to that of checks C4 and C5 (Table 5).

**Table 5.** Local checks average, least significant increase outperforming genotypes number.

Checks	DTH-LSI	Out GN	NS $m^{-2}$ +LSI	Out GN	NKS+LSI	Out GN	TKW+LSI	Out GN	YLD+LSI	Out GN
C1	113.05	3	324.84	0	75.34	2	44.01	10	70.10	1
C2	113.68	3	330.59	0	58.55	57	42.98	10	52.98	14
C3	108.55	0	345.09	0	68.09	13	51.46	0	70.37	1
C4	115.43	6	385.59	0	68.26	14	41.44	20	69.10	1
C5	117.18	14	308.09	5	67.68	14	44.09	10	60.85	4

Out GN: Outperforming genotypes number.

For traits where higher values are desirable, namely NKS, NS  $m^{-2}$ , TKW, and YLD genotypes that exceed the mean performance of the local checks plus LSI threshold are considered superior. Based on this criterion, 22 out of the 107 tested genotypes exhibited YLD values significantly

higher than the benchmark set by the local checks, thereby demonstrating promising agronomic potential. Among these, genotypes such as G111, G11, G54, G30, G57, G60, G61, G62, G67, and G8 notably outperformed the local check C2 in terms of grain yield. Genotype G87 was

particularly outstanding, registering the highest yield at  $7.33 \text{ t ha}^{-1}$ , thus surpassing all five local checks. Furthermore, G87 also exceeded the population mean for NKS (63 grains),  $\text{NS m}^{-2}$  ( $235 \text{ spikes m}^{-2}$ ), and TKW (36.65 g), indicating a robust and well-balanced performance across key yield-contributing traits.

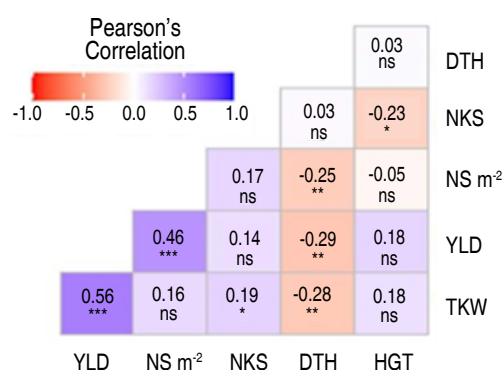
For the number of kernels per spike, the mean value recorded among the local checks was 58.27 grains. Genotypes G26 and G49 exceeded this threshold and outperformed all checks based on the LSI criteria, indicating superior spike fertility. Notably, the local check C4 registered TKW across the entire collection, confirming its strong performance for grain size. Among the tested entries, genotype G65 stood out by surpassing at least one local check for every trait evaluated, reflecting its broad and consistent agronomic superiority.

Selection based on LSI thus enables the identification of genotypes with statistically significant improvements. Specifically, genotypes with trait values greater than (check mean + LSI) for NKS,  $\text{NS m}^{-2}$ , TKW, and YLD or less than (check mean – LSI) for DTH can be classified

as statistically superior. The utility of LSI in identifying promising donors of yield-related traits has been previously validated in bread wheat (Kumar et al. 2018) as well as in rice (Hasan et al. 2020; Mustikarini et al. 2023). If in a new germplasm, YG, exceeds  $\text{YC} + \text{LSI}$ , the resulting increase in yield is considered statistically significant at the 100% level. However, the results reported in the present study do not fully align with those of Kumar et al. (2018).

### Trait relationships and their contribution to grain yield

Strong correlations were observed among the six agromorphological traits assessed in the bread wheat genotypes (Figure 1). Correlation analysis revealed that early heading, high spike density, and increased thousand-kernel weight positively contributed to higher grain yield, particularly in genotype G87. Early-heading genotypes are of particular interest to breeders, as earliness is often associated with improved yield performance under rainfed and drought-prone conditions. Therefore, such genotypes represent valuable candidates for selection programs aiming to combine early maturity with yield-enhancing traits.



ns  $P \geq 0.05$ ; \*  $P < 0.05$ ; \*\*  $P < 0.01$ ; and \*\*\*  $P < 0.001$

**Figure 1.** Correlation heat maps of grain yield and its related traits of studied bread wheat genotypes. DTH: Days to heading; HGT: Plant height; NKS: Number of kernels per spike;  $\text{NS m}^{-2}$ : Number of spikes per square meter; TKW: Thousand kernel weight; YLD: Grain yield; ns: no significant at ( $P \geq 0.05$ ); \*: Represents significance at ( $P < 0.05$ ) level; \*\*: Represents significance at ( $P < 0.01$ ) level; \*\*\*: represents significance at ( $P < 0.001$ ) level.

These findings agree with earlier reports demonstrating significant positive associations between yield and traits such as TKW and  $\text{NS m}^{-2}$  (Kumar et al. 2020; Ullah et al. 2021). In contrast, Kumar et al. (2018) reported a significant negative correlation between DTH and YLD,

which aligns with the present findings. A negative but statistically non-significant relationship was observed between the NKS and HGT, consistent with the results of Arain et al. (2018). Furthermore, Fellahi et al. (2013) identified a significant inverse relationship between NKS

and TKW, suggesting a possible trade-off between spike fertility and grain weight. However, this contrasts with other studies (Djuric et al. 2018), which reported positive associations between these traits. Such discrepancies highlight the complexity of trait interactions and emphasize the importance of context-specific validation in different genetic backgrounds and environmental conditions.

### MGIDI-Based Multi-Trait Selection

In selection based on MGIDI (Table 6), six traits were employed to assess variation among 107 genotypes. The genotype selection aimed at selecting genotypes with lower values (negative gains) for DTH, and higher values (positive gains) for NKS, NS m<sup>2</sup>, TKW, and YLD. For HGT, based on the average height of the germplasm

(90.31 cm), medium straw genotypes are more desirable than short straw genotypes. A selection with a positive gain is more desirable for this study.

The Multi-Trait Genotype-Ideotype Index classifies the studied genotypes by trait interest and exhibits significant genetic gains across all examined traits, resulting in a total genetic gain of 31.19%. The YLD shows the highest selection gain at 20%, while NKS is the only trait exhibiting an undesired gain (Table 6). Among the five local checks, C3 and C4 were chosen. The genotypes G39 and G112 were observed to be near to the cut point, indicated by the red line in Figure 2. These genotypes may serve as promising candidates exhibiting noteworthy traits for future breeding programs.

**Table 6.** Factorial loadings after varimax rotation and predicted genetic gains (PSG) based on the MGIDI.

Traits	Factors	FA1	FA2	SG	SG (%)	Sense	Goal
DTH	FA1	0.60	-0.02	-1.85	-1.52	decrease	100
NS-m <sup>2</sup>	FA1	0.64	0.22	10.10	4.30	increase	100
TKW	FA1	0.69	-0.06	1.65	4.75	increase	100
YLD	FA1	0.85	-0.04	7.40	19.97	increase	100
HGT	FA2	0.17	-0.79	3.83	4.24	increase	100
NKS	FA2	0.19	0.75	-0.34	-0.59	increase	0

SG: Selection gain; SG %: Selection gain percent.

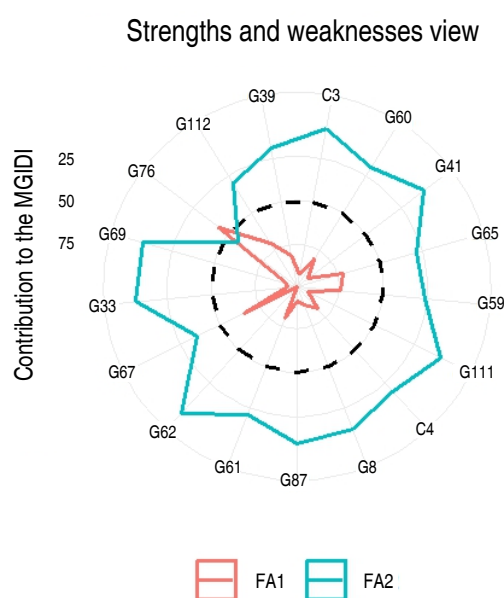


**Figure 2.** View of strengths and weaknesses of selected bread wheat genotypes.



According to Olivoto et al. (2022), the genotype with the lowest MGIDI value is considered the closest to the ideal genotype, exhibiting favorable performance across all traits under evaluation. Understanding the strengths and weaknesses of genotypes provides critical insights for parental selection in future breeding efforts. Out of the 107 evaluated genotypes, 17 were selected, including the

two local checks (C3 and C4). These selected genotypes demonstrated outstanding agronomic performance, particularly in YLD, but also across other desirable traits. Similar Multi-Trait selection (Figure 3) approaches have been successfully applied in wheat (Pour-Aboughadareh and Poczaï 2021; Romena et al. 2022), barley (Pour-Aboughadareh et al. 2021), and rice (Mamun et al. 2022).

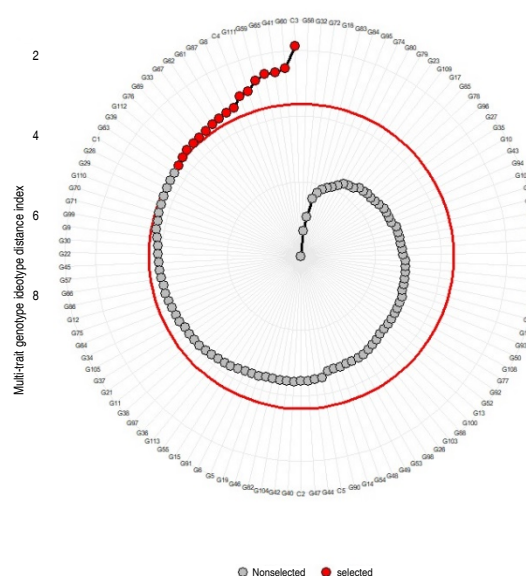


**Figure 3.** Selected bread wheat genotypes using Multi-Trait Genotype Ideotype Index.

## CONCLUSION

The present study revealed significant agro-morphological variability among the evaluated bread wheat genotypes, underscoring the genetic diversity available for selection under semi-arid conditions. The application of both the Least Significant Increase (LSI) method and the Multi-Trait Genotype–Ideotype Distance Index (MGIDI) facilitated the identification of superior genotypes combining desirable agronomic traits. Notably, genotype G65 outperformed at least one local check across all studied traits, while MGIDI highlighted 15 promising genotypes alongside two local checks (C3 and C4) as candidates for future breeding efforts. These findings emphasize the importance of early heading (DTH), high kernel number per spike (NKS), and high thousand-kernel weight (TKW) as key traits positively associated with grain yield performance. These results suggest that integrating genotypes expressing such traits into crossing programs could substantially contribute to the development of high-yielding and well-adapted cultivars

suited to the constraints of semi-arid environments like those found in Algeria. From a broader perspective, the success of breeding programs relies not only on trait-based selection but also on a comprehensive understanding of the interrelationships among traits. Such knowledge is essential for making strategic decisions that maximize genetic gain while minimizing negative correlations. Future research should therefore focus on combining phenotypic data with molecular and genomic approaches to improve selection accuracy. Moreover, the incorporation of diverse germplasm, including landraces and improved lines, into pre-breeding pipelines remains crucial for broadening the genetic base and reinforcing the adaptive potential of new cultivars. The integration of robust statistical tools such as MGIDI with well-designed field evaluations represents a promising strategy for accelerating wheat genetic improvement. These approaches will play a vital role in ensuring food security and climate resilience in regions facing increasing agricultural challenges.

## ACKNOWLEDGMENTS

The present work was financed by the socio-economic impact project "Development of New Varieties of Wheat, with high-quality performance and adapted to the different agroecological zones of the country".

## CONFLICT OF INTERESTS

No competing interests declared.

## REFERENCES

- Arain SM, Sial MA, Jamali KD and Laghari KA (2018) Grain yield performance, correlation, and cluster analysis in elite bread wheat (*Triticum aestivum* L.) lines. *Acta Agrobotica* 71(4): 1747. <https://doi.org/10.5586/aa.1747>
- Aravind J, Mukesh Sankar S, Wankhede DP and Kaur V (2023) augmentedRCBD: analysis of augmented randomised complete block designs (Version 0.1.5.9000) [R package]. <https://aravind-j.github.io/augmentedRCBD/>
- Bekkis S, Benmehaia AM and Kaci A (2023) Price Transmission in the wheat market in Algeria: Threshold cointegration approach. *International Journal of Food and Agricultural Economics* 11(1): 17–32. <https://ideas.repec.org/a/ags/ijfaec/330862.html>
- Djoudi MBI, Cheniti K, Guendouz A and Louahdi N (2024) Modeling the grain yield loss and quality assessment of some durum wheat (*Triticum durum* Desf.) genotypes under semi-arid conditions. *Revista Facultad Nacional de Agronomía Medellín* 77(1): 10563–10572. <https://doi.org/10.15446/rfnam.v77n1.108026>
- Djuric N, Prodanovic S, Brankovic G, Djekic V, Cvijanovic G et al (2018) Correlation-regression analysis of morphological-production traits of wheat varieties. *Romanian Biotechnological Letters* 23(2): 13457–13465. <https://www.researchgate.net/publication/324824808>
- Federer WT (1956) Augmented (or Hoonuiaku) design. *Hawaiiian Planters Record* 55: 191–208.
- Federer WT (1961) Augmented designs with one-way elimination of heterogeneity. *Biometrics* 17(3): 447–473.
- Fellahi Z, Hannachi A, Bouzerzour H and Boutekrabt A (2013) Correlation between traits and path analysis coefficient for grain yield and other quantitative traits in bread wheat under semi-arid conditions. *Journal of Agriculture and Sustainability* 3 (1): 16–26. <https://infinitypress.info/index.php/jas/article/view/96>
- Frih B, Oulmi A, Guendouz A and Benkadia S (2022) Evaluation of grain yield performance of seven (*Triticum durum* Desf.) genotypes grown under semi-arid conditions during two crop seasons in the eastern of Algeria. *Agricultural Science and Technology* 14(3): 26–31. <https://doi.org/10.15547/ast.2022.03.033>
- Hannachi A and Fellahi Z (2023) Efficiency of index-based selection for potential yield in durum wheat [*Triticum turgidum* (L.) ssp. *turgidum* convar. *durum* (Desf.) Mackey] lines. *Italian Journal of Agronomy* 18(1): 2182. <https://doi.org/10.4081/ija.2023.2182>
- Hasan FU, Sari S, Zubair A and Carsono N (2020) New promising rice genotypes of SP87-1-1-2 and SP73-3-17 adaptive to lowland and medium land. *Planta Tropika* 8(1). <https://doi.org/10.18196/pt.2020.110.21-32>
- Khodarahmi M, Soughi H, Shahbazi K, Jafarby J and Khavarinejad MS (2023) Trends in important agronomic traits, grain yield and its components in bread wheat cultivars released in northern warm and humid climate of Iran, 1968–2018. *Cereal Research Communications* 51(4): 1003–1014. <https://doi.org/10.1007/s42976-023-00353-x>
- Kumar A, Sharma PC, Singh R and Kumari J (2018) Bread wheat germplasm evaluation for soil moisture stress tolerance under rainfed condition. *International Journal of Bio-resource and Stress Management* 9(6): 754–761.
- Kumar P, Solanki YPS Singh V and Kiran (2020) Genetic variability and association of morpho-physiological traits in bread wheat (*Triticum aestivum* L.). *Current Journal of Applied Science and Technology* 39(35): 95–105. <https://doi.org/10.9734/cjast/2020/v39i3531059>
- Lamara A, Fellahi Z, Hannachi A and Benniou R (2022) Assessing the phenotypic variation, heritability and genetic advance in bread wheat (*Triticum aestivum* L.) candidate lines grown under rainfed semi-arid region of Algeria. *Revista Facultad Nacional de Agronomía Medellín* 75(3): 10107–10118. <https://doi.org/10.15446/rfnam.v75n3.100638>
- Mamun AA, Islam MM, Adhikary SK and Sultana MS (2022) Resolution of genetic variability and selection of novel genotypes in EMS induced rice mutants based on quantitative traits through MGIDI. *International Journal of Agriculture and Biology* 28(2): 100–112.
- Mustikarini ED, Prayoga GI, Santi R, Yesi and Sari NPE (2023) Potential of Upland Rice Promising Lines in Acid Dry Land at Two Different Seasons. *AGRIVITA Journal of Agricultural Science* 45(1): 31–37. <https://doi.org/10.17503/agrivita.v45i1.3750>
- Olivoto T and Lúcio AD (2020) metan: An R package for multi-environment trial analysis. *Methods in Ecology and Evolution* 11(6): 783–789. <https://doi.org/10.1111/2041-210x.13384>
- Olivoto T and Nardino M (2021) MGIDI: toward an effective multivariate selection in biological experiments. *Bioinformatics* 37(10): 1383–1389. <https://doi.org/10.1093/bioinformatics/btaa981>
- Olivoto T, Diel MI, Schmidt D and Lúcio AD (2022) MGIDI: a powerful tool to analyze plant multivariate data. *Plant Methods* 18: 121. <https://doi.org/10.1186/s13007-022-00952-5>
- ONS - Office Nationale des Statistiques (2023a) Collections Statistiques: Evolution des échanges extérieurs de marchandises de 2017 à 2022 (233). <https://www.ons.dz/spip.php?rubrique315>
- ONS - Office Nationale des Statistiques (2023b) La Production Agricole Campagne 2020/2021 (990). [https://www.ons.dz/IMG/pdf/ProdAgricol2020\\_2021.pdf](https://www.ons.dz/IMG/pdf/ProdAgricol2020_2021.pdf)
- Pour-Aboughadareh A and Pocza P (2021) A dataset on multi-trait selection approaches for screening desirable wild relatives of wheat. *Data in Brief* 39: 107541. <https://doi.org/10.1016/j.dib.2021.107541>
- Pour-Aboughadareh A, Sanjani S, Nikkhah-Chamanabad H, Mehrvar M R, Asadi A and Amini A (2021) Identification of salt-tolerant barley genotypes using multiple-traits index and yield performance at the early growth and maturity stages. *Bulletin of the National Research Centre* 45(1): 117. <https://doi.org/10.1186/s42269-021-00576-0>
- R Core Team (2024) R: A Language and Environment for Statistical Computing. R Foundation for Statistical Computing, Vienna, Austria. <https://www.r-project.org/>
- Romena MH, Najaphy A, Saeidi M and Khoramivafa M (2022) Identification of superior wheat genotypes using multiple-trait selection methods based on agronomic characters and grain protein content under rain-fed conditions. *Genetika* 54(1): 15–26. <https://doi.org/10.2298/genstr2201015r>
- Sivakumar U and Kumar A (2023) Genetic variability, heritability, and genetic advance analysis in bread wheat (*Triticum aestivum* L.).

The Pharma Innovation Journal 12(8): 800-804.

Tutiempo Network SL (2024) Climate Constantine – climate data (station 604190), 2018 and 2019. <https://fr.tutiempo.net/climat/ws-604190.html>

Ullah MI, Mahpara S, Bibi R et al (2021) Grain yield and correlated traits of bread wheat lines: Implications for yield improvement. Saudi

Journal of Biological Sciences 28(10): 5714–5719. <https://doi.org/10.1016/j.sjbs.2021.06.006>

Venske E, dos Santos RS, Busanello C, Gustafson P and Costa de Oliveira A (2019) Bread wheat: a role model for plant domestication and breeding. *Hereditas* 156(1): 16 <https://doi.org/10.1186/s41065-019-0093-9>





# Tomato (*Solanum lycopersicum* L.) leaf disease detection using computer vision



Detección de enfermedades en las hojas del tomate (*Solanum lycopersicum* L.) mediante visión por computadora

<https://doi.org/10.15446/rfnam.v78n3.116493>

Sebastián Palacio Betancur<sup>1\*</sup> and Freddy Bolaños Martínez<sup>1</sup>

## ABSTRACT

### Keywords:

Deep learning  
Object detection  
Plant pathology  
PlantVillage dataset  
Precision agriculture

Tomato cultivation is a key component of global agriculture, but is significantly threatened by pests and diseases that impact yield and trade. To address this, the present study investigates the application of YOLOv9, a state-of-the-art object detection model, for automated disease detection in tomato leaves. Using a dataset of 4,323 images with 15,135 annotations and a modified PlantVillage dataset, YOLOv9 models were trained and evaluated. Among the evaluated models, YOLOv9e yielded the highest mean average precision (mAP) at 0.964, establishing a benchmark for accuracy. In contrast, the YOLOv9t model provided an optimal balance for practical applications, achieving a competitive mAP of 0.95 with a rapid inference time of 8.8 ms. Furthermore, this work contributes a public version of the PlantVillage dataset with bounding box annotations, providing a valuable resource for object detection research and extending the use of the original classification-focused dataset. The results indicate that YOLOv9 models are effective for real-time and accurate detection of various diseases in complex agricultural settings.

## RESUMEN

### Palabras clave:

Aprendizaje profundo  
Detección de objetos  
Fitopatología  
PlantVillage dataset  
Agricultura de precisión

El cultivo de tomate es un componente clave de la agricultura mundial, pero se ve amenazado significativamente por plagas y enfermedades que impactan el rendimiento y el comercio. Para abordar esto, el presente estudio investiga la aplicación de YOLOv9, un modelo de detección de objetos de última generación, para la detección automatizada de enfermedades en las hojas de tomate. Utilizando un conjunto de datos de 4.323 imágenes con 15.135 anotaciones y un conjunto de datos PlantVillage modificado, se entrenaron y evaluaron los modelos YOLOv9. Entre los modelos evaluados, YOLOv9e arrojó la precisión media promedio (mAP) más alta con 0,964, estableciendo un punto de referencia para la exactitud. En contraste, el modelo YOLOv9t proporcionó un equilibrio óptimo para aplicaciones prácticas, logrando un mAP competitivo de 0,95 con un tiempo de inferencia rápido de 8,8 ms. Además, este trabajo aporta una versión pública del conjunto de datos PlantVillage con anotaciones de cuadros delimitadores, proporcionando un recurso valioso para la investigación en detección de objetos y extendiendo el uso del conjunto de datos original enfocado en la clasificación. Los resultados indican que los modelos YOLOv9 son eficaces para la detección precisa y en tiempo real de diversas enfermedades en entornos agrícolas complejos.

<sup>1</sup>Departamento de Energía Eléctrica y Automática, Facultad de Minas, Universidad Nacional de Colombia Sede Medellín, Colombia. [spalaciob@unal.edu.co](mailto:spalaciob@unal.edu.co) , [fbolanosm@unal.edu.co](mailto:fbolanosm@unal.edu.co) 

\*Corresponding author



The cultivation of tomatoes (*Solanum lycopersicum* L.) represents one of the most significant agricultural activities worldwide, both in terms of production and consumption. According to data from the Food and Agriculture Organization of the United Nations (FAO), approximately 186.1 million tons of tomatoes were produced globally in 2022.

During the same year, it is estimated that around 875,436.86 tons of tomatoes were produced in Colombian territory (FAO 2024), underscoring the importance of this crop in the national agricultural context and its contribution to the country's food security and economy.

However, tomato cultivation, like many other crops, faces significant challenges due to plant pests and diseases. These plant pests are responsible for global losses of crops up to 40% and cause annual trade losses of over 220 billion USD (IPPC Secretariat 2021). The conventional response has been a heavy reliance on chemical inputs, with 4.2 million tons of pesticides used worldwide in 2019 (FAO 2021), a practice that raises significant environmental and public health concerns. In this context, early and accurate disease detection emerges as a key strategy to enable targeted interventions, thereby optimizing the use of agrochemicals and promoting more sustainable agricultural practices.

Traditionally, this task of disease detection has been carried out through visual inspection by agricultural experts. However, this approach presents significant limitations in terms of cost, time, and difficulties in implementation in rural areas where access to experts may be limited.

Computer vision has become a powerful tool for detecting tomato leaf diseases using automatic image techniques. The predominant approach is deep learning, which outperforms traditional machine learning by automatically learning relevant features, without the need for manual feature extraction. This adaptability is especially useful given the complexity and variability of tomato leaf images (Tan et al. 2021).

In the field of computer vision applied for detecting tomato leaf diseases, various techniques have been explored to improve the accuracy and generalization of models. These include the use of hybrid models that combine traditional

machine learning with deep learning techniques (Singh et al. 2022), data augmentation through techniques such as Conditional Generative Adversarial Networks (cGAN) (Abbas et al. 2021), the incorporation of pre-trained neural networks such as AlexNet, GoogleNet, DenseNet, SqueezeNet (Abbas et al. 2021; Durmus et al. 2017), and with the use of different versions of You Only Look Once (YOLO) models for plant disease detection (Chairma et al. 2023; Liu and Wang 2020).

It is important to distinguish between classification and detection in this context. While classification focuses on assigning a specific label to an image (i.e., identifying the disease present), detection involves locating and classifying multiple diseases simultaneously in one image, which is crucial for practical real-time applications.

In the specific task of classifying tomato diseases, Mohanty et al. (2016) used convolutional neural networks (CNN), for the sake of identifying 14 distinct classes of vegetal pathologies, including several which affect tomatoes. Accuracy reached in this case was 99 % under controlled circumstances (Mohanty et al. 2016). The main drawback of this reported solution is its low performance when facing real-world images, and varying conditions such as illumination, background, resolution of the images, and so on. Low computational complexity is also a key issue, since the classification models are intended to be implemented in mobile, real-time, and low consumption platforms. Some models, such as MobileNet, EfficientNet, and YoloV5-Lite, have been reported in literature for these purposes (Fuentes et al. 2017).

Regarding the detection of tomato diseases, some deep learning models have been proposed. Among the plethora of alternatives reported in literature, some approaches such as Mask R-CNN, PLPNet, and Yolo highlight (Tang et al. 2023). Recent developments in this subject aim to achieve both high accuracy and low delay time, though such objectives seem to be in conflict.

Despite some of the reported advancements, automatic disease detection models for tomato leaves still face several challenges that impact their performance and accuracy. Issues include unwanted elements in images (such as grass or soil), the need for large, high-quality datasets, the complexity and computational demands of deep learning



models, and difficulties in detecting multiple or similar diseases. Additional challenges arise from varying field conditions, the integration of drones for image capture, and ensuring reliability in open agricultural environments (Sajitha et al. 2024).

Due to the lack of large datasets for training purposes, transfer learning and self-supervised models have been proposed to reduce the model's dependency to large volume of training data. Such is the case of the work reported in Chai et al. (2024), where self-supervised models are proposed for tomato disease recognition. Another proposed approach implies the use of multispectral images, or the complement of traditional RGB images with thermal signals, in order to improve the detection accuracy (Mahlein 2016).

Given these challenges, the YOLOv9 model family presents a promising solution due to its documented efficiency and accuracy in complex environments. To formally assess this potential in the agricultural context, this study aims to evaluate the performance of different YOLOv9 models for detecting tomato leaf diseases in real-time scenarios.

## MATERIALS AND METHODS

### Datasets

#### Dataset for model detection training

The dataset used consists of 4,323 images with 15,135 annotations, including images with simple backgrounds, photos taken of plants, and collages of multiple leaves with different diseases, as shown in Figure 1. This diversity is crucial for training a model capable of functioning in complex, real-world field conditions. This dataset is divided

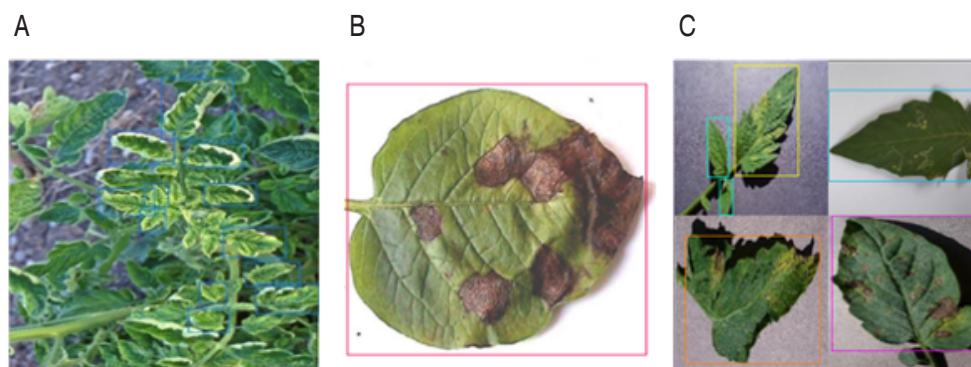


**Figure 1.** Dataset sample. **A.** Yellow leaf curl virus; **B.** Late Blight and **C.** Multiple classes.

into 9 classes, as presented in Table 1, and includes the necessary bounding boxes for detection.

**Table 1.** Distribution of classes in the dataset.

Class	Number of annotations
Yellow Leaf Curl Virus	2,131
Late Blight	1,886
Leaf Mold	1,878
Mosaic Virus	1,788
Septoria	1,713
Healthy	1,691
Early Blight	1,407
Leaf Miner	1,409
Spider Mites	1,232

This distribution follows a standard machine learning convention, ensuring that the model is trained on a

substantial data volume and then evaluated impartially on separate validation and test sets. It is important to note that this dataset is a modified version of a freely available dataset from Roboflow (dyploma 2024) created by a community member. Given its community-sourced origin, guaranteeing the complete precision of every annotation is not feasible. This makes a rigorous evaluation against a standardized benchmark an essential methodological step. For this reason, an additional model validation is performed using the PlantVillage dataset. PlantVillage, being a curated collection of images with single leaves on uniform backgrounds, is less ideal for training a model for complex scenarios but serves as a perfect, unbiased source for validation.

Seventy-five percent of the images were allocated for training, 15% for validation, and 10% for testing.

This distribution follows a standard machine learning convention, ensuring that the model is trained on a substantial data volume and then evaluated impartially on separate validation and test sets. To address class imbalance and enhance model generalization, the “Healthy” class was enriched by augmenting its image count. A structured data augmentation pipeline was applied to the training dataset using the Roboflow platform. This process included converting 15% of the training images to grayscale to reduce color-based bias and improve robustness to variable lighting conditions. Additionally, random crops were applied within bounding boxes with a zoom range of 0–20%, simulating occlusion scenarios and improving localization accuracy for diseases with small lesions, such as Septoria. These augmentations increased the training dataset size from 3,244 to 9,732 images, tripling the available data for model training. Both the enriched and augmented versions of the dataset have been publicly released on Kaggle (Palacio 2024a) to support reproducibility and future research.

### PlantVillage dataset for object detection

The PlantVillage is one of the most widely used data sets in machine learning and deep learning research for plant disease classification of images (Sajitha et al. 2024). It contains an extensive collection of images covering 38 different classes, representing various diseases and health states in plants such as apples, cherries, corn, grapes, and tomatoes, among others, with over 54,000

leaf images (Geetharamani and Arun 2019).

However, PlantVillage is mainly designed for classification tasks and does not include the bounding boxes necessary for working with object detection models like YOLO. This limitation has been addressed by some researchers through manual labeling strategies (Nawaz et al. 2022; Mathew and Mahesh 2022), which, while effective, can be extremely labor-intensive and time-consuming.

To address the challenge of labeling the PlantVillage dataset for object detection more efficiently, a semi-automatic labeling pipeline was developed (Figure 2). First, a YOLOv9 model was trained to generate bounding boxes around plant leaves. This initial model processed the entire dataset, producing candidate regions of interest. Next, the dataset’s inherent folder structure, where images are organized by class labels (e.g., Tomato\_Healthy, Tomato\_Late\_Blight) was leveraged to automate class assignment. A custom Python script mapped folder names to corresponding annotation labels, assigning classes to the bounding boxes generated by the YOLOv9 model. This approach enabled rapid annotation of 54,000+ images while minimizing manual effort. To ensure accuracy, all annotations were manually reviewed, with <5% of labels requiring correction due to misalignments or edge cases (e.g., overlapping leaves). The final labeled dataset, optimized for object detection tasks, has been publicly released on Kaggle (Palacio 2024b). This resource eliminates the need for labor-intensive manual annotation, providing researchers with a scalable foundation for training

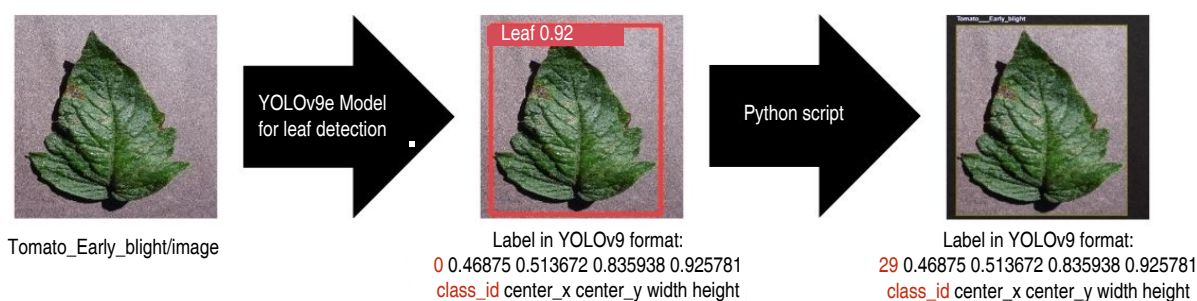


**Figure 2.** Labeling process for the PlantVillage dataset.

and evaluating disease detection models.

### YOLOv9: Detection algorithm

YOLO is a family of deep-learning models designed for real-time object detection in images and videos. Unlike other methods that process images in multiple stages, YOLO

processes an entire image in a single pass, dividing it into a grid and assigning bounding boxes and class probabilities to each cell. This architecture allows YOLO to be extremely fast and efficient, making it ideal for applications requiring rapid and precise detection, such as surveillance, autonomous



driving, and real-time computer vision.

YOLOv9, the ninth version of this model series, represents a significant advancement in terms of accuracy and efficiency. Introduced in 2024, YOLOv9 incorporates key improvements such as Programmable Gradient Information (PGI) and Generalized Efficient Layer Aggregation Network (GELAN). PGI addresses information loss by integrating a reversible auxiliary branch, enhancing gradient generation across deep layers. GELAN optimizes computational complexity, accuracy, and inference speed by enabling the selection of suitable computational blocks and the use of conventional convolution operators instead of more complex techniques. These innovations have allowed YOLOv9 to reduce the number of parameters by 49% and calculations by 43% compared to its predecessor while improving average precision by 0.6% on the MS COCO dataset. These statistics highlight its ability to deliver precise and efficient real-time detection (Wang et al. 2024).

Table 2, with data sourced from the original YOLOv9 paper (Wang et al. 2024), outlines the specifications for each model variant based on their size and computational needs. Parameters (M) show the number of model parameters, measured in millions, which include the weights and biases the model learns. FLOPs (BFLOPS) indicate the number of floating-point calculations required for one pass through the model, measured in billion FLOPs, reflecting

**Table 2.** YOLOv9 models.

Model	Parameters (M)	FLOPs (BFLOPS)
YOLOv9t	2.0	7.7
YOLOv9s	7.2	26.7
YOLOv9m	20.1	76.8
YOLOv9c	25.5	102.8
YOLOv9e	58.1	192.5

its computational demand.

#### Performance metrics

The following metrics are used to evaluate the performance of the proposed method, expressed in Equations 1, 2, 3 and 4:

$$\text{Precision (P)} = \frac{TP}{TP + FP} \quad (1)$$

$$\text{Recall (R)} = \frac{TP}{TP + FN} \quad (2)$$

$$\text{Average precision (AP)} = \int_0^1 P(R) dR \quad (3)$$

Intersection over Union (IoU) = (Area of overlap) / (Area of union)

Where TP is the True Positives, FP is the False Positives, FN is the False Negatives, and C is the Number of Classes.

AP calculates the area under the precision-recall curve, providing a single value that summarizes the model's precision and recall performance across various thresholds (Jocher et al. 2024).

Mean average precision (mAP) extends the concept of AP by averaging the AP values across multiple object classes (Equation 4). This metric is useful in multi-class object detection scenarios to provide a comprehensive evaluation of the model's performance (Jocher et al. 2024).

$$\text{Mean average precision (mAP)} = \frac{1}{C} \sum_{i=1}^C AP_i \quad (4)$$

Intersection over Union (IoU): IoU is a measure that quantifies the overlap between a predicted bounding box and a ground truth bounding box. It plays a fundamental role in evaluating the accuracy of object localization (Jocher et al. 2024).

Confusion Matrix: The confusion matrix provides a detailed view of the results by showing the counts of true positives (TPs), true negatives (TNs), false positives (FPs), and false negatives (FNs) for each class (Jocher et al. 2024).

Inference Time: Indicates the time taken by the model to process a single image and produce predictions. This metric reflects the model's efficiency and speed in real-time applications.

## RESULTS AND DISCUSSION

### Training a custom YOLOv9 on a custom dataset

Training an object detection model like YOLOv9 involves

teaching the network to recognize and localize objects within images by learning associations between visual features and annotated bounding boxes. This process requires a labeled dataset comprising images annotated with class labels and spatial coordinates (bounding boxes) that define the location of objects. During training, the model iteratively adjusts its parameters to minimize prediction errors, learning to correlate specific visual patterns (e.g., color, texture, shape) with their corresponding classes and spatial positions.

In this work, YOLOv9 models were trained using the code available on the official GitHub repository of the model. The training process was executed using Kaggle Notebooks, which provided access to a free Nvidia Tesla P100 GPU with 16 GB of VRAM. Each model was trained for 120 epochs, using images with 640x640 pixels. All other hyperparameters (e.g., learning rate, batch size, optimizer settings) and training configurations were retained from

the repository's default values to ensure alignment with the model's standardized implementation.

#### Validation with the model's training dataset

The initial validation results were obtained using 15% of the images from the dataset used to train the model, with an image of 640x640 pixels.

Table 3 shows YOLOv9e achieved the highest precision (0.945) and mAP (0.964) due to its deeper network (58.1M parameters) and advanced features like PGI, which retains gradient information for fine-grained feature learning. However, its computational cost (192.5 BFLOPs) results in slower inference (48.4 ms), making it less suitable for edge devices. YOLOv9t sacrifices marginal precision (0.92) and mAP (0.95) for speed (8.8 ms), leveraging a lightweight architecture (2.0M parameters, 7.7 BFLOPs). This trade-off aligns with agricultural needs like drone-based monitoring, where real-time performance is critical.

**Table 3.** Performance metrics of the models.

Model	Precision	Recall	mAP	Inference Time (ms)
YOLOv9t	0.92	0.867	0.95	8.8
YOLOv9s	0.924	0.884	0.953	11.8
YOLOv9m	0.906	0.91	0.949	25.2
YOLOv9c	0.927	0.893	0.944	35.7
YOLOv9e	0.945	0.904	0.964	48.4

To further analyze the classification performance of the YOLOv9e model on the primary dataset, a confusion matrix was generated, as shown in Figure 3. For object detection tasks, it is crucial to note that this matrix evaluates both classification accuracy and localization precision. A prediction is only considered a True Positive if the class is correct and the Intersection over Union (IoU) between the predicted and ground truth bounding boxes exceeds a set threshold (0.7). The matrix reveals high values along the main diagonal for most classes, such as Leaf Miner (1.00) and Late Blight (0.95), indicating strong performance in both classifying and localizing these diseases. However, the most significant finding is the rate of False Negatives, represented by the background column. For instance, 31% of Yellow Leaf Curl Virus instances and 27% of Healthy leaf instances were categorized as background misses. This type of error occurs for one of two reasons: either the

model completely failed to detect an object, or it detected the object but with a bounding box of poor quality (IoU < 0.7). In contrast, confusion between the different disease classes was minimal. These results therefore indicate that the primary challenge for the model lies in its detection and localization capabilities, rather than in its ability to differentiate between the pathologies themselves.

Figure 4 shows an example of a YOLOv9e prediction.

#### Validation with the PlantVillage dataset

For this additional validation, the classes that matched between the model's dataset and the PlantVillage dataset were selected. The classes included are the same as those listed in Table 1, except for Leaf Miner, which is not present in the PlantVillage dataset. A total of 14,627 images were used, each with a size of 256x256 pixels.

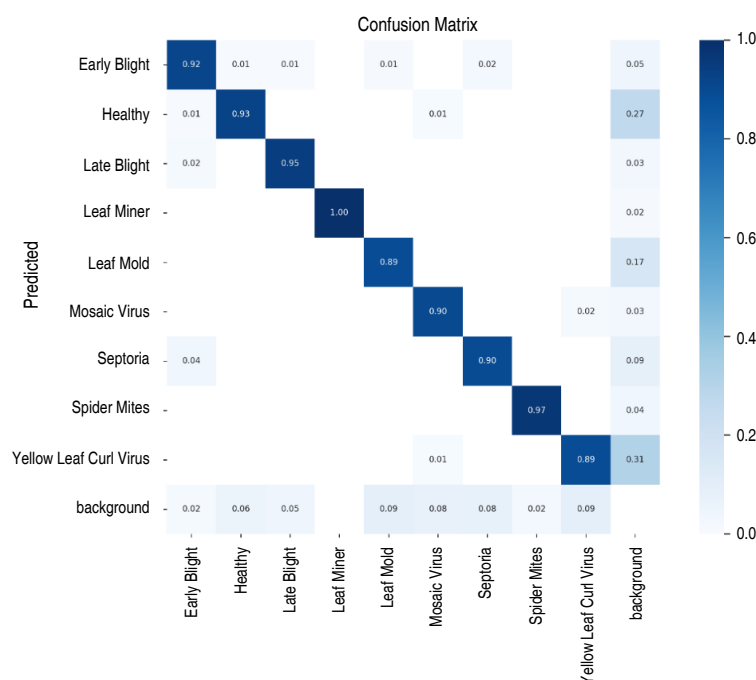


Figure 3. YOLOv9e confusion matrix.

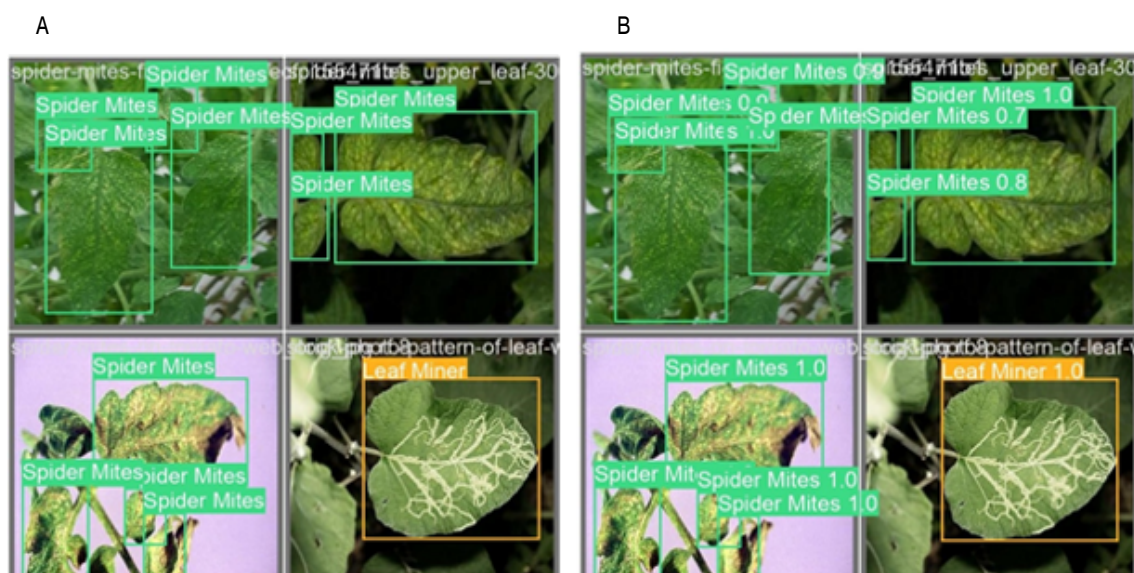


Figure 4. YOLOv9e prediction. A. Expected prediction and B. Model output.

In Table 4, YOLOv9t demonstrated superior performance on the PlantVillage dataset, achieving the highest precision (0.939), recall (0.933), and fastest inference time (1.4 ms). Conversely, YOLOv9e, despite its higher complexity (58.1

M parameters, PGI, and GELAN layers), underperformed relative to its results on the custom dataset, with precision (0.893), recall (0.911), and mAP (0.958) trailing smaller models.

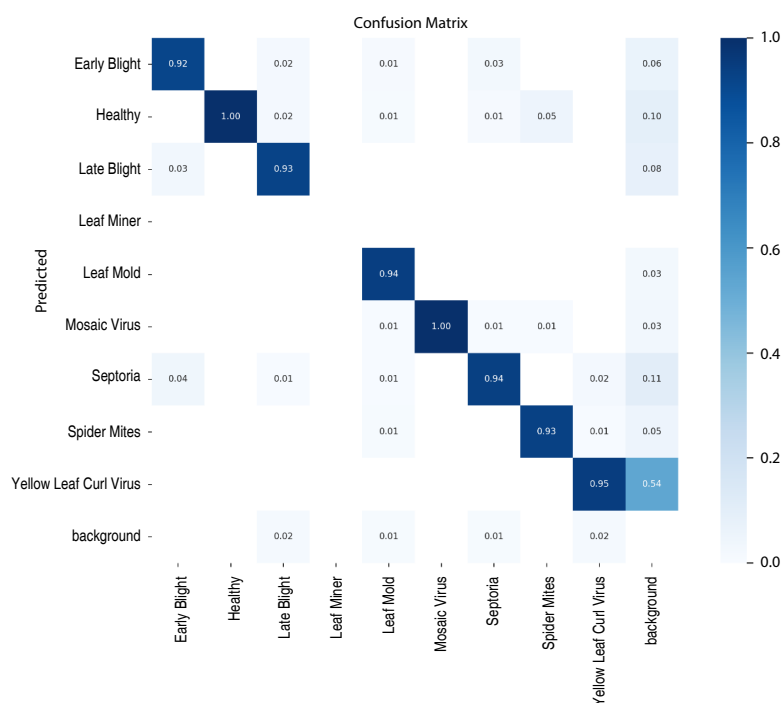
**Table 4.** Performance metrics of the models on the PlantVillage dataset.

Model	Precision	Recall	mAP	Inference Time (ms)
YOLOv9t	0.939	0.933	0.965	1.4
YOLOv9s	0.913	0.919	0.952	2.3
YOLOv9m	0.894	0.883	0.942	4.8
YOLOv9c	0.905	0.896	0.955	6.5
YOLOv9e	0.893	0.911	0.958	9.8

This discrepancy could be attributed to the simplicity of PlantVillage images, which feature uniform backgrounds and controlled lighting, potentially reducing the need for YOLOv9e's advanced feature-extraction capabilities. The model's architectural complexity, optimized for diverse real-world conditions (e.g., overlapping leaves, variable lighting), may have led to overfitting on the more heterogeneous training data, plausibly diminishing its adaptability to simpler, structured datasets. Smaller models like YOLOv9t, with fewer parameters (2.0 M) and lower computational demands (7.7 BFLOPs), could be better suited for such scenarios, suggesting that their efficiency aligns with the dataset's reduced complexity.

These findings underscore the importance of aligning model architecture with dataset characteristics for optimal deployment e.g., lightweight models for high-throughput edge devices versus high-precision models for detailed field diagnostics.

The confusion matrix for the YOLOv9t model on the PlantVillage dataset (Figure 5) reveals an exceptionally high level of accuracy. The model achieved perfect or near-perfect classification for several classes, including Healthy (1.00) and Mosaic Virus (1.00), with all other disease classes scoring 0.92 or higher on the main diagonal.

**Figure 5.** YOLOv9e confusion matrix PlantVillage dataset validation.



Most notably, the False Negative rate, represented by misclassifications into the 'background' class, is reduced across all categories when compared to the model's performance on the more complex primary dataset. This finding strongly supports the previous analysis: the primary source of error encountered in the initial tests was directly

related to environmental complexity and challenges in object localization, rather than an inherent limitation in the model's ability to differentiate between pathologies. When tested on clean, uniform images, the model's performance is excellent.

Figure 6 shows an example of a YOLOv9t prediction.

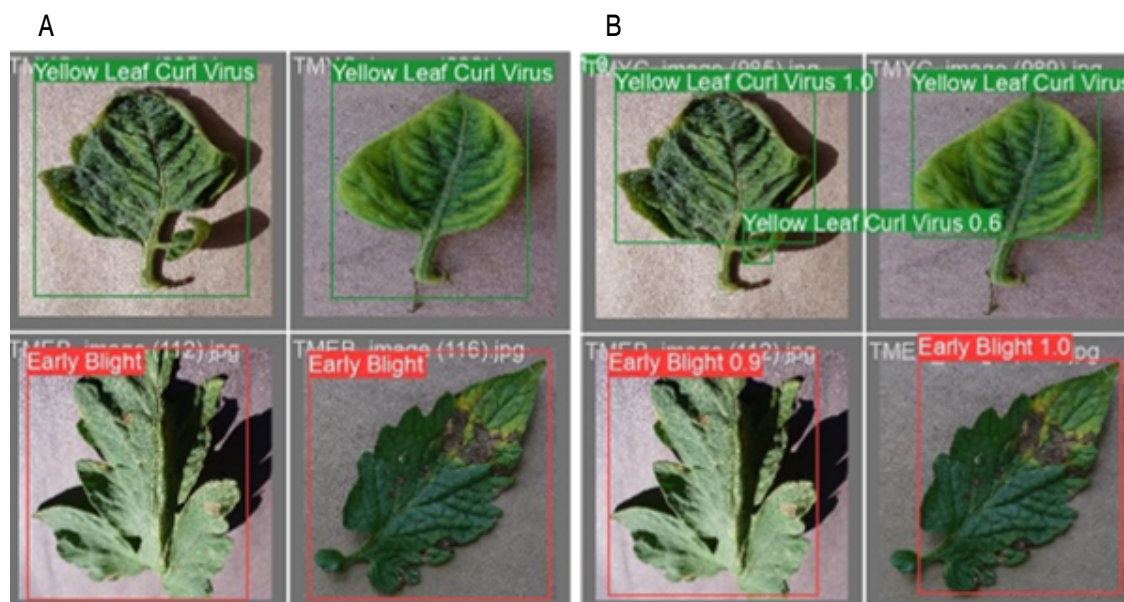


**Figure 6.** YOLOv9t prediction. **A.** Expected prediction and **B.** Model output.

## CONCLUSION

YOLOv9 models exhibit robust performance in tomato leaf disease detection, effectively balancing the dual demands of accuracy and computational efficiency. Among the variants, YOLOv9t emerges as a practical choice for real-time applications, achieving a competitive mean average precision (mAP) of 0.95 with an inference time of 8.8 ms per image. This efficiency—enabled by its lightweight architecture (2.0 M parameters) and reduced FLOPs (7.7 billion)—positions it as ideal for deployment in resource-constrained environments, such as drone-based field monitoring systems requiring rapid, high-throughput processing. In contrast, YOLOv9e prioritizes precision, attaining the highest mAP (0.964) through its advanced Programmable Gradient Information (PGI) and deeper network structure. While its slower inference speed (48.4 ms) may limit its use in time-sensitive scenarios, it remains invaluable for precision-critical tasks, such as greenhouse diagnostics or laboratory analysis, where accuracy is

paramount. These findings underscore the importance of model selection based on operational priorities, offering clear guidance for agricultural stakeholders. Notably, even the slowest model (YOLOv9e) operates within real-time thresholds ( $\geq 20$  FPS), ensuring broad applicability across diverse settings.

A key outcome of this work is the public release of the PlantVillage dataset with bounding box annotations. This initiative adapts the well-known dataset, originally designed for image classification, for a new application in object detection. Providing this resource to the research community removes the need for individual, labor-intensive labeling efforts on this specific dataset and facilitates the training and evaluation of object detection models on a widely recognized set of images. Despite its contributions, this study has certain limitations that should be acknowledged. The training data predominantly featured images from controlled or semi-controlled environments,

which may not fully represent the variability of real-world field conditions. Consequently, the model's robustness could be challenged by factors such as motion blur, variable lighting, and partial leaf occlusions not extensively covered in the training set.

These limitations, however, define clear and compelling directions for future research. First, future work should prioritize validating the models on imagery captured directly from field conditions via drones or handheld devices, which is essential for assessing real-world performance. Furthermore, it is recommended to expand the dataset to include other significant plant stressors, such as nutrient deficiencies and pest infestations, to develop a more comprehensive diagnostic tool. A final and logical progression would be the integration of these validated models into edge-computing or IoT platforms to create and test automated, closed-loop disease management systems.

## ACKNOWLEDGMENTS

The authors would like to thank the following institutions: Universidad Nacional de Colombia, Medellín Headquarters, and Semillero de Instrumentación, Control y Robótica (SinCRo), for their support in the development of the current work.

## CONFLICT OF INTERESTS

The authors declare no potential conflicts of interest.

## REFERENCES

- Abbas A, Jain S, Gour M and Vankudothu S (2021) Tomato plant disease detection using transfer learning with C-GAN synthetic images. *Comput Electron Agric* 187. <https://doi.org/10.1016/j.compag.2021.106279>
- Chai AYH, Lee SH, Tay FS et al (2024) Beyond supervision: Harnessing self-supervised learning in unseen plant disease recognition. *Neurocomputing* 610:128608. <https://doi.org/10.1016/j.neucom.2024.128608>
- Chairma Lakshmi KR, Praveena B, Sahaana G et al (2023) Yolo for Detecting Plant Diseases. In: *Proceedings of the 3rd International Conference on Artificial Intelligence and Smart Energy, ICAIS 2023*. Institute of Electrical and Electronics Engineers Inc., pp 1029–1034.
- Durmus H, Gunes EO and Kirci M (2017) Disease detection on the leaves of the tomato plants by using deep learning. In: *2017 6th International Conference on Agro-Geoinformatics*. IEEE, pp 1–5.
- diploma (2024) Tomato Leaf Diseases Dataset. Roboflow Universe.
- FAO - Food and Agriculture Organization of the United Nations (2024) FAOSTAT. In: FAOSTAT. <https://www.fao.org/faostat/en/#data/QCL>
- FAO - Food and Agriculture Organization of the United Nations (2021) *World Food and Agriculture – Statistical Yearbook 2021*. FAO, Rome.
- Fuentes A, Yoon S, Kim S and Park D (2017) A robust deep-learning-based detector for real-time tomato plant diseases and pests recognition. *Sensors* 17: 2022. <https://doi.org/10.3390/s17092022>
- Geetharamani G and Arun Pandian J (2019) Identification of plant leaf diseases using a nine-layer deep convolutional neural network. *Computers & Electrical Engineering Journal* 76: 323–338. <https://doi.org/10.1016/j.compeleceng.2019.04.011>
- IPPC Secretariat (2021) *International year of plant health – Final report*. FAO, Rome.
- Jocher G, Munawar MR and Vina A (2024) YOLO Métricas de Rendimiento. YOLO Métricas de rendimiento - Ultralytics YOLOv8 Docs.
- Liu J and Wang X (2020) Tomato Diseases and pests detection based on improved Yolo V3 Convolutional Neural Network. *Front Plant Sci* 11: 521544. <https://doi.org/10.3389/fpls.2020.00898>
- Mahlein A-K (2016) Plant disease detection by imaging sensors – parallels and specific demands for precision agriculture and plant phenotyping. *Plant Diseases* 100: 241–251. <https://doi.org/10.1094/PDIS-03-15-0340-FE>
- Mathew MP and Mahesh TY (2022) Leaf-based disease detection in bell pepper plant using YOLO v5. *Signal Image Video Process* 16: 841–847. <https://doi.org/10.1007/s11760-021-02024-y>
- Mohanty SP, Hughes DP and Salathé M (2016) Using deep learning for image-based plant disease detection. *Front Plant Sci* 7. <https://doi.org/10.3389/fpls.2016.01419>
- Nawaz M, Nazir T, Javed A et al (2022) A robust deep learning approach for tomato plant leaf disease localization and classification. *Sci Rep* 12. <https://doi.org/10.1038/s41598-022-21498-5>
- Palacio S (2024a) Tomato leaf diseases dataset for object detection. <https://www.kaggle.com/dsv/9270440>
- Palacio S (2024b) PlantVillage for object detection YOLO. <https://www.kaggle.com/ds/5363572>
- Sajitha P, Diana Andrushia A, Anand N and Naser MZ (2024) A review on machine learning and deep learning image-based plant disease classification for industrial farming systems. *J Ind Inf Integr* 100572. <https://doi.org/10.1016/j.jii.2024.100572>
- Singh A, Sreenivasu S, Mahalaxmi U et al (2022) Hybrid Feature-Based disease detection in plant leaf using convolutional neural network, bayesian optimized SVM, and random forest classifier. *J Food Qual* 2022: 16. <https://doi.org/10.1155/2022/2845320>
- Tan L, Lu J and Jiang H (2021) Tomato leaf diseases classification based on leaf images: A comparison between classical machine learning and deep learning methods. *AgriEngineering* 3: 542–558. <https://doi.org/10.3390/agriengineering3030035>
- Tang Z, He X, Zhou G et al (2023) A precise image-based tomato leaf disease detection approach using PLPNet. *Plant Phenomics* 5:0042. <https://doi.org/10.34133/plantphenomics.0042>
- Wang CY, Yeh I-H and Liao HYM (2024) YOLOv9: Learning what you want to learn using programmable gradient information.

## Response of *Corchorus olitorius* L. to cocoa pod husk powder and urea fertilizer

Respuesta de *Corchorus olitorius* L. al polvo de cáscara de mazorca de cacao y al fertilizante químico de nitrógeno

<https://doi.org/10.15446/rfnam.v78n3.117135>

Tajudeen Bamidele Akinrinola<sup>1\*</sup>, Miracle Oluwaseyi Aponjolosun<sup>1</sup> and Olajire Fagbola<sup>2</sup>

### ABSTRACT

#### Keywords:

Inorganic fertilizer  
Jute mallow  
Recycling waste  
Sustainable production



Jute mallow is a crop with versatile applications in industries and as a food source. Low yield resulting from land degradation has necessitated the use of cocoa pod husk as a nutrient source, although it may require inorganic fertilizers to enhance its efficiency. The aim was to determine the effects of Cocoa Pod Husk Powder (CPHP) and urea fertilizer on Jute mallow performance. In a repeated 3x3 factorial pot experiment, CPHP [0 ( $C_0$ ), 30 ( $C_{30}$ ), and 60 ( $C_{60}$ ) kg N ha<sup>-1</sup>] and urea fertilizer [0 ( $U_0$ ), 30 ( $U_{30}$ ), and 60 ( $U_{60}$ ) kg N ha<sup>-1</sup>] were evaluated on Jute growth, fresh and dry biomasses using a randomized complete block design with five replicates. Applying CPHP increased the growth parameters but reduced fresh and dry biomass of Jute mallow in both plantings. The plants treated with  $U_{60}$  had significantly higher fresh biomass than the control during the first planting, but were similar in the second planting. The sole CPHP and urea treatments performed better for the parameters observed. However,  $C_{30}U_{60}$  had similar fresh weights (11.14 and 11.40 g per plant) with  $C_0U_{60}$  (12.76 and 15.07 g per plant) during the first and second plantings, respectively. Jute mallow dry biomass ranged from 1.64 ( $C_{60}U_{30}$ ) to 2.12 ( $C_{30}U_{60}$ ) g per plant and differed significantly between  $C_0U_{30}$  (1.30 g per plant) and  $C_0U_{60}$  (3.00 g per plant) during the first and second plantings, respectively. Cocoa pod husk powder at 30 kg N combined with urea at 60 kg N ha<sup>-1</sup> is recommended for improving crop and soil quality.

### RESUMEN

#### Palabras clave:

Fertilizante inorgánico  
Malva de yute  
Reciclaje de residuos  
Producción sostenible

El jute mallow es un cultivo con aplicaciones versátiles en industrias y como fuente de alimento. El bajo rendimiento resultante de la degradación del suelo ha hecho necesario el uso de cáscaras de mazorcas de cacao como fuente de nutrientes, aunque puede requerir fertilizantes inorgánicos para mejorar su eficiencia. Este estudio determinó los efectos del polvo de cáscara de mazorca de cacao (CPHP) y el fertilizante de urea en el rendimiento del jute mallow. En un experimento repetido en macetas con un diseño factorial 3x3, se evaluaron el CPHP [0 ( $C_0$ ), 30 ( $C_{30}$ ) y 60 ( $C_{60}$ ) kg N ha<sup>-1</sup>] y el fertilizante de urea [0 ( $U_0$ ), 30 ( $U_{30}$ ) y 60 ( $U_{60}$ ) kg N ha<sup>-1</sup>] sobre el crecimiento del jute, biomasa fresca y seca utilizando un diseño de bloques completamente al azar con cinco réplicas. La aplicación de CPHP aumentó los parámetros de crecimiento, pero redujo la biomasa fresca y seca del jute mallow en ambas siembras. Las plantas tratadas con  $U_{60}$  tuvieron una biomasa fresca significativamente más alta que el control durante la primera siembra, pero fueron similares en la segunda siembra. Los tratamientos de CPHP y urea por sí solos tuvieron un mejor rendimiento en los parámetros observados. Sin embargo,  $C_{30}U_{60}$  tuvo pesos frescos similares (11.14 y 11.40 g por planta) con  $C_0U_{60}$  (12.76 y 15.07 g por planta) durante las primeras y segundas siembras, respectivamente. La biomasa seca de la malva de yute varió de 1.64 ( $C_{60}U_{30}$ ) a 2.12 ( $C_{30}U_{60}$ ) g por planta y diferenció significativamente entre  $C_0U_{30}$  (1.30 g por planta) y  $C_0U_{60}$  (3.00 g por planta) durante las primeras y segundas siembras, respectivamente. Se recomienda el polvo de cáscara de vaina de cacao a 30 kg N combinado con urea a 60 kg N ha<sup>-1</sup> para mejorar la calidad del cultivo y del suelo.

<sup>1</sup>Department of Crop and Horticultural Sciences, Agronomy Building, University of Ibadan, Ibadan, Nigeria. [tb.akinrinola@gmail.com](mailto:tb.akinrinola@gmail.com) , [earlpappi@gmail.com](mailto:earlpappi@gmail.com) 

<sup>2</sup>Department of Soil Resources Management, Agronomy Building, University of Ibadan, Ibadan, Nigeria. [Fagbola1111@gmail.com](mailto:Fagbola1111@gmail.com) 

\*Corresponding author

**C***orchorus olitorius* (L) called Jute mallow, is the most versatile natural herb of the family Malvaceae valued for its eco-friendly fiber in textile, packaging, and agriculture (Vaishnavi and Krishnaveni 2022). It is a biodegradable, low-carbon, and renewable source that offers a natural alternative to synthetic fiber (Maiti et al. 2022). The leaves and young stems can be consumed by boiling or added to soup (Rumanuzzaman et al. 2024). Economically, Jute mallow provides livelihood opportunities for millions of farmers in developing countries through cultivation, processing, and manufacturing, consequently, boosting export earnings and employment generation (Shahinur et al. 2022). Jute cultivation also enhances soil health by enriching organic matter in the soil, suppressing weed growth, and reducing pest and disease occurrence in subsequent crops through natural rotation (Shahinur et al. 2022).

Jute cultivation requires nitrogen, phosphorus, and potassium for optimal growth and yield. Nitrogen is essential for vegetative growth, phosphorus promotes root development, and potassium enhances plant vigor and disease resistance (Govindasamy et al. 2023). In addition, Jute also requires micronutrients, all of which are often deficient in tropical soils (Rumanuzzaman et al. 2024). Consequently, maintaining proper soil fertility status is crucial for sustainable Jute cultivation. Nutrient deficiencies can negatively affect Jute growth and yield, especially in tropical soils that rapidly lose nutrient status and are devoid of soil organic matter due to high rates of weathering and intensive rainfall coupled with continuous cropping (Zhao and Riaz 2024). Thus, fertilizer application is crucial for successful Jute mallow cultivation.

Inorganic and organic fertilizers applied solely have significantly contributed to Jute mallow production (Sahoo et al. 2023). However, limited attention is given to inorganic fertilizers due to their effect on crop quality reduction and adverse impact on soil quality and the ecosystem (Zhao and Riaz 2024). Organic fertilizers, including animal manure, green manure, compost, and crop residues, contribute to nutrient cycling and improve soil organic carbon, which are critical for sustaining Jute mallow yield in tropical soils (Sahoo et al. 2023). They also help lower greenhouse gas emissions than synthetic fertilizers through carbon sequestration during production and application (He et al. 2023). Organic fertilizers release nutrients slowly over

time as they undergo decomposition, reducing the risk of nutrient leaching and run-off (Anas et al. 2020). The slow-release nutrients, in alignment with the plant growth requirements, minimize nutrient wastage and improve nutrient use efficiency (Anas et al. 2020). Poultry manure and cow dung applications have the problem of transporting large quantities to the farm and are often not in sufficient quantity (Liu and Wang 2020). Therefore, the need for alternative sources for improving crop performance within the farmers fields.

The use of cocoa pod husk powder (CPHP) as an organic manure for vegetable production serves as a way of recycling farm waste and reducing the build-up of black pod disease in cocoa plantations (Fidelis and Rajashekhar Rao 2017). Cocoa pod husk (CPH) is a by-product obtained after extracting cocoa beans and consists of the outer shell of cocoa pods. Its nutrient composition can vary depending on cocoa variety, pod maturity, and processing methods. Generally, CPH contains significant amounts of organic matter, nitrogen, phosphorus, potassium, and other essential nutrients (Hougni et al. 2021). Cocoa pod husk is rich in organic matter, which contributes to improving soil structure, moisture retention, and nutrient-holding capacity. Its use as compost, biochar, ash, and powdery form for crop improvement are documented (Munongo et al. 2017; Doungous et al. 2018; Tamfuh et al. 2021; Kayode and Adeoye 2021). Like many other organic fertilizer sources, reports have shown that CPH is limited in the adequate quantity of N required for proper crop growth (Hougni et al. 2021).

Consequently, combining CPHP with urea demonstrates a renewed interest in integrating nutrient management strategies to increase crop production. Urea is the preferred and predominant source of N due to relatively higher nitrogen contents and low cost (Swify et al. 2024). Urea can be applied to increase crop yields, such as cereals, vegetables, and fruit trees (Anas et al. 2020). It can be applied as a top dressing, incorporated into the soil, or used in foliar sprays, providing flexibility in application methods (Swify et al. 2024). The excessive use of sole urea in crop production reportedly causes groundwater pollution and environmental hazards. However, the combination with organic sources of fertilizer limits negative effects on the environment (Swify et al. 2024). Its combination with organic fertilizers reduces the quantity



needed to achieve the desired nitrogen supply, minimizing transportation, storage, and application costs (Gheith et al. 2022). Composted CPH and urea combination improves cocoa performance (Doungous et al. 2018). The integrated application enhanced nutrient uptake and improved soil fertility, ultimately contributing to increased yield. Nevertheless, empirical evidence remains scarce regarding the effects of CPHP, either individually or in conjunction with urea, on the growth, development, and yield performance of short-duration, high-value crops such as jute (*Corchorus olitorius* L.). Accordingly, the present study sought to elucidate the impacts of CPHP, urea, and their interaction on the growth dynamics of jute.

## MATERIALS AND METHODS

### Experimental site

The experiments for the first and second studies were carried out in the screenhouse between April to June and June to August 2023 for the first and second plantings, respectively, at the Department of Crop and Horticultural Sciences, University of Ibadan, Ibadan, Nigeria. The coordinates of the screenhouse are latitude 7°27'6" N and longitude 3°53'46" E.

### Experimental design and treatments

Cocoa Pod Husk Powder (CPHP) at 0, 30, and 60 kg of N ha<sup>-1</sup> and urea at 0, 30, and 60 kg of N ha<sup>-1</sup> were evaluated in a 3×3 factorial experiment. The experimental design was a randomized complete block design and each treatment was replicated five times. Treatments include 0 CPHP × 0 urea (control), 0 CPHP × 30 urea, 0 CPHP × 60 urea, 30 CPHP × 0 urea, 30 CPHP × 30 urea, 30 CPHP × 60 urea, 60 CPHP × 0 urea, 60 CPHP × 30 urea, and 60 CPHP × 60 urea. The treatments were the same for the second planting. By implication, the CPHP was applied at 0, 7.13, and 14.27 g per pot of 4 kg soil, which were equivalent to 0, 3,567.18, and 7,134.36 kg ha<sup>-1</sup>, respectively. The urea levels were applied at 0, 0.13, and 0.26 g per pot of 4 kg soil, which amounted to 0, 65.22, and 130.44 kg ha<sup>-1</sup>.

### Soil sample collection and analysis

Topsoil was collected from the Department of Crop and Horticultural Sciences research field, University of Ibadan, Ibadan, Nigeria. The collected soil was thoroughly mixed for homogeneity, sieved with a 2 mm mesh, and air-dried. A soil sample from the mixed treatment was analyzed at

the Soil Service Laboratory, Department of Soil Resources Management, University of Ibadan, to determine its routine chemical and physical properties. Soil pH was measured using a glass electrode pH meter, while soil organic carbon was determined by the dichromate wet oxidation method of Walkley and Black (Poudel 2020). Macro-kjeldhal and Bray P-1 methods were used to determine the soil total N and available P contents, respectively (FAO 2021). The Ca and Mg were determined using the EDTA titration method (FAO 2020). Exchangeable K and Na were determined using an EEL flame photometer. The hydrometer method was used in determining the soil textural classification (Hossain et al. 2022).

### Analysis of cocoa pod husk powder

The cocoa husk ash was analyzed for nutrient content. Total nitrogen was measured using the Micro-Kjeldahl method. The other nutrients were assessed using a wet digestion technique (AOAC 1990). After digestion, the same methods applied to soil were used to evaluate P, K, Ca, and Mg.

### Material sources and collection

The materials used in the experiment included seeds obtained from the National Horticultural Research Institute (NIHORT), Ibadan, Nigeria. The CPHP was collected from the Department of Crop and Horticultural Sciences. Additionally, the urea used in the study was sourced from an agricultural enterprise in Bodija, Ibadan. The Department of Crop and Horticultural Sciences provided the black polyethylene bags of 45 pieces filled with 4 kg of soil, as a larger soil weight may offer more nutrients and obscure the true impact of experimental treatments. The polyethylene bags were labeled properly, based on the type and rate of treatment to be given to the soil sample for the experiment. There were nine treatments.

To ensure accurate measurement of all treatments, an electronic sensitive scale (Qun Ze High Precision Portable scale) was used. In the case of the CPHP treatments, it was added to the soil one week before the planting process in all the designated pots. After two weeks of planting, urea was added to the experimental pots where required, based on the treatment specifications. This sequential application of CPHP and urea allowed for proper nutrient management and ensured that the desired experimental conditions were achieved.

### Planting and establishment

Before sowing, the pots were appropriately spaced to ensure proper plant growth and development. In all treatment pots, Jute seeds treated with hot water were sown on the soil surface. Two seedlings were initially raised, then thinned to one each per pot 10 days after sowing (WAS). The sowing of seeds took place on 25th April 2023 and was followed by light irrigation to provide initial moisture. To ensure adequate moisture for the proper emergence and development of Jute roots, the pots were watered in the morning and evening every day. A measuring cylinder was used for watering, and an equal amount of water was provided to each pot. At the initial stage, 20 mm of water is added per day to ensure the surface of the soil is not dry and the volume increases to 100 mL with plant size increase. The consistent watering regimens were aimed at facilitating optimal moisture uptake and promoting the healthy growth of the Jute plants.

### Maintenance

One week after planting, thinning was conducted to minimize competition among the Jute plants for space, light, nutrients, and water. The most vigorous and healthy plant stands were carefully selected to remain in the experimental pots. Thinning was done in all pots to ensure optimal plant growth and development. Similarly, weed removal was performed to prevent the growth of unwanted and harmful plants that could compete with the Jute. Careful attention was given during the weeding process to minimize potential damage to the growing Jute stems and leaves. Weeds were hand-picked, and no chemical weed control methods were used.

### Data collection

Throughout the experiment, observations on plant height and stem diameter were measured, and the number of leaves was counted at 2, 3, 4, and 5 weeks after sowing (WAS). To obtain accurate measurements, a Vernier caliper was used to measure the stem diameter, and a flexible meter ruler was used to measure the height of the plants. At 6 WAS, the plant was harvested, and its fresh weights were taken using a sensitive scale. This was done before the plants start partitioning assimilates for flower and seed formation. Additionally, the harvested plants were oven-dried and the dry biomass weights were taken.

### Statistical analysis

The agronomic data collected were analyzed using GenStat

version 8.1. Means that showed significant differences were separated using Duncan's Multiple Range Test at a probability level of 0.05

## RESULTS AND DISCUSSION

### Chemical and particle size analysis of the soil at the experimental site

Chemical analysis of the soil at the experimental site showed that the soil was neutral with a pH of 7.09 (Table 1). However, the total nitrogen content in the soil was 3.3 g kg<sup>-1</sup>. The potassium value was determined to be 0.36 cmol kg<sup>-1</sup>, while the available phosphorus content was 16.1 mg kg<sup>-1</sup>. The particle size result indicated the soil textural class was loamy sand. The study site soil has a nitrogen level below the critical level for Jute production (Huat et al. 2017). Considering the soil texture with a low soil organic matter content. Therefore, there is an urgent need to increase the available nitrogen in the soil to ensure the establishment and production of Jute. Organic fertilizers are well-known for their beneficial effect on crop growth and development (Anas et al. 2020).

**Table 1.** Chemical and physical properties of the experimental soil.

Parameters	Values
Organic C (g kg <sup>-1</sup> )	30.08
Total N (g kg <sup>-1</sup> )	3.3
Available P (mg kg <sup>-1</sup> )	16.1
pH (H <sub>2</sub> O)	7.09
<b>Exchangeable bases (cmol kg<sup>-1</sup>)</b>	
K	0.36
Mg	0.83
Na	0.29
Ca	2.71
Exchangeable acidity	0.4
<b>Extractable micronutrients (mg kg<sup>-1</sup>)</b>	
Fe	92
Cu	1.35
Mn	76
Zn	1.86
<b>Textural class (g kg<sup>-1</sup>)</b>	
Sand	800
Silt	130
Clay	62
Textural class	Loamy sand

### Cocoa pod Husk powder properties

The chemical properties of the CPHP used revealed that the C: N ratio was 17.60, indicating an organic material with a low C: N ratio (Table 2). Health-conscious individuals

often prefer to consume farm produce cultivated using organic materials. These organic materials serve as valuable sources of nutrients for plants, enhancing the soil's

water-holding capacity and improving nutrient availability, thus creating favorable conditions for Jute root growth and nutrient uptake (Fidelis and Rajashekhar Rao 2017).

**Table 2.** Chemical properties of the cocoa pod husk powder used in the study.

Total N (%)	Organic C (%)	Total P (%)	Ca (%)	Mg (%)	K (%)	Na (%)	Mn (mg kg <sup>-1</sup> )	Fe (mg kg <sup>-1</sup> )	Zn (mg kg <sup>-1</sup> )
0.841	14.804	0.143	0.531	0.227	2.058	0.398	48.65	1467.25	64.55

### Effects of fertilizers on the height of Jute mallow plants

The CPHP application resulted in significant ( $P < 0.05$ ) variations among treatments in the height of the Jute plants during the first and second cropping (Table 3). In the first planting, the CPH-treated plants at 30 kg of N ha<sup>-1</sup> had significantly higher height than the control at 2 and 3 WAS. At 4 WAS, the CPHP application at 60 kg of N ha<sup>-1</sup> had significantly taller plants than the control, while the difference was not significant at 5 WAS. In the second planting, CPHP at 30 kg of N ha<sup>-1</sup> had significantly taller plants than the other treatments at 2 and 3 WAS, while the difference was not significant at 4 WAS. The control treatment had the lowest height throughout the

observation periods. These results suggest that CPHP at 30 kg N ha<sup>-1</sup> is effective for early growth, while higher rates (60 kg N ha<sup>-1</sup>) may be better for later stages. The taller the plants, the better the access to light, leading to more developed root systems for nutrient and water absorption (Rumanuzzaman et al. 2024). The results of the CPHP application demonstrated improvements in the plant height over the control. The nutrient composition of cocoa pod husk includes nitrogen, phosphorus, and potassium, which serve as a source of plant-available nutrients, supporting crop growth, development, and productivity (Munongo et al. 2017). These results were consistent with earlier reports that organic soil amendments improved crop growth parameters (Bai et al. 2023).

**Table 3.** Effect of Cocoa pod husk, urea, and their interactions on Jute plant height (cm).

	First planting (WAS)				Second planting (WAS)			
	2	3	4	5	2	3	4	5
<b>CPHP (kg of N ha<sup>-1</sup>)</b>								
0	8.13 <sup>b</sup>	15.97 <sup>b</sup>	24.13 <sup>b</sup>	37.40	8.67 <sup>b</sup>	16.44 <sup>c</sup>	25.44	39.56
30	11.23 <sup>a</sup>	21.86 <sup>a</sup>	29.53 <sup>ab</sup>	38.07	11.56 <sup>a</sup>	22.98 <sup>a</sup>	29.78	39.44
60	9.90 <sup>a</sup>	20.99 <sup>a</sup>	30.87 <sup>a</sup>	43.13	9.78 <sup>ab</sup>	19.83 <sup>b</sup>	29.44	42.33
SE	0.58	0.81	1.98	2.70	0.72	0.93	2.80	3.86
<b>Urea (kg of N ha<sup>-1</sup>)</b>								
0	8.57 <sup>b</sup>	18.56 <sup>b</sup>	26.33	38.07	8.61 <sup>b</sup>	19.22 <sup>ab</sup>	27.89	39.33
30	11.17 <sup>a</sup>	22.10 <sup>a</sup>	29.80	39.67	11.56 <sup>a</sup>	21.94 <sup>a</sup>	29.56	41.56
60	9.53 <sup>ab</sup>	18.16 <sup>b</sup>	28.40	40.87	9.83 <sup>ab</sup>	18.09 <sup>b</sup>	27.22	40.44
SE	0.58	0.81	1.98	2.70	0.72	0.93	2.80	3.87
<b>Interactions</b>								
C <sub>0</sub> U <sub>0</sub>	9.80 <sup>a-c</sup>	17.80 <sup>cd</sup>	24.60 <sup>ab</sup>	36.20	10.33 <sup>ab</sup>	17.67 <sup>cd</sup>	23.00	36.33
C <sub>0</sub> U <sub>30</sub>	6.20 <sup>d</sup>	13.70 <sup>e</sup>	22.20 <sup>b</sup>	34.40	6.33 <sup>c</sup>	14.50 <sup>d</sup>	25.33	34.67
C <sub>0</sub> U <sub>60</sub>	8.40 <sup>cd</sup>	16.40 <sup>de</sup>	25.60 <sup>ab</sup>	41.60	9.33 <sup>a-c</sup>	17.17 <sup>cd</sup>	28.00	47.67
C <sub>30</sub> U <sub>0</sub>	11.90 <sup>a</sup>	25.30 <sup>a</sup>	31.40 <sup>ab</sup>	37.80	12.00 <sup>a</sup>	25.50 <sup>a</sup>	30.33	39.00
C <sub>30</sub> U <sub>30</sub>	10.30 <sup>a-c</sup>	21.30 <sup>a-c</sup>	25.20 <sup>ab</sup>	35.00	9.83 <sup>a-c</sup>	23.17 <sup>ab</sup>	28.00	40.00

Table 3

	First planting (WAS)				Second planting (WAS)			
	2	3	4	5	2	3	4	5
<b>Interactions</b>								
C <sub>30</sub> U <sub>60</sub>	11.50 <sup>ab</sup>	18.98 <sup>cd</sup>	32.00 <sup>ab</sup>	41.40	12.83 <sup>a</sup>	20.27 <sup>bc</sup>	31.00	39.33
C <sub>60</sub> U <sub>0</sub>	11.80 <sup>a</sup>	23.20 <sup>ab</sup>	33.40 <sup>a</sup>	45.00	12.33 <sup>a</sup>	22.67 <sup>ab</sup>	35.33	49.33
C <sub>60</sub> U <sub>30</sub>	9.20 <sup>a-c</sup>	20.68 <sup>bc</sup>	31.60 <sup>ab</sup>	44.80	9.67 <sup>a-c</sup>	20.00 <sup>bc</sup>	30.33	43.33
C <sub>60</sub> U <sub>60</sub>	8.70 <sup>b-d</sup>	19.10 <sup>cd</sup>	27.60 <sup>ab</sup>	39.60	7.33 <sup>bc</sup>	16.83 <sup>cd</sup>	22.67	34.33
SE	1.00	1.41	3.43	4.68	1.25	1.61	4.85	6.69

CPHP = Cocoa Pod Husk Powder; WAS = Weeks After Sowing; CPHP at 0 (C<sub>0</sub>), 30 (C<sub>30</sub>) and 60 (C<sub>60</sub>) kg of N ha<sup>-1</sup>; Urea fertilizer at 0 (U<sub>0</sub>), 30 (U<sub>30</sub>) and 60 (U<sub>60</sub>) kg of N ha<sup>-1</sup>; Mean values within the same column and with similar letter(s) are not significantly ( $P < 0.05$ ) different, as determined by Duncan's Multiple Range Test.

Urea application at 30 kg of N ha<sup>-1</sup> resulted in significantly ( $P < 0.05$ ) higher plant height than the control in the second week of sowing in the first planting. At 3 WAS, the other treatments had significantly lower height than the effect of urea at 30 kg of N ha<sup>-1</sup>. The variations in plant height at 4 and 5 WAS were similar for the treatments. However, urea at 30 and 60 kg of N ha<sup>-1</sup> had the tallest plants at 4 and 5 WAS, respectively, while the control treatment had the shortest plants. At 2 and 3 WAS in the second planting, plants treated with urea at 30 kg of N ha<sup>-1</sup> were significantly taller than plants under the control and urea at 60 kg of N ha<sup>-1</sup>, respectively. Plant heights at 4 and 5 WAS were not significantly different but ranged from 27.22 (60 kg of N ha<sup>-1</sup>) to 29.56 cm (30 kg of N ha<sup>-1</sup>) and 39.33 (control) to 41.56 cm (30 kg of N ha<sup>-1</sup>), respectively. Urea fertilizer application at varying levels led to a significant increase in the observed growth parameters of Jute mallow, but the effect may be more pronounced early in growth. This is due to its high solubility in water, which allows for easy uptake by plant roots (Gheith et al. 2022). Urea fertilizer effectively ameliorates the nitrogen status in N-deficient soils, thereby increasing the available nitrogen required for cell mitosis at the meristem, causing stem height increase (Govindasamy et al. 2023; Swify et al. 2024). This conforms with Luo et al. (2020) report that improved N availability for crop uptake promotes plant height increase.

Cocoa pod husk powder and urea applications resulted in significantly ( $P < 0.05$ ) different Jute mallow heights in the first and second plantings (Table 3). The C<sub>60</sub>U<sub>30</sub> interaction resulted in the highest plant height at 2 and 3 WAS in the first planting. Also, C<sub>60</sub>U<sub>30</sub> significantly

increased Jute height compared to C<sub>0</sub>U<sub>30</sub> at 4 WAS, while the treatments were all similar at 5 WAS. During the second planting, the C<sub>30</sub>U<sub>60</sub> and C<sub>30</sub>U<sub>0</sub> had the tallest plants at 2 and 3 WAS, respectively, while C<sub>0</sub>U<sub>30</sub> had the shortest plants. This indicated that soil physical property improvement through CPHP application was a major factor for height increase. The CPHP and urea interactions did not significantly influence variation among the treatments at 4 and 5 WAS. However, the heights ranged from 23.00 (C<sub>0</sub>U<sub>30</sub>) to 35.33 cm (C<sub>60</sub>U<sub>0</sub>) and 34.33 (C<sub>60</sub>U<sub>60</sub>) to 49.33 cm (C<sub>60</sub>U<sub>0</sub>) at 4 and 5 WAS, respectively. Integrating organic and inorganic fertilizers is a strategy to promote plant growth and maintain soil health (Bai et al. 2023; Akinrinola and Ojo 2024). However, the finding in this study did not conform to this assertion, in that the sole CPHP treatments had taller plants with the increase in application levels. These results suggest CPHP is more effective than urea in promoting Jute height, which could be due to improved nutrient supply and soil physical condition, as supported by Doungous et al. (2018).

#### Effects of fertilizers on the stem diameter of Jute

The effects of CPH, urea fertilizers, and their combinations on Jute stem diameter showed similar responses during the first and second plantings (Table 4). At 2 and 3 WAS, CPHP applications at 30 kg of N ha<sup>-1</sup> and 60 kg of N ha<sup>-1</sup> significantly ( $P < 0.05$ ) increased Jute mallow stem diameter compared to the 0 kg of N ha<sup>-1</sup> during the first planting. There was no significant difference in stem diameter at 4 WAS, while CPHP at 60 kg of N ha<sup>-1</sup> significantly improved stem diameter compared to the other treatments at 5 WAS.

During the second planting, CPHP applications at 30 and 60 kg of N ha<sup>-1</sup> significantly increased Jute stem diameter at 2 and 5 WAS, respectively, compared to the control. However, the variations among treatments at 3 and 4 WAS were nonsignificant. This finding conformed with Tamfuh et al. (2021) that applying CPH resulted in the stem diameter increase in okra. The influence of CPH powder could be attributed to the availability of assimilates that encourage an increase in cell division or enlargement of the lateral meristematic tissue, thus resulting in the thickness of plants' stems.

Jute plants treated with urea were not significantly ( $P < 0.05$ ) different throughout the observation periods during both plantings (Table 4). This observation suggests that urea has a weak influence on stem diameter. However, urea

treatment at 30 kg of N ha<sup>-1</sup> had relatively higher stem diameters during observation periods. These results implied that urea application at 30 kg N ha<sup>-1</sup> is sufficient to promote stem diameter, but increasing the level to 60 kg N ha<sup>-1</sup> offers little additional benefit, possibly due to nutrient saturation or allocation to other growth parameters. This assertion supported Luo et al. (2020) report that the response to nitrogen increase is minimal after the optimum plant requirement.

At 2, 3, and 5 WAS during the first planting, there were significant differences among fertilizer combinations. The plants treated with C<sub>30</sub>U<sub>0</sub> had the highest stem diameter at 2 WAS, while C<sub>30</sub>U<sub>30</sub>, C<sub>60</sub>U<sub>30</sub>, and C<sub>60</sub>U<sub>0</sub> treatments had higher values at 3 WAS. At 5 WAS, C<sub>60</sub>U<sub>60</sub>-treated plants had the highest stem diameter. During the second planting,

**Table 4.** Effect of cocoa pod husk and urea applications on Jute stem diameter (cm).

	First planting (WAS)				Second planting (WAS)			
	2	3	4	5	2	3	4	5
<b>CPHP (kg of N ha<sup>-1</sup>)</b>								
0	0.18 <sup>b</sup>	0.25 <sup>b</sup>	0.24	0.32 <sup>b</sup>	0.18 <sup>b</sup>	0.26	0.26	0.33 <sup>b</sup>
30	0.22 <sup>a</sup>	0.27 <sup>a</sup>	0.27	0.35 <sup>b</sup>	0.22 <sup>a</sup>	0.27	0.27	0.35 <sup>ab</sup>
60	0.21 <sup>a</sup>	0.27 <sup>a</sup>	0.28	0.41 <sup>a</sup>	0.20 <sup>ab</sup>	0.27	0.27	0.40 <sup>a</sup>
SE	0.01	0.01	1.14	0.02	0.01	0.01	0.01	0.02
<b>Urea (kg of N ha<sup>-1</sup>)</b>								
0	0.19	0.27	0.25	0.34	0.19	0.27	0.27	0.35
30	0.21	0.27	0.27	0.37	0.22	0.27	0.27	0.40
60	0.19	0.26	0.26	0.36	0.20	0.26	0.26	0.33
SE	0.01	0.01	1.14	0.01	0.01	0.01	0.01	0.02
<b>Interactions</b>								
C <sub>0</sub> U <sub>0</sub>	0.19 <sup>b-e</sup>	0.26 <sup>ab</sup>	0.21	0.35 <sup>a-c</sup>	0.19 <sup>a-c</sup>	0.27	0.27	0.38 <sup>a-c</sup>
C <sub>0</sub> U <sub>30</sub>	0.15 <sup>e</sup>	0.25 <sup>b</sup>	0.25	0.28 <sup>c</sup>	0.15 <sup>c</sup>	0.25	0.25	0.28 <sup>c</sup>
C <sub>0</sub> U <sub>60</sub>	0.19 <sup>c-e</sup>	0.25 <sup>b</sup>	0.26	0.34 <sup>a-c</sup>	0.21 <sup>ab</sup>	0.27	0.27	0.33 <sup>a-c</sup>
C <sub>30</sub> U <sub>0</sub>	0.23 <sup>a</sup>	0.27 <sup>ab</sup>	0.27	0.37 <sup>ab</sup>	0.23 <sup>a</sup>	0.27	0.27	0.39 <sup>a-c</sup>
C <sub>30</sub> U <sub>30</sub>	0.21 <sup>a-d</sup>	0.28 <sup>a</sup>	0.28	0.35 <sup>a-c</sup>	0.20 <sup>ab</sup>	0.28	0.28	0.36 <sup>a-c</sup>
C <sub>30</sub> U <sub>60</sub>	0.22 <sup>a-c</sup>	0.26 <sup>ab</sup>	0.26	0.32 <sup>bc</sup>	0.23 <sup>a</sup>	0.26	0.26	0.31 <sup>bc</sup>
C <sub>60</sub> U <sub>0</sub>	0.22 <sup>ab</sup>	0.28 <sup>a</sup>	0.28	0.40 <sup>ab</sup>	0.23 <sup>a</sup>	0.29	0.29	0.43 <sup>a</sup>
C <sub>60</sub> U <sub>30</sub>	0.21 <sup>a-d</sup>	0.28 <sup>a</sup>	0.28	0.41 <sup>a</sup>	0.21 <sup>ab</sup>	0.28	0.28	0.40 <sup>ab</sup>
C <sub>60</sub> U <sub>60</sub>	0.18 <sup>de</sup>	0.26 <sup>ab</sup>	0.27	0.42 <sup>a</sup>	0.17 <sup>bc</sup>	0.24	0.25	0.36 <sup>a-c</sup>
SE	0.01	0.01	1.98	0.03	0.01	0.01	0.01	0.04

CPHP = Cocoa Pod Husk Powder; WAS = Weeks After Sowing; CPHP at 0 (C<sub>0</sub>), 30 (C<sub>30</sub>) and 60 (C<sub>60</sub>) kg of N ha<sup>-1</sup>; Urea fertilizer at 0 (U<sub>0</sub>), 30 (U<sub>30</sub>) and 60 (U<sub>60</sub>) kg of N ha<sup>-1</sup>; Mean values within the same column and with a similar letter(s) are not significantly ( $P < 0.05$ ), as determined by Duncan's Multiple Range Test.



CPHP and urea interactions significantly improved Jute stem diameter at 2 and 5 WAS, with  $C_{30}U_{60}$  having the highest value among the interactions. The  $C_0U_{30}$  consistently had the lowest values during the observation period. These findings at the last observation before harvest were inconsistent with Kayode and Adeoye's (2021) report that CPHP combined with NPK fertilizer further increased okra stem diameter. While the first planting supported Kayode and Adeoye's (2021) report, the second planting was against it, though the readings were similar. It can be inferred that the attributes of CPHP as fertilizer were sufficient to supply the required Jute mallow stem increase. The low responses from urea application as compared to its combination with CPHP may reflect the absence of complementary nutrients in urea compared to CPHP.

### Effects of fertilizers on the number of leaves

During the first planting, the CPHP application at 30 kg of N ha<sup>-1</sup> significantly ( $P < 0.05$ ) increased the number of leaves in Jute mallow compared to the control at 2 and 3 WAS (Table 5). At 4 WAS, 60 kg of N ha<sup>-1</sup> of CPHP had a significantly higher number of leaves than the control, while the variation among treatments was not significantly different at 5 WAS. A similar trend of observations was made in the second planting, except that the variations at 4 WAS were not significantly different. The number of leaves produced by a plant indicates its light interception ability and the net carbon gain it can achieve (Luo et al. 2020). It is an indicator often used interchangeably with leaf area to monitor a plant's growth rate. During the two plantings, CPHP-treated plants had more numbers of leaves than the control treatment.

**Table 5.** Influence of Cocoa pod husk, urea, and interactions on Jute number of leaves.

	First planting (WAS)				Second planting (WAS)			
	2	3	4	5	2	3	4	5
<b>CPHP (kg of N ha<sup>-1</sup>)</b>								
0	7.93 <sup>b</sup>	13.07 <sup>b</sup>	12.20 <sup>b</sup>	15.40	8.11 <sup>b</sup>	12.44 <sup>b</sup>	11.56	14.56
30	9.00 <sup>a</sup>	14.60 <sup>a</sup>	13.20 <sup>ab</sup>	16.80	9.11 <sup>a</sup>	14.56 <sup>a</sup>	12.89	16.22
60	8.60 <sup>ab</sup>	14.13 <sup>ab</sup>	14.27 <sup>a</sup>	16.87	8.67 <sup>ab</sup>	13.44 <sup>ab</sup>	13.56	15.67
SE	0.35	0.41	0.45	0.59	0.37	0.48	0.58	0.79
<b>Urea (kg of N ha<sup>-1</sup>)</b>								
0	8.00	13.27	13.07	16.07	8.00	12.78	12.56	15.22
30	8.93	14.13	13.33	16.13	9.11	14.00	12.78	15.22
60	8.60	14.40	13.27	16.87	8.78	13.67	12.67	16.00
SE	0.35	0.41	0.45	0.60	0.38	0.48	0.58	0.79
<b>Interactions</b>								
$C_0U_0$	8.60 <sup>ab</sup>	14.00 <sup>ab</sup>	12.60 <sup>a-c</sup>	15.20 <sup>b</sup>	8.67 <sup>a-d</sup>	13.00 <sup>ab</sup>	11.33	13.00
$C_0U_{30}$	7.20 <sup>b</sup>	12.40 <sup>b</sup>	12.20 <sup>bc</sup>	15.40 <sup>ab</sup>	7.00 <sup>d</sup>	12.33 <sup>b</sup>	12.33	15.67
$C_0U_{60}$	8.00 <sup>ab</sup>	12.80 <sup>b</sup>	11.80 <sup>c</sup>	15.60 <sup>ab</sup>	8.67 <sup>a-d</sup>	12.00 <sup>b</sup>	11.00	15.00
$C_{30}U_0$	9.20 <sup>a</sup>	15.00 <sup>a</sup>	13.60 <sup>a-c</sup>	17.40 <sup>ab</sup>	9.00 <sup>a-c</sup>	15.33 <sup>ab</sup>	13.33	17.00
$C_{30}U_{30}$	8.40 <sup>ab</sup>	13.40 <sup>ab</sup>	12.40 <sup>a-c</sup>	16.20 <sup>ab</sup>	8.00 <sup>b-d</sup>	13.00 <sup>ab</sup>	11.67	15.00
$C_{30}U_{60}$	9.40 <sup>a</sup>	15.40 <sup>a</sup>	13.60 <sup>a-c</sup>	16.80 <sup>ab</sup>	10.33 <sup>a</sup>	15.33 <sup>a</sup>	13.67	16.67
$C_{60}U_0$	9.00 <sup>a</sup>	13.40 <sup>b</sup>	13.80 <sup>a-c</sup>	15.80 <sup>ab</sup>	9.67 <sup>ab</sup>	13.67 <sup>ab</sup>	13.67	15.67
$C_{60}U_{30}$	8.40 <sup>ab</sup>	14.00 <sup>ab</sup>	14.60 <sup>a</sup>	16.60 <sup>ab</sup>	9.00 <sup>a-c</sup>	13.00 <sup>ab</sup>	13.67	15.00
$C_{60}U_{60}$	8.40 <sup>ab</sup>	15.00 <sup>a</sup>	14.40 <sup>ab</sup>	18.20 <sup>a</sup>	7.33 <sup>cd</sup>	13.67 <sup>ab</sup>	13.33	16.33
SE	0.60	0.71	0.78	1.03	0.65	0.83	1.01	1.37

CPHP = Cocoa Pod Husk Powder; WAS = Weeks After Sowing; CPHP at 0 ( $C_0$ ), 30 ( $C_{30}$ ) and 60 ( $C_{60}$ ) kg of N ha<sup>-1</sup>; Urea fertilizer at 0 ( $U_0$ ), 30 ( $U_{30}$ ) and 60 ( $U_{60}$ ) kg of N ha<sup>-1</sup>; Mean values within the same column and with similar letter(s) are not significantly ( $P < 0.05$ ) different, as determined by Duncan's Multiple Range Test.

All urea fertilizer treatments showed a nonsignificant difference in the number of leaves throughout the observation period in both plants (Table 5). However, plants treated with urea fertilizer at 30 kg of N ha<sup>-1</sup> and 60 kg of N ha<sup>-1</sup> relatively had higher values in the first planting. The differences among treatments were not significant during the second planting. However, urea-treated plants at 30 kg of N ha<sup>-1</sup> had a relatively higher number of leaves at 2, 3, and 4 WAS, while the control had the lowest values. This observation possibly suggests nutrient allocation to other traits. The results did not justify the cost of increasing soil nitrogen from urea fertilizer, to support the increase in the number of leaves in Jute mallow as reported by Gheith et al. (2022).

The interactions between CPHP and urea indicated significant differences among treatments for the number of leaves during the first planting (Table 5). The highest number of leaves at 2 and 3 WAS were observed in plants treated with C<sub>30</sub>U<sub>60</sub>, while C<sub>60</sub>U<sub>30</sub> and C<sub>30</sub>U<sub>0</sub> had the highest values at 4 and 5 WAS, respectively. During the second planting, the plants treated with C<sub>30</sub>U<sub>60</sub> had a significantly higher number of leaves than C<sub>0</sub>U<sub>30</sub> at 2 and 3 WAS. However, the differences at 4 and 5 WAS were nonsignificant. The consistency and similarity in the values observed for combined CPHP and urea fertilizers during the two plantings consolidated the reports of earlier studies (Doungous et al. 2018; Kayode and Adeoye 2021). However, the consistent low response from C<sub>0</sub>U<sub>30</sub> aligns with Table 1, substantiating that urea was inefficient without CPHP,

probably due to poor uptake. The combined CPHP and urea fertilizer application during the two plantings promoted the Jute mallow plant's growth rate and soil health condition more than the control. These findings suggest moderate CPHP levels optimize this parameter, but high urea levels may not justify additional costs, given their minimal influence.

### Effects of fertilizers on the fresh biomass and dry biomass at harvest

The responses observed for plant height, stem diameter, and number of leaves in Jute mallow plants were similar for CPHP, urea, and their interactions, except for slight variations during observation periods. These responses result from variations in soil health, cumulated to determine the fresh and dry biomasses accumulated during growth periods. The effect of CPHP treatments on Jute mallow fresh weight at harvest was nonsignificant during the two plantings (Table 6). However, the fresh weight ranges from 9.76 g (30 kg of N ha<sup>-1</sup>) to 11.16 g (0 kg of N ha<sup>-1</sup>) and from 10.03 g (30 kg of N ha<sup>-1</sup>) to 11.81 g (0 kg of N ha<sup>-1</sup>) during the first and second plantings, respectively. Similarly, the plants under the control treatment had significantly higher dry biomass yields than those under CPHP at 30 and 60 kg N ha<sup>-1</sup> during the first planting (Table 6). The reduced biomass seen at higher CPHP levels (30 and 60 kg N ha<sup>-1</sup>) may indicate nutrient imbalances or toxicity, especially because of the high Fe content in the material. Rout and Sahoo (2015) reported that organic manure could be a source through which heavy metals are deposited in the soil, thereby leading to nutrient imbalance.

**Table 6.** Effect of Cocoa pod husk and urea on fresh and dry biomass at harvest.

	First planting (g per plant)		Second planting (g per plant)	
	Fresh weight	Dry weight	Fresh weight	Dry weight
<b>CPHP (kg of N ha<sup>-1</sup>)</b>				
0	11.16	2.62 <sup>a</sup>	11.81	2.73 <sup>a</sup>
30	9.79	1.86 <sup>b</sup>	10.03	1.70 <sup>b</sup>
60	9.96	1.93 <sup>b</sup>	10.36	1.88 <sup>ab</sup>
SE	0.71	0.22	0.84	0.31
<b>Urea (kg of N ha<sup>-1</sup>)</b>				
0	9.45 <sup>b</sup>	2.03	9.86	1.98
30	9.86 <sup>ab</sup>	2.16	10.36	2.09
60	11.60 <sup>a</sup>	2.23	11.99	2.24
SE	0.72	0.22	0.84	0.32

Table 6

	First planting (g per plant)		Second planting (g per plant)	
	Fresh weight	Dry weight	Fresh weight	Dry weight
<b>Interactions</b>				
C <sub>0</sub> U <sub>0</sub>	11.32 <sup>ab</sup>	2.56	10.90 <sup>a-c</sup>	2.27 <sup>ab</sup>
C <sub>0</sub> U <sub>30</sub>	9.40 <sup>a-c</sup>	2.68	9.47 <sup>bc</sup>	2.93 <sup>ab</sup>
C <sub>0</sub> U <sub>60</sub>	12.76 <sup>a</sup>	2.62	15.07 <sup>a</sup>	3.00 <sup>a</sup>
C <sub>30</sub> U <sub>0</sub>	7.36 <sup>c</sup>	1.70	7.87 <sup>c</sup>	1.70 <sup>ab</sup>
C <sub>30</sub> U <sub>30</sub>	10.88 <sup>a-c</sup>	1.76	10.83 <sup>a-c</sup>	1.30 <sup>b</sup>
C <sub>30</sub> U <sub>60</sub>	11.14 <sup>ab</sup>	2.12	11.40 <sup>a-c</sup>	2.10 <sup>ab</sup>
C <sub>60</sub> U <sub>0</sub>	10.90 <sup>a-c</sup>	2.22	12.30 <sup>ab</sup>	2.30 <sup>ab</sup>
C <sub>60</sub> U <sub>30</sub>	8.08 <sup>bc</sup>	1.64	9.27 <sup>bc</sup>	1.70 <sup>ab</sup>
C <sub>60</sub> U <sub>60</sub>	10.90 <sup>a-c</sup>	1.94	9.50 <sup>bc</sup>	1.63 <sup>ab</sup>
SE	1.24	0.38	1.45	0.54

CPHP = Cocoa Pod Husk Powder; CPHP at 0 (C<sub>0</sub>), 30 (C<sub>30</sub>) and 60 (C<sub>60</sub>) kg of N ha<sup>-1</sup>; Urea fertilizer at 0 (U<sub>0</sub>), 30 (U<sub>30</sub>) and 60 (U<sub>60</sub>) kg of N ha<sup>-1</sup>; Mean values within the same column and with similar letter(s) are not significantly ( $P < 0.05$ ) different, as determined by Duncan's Multiple Range Test.

During the second planting, however, the control treatment had significantly higher dry biomass than the CPHP treatment at 30 kg of N ha<sup>-1</sup> but was comparable with the 60 kg of N ha<sup>-1</sup> treated plants. The results of the CPHP application demonstrated through the improvements in the plant height, stem diameter, and number of leaves over the control, consolidated the accumulation of photosynthates for growth and development. The nutrient-rich profile of CPHP supported their growth, development, and productivity (Munongo et al. 2017). These results were consistent with earlier reports that organic soil amendments improved crop growth parameters (Kayode and Adeoye 2021; Bai et al. 2023). The contribution of CPHP as an organic amendment in crop growth enhancement is achieved through the improvement in soil structure, crop nutrition, and an increase in microbial diversity and activities (Hougni et al. 2021). The results showed that CPHP at 30 kg of N ha<sup>-1</sup> supported early growth (2 and 4 WAS), while 60 kg of N ha<sup>-1</sup> was better at 4 and 5 WAS. Songsong et al. (2019) suggest that at the early stage of development, the higher level promoted higher microbial diversity that led to the immobilization of available nutrients for plant growth. At the lower level of the CPHP application, soil microbes were less active, thus causing minimal nutrient immobilization, thereby promoting growth (Songsong et al. 2019). This must have accounted for the improvement in the observed growth parameters after 3 WAS. The higher nitrogen from

CPHP resulted in reduced biomass accumulation, possibly due to excessive microbial activities promoted rather than at the expense of biomass increase. This outcome warrants further investigation into soil dynamics or plant uptake efficiency. High Fe could have limited the plant's ability to accumulate assimilates, leading to lowered fresh and dry biomass yields (Rout and Sahoo 2015).

The response of Jute mallow to urea application at 60 kg of N ha<sup>-1</sup> significantly ( $P < 0.05$ ) increased the fresh weight in Jute mallow compared to the control during the first planting. Jute mallow fresh weight ranged from 9.86 to 11.99 g per plant for plants treated under the control and urea at 60 kg of N ha<sup>-1</sup>, respectively. However, the variation was not significantly different during the second planting. Also, the variations in dry biomass among plants treated with urea fertilizer were not significantly different during the first and second plantings. However, it ranged from 2.03 to 2.23 g per plant and 1.98 to 2.24 g per plant for the control and urea application at 60 kg of N ha<sup>-1</sup> during the first and second plantings, respectively. Applying urea fertilizer encourages biomass accumulation due to its high solubility in water, which allows for easy uptake by plant roots (Gheith et al. 2022). Urea fertilizer effectively ameliorates the nitrogen status in N-deficient soils, thereby increasing the available nitrogen to improve crop performance (Govindasamy et al. 2023; Swify et



al. 2024). Urea is a concentrated source of nitrogen, an essential nutrient for plant growth, chlorophyll synthesis, and protein production. Therefore, adequate nitrogen supply from urea increases shoot and root growth, resulting in enhanced plant biomass production (Huat et al. 2017; Akinrinola and Ojo 2024). This report is substantiated when a higher level of urea fertilizer application (60 kg of N ha<sup>-1</sup>) did not further increase the response of Jute than the (30 kg of N ha<sup>-1</sup>), except for plant height. This suggests that excessive nitrogen application through urea may have caused nutrient imbalance or toxicity, thereby reducing photoassimilate accumulation. These findings are consistent with the report of Swify et al. (2024), which indicated that higher rates of urea fertilization can further enhance maize yield.

The plants treated with C<sub>0</sub>U<sub>60</sub> had significantly higher fresh weight compared to C<sub>30</sub>U<sub>0</sub> and C<sub>60</sub>U<sub>30</sub> treatments during the first planting. However, C<sub>0</sub>U<sub>60</sub> treatment significantly increased Jute mallow fresh weight more than C<sub>0</sub>U<sub>30</sub>, C<sub>30</sub>U<sub>0</sub>, C<sub>60</sub>U<sub>30</sub>, and C<sub>60</sub>U<sub>60</sub> during the second planting. Furthermore, the improvement in dry biomass at harvest for CPHP and urea was not significant during the first planting but ranged from 1.64 (C<sub>60</sub>U<sub>30</sub>) to 2.68 g per plant (C<sub>0</sub>U<sub>30</sub>). During the second planting, C<sub>30</sub>U<sub>30</sub>-treated plants had significantly lower dry biomass than C<sub>0</sub>U<sub>60</sub>, while other treatments were similar. Among the interactions, the plants treated with individual applications of CPHP and urea indicated better growth. However, this tended to be at par with the combined CPHP and urea during the first and second plantings in the study. This study conforms to Govindasamy et al. (2023) and He et al. (2023), who report that the use of sole organic or inorganic sources is being less recognized because of their environmental impact on climate change and socio-economic implications. Combining CPHP at 60 kg of N ha<sup>-1</sup> × urea at 30 kg of N ha<sup>-1</sup> yielded the highest, surpassing the other treatments. This may be due to CPHP, an organic fertilizer that slowly mineralizes nutrients in the soil, promoting rapid growth. As a result, the development of short-duration crops like Jute mallow may be at a disadvantage. Proper application level and concise timing are crucial to maximize crop response and achieve optimal yields (Dhakal and Lange 2021). The relatively reduced response from the other CPHP and urea interactions demonstrated that the release of nutrients immobilized by microbes did not coincide with the need for crops for nutrients to increase growth.

In contrast, longer-duration crops like maize may benefit more from CPHP as a fertilizer. Additionally, the microbes found in the soil must have prioritized the mineralization of nutrients in CPHP, thereby influencing the mineralization rate of existing mineral nutrients in the soil. This ultimately leads to the reduced effectiveness of the CPHP treatments. However, the low dry weight with high CPHP levels may indicate nutrient imbalance, luxury consumption, or water retention rather than productive growth. The response of Jute mallow to C<sub>30</sub>U<sub>60</sub> indicated the level at which there was a balance in the spontaneous supply of the available nutrients for Jute growth and the microbial nutrient demand. The substitution of N in the CPHP at 30 kg of N ha<sup>-1</sup> with urea fertilizer must have encouraged better Jute performance than the other interactions. This result is supported by He et al. (2023) report, that maize and wheat performed better when N in organic and inorganic fertilizers was substituted. Also, Doungous et al. (2018) reported improved *Theobroma cacao* seedlings performance due to CPH compost and urea fertilizer application. This substitution of inorganic N with organic sources would minimize the pressurized growth induced by chemical fertilizers and mitigate their negative effects on the environment, which causes global warming. Similarly, the challenges of CPHP that limit crop growth and development are overcome, thus creating an avenue to manage the waste from cocoa production.

## CONCLUSION

Applying cocoa pod husk powder increased the growth parameters but reduced Jute mallow fresh and dry biomass during the first and second plantings. Response of Jute mallow plants to urea fertilizer was highest at 60 kg of N ha<sup>-1</sup>. Although the individual applications of cocoa pod husk powder and urea treatments performed better for the parameters observed, their combinations were comparable. The treatment of cocoa pod husk powder at 30 kg of N ha<sup>-1</sup> × urea at 60 kg of N ha<sup>-1</sup> performed better in terms of growth and yield parameters. Consequently, cocoa pod husk powder at 30 kg of N ha<sup>-1</sup> with urea at 60 kg of N ha<sup>-1</sup> was suggested for promoting Jute mallow performance. For further research, the nutrient release dynamics of cocoa pod husk powder and its effects on soil physical, chemical, and biological properties could explain the variations observed and should be considered.

## CONFLICT OF INTEREST

The authors have no conflict of interest to declare.

## REFERENCES

- Akinrinola TB and Ojo AB (2024) Radish Response to cocoa pod husk and urea fertilizer applications. *Agricultura* 131(3-4): 106-122.
- Anas M, Liao F, Verma KK, Sarwar MA, Mahmood A et al (2020) Fate of nitrogen in agriculture and environment: Agronomic, eco-physiological and molecular approaches to improve nitrogen use efficiency. *Biology Research* 53: 47. <https://doi.org/10.1186/s40659-020-00312-4>
- AOAC - Association of Official Agricultural Chemists (1990) Official methods of analysis. 15th edition, Association of Official Analytical Chemist, Washington DC. 771 p. <https://law.resource.org/pub/us/cfr/ibr/002/aoac.methods.1.1990.pdf>
- Bai J, Qiu S, Zhang S, Huang S, Xu X, Zhao S, He P and Zhou W (2023) Effects of the combined application of organic and chemical nitrogen fertilizer on soil aggregate carbon and nitrogen: A 30-year study. *Journal of Integrative Agriculture* 22(11): 3517-3534. <https://doi.org/10.1016/j.jia.2023.09.012>
- Dhakal C and Lange K (2021) Crop yield response functions in nutrient application: A review. *Agronomy Journal* 113: 5222-5234. <https://doi.org/10.1002/agj2.20863>
- Doungous O, Minyaka E, Longue EAM and Nkengafac NJ (2018) Potentials of cocoa pod husk-based compost on *Phytophthora* pod rot disease suppression, soil fertility, and *Theobroma cacao* L. growth. *Environmental Science and Pollution Research* 25: 25327-25335. <https://doi.org/10.1007/s11356-018-2591-0>
- FAO - Food and Agriculture Organization of the United Nations (2020) Standard operating procedure for soil calcium carbonate equivalent. Titrimetric method. Rome. 16 p.
- FAO - Food and Agriculture Organization of the United Nations (2021) Standard operating procedure for soil available phosphorus, Bray I and Bray II method. Rome. 17 p.
- Fidelis C and Rajashekhar Rao BK (2017) Enriched cocoa pod composts and their fertilizing effects on hybrid cocoa seedlings. *International Journal of Recycled Organic Waste in Agriculture* 6: 99-106. <https://doi.org/10.1007/s40093-017-0156-8>
- Gheith EM, Lamlo M Z, Ali HM, Siddiqui MH, Ghareeb RY et al (2022) Maize (*Zea mays* L) productivity and nitrogen use efficiency in response to nitrogen application levels and time. *Frontiers in Plant Science* 13: 941343. <https://doi.org/10.3389/fpls.2022.941343>
- Govindasamy P, Muthusamy SK, Bagavathiannan M, Mowrer J, Jagannadham PTK et al (2023) Nitrogen use efficiency-A key to enhance crop productivity under a changing climate. *Front. Plant Science* 14: 1121073. <https://doi.org/10.3389/fpls.2023.1121073>
- He Z, Ding B, Pei S, Cao H, Liang J and Li Z (2023) The impact of organic fertilizer replacement on greenhouse gas emissions and its influencing factors. *Science of The Total Environment* 905: 166917. <https://doi.org/10.1016/j.scitotenv.2023.166917>
- Hossain S, Islam A, Badhon FF and Imtiaz T (2022) Properties and behavior of soil – online lab. Manual. 111 p.
- Hougni D-GJM, Schut AGT, Woittiez LS, Vanlauwe B and Giller KE (2021) How nutrient rich are decaying cocoa pod husks? The kinetics of nutrient leaching. *Plant and Soil* 463: 155-170. <https://doi.org/10.1007/s11104-021-04885-1>
- Huat J, Toure A, Tanaka A and Amadiji G (2017) Critical nitrogen dilution curve and nitrogen nutrition index for jute mallow (*Corchorus olitorius* L.) in southern Benin. *Experimental Agriculture* 54(4): 549–562. <https://doi.org/10.1017/S0014479717000230>
- Kayode CO and Adeoye GO (2021) Dry matter yield of okra and nutrient dynamics with cocoa pod husk-based compost and NPK fertilizer in an Ultisol. *Eurasian Journal of Soil Science* 10(1): 77-86. <https://doi.org/10.18393/ejss.816577>
- Liu Z and Wang X (2020) Chapter 26 - Manure treatment and utilization in production systems. *Animal Agriculture* 455-467. <https://doi.org/10.1016/B978-0-12-817052-6.00026-4>
- Luo L, Zhang Y and Xu G (2020) How does nitrogen shape plant architecture? *Journal of Experimental Botany* 71(15): 4415-4427. <https://doi.org/10.1093/jxb/eraa187>
- Maiti S, Islam MR, Uddin MA, Afroj S, Eichhorn SJ and Karim N (2022) Sustainable fiber-reinforced composites: A review. *Advanced Sustainable Systems* 6(11): 2200258. <https://doi.org/10.1002/adss.202200258>
- Munongo ME, Nkeng GE and Njukeng JN (2017) Production and characterization of compost manure and biochar from cocoa pod husks. *International Journal of Advanced Scientific Research and Management* 2(2): 26-31. [https://ijasrm.com/wp-content/uploads/2017/02/IJASRM\\_V2S1\\_185\\_26\\_31.pdf](https://ijasrm.com/wp-content/uploads/2017/02/IJASRM_V2S1_185_26_31.pdf)
- Poudel S (2020) Organic Matter determination (Walkley - Black method) <http://doi.org/10.13140/RG.2.2.22043.00807>
- Rout GR and Sahoo S (2015) Role of iron in plant growth and metabolism. *Reviews in Agricultural Science* 3: 1-24. <https://doi.org/10.7831/ras.3.1>
- Rumanuzzaman K, Hossain ME, Syed M, Rahman MH, Rakibuzzaman M and Rahman MK (2024) Assessment of soil fertility in jute (*Corchorus olitorius* L) cultivated land and nutritive value of its plant parts. *Journal of Biodiversity Conservation and Bioresource Management* 10(1): 35-44. <https://doi.org/10.3329/jbcm.v10i1.74594>
- Sahoo P, Mishra S, Jena B, Nayak RK, Mohanty S and Das J (2023) Spatial variation in soil nutrient status under intensively jute cultivated areas of the coastal ecosystem. *Agriculture Association of Textile Chemical and Critical Reviews Journal* 11(2): 241-245. <http://aatcc.peerjournals.net/wp-content/uploads/2023/05/Spatial-Variation-in-Soil-Nutrient-Status-under-Intensively-Jute-Cultivated-Areas-of-the-Coastal-Ecosystem.pdf>
- Shahinur S, Alamgir Sayeed MM, Hasan M, Muhammad Sayem AS, Haider J and Ura S (2022) Current development and future perspective on natural jute fibers and their biocomposites. *Polymers* 14(7): <https://doi.org/10.3390/polym14071445>
- Songsong G, Hu Q, Cheng Y, Bai L, Liu Z et al (2019) Application of organic fertilizer improves microbial community diversity and alters microbial network structure in tea (*Camellia sinensis*) plantation soils. *Soil and Tillage Research* 195: 104356. <https://doi.org/10.1016/j.still.2019.104356>
- Swify S, Mažeika R, Baltrusaitis J, Drapanauskaitė D and Barčauskaitė K (2024) Review: Modified urea fertilizers and their effects on improving nitrogen use efficiency (NUE). *Sustainability* 16(1): 188. <https://doi.org/10.3390/su16010188>
- Tamfuh PA, Agbor-Ambang ST, Bitondo D, Ndzana GM, Singwa AA et al (2021) Soil fertility amendment using cocoa pod husk and plantain peels powders for Okra (*Abelmoschus esculentus*, kirikou variety) production in Dschang (Cameroon Western Highlands).

AGBIR 37(6): 204-212.

Vaishnavi A and Krishnaveni V (2022) A Review - Studies on jute properties, characteristics and application in textile industry. International Journal of Research Publication and Reviews 3(10): 689-692. <https://doi.org/10.55248/gengpi.2022.3.10.30>

Zhao S and Riaz M (2024) Plant–soil interactions and nutrient cycling dynamics in tropical rainforests. In: Fahad S, Saud S, Nawaz T, Gu L, Ahmad M, and Zhou R (eds) Environment, climate, plant and vegetation growth. Springer, Cham. 229-264. [https://doi.org/10.1007/978-3-031-69417-2\\_8](https://doi.org/10.1007/978-3-031-69417-2_8)





# Efficacy of *Tithonia diversifolia* and NPK fertilizers on papaya seedling growth in marginal soils

Eficacia de fertilizantes de *Tithonia diversifolia* y NPK en plántulas de papaya en suelos marginales

<https://doi.org/10.15446/rfnam.v78n3.119222>

Indra Purnama<sup>1\*</sup>, Rizki Nurmadani<sup>2</sup>, Corilia Dawiteratika<sup>2</sup>, Muhammad Rizal<sup>2</sup> and Anisa Mutamima<sup>3</sup>

## ABSTRACT

### Keywords:

*Carica papaya* seedlings  
Low fertility soils  
Organic fertilizers  
Soil nutrient availability  
Sustainable agriculture

The utilization of marginal soils, particularly peat (Histosol) and Ultisol, presents challenges due to low fertility and unfavorable physical and chemical characteristics. This study evaluates the efficacy of liquid organic fertilizer derived from *Tithonia diversifolia* (wild sunflower) and compound NPK fertilizer (with a ratio 16:16:16) in stimulating the growth of papaya (*Carica papaya* L.) seedlings in tropical marginal soils. The soil samples were collected from agricultural lands in Riau Province, Indonesia, where both peat and Ultisol soils are dominant and commonly used for farming. A factorial experiment was conducted using a split-split plot design with two factors: *T. diversifolia* liquid fertilizer (0, 100, and 200 mL L<sup>-1</sup>) and NPK fertilizer (0, 1.5, and 3 g per polybag), applied to both peat and Ultisol soils. Each treatment combination was replicated three times in an open-field setting, with three seedlings grown in individual polybags per replicate. Significant interaction effects between *T. diversifolia* liquid fertilizer and NPK were observed on growth parameters, including plant height, stem diameter, leaf number, and leaf length. The combination of 200 mL L<sup>-1</sup> *T. diversifolia* liquid fertilizer and 3 g per polybag of NPK resulted in the highest growth across both soil types. Peat soil showed comparatively better growth performance, attributed to higher water retention and organic matter content. These findings provide empirical evidence supporting the use of integrated organic and chemical fertilizers to enhance papaya seedling growth in low-fertility tropical soils.




## RESUMEN

### Palabras clave:

Plántulas de *Carica papaya*  
Suelos de baja fertilidad  
Fertilizantes orgánicos  
Disponibilidad de nutrientes del suelo  
Agricultura sostenible

El uso de suelos marginales, particularmente turba (Histosol) y Ultisol, presenta desafíos debido a su baja fertilidad y características físicas y químicas desfavorables. Este estudio evaluó la eficacia de un fertilizante orgánico líquido derivado de *Tithonia diversifolia* (girasol silvestre) y un fertilizante NPK compuesto (con proporción 16:16:16) en la estimulación del crecimiento de plántulas de papaya (*Carica papaya* L.) en suelos marginales tropicales. Las muestras de suelo se recolectaron en tierras agrícolas de la provincia de Riau, Indonesia, donde los suelos de turba y Ultisol son dominantes y se utilizan comúnmente para la agricultura. Se realizó un experimento factorial utilizando un diseño de parcelas divididas y subdivididas con dos factores: fertilizante líquido de *T. diversifolia* (0, 100 y 200 mL L<sup>-1</sup>) y fertilizante NPK (0, 1,5 y 3 g por bolsa), aplicados tanto en suelos de turba como en Ultisol. Cada combinación de tratamiento se replicó tres veces en condiciones de campo abierto, con tres plántulas cultivadas en bolsas individuales por repetición. Se observaron efectos de interacción significativos entre el fertilizante líquido de *T. diversifolia* y el NPK sobre los parámetros de crecimiento, incluidos la altura de planta, el diámetro del tallo, el número de hojas y la longitud de las hojas. La combinación de 200 mL L<sup>-1</sup> de fertilizante líquido de *T. diversifolia* y 3 g de NPK por bolsa resultó en el mayor crecimiento en ambos tipos de suelo. El suelo de turba mostró un rendimiento de crecimiento comparativamente mejor, atribuido a su mayor retención de agua y contenido de materia orgánica. Estos hallazgos proporcionan evidencia empírica que respalda el uso de fertilizantes orgánicos y químicos integrados para mejorar el crecimiento de plántulas de papaya en suelos tropicales de baja fertilidad.

<sup>1</sup>Graduate School of Agricultural Sciences, School of Graduate Studies, and Center for Sustainable Tropical Agricultural Research, Universitas Lancang Kuning, Indonesia. [indra.purnama@unilak.ac.id](mailto:indra.purnama@unilak.ac.id) 

<sup>2</sup>Department of Agrotechnology, Faculty of Agriculture, Universitas Lancang Kuning, Indonesia. [rizkinurmadani99@gmail.com](mailto:rizkinurmadani99@gmail.com) , [coriliadawiteratika@gmail.com](mailto:coriliadawiteratika@gmail.com) , [m.rizal@unilak.ac.id](mailto:m.rizal@unilak.ac.id) 

<sup>3</sup>Department of Chemical Engineering, Faculty of Engineering, Universitas Riau, Indonesia. [anisamutamima@eng.unri.ac.id](mailto:anisamutamima@eng.unri.ac.id) 

\*Corresponding author

**M**arginal soils, including peat (Histosols) and Ultisols, differ fundamentally in their parent materials—organic and mineral, respectively—and are characterized by low fertility, high acidity, and poor structural stability, which pose significant challenges to agricultural productivity (Csikós and Tóth 2023). However, these soils represent a vast reserve for agricultural expansion, particularly in tropical regions where arable land is becoming increasingly scarce (Purnama et al. 2023). Mitigating the limitations of these soils is essential for sustainable agricultural intensification, particularly in high-value crops such as papaya (*Carica papaya* L.), a species of recognized nutritional and economic significance (Schut et al. 2016).

Organic amendments have been extensively investigated for their potential to enhance soil quality and nutrient availability (Purnama et al. 2023). Liquid organic fertilizers derived from *Tithonia diversifolia* (wild sunflower) have attracted considerable attention due to their favorable nutrient composition—particularly 2.7–3.59% nitrogen, 0.14–0.47% phosphorus, and 0.25–4.10% potassium—which are critical for early seedling development (Wang et al. 2021). In several tropical farming systems, *T. diversifolia* has been applied either alone or in combination with mineral inputs to improve soil health and crop performance. Nevertheless, the integration of *T. diversifolia*-based liquid fertilizers with chemical fertilizers such as NPK remains insufficiently studied, particularly in the context of marginal soils.

Research on the synergistic effects of organic and inorganic fertilizers has shown promising results. Khairi et al. (2023) demonstrated that integrating organic amendments with NPK fertilizer enhances nutrient availability, microbial activity, and plant growth. Annisa and Gustia (2017) reported that the application of *T. diversifolia*-based liquid organic fertilizer, which was poured directly onto the soil and plant base, in combination with reduced NPK doses, influenced flowering traits and maintained fruit yield and quality in melon (*Cucumis melo* L.), demonstrating its potential as a complementary nutrient source in horticultural production. However, most studies have focused on mineral soils, leaving a knowledge gap regarding their application in marginal soils such as peat and Ultisol.

Peat soils, while rich in organic matter, suffer from nutrient imbalances, high acidity, and poor drainage, which can limit crop growth. Conversely, Ultisol soils are highly weathered and nutrient-deficient but have better drainage and structure compared to peat (Hewitt et al. 2021). The contrasting characteristics of these soils suggest that fertilization strategies must be tailored to optimize nutrient use efficiency and crop performance. Although several studies, including Watini et al. (2023), have evaluated the individual effects of *T. diversifolia* and NPK on crop performance, limited attention has been given to their combined application on fruit crops grown in marginal soils. Papaya (*Carica papaya* L.) is a high-value tropical fruit that is moderately sensitive to soil fertility constraints, making it a suitable indicator for assessing soil amendment strategies. However, research examining the interaction effects of *T. diversifolia*-based liquid organic fertilizer and NPK on papaya seedling performance, particularly in contrasting soil types such as Ultisols and peat, remains scarce. To address this gap, plant growth responses and changes in soil properties were evaluated under integrated fertilization strategies combining *T. diversifolia* liquid fertilizer with NPK.

This study aimed to evaluate the synergistic effects of organic liquid fertilizer from *Tithonia diversifolia* and NPK fertilizer on the growth of *C. papaya* seedlings in two types of marginal soils: peat and Ultisol. It was hypothesized that the integrated application would enhance seedling performance more effectively than sole inputs, particularly in nutrient-depleted Ultisols. By analyzing growth responses across treatments and soil types, this study contributes to the development of effective fertilization strategies for the sustainable management of low-fertility tropical soils.

## MATERIALS AND METHODS

### Study site and experimental design

The study was conducted at the Experimental Farm of the Faculty of Agriculture, Universitas Lancang Kuning, Pekanbaru, Indonesia (0°32'N, 101°27'E). The site is characterized by a tropical climate with an average temperature of 31 °C and a relative humidity of 80%. The soils used in the study were peat and Ultisol, collected from agricultural lands in Riau, Indonesia. Peat and Ultisol soils were selected based on their dominance in Riau



Province, Indonesia, where both soil types are widely used for agricultural production, including papaya cultivation. These soils represent contrasting fertility conditions that are commonly encountered in tropical farming systems. A split-split plot design was used to evaluate the effects of soil type (peat and Ultisol), *T. diversifolia* liquid fertilizer (P0: 0 mL L<sup>-1</sup>, P1: 100 mL L<sup>-1</sup>, P2: 200 mL L<sup>-1</sup>), and NPK fertilizer (16:16:16 formulation), applied at rates of 0 g (N0), 1.5 g (N1), and 3 g (N2) per polybag. The P0N0 combination (no *T. diversifolia* liquid fertilizer and no NPK) was used as the control treatment. Soil type was assigned to the main plot, liquid organic fertilizer to the subplot, and NPK fertilizer to the sub-subplot. All treatments were applied in an open-field setting at the same location and time, with three replications per treatment combination. Each replicate consisted of three seedlings grown individually in polybags.

#### Preparation of liquid organic fertilizer

The liquid organic fertilizer was prepared using fresh biomass of *T. diversifolia* collected from local fields in Pekanbaru. The biomass was chopped and mixed with a solution of molasses and water at a 1:10 (w/v) ratio, where 1 part molasses was diluted in 10 parts water. The mixture was then added to the biomass at a ratio of 1:1 (w/w) and fermented anaerobically for 14 days. During the anaerobic fermentation process, pH was monitored and stabilized between 5.2 and 5.5 by day 14. While the microbial composition and C/N ratio were not characterized in this study, the preparation followed standardized protocols as outlined by Annisa and Gustia (2017), which have demonstrated efficacy and consistency in extracting nutrients from *Tithonia* biomass. The fermented solution was filtered and stored in plastic containers at room temperature for seven days before application.

#### Planting materials and soil preparation

Seeds of papaya (*Carica papaya* L., var. California) were procured from a certified supplier in Pekanbaru, Indonesia. The seeds were first germinated in small polybags containing a mixture of sterilized sand to support uniform seedling development. The seedlings were maintained in these small polybags for one month to ensure proper root development before being transplanted into 30×25 cm polybags filled with a soil mixture. The planting medium was prepared by mixing peat or Ultisol soils with cow manure compost and rice husk biochar in a 2:1:1 ratio (v/v/v), respectively representing peat or Ultisol, cow manure,

and rice husk biochar. These organic amendments were applied uniformly across all treatments to standardize the base growing medium and ensure comparability of fertilizer effects. This mixture was designed to improve soil aeration, water retention, and nutrient availability, facilitating optimal root growth. Before planting, the soils were analyzed for pH, organic carbon, total nitrogen, and cation exchange capacity (CEC) to assess baseline soil properties (Purnama et al. 2023).

#### Fertilizer application

The *Tithonia diversifolia*-based liquid fertilizer (TLF) was applied starting at 7 days after transplanting (DAT), then reapplied at two-week intervals for a total of three applications, and discontinued two weeks before the final observation. The TLF was prepared at 100- and 200-mL L<sup>-1</sup> concentration according to the treatment levels. These concentrations were selected based on previous studies showing enhanced plant growth responses within this range (Annisa and Gustia 2017), as well as preliminary observations indicating no signs of phytotoxicity or nutrient imbalance at these dosages.

Applications were carried out in the early morning using a hand sprayer equipped with a fine-mist nozzle to ensure uniform foliar coverage while minimizing excessive run-off. Each plant received 50 mL of TLF solution per application. After a light foliar misting, any remaining volume from the 50 mL was applied directly to the soil surface around the plant base to enhance nutrient availability in the root zone. Prior to each application, plants were irrigated on the previous day to ensure adequate soil moisture and to minimize stress-related variability in nutrient uptake. The experimental NPK fertilizer (16:16:16; Petro Nitrat, PT Petrokimia Gresik, Indonesia) was applied in two split doses, with half of the total treatment applied at 15 DAT and the remaining half at 45 DAT.

#### Growth parameter measurements

Plant height, stem diameter, leaf number, and leaf length were recorded at 90 days after transplanting (DAT). Plant height was measured from the soil surface to the tip of the highest leaf using a measuring tape (Stanley Tools, United Kingdom). Stem diameter was measured at 2 cm above the soil surface using a digital caliper (Mitutoyo, Japan). Leaf number was counted manually by recording all fully expanded leaves per plant. Leaf length was measured



from the base of the petiole to the tip of the leaf blade using a standard ruler (Faber-Castell, Germany), taken from the second fully expanded leaf from the apex to ensure consistency.

### Soil and fertilizer analysis

The chemical composition of the TLF was analyzed for total nitrogen, phosphorus, and potassium content using standard procedures (AOAC 2019). Prior to planting, composite soil samples were collected from the top 0–20 cm layer of each soil type (Ultisol and peat), with three replicates per type to ensure representativeness. Soil pH was measured in a 1:2.5 soil-to-water suspension; organic carbon was determined using the Walkley–Black method; total nitrogen was analyzed using the Kjeldahl method; and cation exchange capacity (CEC) was measured via ammonium acetate extraction at pH=7.0. The peat soil used in this study was classified as sapric in decomposition stage, obtained from a shallow peatland (< 1 m depth) in Riau, Indonesia. The field moisture content was approximately 350%, and all analyses were corrected to an oven-dry basis at 105 °C prior to testing. At the end of the experiment, post-treatment soil samples were collected from each treatment pot. Available phosphorus was analyzed using the Bray I extraction method, while

exchangeable potassium was measured using ammonium acetate extraction, following procedures described by Purnama et al. (2023).

### Data analysis

All data were subjected to analysis of variance (ANOVA) using SPSS software (version 26.0, IBM Corp., Armonk, NY, USA). Significant differences between treatment means were determined using Duncan's Multiple Range Test (DMRT) at a 5% significance level.

## RESULTS AND DISCUSSION

**Soil Characteristics and the Role of Organic Amendments**  
The characteristics of Ultisol and peat soil significantly influence their suitability for crop growth, necessitating the use of fertilization strategies to enhance soil fertility and support plant development. Based on the soil analysis (Table 1), Ultisol is characterized by low organic carbon (1.2%), low total nitrogen (0.09%), and limited phosphorus availability (12.4 mg kg<sup>-1</sup>). These factors make Ultisols highly weathered and nutrient-poor, which aligns with previous findings indicating that Ultisols are often strongly leached, acidic, and have low CEC, thus requiring appropriate fertilization strategies to support sustainable agricultural productivity (Lestari et al. 2022).

**Table 1.** Comparison of initial and post-treatment (P2N2) soil properties in Ultisol and peat soil.

Parameter	Ultisol (before)	Ultisol (after P2N2)	Peat soil (before)	Peat soil (after P2N2)
pH (H <sub>2</sub> O)	4.80±0.10 <sup>b</sup>	5.30±0.08 <sup>a</sup>	3.90±0.05 <sup>b</sup>	4.40±0.06 <sup>a</sup>
Organic carbon (%)	1.20±0.12 <sup>b</sup>	2.80±0.15 <sup>a</sup>	47.50±1.10 <sup>b</sup>	50.20±1.25 <sup>a</sup>
Total nitrogen (%)	0.09±0.01 <sup>b</sup>	0.21±0.02 <sup>a</sup>	1.20±0.04 <sup>b</sup>	1.45±0.05 <sup>a</sup>
Available phosphorus (mg kg <sup>-1</sup> )	12.40±1.05 <sup>b</sup>	18.50±1.12 <sup>a</sup>	5.20±0.30 <sup>b</sup>	7.90±0.44 <sup>a</sup>
Exchangeable potassium (cmol kg <sup>-1</sup> )	0.15±0.01 <sup>b</sup>	0.28±0.02 <sup>a</sup>	0.10±0.01 <sup>b</sup>	0.16±0.01 <sup>a</sup>
Cation exchange capacity (cmol kg <sup>-1</sup> )	8.50±0.45 <sup>b</sup>	10.20±0.52 <sup>a</sup>	34.70±0.90 <sup>b</sup>	36.50±0.88 <sup>a</sup>

Note. Values are presented as mean ± SD (n=3). Different letters within rows indicate significant differences at  $P<0.05$  based on Duncan's Multiple Range Test (DMRT). P2N2 = 200 mL L<sup>-1</sup> TLF + 3 g NPK per polybag.

Conversely, peat soil exhibits a significantly higher organic carbon content (47.5%) and total nitrogen (1.20%), which contribute to greater nutrient retention and microbial activity. However, its low pH (3.9) and limited phosphorus availability (5.2 mg kg<sup>-1</sup>) can inhibit nutrient uptake and root development (Gillespie et al. 2020). The CEC of peat soil (34.7 cmol kg<sup>-1</sup>) is substantially higher than that of Ultisol (8.5 cmol kg<sup>-1</sup>), suggesting that peat can retain more nutrients but may also lead to nutrient imbalances,

particularly potassium deficiency (Woittiez et al. 2019). This justifies the need for external nutrient supplementation to optimize plant growth.

To address the fertility constraints of both soil types, organic amendments such as TLF play a crucial role in enhancing nutrient availability and improving soil structure. As shown in Table 2, the TLF contains essential macronutrients—total nitrogen (2.1%), phosphorus (0.45%), and potassium

(2.9%)—which help address the nutrient deficiencies in both Ultisol and peat soils. These values are consistent with previous studies reporting high nutrient concentrations in both the biomass and liquid extracts of *T. diversifolia* (Olabode et al. 2007), confirming its potential as a nutrient-rich organic input for marginal soils.

**Table 2.** Composition of TLF after 14 days of fermentation.

Parameter	<i>T. diversifolia</i> fertilizer
pH	5.5
Total nitrogen (%)	2.1
Total phosphorus (%)	0.45
Total potassium (%)	2.9
C/N ratio	15.4

The C/N ratio of TLF (15.4) indicates a moderate decomposition rate, ensuring a steady release of nitrogen into the soil, supporting prolonged plant growth without rapid nutrient depletion (Kagan et al. 2024). Moreover, the pH of TLF (5.5) suggests that its application can help neutralize the acidity of peat soil and moderately improve the pH of Ultisol, making essential nutrients more bioavailable (Johan et al. 2021). Several studies have shown that *T. diversifolia*-based fertilizers can enhance soil organic matter, microbial activity, and nutrient cycling, contributing to increased crop yields and soil sustainability in degraded lands (Ewané et al. 2020).

Following the application of TLF and NPK (P2N2 treatment), improvements in soil chemical properties—such as increased pH, organic carbon, total nitrogen, available phosphorus, and exchangeable potassium—were recorded (Table 1). The pH of Ultisol increased from 4.8 to 5.3, indicating that the treatment contributed to reducing soil acidity, which is often associated with improved nutrient availability. In peat soil, pH increased from 3.9 to 4.4, suggesting that while the treatment helped buffer acidity, additional amendments may still be necessary for long-term pH stabilization. The organic carbon content of Ultisol increased from 1.2 to 2.8%, highlighting the role of TLF in enhancing soil structure, microbial activity, and organic matter accumulation. In peat soil, organic carbon remained

high at 50.2%, ensuring adequate carbon availability for microbial processes.

In terms of macronutrient availability, total nitrogen content increased significantly in both soil types (Ultisol: 0.09 to 0.21%; Peat: 1.20 to 1.45%), reinforcing the role of TLF in supplying plant-available nitrogen. The application of TLF and NPK also improved phosphorus availability (Ultisol: 12.4 to 18.5 mg kg<sup>-1</sup>; Peat: 5.2 to 7.9 mg kg<sup>-1</sup>), demonstrating that organic amendments help reduce phosphorus fixation and enhance plant uptake in acidic soils. Exchangeable potassium also increased (Ultisol: 0.15 to 0.28 cmol kg<sup>-1</sup>; Peat: 0.10 to 0.16 cmol kg<sup>-1</sup>), reflecting the contribution of TLF in maintaining potassium availability. Additionally, the CEC of Ultisol improved from 8.5 to 10.2 cmol kg<sup>-1</sup>, while peat soil increased from 34.7 to 36.5 cmol kg<sup>-1</sup>, confirming that TLF enhances nutrient retention capacity.

These results demonstrated that the combined application of TLF and NPK not only supports plant growth but also significantly improves soil fertility. The improvements in organic matter content, pH, and nutrient availability under the P2N2 treatment highlight the potential of TLF as an effective organic fertilizer for sustaining soil health and optimizing plant productivity in marginal soils. Although TLF was primarily applied as a foliar spray, excess solution was also applied to the soil surface, allowing for partial absorption through the root zone. This dual application contributed to enhanced soil chemical properties. The findings further support the integration of organic and inorganic fertilizers as a sustainable strategy to improve soil fertility and enhance agricultural productivity in degraded land areas.

### Effects of TLF and NPK on plant growth

The application of TLF and NPK significantly enhanced the growth of papaya seedlings, as demonstrated by improvements in plant height, leaf number, stem diameter, and leaf length (Figure 1, Table 3). The combination of 200 mL L<sup>-1</sup> TLF and 3 g per polybag NPK (P2N2) consistently produced the highest growth performance in both Ultisol and peat soil, reinforcing the effectiveness of integrated organic and inorganic fertilization in improving nutrient uptake and plant vigor.

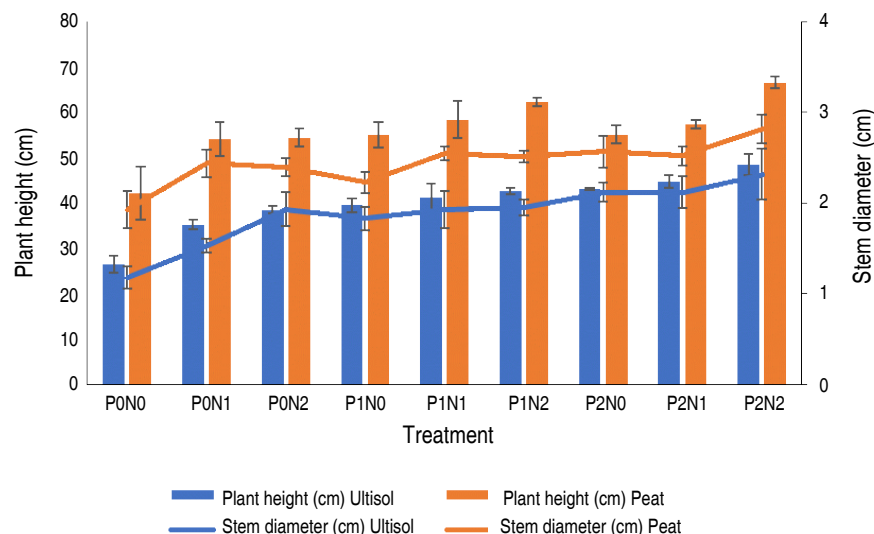


**Figure 1.** Effect of integrated TLF and NPK treatments on plant height and stem diameter of papaya seedlings grown in Ultisol and peat soils. Bars represent mean values ( $n=3$ )  $\pm$  SD.

**Table 3.** Leaf number and leaf length of papaya seedlings in Ultisol and peat soils under TLF and NPK treatments.

Treatment	Leaf number		Leaf length (cm)	
	Ultisol	Peat	Ultisol	Peat
P0N0	8.00 $\pm$ 2.01 <sup>a</sup>	8.53 $\pm$ 1.80 <sup>a</sup>	12.52 $\pm$ 0.50 <sup>a</sup>	17.50 $\pm$ 0.29 <sup>a</sup>
P0N1	9.33 $\pm$ 0.63 <sup>ab</sup>	11.00 $\pm$ 2.62 <sup>ab</sup>	17.92 $\pm$ 1.89 <sup>b</sup>	23.40 $\pm$ 1.80 <sup>b</sup>
P0N2	9.50 $\pm$ 1.21 <sup>ab</sup>	10.17 $\pm$ 1.44 <sup>ab</sup>	18.02 $\pm$ 2.50 <sup>b</sup>	24.17 $\pm$ 1.61 <sup>b</sup>
P1N0	8.33 $\pm$ 1.96 <sup>ab</sup>	10.50 $\pm$ 1.44 <sup>ab</sup>	17.77 $\pm$ 0.58 <sup>b</sup>	23.83 $\pm$ 0.87 <sup>b</sup>
P1N1	11.00 $\pm$ 0.60 <sup>bc</sup>	11.17 $\pm$ 0.50 <sup>ab</sup>	19.93 $\pm$ 0.50 <sup>c</sup>	24.00 $\pm$ 0.29 <sup>b</sup>
P1N2	11.00 $\pm$ 2.52 <sup>bc</sup>	12.17 $\pm$ 1.32 <sup>bc</sup>	20.08 $\pm$ 1.00 <sup>c</sup>	24.50 $\pm$ 1.26 <sup>bc</sup>
P2N0	10.17 $\pm$ 0.76 <sup>bc</sup>	12.67 $\pm$ 1.33 <sup>bc</sup>	18.08 $\pm$ 1.26 <sup>b</sup>	24.87 $\pm$ 1.26 <sup>bc</sup>
P2N1	11.00 $\pm$ 1.08 <sup>bc</sup>	19.67 $\pm$ 1.89 <sup>d</sup>	20.73 $\pm$ 0.50 <sup>cd</sup>	25.33 $\pm$ 0.76 <sup>bc</sup>
P2N2	12.17 $\pm$ 1.73 <sup>c</sup>	23.33 $\pm$ 1.96 <sup>e</sup>	20.87 $\pm$ 1.04 <sup>d</sup>	29.13 $\pm$ 0.50 <sup>c</sup>

Note. Values are presented as mean  $\pm$  SD ( $n=3$ ). Different letters within the same column indicate significant differences at  $P<0.05$  based on Duncan's Multiple Range Test (DMRT). P0: 0 mL L<sup>-1</sup> TLF; P1: 100 mL L<sup>-1</sup> TLF; P2: 200 mL L<sup>-1</sup> TLF and N0: 0 g NPK per polybag; N1: 1.5 g NPK per polybag; N2: 3 g NPK per polybag.

The increase in plant height was particularly evident, with the P2N2 treatment yielding 48.50 cm in Ultisol and 66.58 cm in peat soil, significantly higher than the control (P0N0) at 26.50 and 42.17 cm, respectively — representing an 83.02% increase in Ultisol and 57.84% increase in peat. These results highlight the role of nitrogen and potassium in stimulating vegetative growth, as both nutrients are essential for cell division, elongation, and photosynthesis efficiency (Jasim et al. 2016). The improved response

in peat soil compared to Ultisol is likely due to its higher organic matter content and superior water retention capacity, which enhance nutrient availability. However, the significant improvements observed in Ultisol following fertilization demonstrate the ability of TLF and NPK to replenish soil nutrients and mitigate fertility constraints, making nutrient-poor soils more suitable for cultivation. The post-treatment soil analysis (Table 1) further supports this finding, showing increased nitrogen, phosphorus, and

exchangeable potassium levels in both soil types, which contributed to improved plant height.

Leaf number, an essential indicator of plant health and photosynthetic capacity, also exhibited a strong response to fertilization. The highest leaf production was observed in the P2N2 treatment, reaching 12.17 leaves per plant in Ultisol and 23.33 leaves per plant in peat soil, significantly higher than the control (P0N0) with 8.00 and 8.53 leaves, respectively — equivalent to an increase of 52.13% in Ultisol and 173.52% in peat. The increased leaf number is likely attributed to the steady supply of nitrogen and phosphorus, which are essential for leaf expansion, chlorophyll biosynthesis, and photosynthetic activity (Malhotra et al. 2018). This aligns with previous research indicating that *T. diversifolia*-based fertilizers enhance foliage development in tropical crops by improving soil nutrient availability and microbial activity (Ewané et al. 2024).

A similar trend was observed in stem diameter, where P2N2 produced the thickest stems (2.32 cm in Ultisol and 2.82 cm in peat soil), significantly greater than the control (P0N0) at 1.18 and 1.93 cm, respectively — an increase of 96.61% in Ultisol and 46.11% in peat. The increase in stem diameter suggests stronger plant structural integrity, which is essential for nutrient transport, water conduction, and overall plant stability. Organic fertilizers such as *T. diversifolia* have been reported to improve stem robustness and increase seedling drought resistance, likely due to their slow nutrient release and ability to enhance soil physical properties (Setyowati et al. 2022). The enhanced structural growth in Ultisol demonstrates the potential of TLF to improve nutrient retention and soil fertility, reducing the constraints associated with highly weathered tropical soils.

Leaf length, another key growth parameter, also significantly increased following fertilization. The longest leaves were recorded in the P2N2 treatment (20.87 cm in Ultisol and 29.13 cm in peat soil), compared to the control (P0N0), which only reached 12.52 and 17.50 cm, respectively — corresponding to an increase of 66.70% in Ultisol and 66.46% in peat. The elongation of leaves is strongly associated with higher nitrogen and potassium availability, as these nutrients facilitate cell expansion, metabolic activity, and photosynthetic efficiency (Shah et al. 2024). The positive effects of *T. diversifolia* on leaf

growth are consistent with previous studies, where organic amendments contributed to increased leaf surface area, chlorophyll content, and overall plant productivity (Gao et al. 2020).

The differences in growth responses between Ultisol and peat soil highlight the distinct soil characteristics and their interactions with fertilization. While peat soil supported higher overall growth, particularly in plant height and leaf number, due to its higher organic carbon (50.2%) and total nitrogen content (1.45%) after P2N2 application (Table 1), Ultisol showed greater relative improvements in nutrient availability, particularly in total nitrogen (0.21%), available phosphorus (18.5 mg kg<sup>-1</sup>), and exchangeable potassium (0.28 cmol kg<sup>-1</sup>), which helped mitigate its initial fertility limitations. The increase in CEC observed in both soil types under the P2N2 treatment further supports the contribution of organic amendments to improved soil nutrient retention, which is critical for long-term soil fertility.

The results indicate that the combination of TLF and NPK fertilization significantly outperformed single fertilizer applications, reinforcing the importance of balanced nutrient management in optimizing seedling growth. The application of *T. diversifolia*-based liquid fertilizer (TLF) led to improved soil nutrient indicators (e.g., total N, available P, and exchangeable K) in Ultisol, where baseline fertility was limited. However, as nutrient uptake by plant tissues was not directly measured in this study, conclusions regarding actual nutrient use efficiency remain tentative and warrant further investigation. These findings support the integration of organic and inorganic fertilizers as a sustainable strategy for improving plant growth in marginal soils, providing both short-term nutrient availability and long-term soil health benefits.

#### Comparison of ultisol and peat soil in supporting growth

The results of this study demonstrated that peat soil supported better overall growth performance than Ultisol, as evidenced by higher plant height, greater leaf number, thicker stem diameter, and longer leaves. This disparity is largely explained by the inherent differences in soil properties. Compared to Ultisol, peat soil had substantially higher organic carbon (50.2 vs. 2.8%), total nitrogen (1.45 vs. 0.21%), and cation exchange capacity (36.5 vs. 10.2 cmol kg<sup>-1</sup>) (Table 1). These properties are known to enhance nutrient retention and availability in



the rhizosphere, thereby supporting more robust plant growth (Ali et al. 2025). Despite these initial differences, the application of TLF and NPK significantly improved growth performance in both soil types, as confirmed by ANOVA and DMRT analyses, suggesting that organic and inorganic fertilization can enhance the productivity of even nutrient-poor soils like Ultisol.

Figure 2 shows the visual comparison of papaya seedling growth in Ultisol and peat soil following the application of TLF and NPK. The image on the left represents the peat soil experiment, where seedlings exhibit denser foliage,

greater stem robustness, and enhanced vigor compared to those grown in Ultisol (right image). The improved growth in peat soil aligns with its higher organic carbon and nitrogen content, which facilitates better nutrient retention and water availability, thereby supporting enhanced physiological development. Conversely, while the Ultisol-grown seedlings initially exhibited slower growth, the integration of TLF and NPK significantly improved plant height, stem diameter, leaf number, and leaf length, demonstrating the potential of combined organic and inorganic amendments in mitigating the fertility limitations of highly weathered soils.



**Figure 2.** Growth performance of papaya (*Carica papaya* L.) seedlings in peat soil (A) and Ultisol (B) under *Tithonia diversifolia* liquid fertilizer and NPK application.

The superior performance of papaya seedlings in peat soil is primarily linked to its high organic carbon content (47.5%) and total nitrogen (1.20%), which create a nutrient-rich growing environment that supports root development and vegetative growth. Organic matter plays a crucial role in improving soil structure, enhancing microbial activity, and increasing nutrient retention, making peat soil inherently more fertile than Ultisol (Liu et al. 2019). Additionally, peat soil's high CEC (34.7 cmol kg<sup>-1</sup>) allows it to retain nutrients more effectively, reducing leaching losses and ensuring a more consistent supply of essential macronutrients like nitrogen and potassium. However, its low pH (3.9) and phosphorus availability (5.2 mg kg<sup>-1</sup>) present challenges for long-term crop production, as extreme soil acidity can reduce nutrient solubility and inhibit root nutrient uptake (Gillespie et al. 2020).

In contrast, Ultisol exhibited significantly lower growth performance under unfertilized conditions, as reflected in shorter plants, fewer leaves, smaller stem diameters, and shorter leaf lengths. Ultisol is highly weathered and characterized by low organic carbon (1.2%), limited total nitrogen (0.09%), and poor phosphorus availability (12.4 mg kg<sup>-1</sup>), which restricts its ability to support vigorous plant growth without external fertilization (Malhotra et al. 2018). The low CEC of Ultisol (8.5 cmol kg<sup>-1</sup>) suggests that it has poor nutrient retention, making it more prone to leaching, particularly under high rainfall conditions. Without intervention, these limitations lead to low nutrient availability and suboptimal plant development. However, the significant improvements observed after fertilization indicate that Ultisol can be managed effectively through the integration of organic and inorganic amendments.

The ANOVA results confirmed that both soil type and fertilization significantly affected all measured growth parameters ( $P < 0.05$ ), with a notable interaction effect between TLF and NPK. The DMRT analysis further revealed that P2N2 (200 mL L<sup>-1</sup> TLF + 3 g per polybag NPK) produced the best results, significantly increasing plant height, leaf number, stem diameter, and leaf length compared to other treatments. These findings highlight the importance of balanced nutrient management, particularly in marginal soils, to optimize seedling growth.

For plant height, seedlings grown in peat soil consistently outperformed those in Ultisol, particularly in the P2N2 treatment, where plant height reached 66.58 cm in peat soil and 48.50 cm in Ultisol. The statistical difference between these values ( $P < 0.05$ ) suggests that peat soil's higher nitrogen and organic matter content contributed to more robust shoot elongation, whereas Ultisol's lower fertility limited plant growth unless supplemented with fertilization. The increase in plant height with fertilization aligns with previous studies that demonstrated *T. diversifolia*'s ability to enhance nitrogen availability and stimulate vegetative growth in degraded soils (Suyanto and Astar 2024).

Similarly, leaf number increased significantly with higher doses of TLF and NPK, particularly in peat soil, where P2N2 resulted in 23.33 leaves per plant, compared to 12.17 leaves per plant in Ultisol. This difference was statistically significant ( $P < 0.05$ ), reinforcing the role of TLF as a nitrogen source that enhances leaf expansion and chlorophyll biosynthesis. The integration of organic and inorganic fertilizers allowed for both immediate and sustained nitrogen availability, promoting healthier leaf development and higher photosynthetic efficiency, which are essential for strong seedling establishment (Moe et al. 2019).

A similar pattern was observed in stem diameter, where P2N2 produced significantly thicker stems (2.82 cm in peat soil and 2.32 cm in Ultisol) compared to unfertilized treatments. Stem diameter is a key parameter indicating plant strength and structural stability, with thicker stems facilitating better water and nutrient transport. The improvement in stem diameter following fertilization is consistent with previous findings that organic amendments enhance root activity, increase biomass allocation, and promote drought resistance (Benaffari et al. 2022). The

fact that Ultisol, despite its lower initial fertility, showed significant improvement in stem thickness after TLF and NPK application, suggests that integrated fertilization can strengthen plant architecture even in nutrient-poor soils.

The same trend was evident in leaf length, where P2N2-treated plants in peat soil recorded 29.13 cm, while those in Ultisol reached 20.87 cm. The ANOVA and DMRT results confirmed that both soil type and fertilization had a statistically significant impact on leaf elongation ( $P < 0.05$ ), with TLF and NPK enhancing cell expansion and leaf development. Longer leaves contribute to greater light interception and higher photosynthetic efficiency, further promoting seedling growth and vigour (Anthony et al. 2020).

Collectively, these findings demonstrate that while peat soil provides a more favorable growing environment for papaya seedlings due to its higher organic matter content and nutrient retention capacity, its low pH and phosphorus deficiency require external supplementation to sustain long-term plant productivity. Meanwhile, Ultisol, despite its lower initial fertility, responded well to fertilization, showing significant improvements in all growth parameters after TLF and NPK application. These results support the use of *T. diversifolia* as an effective organic amendment for enhancing soil fertility and optimizing plant growth in marginal soils, offering both immediate nutrient benefits and long-term improvements in soil health. The statistical validation through ANOVA and DMRT confirms that P2N2 (200 mL L<sup>-1</sup> TLF + 3 g per polybag NPK) was the most effective treatment, reinforcing the importance of integrated organic and inorganic fertilizer strategies for sustainable agricultural development.

#### **Potential of *Tithonia diversifolia* as an organic fertilizer**

The findings of this study confirm that TLF significantly enhances papaya seedling growth in marginal soils, particularly Ultisol and peat soil, which exhibit inherent fertility constraints. The observed improvements in plant height, leaf number, stem diameter, and leaf length following TLF application highlight its nutrient-rich composition, particularly its high nitrogen (2.1%) and potassium (2.9%) content, which support vegetative growth, root development, and overall plant health. The role of *T. diversifolia* in improving soil nutrient availability aligns with previous studies demonstrating that it enhances CEC, soil organic matter, and microbial



activity, thereby mitigating the nutrient deficiencies commonly associated with highly weathered tropical soils (Ewané et al. 2020).

The application of TLF has a profound impact on soil properties post-treatment, as shown in Table 1. In Ultisol, TLF application increased organic carbon, nitrogen, and phosphorus levels while slightly improving soil pH, making nutrients more bioavailable for plant uptake. Similarly, in peat soil, TLF contributed to reducing extreme acidity and enhancing phosphorus availability, which are crucial factors in improving plant nutrient absorption. These effects suggest that TLF not only acts as a direct nutrient source but also serves as a soil conditioner, facilitating improved nutrient retention and microbial processes.

Compared to other organic fertilizers, such as compost tea and cow manure extract, TLF offers a more concentrated source of readily available nutrients. Compost tea has been shown to improve microbial biomass and nutrient uptake, but often contains lower levels of macronutrients (Raza et al. 2023). Similarly, cow manure extract enhances soil fertility through microbial activity and organic matter content, yet its nutrient release tends to be slower and less consistent (Ikeh et al. 2023). In contrast, TLF, with its high nitrogen and potassium content and rapid nutrient release due to fermentation, provides faster stimulation of vegetative growth in nutrient-poor soils. Additionally, its liquid form facilitates integration with fertigation systems, providing an advantage over solid compost or manure applications, as summarized in Table 4.

**Table 4.** Comparative characteristics of *Tithonia diversifolia* liquid fertiliser (TLF) and other organic fertilizers commonly used in marginal soils.

Parameter	<i>Tithonia diversifolia</i> Liquid Fertilizer	Compost tea*	Cow manure extract**
Form	Liquid	Liquid	Liquid
N content (%)	2.10	0.007–0.036	0.20
K content (%)	2.90	0.003–0.005	0.29
Mode of action	Fast nutrient release, microbial boost	Microbial biomass enhancer	Organic matter enrichment
Effect on seedling growth	High	Moderate	Moderate
Ease of application	High (e.g., fertigation)	Moderate	Moderate
Additional benefit	Biopesticidal potential	Enhances microbial activity	Improves soil structure

\*(Raza et al. 2023); \*\* (Ikeh et al. 2023).

While this study specifically assessed the organic fertilizer potential of *T. diversifolia*, previous studies have reported its antimicrobial and pesticidal properties, owing to bioactive compounds such as flavonoids, tannins, and alkaloids (Purnama et al. 2024). These attributes warrant further investigation, particularly in the context of integrated pest and nutrient management (Anggrayni et al. 2025). Future studies should explore its biopesticidal efficacy under field conditions, alongside its long-term impacts on soil microbiota and crop protection.

## CONCLUSION

This study demonstrated that *Tithonia diversifolia* liquid fertiliser (TLF) significantly improved the early growth of *Carica papaya* L. seedlings in both peat and Ultisol soils, with the P2N2 treatment (200 mL L<sup>-1</sup> TLF + 3 g NPK per polybag) resulting in the highest performance in terms

of plant height, stem diameter, and leaf development. Peat soil supported better seedling growth, likely due to its higher organic matter content and favorable moisture retention characteristics, whereas Ultisol—despite its low initial fertility—showed notable responsiveness to integrated fertilization. These findings support the potential of combining organic and inorganic fertilizers to enhance seedling establishment in degraded tropical soils. However, the results are based on a short-term, container-based experiment conducted under controlled conditions without biotic stressors. Therefore, extrapolation to other crops, soil types, or field-scale conditions should be approached with caution. Future studies should incorporate longer-term trials under field conditions, assess microbial and root dynamics, and evaluate pest interactions to more comprehensively understand TLF's multifunctional roles. Additionally, cost-effectiveness analysis and elucidation of

the phytochemical contributions of *T. diversifolia* will further inform its potential in sustainable nutrient management systems. To better understand soil organic carbon turnover and its link with fertilizer-induced changes, future research should also employ more detailed carbon fractionation methods or stable isotope tracing techniques.

## ACKNOWLEDGMENTS

This research was funded by the Ministry of Higher Education, Science, and Technology of the Republic of Indonesia under the fundamental grant scheme, contract number: 138/C3/DT.05.00/PL/2025.

## CONFLICT OF INTERESTS

The authors declare no competing interests.

## REFERENCES

- Ali A, Jabeen N, Chachar Z et al (2025) The role of biochar in enhancing soil health & interactions with rhizosphere properties and enzyme activities in organic fertilizer substitution. *Frontiers in Plant Science* 16: 1595208. <https://doi.org/10.3389/fpls.2025.1595208>
- Anggrayni D, Purnama I, Saidi NB et al (2025) Antifungal and phytotoxicity of wood vinegar from biomass waste against *Fusarium oxysporum* f. sp. *cubense* TR4 infecting banana plants. *Discover Food* 5(1): 98. <https://doi.org/10.1007/s44187-025-00377-8>
- Annisia P and Gustia H (2017) Respon pertumbuhan dan produksi tanaman melon terhadap pemberian pupuk organik cair *Tithonia diversifolia*. *Prosiding Semnastan*: 104-114.
- Anthony B, Serra S and Musacchi S (2020) Optimization of light interception, leaf area and yield in "WA38": comparisons among training systems, rootstocks and pruning techniques. *Agronomy* 10(5): 689. <https://doi.org/10.3390/agronomy10050689>
- AOAC - Official Methods of Analysis of the Association of Official Analytical Chemists (2019) Official methods of analysis of AOAC International. 21st Edition, AOAC, Washington DC.
- Benaffari W, Boutasknit A, Anli M et al (2022) The native arbuscular mycorrhizal fungi and vermicompost-based organic amendments enhance soil fertility, growth performance, and the drought stress tolerance of quinoa. *Plants* 11(3): 393. <https://doi.org/10.3390/plants11030393>
- Csikós N and Tóth G (2023) Concepts of agricultural marginal lands and their utilisation: A review. *Agricultural Systems* 204: 103560. <https://doi.org/10.1016/j.agry.2022.103560>
- Ewané CA, Tatseguouck RN, Meshuneke A and Niemenak N (2020) Field efficacy of a biopesticide based on *Tithonia diversifolia* against black sigatoka disease of plantain (*Musa* spp., AAB). *Agricultural Sciences* 11(08): 730. <https://doi.org/10.4236/as.2020.118048>
- Ewané CA, Meshuneke A, Mbang GE et al (2024) Stimulatory effect of *Tithonia diversifolia*-by products on plantain banana vivoplants in nursery (A Review). *American Journal of Plant Sciences* 15(9): 726-745. <https://doi.org/10.4236/ajps.2024.159047>
- Gao C, El-Sawah AM, Ali DFI et al (2020) The integration of bio and organic fertilizers improve plant growth, grain yield, quality and metabolism of hybrid maize (*Zea mays* L.). *Agronomy* 10(3): 319. <https://doi.org/10.3390/agronomy10030319>
- Gillespie DP, Kubota C and Miller SA (2020) Effects of low pH of hydroponic nutrient solution on plant growth, nutrient uptake, and root rot disease incidence of basil (*Ocimum basilicum* L.). *HortScience* 55(8):1251-1258.
- Hewitt AE, Balks MR and Lowe DJ (2021) Ultic soils. In *The soils of Aotearoa New Zealand* (pp. 249-265). Cham: Springer International Publishing. [https://doi.org/10.1007/978-3-030-64763-6\\_16](https://doi.org/10.1007/978-3-030-64763-6_16)
- Ikeh AO, Okocha IO, Umekwe PN et al (2023) Effect of foliar application of cow dung extract on growth and yield of waterleaf (*Talinum triangulare* Jacq.) in an ultisol. *Journal of Current Opinion in Crop Science* 4(3): 103-111. <https://doi.org/10.62773/jcocs.v4i3.203>
- Jasim AH, Rashid HM and Ghani MM (2016) Effect of foliar nutrition of phosphorous and potassium on vegetative growth characteristics and yield of broad bean. *Euphrates Journal of Agricultural Science* 8(3): 50-55.
- Johan PD, Ahmed OH, Omar L and Hasbullah NA (2021) Phosphorus transformation in soils following co-application of charcoal and wood ash. *Agronomy* 11(10): 2010. <https://doi.org/10.3390/agronomy11102010>
- Kagan K, Jonak K and Wolińska A (2024) The impact of reduced N fertilization rates according to the "farm to fork" strategy on the environment and human health. *Applied Sciences* 14(22): 10726. <https://doi.org/10.3390/app142210726>
- Khairi A, Jayaputra J, Padusung P, Tejowulan S and Nurrachman N (2023) Combination of bio-organo-mineral fertilizers on optimizing the growth and production of tomatoes (*Solanum lycopersicum* L.) in dryland environment. *Jurnal Ilmiah Pertanian* 20(2): 127-138. <https://doi.org/10.31849/jip.v20i2.10901>
- Lestari IP, Susila AD, Sutandi A and Nursyamsi D (2022) Study of P nutrient soil test calibration in determining P fertilization recommendations shallots in ultisol soil. In *IOP Conference Series: Earth and Environmental Science* (Vol. 978, No. 1, p. 012009). IOP Publishing.
- Liu B, Talukder MJH and Terhonen E et al (2019) The microbial diversity and structure in peatland forest in Indonesia. *Soil Use and Management* 36(1): 123-138. <https://doi.org/10.1111/sum.12543>
- Malhotra H, Vandana, Sharma S and Pandey R (2018) Phosphorus nutrition: plant growth in response to deficiency and excess. In *Plant Nutrients and Abiotic Stress Tolerance*: 171-190. [https://doi.org/10.1007/978-981-10-9044-8\\_7](https://doi.org/10.1007/978-981-10-9044-8_7)
- Moe K, Moh SM, Htwe AZ et al (2019) Effects of integrated organic and inorganic fertilizers on yield and growth parameters of rice varieties. *Rice Science* 26(5): 309-318. <https://doi.org/10.1016/j.rsci.2019.08.005>
- Olabode OS, Sola O, Akanbi WB, Adesina GO and Babajide PA (2007) Evaluation of *Tithonia diversifolia* (Hemsl.) A gray for soil improvement. *World Journal of Agricultural Sciences* 3(4): 503-507.
- Purnama I, Mutryarny E and Wijaya RT (2023) Avanzando en el crecimiento de porang (*Amorphophallus muelleri*) en suelos podzólicos rojo-amarillos: un análisis experimental de la interacción entre el guano sólido y el fertilizante orgánico líquido. *Idesia (Arica)* 41(3): 9-14. <https://doi.org/10.4067/S0718-34292023000300009>
- Purnama I, Swebrock T, Ihsan F, Mutamima A et al (2024) Evaluation of four Indonesian leaf extracts for their antimicrobial activity against *Staphylococcus aureus* (MRSA) & *Escherichia coli* (K-12).

In E3S Web of Conferences (Vol. 593, p. 05001). EDP Sciences. <https://doi.org/10.1051/e3sconf/202459305001>

Raza A, Ali Z and Ali SA (2023) Standardization of protocol for the formulation of compost tea and its efficacy study on potato. *Pure and Applied Biology (PAB)* 12(2): 1044-1055. <https://doi.org/10.19045/bspab.2023.120107>

Schut M, van Asten P, Okafor C et al (2016) Sustainable intensification of agricultural systems in the Central African Highlands: The need for institutional innovation. *Agricultural Systems* 145: 165-176. <https://doi.org/10.1016/j.agsy.2016.03.005>

Shah IH, Jinhui W, Li X, Hameed MK et al (2024) Exploring the role of nitrogen and potassium in photosynthesis implications for sugar: Accumulation and translocation in horticultural crops. *Scientia Horticulturae* 327: 112832. <https://doi.org/10.1016/j.scienta.2023.112832>

Setyowati N, Hutapea JV and Mukhtar Z (2022) Mexican sunflower (*Tithonia diversifolia*) compost as substitution of synthetic fertilizers for

sweet corn in Ultisols. *International Journal of Agricultural Technology* 18(6): 2607-2616.

Suyanto A and Astar I (2024) Effect of using *Tithonia diversifolia* green manure and *Trichoderma* sp. secondary metabolites on the growth and yield of tomato plants (*Solanum lycopersicum* L.) on alluvial soil. *Journal of Smart Science and Technology* 4(2): 54-63.

Wang Y, Chen YF and Wu WH (2021) Potassium and phosphorus transport and signaling in plants. *Journal of Integrative Plant Biology* 63(1): 34-52. <https://doi.org/10.1111/jipb.13053>

Watini W, Zulfita D and Rahmadiyah R (2023) Pengaruh pupuk hijau paitan dan npk terhadap pertumbuhan dan hasil kailan pada tanah gambut. *Jurnal Sains Pertanian Equator* 12(3): 292-302.

Woittiez LS, Turhina SRI, Deccy D et al (2019) Fertiliser application practices and nutrient deficiencies in smallholder oil palm plantations in Indonesia. *Experimental Agriculture* 55(4): 543-559. <https://doi.org/10.1017/S0014479718000182>

# *In vitro* propagation of sweet cucumber (*Solanum muricatum* Ait): Effects of auxins and cytokinins

Propagación *in vitro* de pepino dulce (*Solanum muricatum* Ait): Efectos de las auxinas y las citoquininas

<https://doi.org/10.15446/rfnam.v78n3.118004>

Cecilia Lazaro-Rodriguez<sup>1</sup>, Lia Loana Bendezu-Granda<sup>1</sup>, Julio A. Olivera-Soto<sup>2</sup>, Alvaro Tumpe-Jaquehua<sup>1</sup>, Graciela Gomez-Fuentes<sup>1</sup>, Maria Vicente-Vega<sup>1</sup> and Luz Sanchez-Quispe<sup>1\*</sup>

## ABSTRACT

### Keywords:

Cytokinin  
Plant growth regulators  
Plant tissue culture

Sweet cucumber (*Solanum muricatum* Ait.) is a perennial shrub native to the Andean region and closely related to tomato and potato. Its fruit is valued for its high-water content and nutritional properties, including antioxidants, potassium, and vitamin C. However, its agricultural potential is constrained by low germination rates, high heterozygosity, and susceptibility to diseases. *In vitro* culture techniques offer a viable alternative for obtaining plant material with high genetic and phytosanitary quality. This study evaluated the *in vitro* regeneration of *S. muricatum* through organogenesis and shoot proliferation. During the establishment phase on semi-solid MS medium, supplementation with 1.5 mg L<sup>-1</sup> indole-3-acetic acid (IAA) enhanced bud regeneration, increased shoot height (2.69 cm), and promoted root formation, whereas higher concentrations (2.0 mg L<sup>-1</sup>) negatively affected regeneration. Shoot proliferation was stimulated by specific combinations of auxins and cytokinins, particularly IAA+BAP (1.0 + 0.2 mg L<sup>-1</sup>), which produced taller explants (7.7 cm) with a greater number of leaves (11.9). These findings provide useful information for optimizing *in vitro* propagation conditions for *S. muricatum*, with potential applications in germplasm conservation, production of disease-free plants, and genetic improvement of this underutilized species.

## RESUMEN

### Palabras clave:

Citocinina  
Reguladores del crecimiento de las plantas  
Cultivo de tejidos vegetales

El pepino dulce (*Solanum muricatum* Ait.) es un arbusto perenne originario de la región andina y estrechamente relacionado con el tomate y la papa. Su fruto es valorado por su alto contenido de agua y propiedades nutricionales, incluidos antioxidantes, potasio y vitamina C. Sin embargo, su potencial agrícola se ve limitado por las bajas tasas de germinación, la alta heterocigosidad y la susceptibilidad a las enfermedades. Las técnicas de cultivo *in vitro* ofrecen una alternativa viable para la obtención de material vegetal de alta calidad genética y fitosanitaria. Este estudio evaluó la regeneración *in vitro* de *S. muricatum* a través de la organogénesis y la proliferación de brotes. Durante la fase de establecimiento en medio MS semisólido, la suplementación con 1,5 mg L<sup>-1</sup> de ácido indol-3-acético (IAA) mejoró la regeneración de las yemas, aumentó la altura de los brotes (2,69 cm) y promovió la formación de raíces, mientras que las concentraciones más altas (2,0 mg L<sup>-1</sup>) afectaron negativamente la regeneración. La proliferación de brotes fue estimulada por combinaciones específicas de auxinas y citoquininas, particularmente IAA+BAP (1,0+0,2 mg L<sup>-1</sup>), que produjeron explantes más altos (7,7 cm) con un mayor número de hojas (11,9). Estos hallazgos proporcionan información útil para optimizar las condiciones de propagación *in vitro* de *S. muricatum*, con aplicaciones potenciales en la conservación de germoplasma, la producción de plantas libres de enfermedades y el mejoramiento genético de esta especie subutilizada.

<sup>1</sup>Escuela Profesional de Agronomía, Facultad de Ciencias Agrarias, Universidad Nacional de Cañete, San Luis, Cañete, Lima, Perú. [lazarorosa0320@gmail.com](mailto:lazarorosa0320@gmail.com), [liabendezu3@gmail.com](mailto:liabendezu3@gmail.com), [alvarotumpej@gmail.com](mailto:alvarotumpej@gmail.com), [gofugraci@gmail.com](mailto:gofugraci@gmail.com), [Mariavicenteagro@gmail.com](mailto:Mariavicenteagro@gmail.com), [Dquesanchez53@gmail.com](mailto:Dquesanchez53@gmail.com)

<sup>2</sup>Laboratorio de cultivo in vitro de tejidos vegetales, Centro Internacional de Investigación para la Sustentabilidad, Universidad Nacional de Cañete, Lunahuaná, Cañete, Lima, Perú. [agols4407@gmail.com](mailto:agols4407@gmail.com)

\*Corresponding author

The sweet cucumber (*Solanum muricatum* Ait.) is a species native to the Andean region and is cultivated for its fruit, which contains 92% water and has a soft texture (Angulo 2024). It provides antioxidants, potassium, vitamin C, and dietary fiber (Campos et al. 2018) and has been associated with potential benefits such as weight management, immune system support, and relief of digestive discomfort (Cavusoglu and Sulusoglu-Durul 2013). The crop is grown in Peru, particularly in Arequipa, Ayacucho, Áncash, La Libertad, and Lima (Pickersgill 2007). Additionally, it has been introduced and adapted in countries including Spain, New Zealand, Turkey, Israel, the United States, and Japan (Torrent 2014).

Nevertheless, the cultivation of this species encounters several challenges, including low seed germination rates and high heterozygosity, which leads to progeny displaying significant variability in characteristics such as leaf type, fruit shape, color, and sensory attributes (González et al. 2015). Furthermore, production fields are impacted by diseases caused by bacteria, fungi, viruses, and mites pests (Kim et al. 2017). This issue is exacerbated when farmers propagate plants using cuttings from existing fields without implementing proper phytosanitary management, often resulting in reduced crop yields. To address these obstacles, the development and optimization of *in vitro* propagation protocols have emerged as a strategic approach to ensure genetic uniformity, quality, and plant health (Shahnawaz et al. 2021). This technique involves isolating cells, tissues, or organs under carefully controlled nutritional and environmental conditions, adhering to rigorous aseptic standards, in order to regenerate whole plants from tissue fragments (explants) (Sharry et al. 2015). Explants are cultivated in media such as Murashige and Skoog (MS) (Gonzales-Arteaga et al. 2023), supplemented with plant growth regulators, particularly auxins and cytokinins. Common auxin hormones used include indole-3-butyric acid (IBA) and indole-3-acetic acid (IAA).

Indole-3-butyric acid (IBA) functions as a hormone that remains active in the culture medium, promoting cell differentiation and elongation, which are necessary for root development. In contrast, indole-3-acetic acid (IAA) regulates cell division, elongation, and differentiation

for both shoot and root formation; however, it is rapidly degraded in the culture medium. Cytokinins such as kinetin (KIN) stimulate shoot multiplication and formation, thereby enhancing organogenesis and plant regeneration. 6-Benzylaminopurine (BAP) promotes cell division and supports the robust development of shoots. The combination of IAA and BAP enables the regeneration of apical buds and shoot proliferation, whereas the combination of IBA and BAP creates a balance between shoot and root formation.

This study proposes the incorporation of auxins and cytokinins into an MS culture medium to achieve efficient establishment, multiplication, and rooting of *Solanum muricatum*.

## MATERIALS AND METHODS

### Plant material

The sweet cucumber cuttings (*S. muricatum* Ait.) were collected from mother plants of a local Lunahuaná ecotype, Cañete. Plants met phytosanitary and maturity standards. Cuttings were potted in peat and agricultural soil until new shoots formed. All activities took place at the International Research Center for Sustainability (CIIS) of the Universidad Nacional de Cañete, Peru.

### *In vitro* establishment

The new shoots were defoliated and cleaned under running water using eucalyptus-based antibacterial soap from the Aval brand, then rinsed with distilled water. The plant material was placed in a laminar flow hood for disinfection: first with 70% alcohol for 1 min, followed by treatment with 1.5% sodium hypochlorite containing one drop of Tween 20 for 10 min. Finally, the material was rinsed three times with sterile distilled water. The treatments used the Murashige and Skoog basal medium (Gonzales-Arteaga et al. 2023) obtained from Caisson Lab, supplemented with sucrose, 8 g L<sup>-1</sup> of agar, and 100 mL L<sup>-1</sup> of myo-inositol at varying concentrations. Indole-3-butyric acid (IBA) (0.5, 1.0, 1.5, and 2.0) and indole-3-acetic acid (IAA) (0.5, 1.0, 1.5, and 2.0), both sourced from Caisson Lab, United States, were applied independently as treatments. The pH was adjusted to 5.7, and the medium was sterilized by autoclaving at 121 °C for 20 min under a pressure of 1.2 kg cm<sup>-2</sup>. Treatments were incubated at a constant temperature of 24 °C and evaluated after 45 days.



### In vitro multiplication

During this phase, plant material from the establishment stage was utilized, specifically handling axillary and apical buds. The MS medium culture included sucrose, 8 g L<sup>-1</sup> of agar, and 100 mL L<sup>-1</sup> of myo-inositol. Growth regulators applied were kinetin (KIN) and 6-benzylaminopurine (BAP), both individually and in combinations with indole-3-butyric acid (IBA) and indole-3-acetic acid (IAA). Treatments were maintained at a constant temperature of 24 °C in the incubation area and evaluated after 45 days.

### Ex vitro acclimatization

The plantlets were removed from the culture medium, and their roots were washed with sterile distilled water to eliminate residual agar. A pre-acclimatization process was conducted in trays covered with transparent plastic to create a microclimate of elevated relative humidity, which was gradually decreased. Subsequently, the plantlets were transplanted into black low-density polyethylene (LDPE) bags containing UV additives, produced by the Peruvian company Maruplast. These bags were filled with a substrate composed of fine sand and agricultural soil at a 2:1 ratio and placed in a greenhouse to facilitate adaptation to external environmental conditions.

### Experimental design and statistical analysis

The experiment was conducted using a completely randomized design (CRD), with each experimental unit consisting of a single cultured explant. For *in vitro* establishment, five explants per treatment were used, while 16 explants were used for multiplication. The Shapiro–Wilk test assessed the normality of sample distributions, and Bartlett's test verified homogeneity of variance. *In vitro* establishment data were analyzed by analysis of variance (ANOVA), and treatment means were compared using Tukey's test at  $P \leq 0.05$  (Nanda et al. 2021). *In*

*vitro* multiplication data that did not meet assumptions of normality and homogeneity were analyzed using the non-parametric Kruskal–Wallis test to determine significant differences among treatments. Dunn's post-hoc test was performed to identify group differences at a significance level of  $P \leq 0.05$ . All analyses were performed using R version 4.4.2 for Windows.

## RESULTS AND DISCUSSION

### In vitro establishment

*In vitro* establishment of sweet cucumber (*S. muricatum* Ait.), statistically significant differences were observed among treatments based on the type and concentration of growth regulator used. Regarding plantlet height, the treatment with 1.5 mg L<sup>-1</sup> of indole-3-acetic acid (IAA) produced the highest mean value (2.69 cm), suggesting that this concentration effectively promotes plantlet height development. On the other hand, the treatment with 2.0 mg L<sup>-1</sup> of IAA resulted in the lowest mean height (1.53 cm), indicating a potential inhibitory effect on growth caused by the higher concentration of the growth regulator.

In terms of leaf number, the combination of 1.0 mg L<sup>-1</sup> (IBA) and 0.5 mg L<sup>-1</sup> (IAA) yielded the highest mean value of 6.40 cm, suggesting that these concentrations are optimal for promoting foliar development. In contrast, the treatment with 2.0 mg L<sup>-1</sup> (IBA) and 2.0 mg L<sup>-1</sup> (IAA) resulted in the lowest leaf number, indicating a potential inhibitory effect associated with higher growth regulator concentrations.

For root length and root number, 1.5 mg L<sup>-1</sup> (IAA) yielded the most favorable results, with mean values of 1.48 and 9.50 cm, respectively. Conversely, 2.0 mg L<sup>-1</sup> (IBA) was the least effective, resulting in a mean root length of 0.11 cm and only 1.10 cm on average. Detailed data for all treatments are provided in Table 1.

**Table 1.** Effect of Growth Regulators (PGR) on *in vitro* establishment of sweet cucumber (*Solanum muricatum* Ait).

Plant Growth Regulator	Concentration (mg L <sup>-1</sup> )	Shoot length (cm)	Number of leaves	Root length (cm)	Number of roots
Control	0	1.93 <sup>bcd</sup>	5.50 <sup>ab</sup>	1.36 <sup>bc</sup>	2.70 <sup>cd</sup>
	0.5	1.93 <sup>bcd</sup>	6.20 <sup>ab</sup>	2.75 <sup>a</sup>	4.40 <sup>bc</sup>
IBA	1.0	2.46 <sup>ab</sup>	6.40 <sup>a</sup>	1.26 <sup>bc</sup>	3.30 <sup>cd</sup>
	1.5	1.65 <sup>cd</sup>	5.00 <sup>ab</sup>	0.15 <sup>d</sup>	3.30 <sup>cd</sup>
	2.0	1.57 <sup>d</sup>	4.70 <sup>b</sup>	0.11 <sup>d</sup>	1.10 <sup>d</sup>



Table 1

Plant Growth Regulator	Concentration (mg L <sup>-1</sup> )	Shoot length (cm)	Number of leaves	Root length (cm)	Number of roots
IAA	0.5	2.21 <sup>abc</sup>	6.40 <sup>a</sup>	0.62 <sup>cd</sup>	1.60 <sup>d</sup>
	1.0	1.87 <sup>cd</sup>	6.30 <sup>a</sup>	0.43 <sup>d</sup>	2.10 <sup>cd</sup>
	1.5	2.69 <sup>a</sup>	6.00 <sup>ab</sup>	1.48 <sup>b</sup>	9.50 <sup>a</sup>
	2.0	1.53 <sup>d</sup>	6.20 <sup>ab</sup>	1.42 <sup>b</sup>	6.80 <sup>a</sup>

Values followed by different letters within each column are significantly different according to Tukey's test (\*\* $P \leq 0.05$ ).

Moreover, IAA treatments were superior, resulting in increased plant height, leaf number, and root production

(Figure 1B), in comparison with IBA treatments (Figure 1A) and the control.

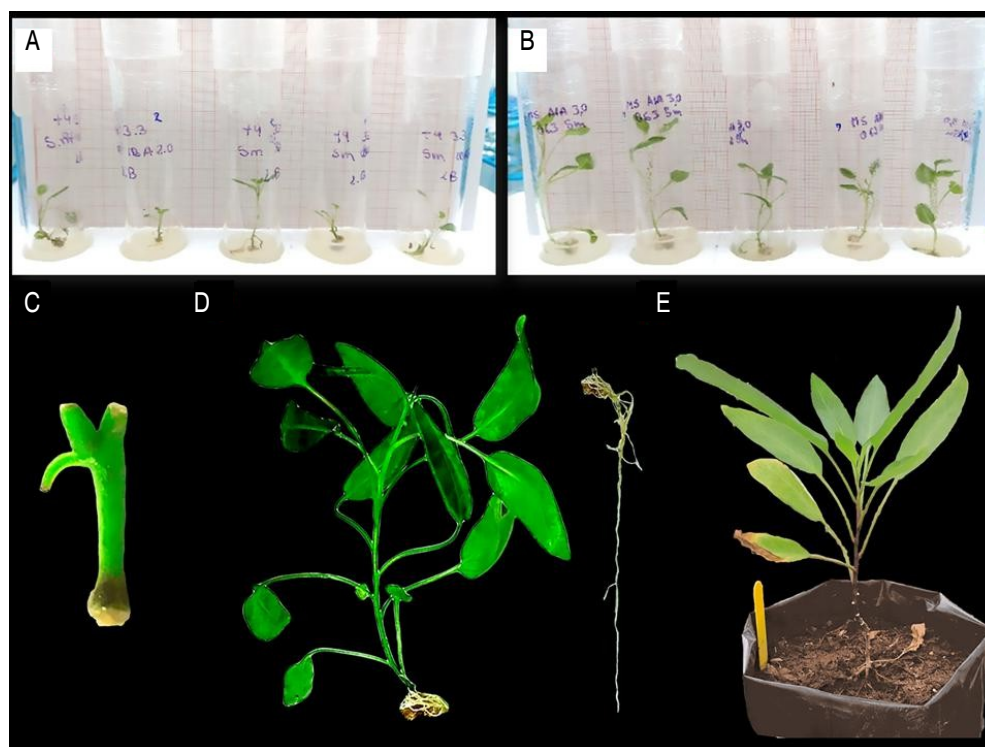


**Figure 1.** *In vitro* establishment and multiplication of sweet cucumber (*S. muricatum* Ait.). **A.** Treatment supplemented with IBA (2.0 mg L<sup>-1</sup>) during *in vitro* establishment; **B.** Treatment supplemented with IAA (1.5 mg L<sup>-1</sup>) during *in vitro* establishment; **C.** Shoots without roots in MS medium supplemented with BAP (1.0 mg L<sup>-1</sup>); **D.** Plantlet with fully developed roots in medium enriched with IAA+BAP (1.0 + 0.1 mg L<sup>-1</sup>); **E.** An *in vitro*-grown plant is fully acclimatized to *ex vitro* conditions.

The synergistic effect of auxins has been shown to induce notable responses in solanaceous crops, significantly influencing leaf number, shoot height, root number, and root length. Studies such as Rehman et al. (2019) reported that the combination of BAP (1.2 mg L<sup>-1</sup>) + IBA (2.0 mg L<sup>-1</sup>) led to increased numbers of roots and shoots, achieving a hormonal balance. Similarly, Iftikhar et al.

(2015) observed efficient rooting in *Solanum villosum* with 1.0 mg L<sup>-1</sup> of IBA, which aligns with the present study on *S. muricatum*, as IBA stimulates the H<sup>+</sup>-ATP<sub>ase</sub> proton pump in the plasma membrane, acidifying the cell wall and activating proteins that facilitate cell elongation under turgor pressure. *Solanum muricatum*, phylogenetically related to major commercial crops such as *S. lycopersicum* and

*S. tuberosum* (Saldaña et al. 2022), has shown a similar response to auxin treatments. Higher concentrations of indole-3-acetic acid (IAA) have been observed to elicit better responses in these two crops (Agurto et al. 2024). In contrast, indole-3-butyric acid (IBA) tends to yield better results at lower concentrations. The application of IBA at 1.0 mg L<sup>-1</sup> in *S. muricatum* resulted in a high shoot length (2.46 cm), as shown in Table 1, indicating a stimulating effect on shoot growth. This finding is consistent with Jabeen et al. (2021) in *Solanum tuberosum*, where moderate concentrations of IBA promoted optimal shoot elongation. Several studies have demonstrated that IBA has a greater capacity to promote adventitious root formation compared to IAA. Furthermore, IBA is more stable and less susceptible to enzymatic degradation, making it a more efficient source of free auxin. However, the present results for *S. muricatum* suggest that IAA may be more effective, as also reported by Cavusoglu and Sulusoglu-Durul (2013), highlighting the need for further exploration of optimal auxin conditions depending on the species and the developmental process under investigation.

### In vitro multiplication

Explants of *S. muricatum* Ait. cultivated in MS medium supplemented with combinations of auxins and cytokinins (IAA+BAP and IBA+BAP) produced the highest number of shoots. The treatment with IBA+BAP (1.0 + 0.1 mg L<sup>-1</sup>)

yielded the best results, with an average of 7.5 shoots. However, this treatment did not show a statistically significant difference compared to treatments with 0.5 and 1.0 mg L<sup>-1</sup> of KIN. On the other hand, treatments with 0.5, 1.0, 1.5, and 2.0 mg L<sup>-1</sup> of BAP resulted in significantly lower averages, not exceeding 0.9 shoots, with minimal growth and callus formation at the cutting site (Figure 1C). This condition impeded root development and nutrient uptake during the initial stages, resulting in challenges to acclimatization due to unstructured morphogenesis, aberrant leaf formation, and hyperhydricity. Following 45 days of treatment, results demonstrated that combinations of auxins and cytokinins—specifically IAA + BAP and IBA + BAP—significantly improved plant size, vigor, firmness, and produced an intense, uniformly green coloration (Figure 1D).

After 45 days of cultivation, explants were evaluated based on the effects of different treatments. Combinations of auxins and cytokinins (IAA+BAP and IBA+BAP) produced significant variations in explant height. The treatment with 1.0 + 0.2 mg L<sup>-1</sup> (IAA+BAP) yielded the best results in terms of height, with an average of 7.7 cm, ranging from 3.7 to 11.5 cm. This treatment was significantly superior compared to others, such as those containing only KIN or BAP, which resulted in lower average shoot lengths (Table 2).

**Table 2.** Influence of plant growth regulators on *in vitro* shoot multiplication of sweet cucumber (*Solanum muricatum* Ait.).

Growth Regulator	Concentration (mg L <sup>-1</sup> )	Number of shoots	Shoot length (cm)	Root length (cm)	Number of leaves
KIN	0.5	3.6 <sup>ab</sup>	3.1 <sup>abc</sup>	4.7 <sup>ab</sup>	9 <sup>ab</sup>
	1.0	2.9 <sup>abc</sup>	2.9 <sup>abc</sup>	4.5 <sup>ab</sup>	7.9 <sup>abc</sup>
	1.5	1.9 <sup>bcd</sup>	2.1 <sup>bcd</sup>	4.1 <sup>ab</sup>	6.2 <sup>acd</sup>
	2.0	1.6 <sup>bcd</sup>	1.6 <sup>bd</sup>	2.8 <sup>bc</sup>	5 <sup>cde</sup>
BAP	0.5	0.9 <sup>cd</sup>	1.0 <sup>bd</sup>	0 <sup>c</sup>	4.1 <sup>cde</sup>
	1.0	0.8 <sup>d</sup>	0.8 <sup>d</sup>	0.1 <sup>c</sup>	2.9 <sup>de</sup>
	1.5	0.7 <sup>d</sup>	0.7 <sup>d</sup>	0 <sup>c</sup>	0.6 <sup>e</sup>
	2.0	0.8 <sup>d</sup>	0.7 <sup>d</sup>	0 <sup>c</sup>	0.4 <sup>e</sup>
IAA+BAP	1.0+0.1	7.2 <sup>a</sup>	6.5 <sup>ac</sup>	7.2 <sup>ab</sup>	10.6 <sup>ab</sup>
	1.0+0.2	6.7 <sup>a</sup>	7.7 <sup>a</sup>	10.8 <sup>a</sup>	11.9 <sup>b</sup>
IBA+BAP	1.0+0.1	7.5 <sup>a</sup>	7.2 <sup>a</sup>	7.6 <sup>a</sup>	9.4 <sup>ab</sup>
	1.0+0.2	6.9 <sup>a</sup>	7.3 <sup>a</sup>	8.5 <sup>a</sup>	10.5 <sup>ab</sup>

Values followed by different letters within each column are significantly different according to Tukey's test (\*\* $P \leq 0.05$ ).

*In vitro* multiplication of *S. muricatum* from explants in MS medium enriched with kinetin (KIN), a cytokinin, has proven effective for shoot formation and shoot elongation, particularly at concentrations of 0.5 and 1.0 mg L<sup>-1</sup>. In this regard, Toma et al. (2021) reported that during the multiplication phase, treatments with KIN at 1.0, 2.0, and 3.0 mg L<sup>-1</sup> produced averages of 1.6, 1.6, and 2.3 shoots, respectively, with shoot lengths of 2.16, 2.83, and 3.6 cm. In the present study, concentrations of 0.5 and 1.0 mg L<sup>-1</sup> resulted in average values of 2.9±0.7 and 1.6±0.5 shoots, and shoot lengths of 2.9±0.7 and 1.6±0.7 cm. Previous studies on *S. muricatum* have also shown that a combination of 2 + 1 mg L<sup>-1</sup> (BAP+KIN) yields the best response in shoot number, while 1 + 1 mg L<sup>-1</sup> (BAP+KIN) is optimal for shoot length (Aghdaei et al. 2019).

As for BAP-based treatments, they were the least effective compared to other approaches. However, among BAP-only treatments, concentrations of 0.5 and 1.0 mg L<sup>-1</sup> showed the best performance, with averages of 0.9±0.3 and 0.8±0.4 shoots and shoot lengths of 1.0±0.4 and 0.8±0.4 cm, respectively. These findings contrast with those reported by Cavusoglu and Sulusoglu-Durul (2013), who found that optimal BAP concentrations of 1, 2, and 3 mg L<sup>-1</sup> resulted in shoot numbers of 3.33, 4.58, and 4.35, and shoot lengths of 1.49, 1.21, and 0.88 cm, respectively. Interestingly, the control treatment without any growth regulator outperformed all BAP treatments in shoot number. This discrepancy may be attributed to possible inhibition caused by the culture medium, which contains additional vitamins. While BAP is known to play a role in plant growth and development during organogenesis (Khatoun et al. 2022), the specific medium conditions in this study may have negatively affected its efficacy. Notably, in other solanaceous crops such as *Solanum tuberosum* (Nezami et al. 2018), *S. lycopersicum* (Kumari et al. 2024), and *S. melongena* (Foo et al. 2018), BAP has shown positive responses in shoot induction. These findings suggest that BAP effectiveness can vary considerably depending on the medium and the plant species used in the experiment. As noted by García and Javier (2016), morphological responses are determined by genotype and medium composition. Furthermore, optimal organogenesis is achieved through a specific balance between auxins and cytokinins, and their concentrations—used individually or in combination—depend on the developmental process being targeted (Alcantara-Cortes et al. 2019).

Treatments with auxins and cytokinins (IAA+BAP and IBA+BAP) resulted in the highest numbers of leaves. The treatment with 1.0 + 0.2 mg L<sup>-1</sup> (IAA+BAP) produced the best results, with an average of 11.9 leaves, ranging from 8 to 26. This treatment outperformed others, including 1.0+0.1 mg L<sup>-1</sup> (IAA+BAP), which had an average of 10.6 leaves. However, IBA+BAP treatments were also effective, with averages of 9.4 and 10.5 leaves. In contrast, KIN and BAP used individually showed significantly lower performance in leaf production, especially at higher BAP concentrations, which caused developmental issues such as thinner stems, reduced vigor, lower resistance, and pale coloration.

Explants treated with 1.0+0.2 mg L<sup>-1</sup> IAA+BAP showed the best root length results, averaging 10.8 cm (range: 4.0–19.5 cm). IBA+BAP treatments also showed effectiveness, with mean root lengths of 7.6 and 8.5 cm. Figure 1D shows a plant with well-formed green leaves and an adequate root system capable of nutrient uptake, supporting development and acclimatization to *ex vitro* conditions. Auxins like IAA and IBA play a key role in the early stages of root formation. However, KIN and BAP alone resulted in significantly lower root lengths, particularly at higher BAP concentrations, as observed in Figure 1C, where no roots or leaves were visible.

*In vitro* multiplication of *S. muricatum* showed the best responses in terms of number of leaves and root length when treated with auxin + cytokinin combinations (IAA+BAP or IBA+BAP). It has been reported that 1.0 mg L<sup>-1</sup> BAP and 3.0 mg L<sup>-1</sup> KIN are individually effective for leaf formation (Toma et al. 2021). Particularly, good root lengths were observed with 0.2 and 0.3 mg L<sup>-1</sup> IAA and 0.1 mg L<sup>-1</sup> IBA, averaging over 6.33 cm, especially in media enriched with 3.0 mg L<sup>-1</sup> KIN. These findings support the effectiveness of auxin-cytokinin combinations in promoting vegetative structure formation in this species. Nonetheless, the combined treatments (IAA+BAP and IBA+BAP) were superior across all parameters evaluated, partially aligning with the findings by Toma et al. (2021). Furthermore, BAP treatments were not as effective for root induction, as also documented by Cavusoglu and Sulusoglu-Durul (2013).

Statistical analysis confirmed that IAA+BAP and IBA+BAP combinations were significantly more effective for multiplication compared to KIN or BAP alone. Specifically, the combination 1.0+0.2 mg L<sup>-1</sup> (IAA+BAP) achieved a

shoot length average of 1.08 cm, while 1.0±0.2 mg L<sup>-1</sup> (IBA+BAP) reached 8.5 cm. Additionally, IBA has proven effective for root formation in *S. lycopersicum* (Alatar et al. 2017) and for root elongation in *S. tuberosum* (Jabeen et al. 2021). Similarly, IAA has shown high efficiency in both root formation and elongation (Bentes et al. 2022), supporting its inclusion in media aimed at root development.

### **Ex vitro acclimatization**

After *in vitro* rooting, plantlets were pre-acclimatized for five days under high humidity, which was then reduced to harden the cuticle and minimize water loss. A 2:1 fine sand to agricultural soil mix achieved 95% survival after 45 days, with no pathogen issues. Figure 1E shows a vigorous plant with normal growth and no abnormal morphological features. Cavusoglu and Sulusoglu-Durul (2013) reported an 80–100% adaptation rate for this species. Similarly, Toma et al. (2021) achieved a 100% survival rate by acclimatizing plantlets in a greenhouse. In *S. tuberosum*, a 100% survival rate was reached after 28 days using a peat substrate, and a 90% acclimatization rate was achieved using a 2:1 peat-to-sand ratio (Aleaga 2023). Tacoronte et al. (2017) reported that the use of cellophane bags mitigated stress during acclimatization, while high humidity conditions enabled previously malformed *in vitro* roots to become fully functional. The success of this stage is contingent upon effective *in vitro* root development and the plantlets' progressive adaptation to their environment, given that *in vitro*-derived plantlets depend on external carbon sources from the culture medium rather than photosynthesis. Furthermore, these plantlets are maintained under low-light and high-humidity conditions, which are markedly different from those encountered in their natural habitats.

### **CONCLUSION**

*In vitro* plant regeneration and shoot proliferation are key processes in plant micropropagation systems. The study indicates that indole-3-acetic acid (IAA) influences the *in vitro* regeneration of sweet cucumber through organogenesis and assists root induction. Additionally, when higher concentrations of auxin (IAA) are combined with lower concentrations of cytokinin (BAP) in MS medium, increased shoot proliferation from explants is observed. These findings suggest that the auxin-to-cytokinin ratio in the culture medium influences morphogenetic responses in *S. muricatum*. The present study provides preliminary data that can contribute to optimizing the use of plant

growth regulators in the micropropagation of this species and guide future protocol adjustments.

### **ACKNOWLEDGMENTS**

The authors express their sincere gratitude to the Universidad Nacional de Cañete for the funding provided through the Semillero de Investigación program, supported by Presidential Resolution No. 212-2022-CO-UNDC/P. This support has been instrumental in the development of this research, fostering significant advancements in scientific investigation and benefiting both undergraduate students and faculty members.

### **CONFLICT OF INTEREST**

The authors declare no conflict of interest.

### **REFERENCES**

- Aghdaei M, Nemati S, Samiei L and Sharifi A (2019) Effect of Medium and Plant Growth Regulators on Micropropagation of Pepino (*Solanum muricatum* Aiton) *in vitro* Condition. *Journal of Horticultural Science* 33(3): 467–479. <https://doi.org/10.22067/jhorts4.v33i3.76833>
- Agurto C, Michel L, Frías F, Chinachi W, Pinto T et al (2024) Effect of different phytohormones on *in vitro* multiplication of *Solanum tuberosum* L. var. Cecilia. *Bionatura Journal* 1: 1–20. <https://doi.org/10.70099/BJ/2024.01.03.22>
- Alatar A, Faisal M, Abdel-Salam E, Canto T, Saquib Q et al (2017) Efficient and reproducible *in vitro* regeneration of *Solanum lycopersicum* and assessment genetic uniformity using flow cytometry and SPAR methods. *Saudi Journal of Biological Sciences* 24(6): 1430–1436. <https://doi.org/10.1016/j.sjbs.2017.03.008>
- Alcantara-Cortes J, Acero-Godoy J, Alcantara-Cortes J, Sánchez-Mora R et al (2019) Principales reguladores hormonales y sus interacciones en el crecimiento vegetal. *Nova* 17(32): 109–129. [http://www.scielo.org.co/scielo.php?script=sci\\_arttext&pid=S1794-24702019000200109](http://www.scielo.org.co/scielo.php?script=sci_arttext&pid=S1794-24702019000200109)
- Aleaga P (2023) Influencia de fitohormonas en la regeneración *in vitro* de *Solanum tuberosum* L. vía organogénesis directa. <https://repositorio.uta.edu.ec/handle/123456789/37455>
- Angulo P (2024) Conoce la fruta exótica de los incas que ayuda a regular los niveles de glucosa y es beneficiosa para el corazón. <https://www.infobae.com/peru/2024/05/16/descubre-la-fruta-exotica-de-los-incas-que-ayuda-a-regular-los-niveles-de-glucosa-y-es-beneficiosa-para-el-corazon/>
- Campos D, Chirinos R, Gálvez-Ranilla L and Pedreschi R (2018) Chapter Eight—Bioactive potential of andean fruits, seeds, and tubers. In F. Toldrá (Ed.), *Advances in Food and Nutrition Research* (Vol. 84, pp. 287–343). Academic Press. <https://doi.org/10.1016/bs.afnr.2017.12.005>
- Cavusoglu A and Sulusoglu-Durul M (2013) *In vitro* propagation and acclimatization of pepino (*Solanum muricatum*). *Journal of Food, Agriculture and Environment* 11: 410–415. <https://www.wfpublisher.com/Abstract/3897>
- Bentes L, Andrade M, Castellane T, Carvalho R, Rigobelo E et al (2022) Effect of indole-3-acetic acid on tomato plant growth. *Microorganisms* 10(11): 2212. <https://doi.org/10.3390/>



microorganisms10112212

Foo P, Lee Z, Chin C, Subramaniam S, Chew B et al (2018) Shoot induction in white eggplant (*Solanum melongena* L. Cv. Bulat Putih) using 6- Benzylaminopurine and kinetin. Tropical Life Sciences Research 29(2): Article 2. <https://doi.org/10.21315/tlsr2018.29.2.9>

García H and Javier F (2016) Desarrollo de herramientas morfológicas y genómicas para el estudio del pepino dulce (*Solanum muricatum*) y especies relacionadas. Caracterización de su valor nutracéutico, Universitat Politècnica de València.

González S, Bazán G and Chavez L (2015) *Solanum Lycopersicum* L. "Tomate" y *Solanum muricatum* Aiton "Pepino" (Solanaceae) dos frutas utilizadas en el Perú Prehispánico. Araldoa 22(1): Article 1. <https://www.biodiversitylibrary.org/part/220555>

Gonzales-Arteaga J, Rodríguez-Layza J, Romero-Rivas L, Párraga-Quintanilla A and Olivera-Soto J (2023) El rol del AIA y BAP en la regeneración y formación de brotes *in vitro* de tres variedades de fresa (*Fragaria x ananassa* Duch). Agroindustrial Science 13(2): 93-102. <https://revistas.unitru.edu.pe/index.php/agroindscience/article/view/5446/5597>

Iftikhar A, Qureshi R, Munir M, Shabbir G, Hussain M et al (2015) *In vitro* micropropagation of *Solanum villosa* potential alternative food plant. Pakistan Journal of Botany 47: 1495–1500.

Jabeen F, Arshad M, Qayyum M, Zaman M and Shafique I (2021) Exploring the effects of indole butyric acid (IBA) on *in vitro* growth of potato (*Solanum tuberosum*). Advances in Agriculture and Biology 4(1): Article 1. <https://doi.org/10.63072/aab.21005>

Khatoun S, Liu W, Ding C, Liu X, Zheng Y et al (2022) *In vitro* Evaluation of the effects of BAP concentration and pre-cooling treatments on morphological, physiological, and biochemical traits of different olive (*Olea europaea* L.) cultivars. Horticulturae 8(12): Article 12. <https://doi.org/10.3390/horticulturae8121108>

Kim O, Ishikawa T, Yamada Y, Sato T, Shinohara H et al (2017) Incidence of pests and viral disease on pepino (*Solanum muricatum* Ait.) in Kanagawa Prefecture, Japan. Biodiversity Data Journal 5: e14879. <https://doi.org/10.3897/BDJ.5.e14879>

Kumari A, Nagpal A and Katnoria J (2024) Potential of some explants for callus induction and plantlet regeneration in *Solanum lycopersicum* L. under treatment of different plant growth regulators. Biotechnologia 105(3): 227–247. <https://doi.org/10.5114/bta.2024.141803>

Nanda A, Bhusan B, Kumar A, Kumar A and Kumar A (2021) Multiple

comparison test by Tukey's honestly significant difference (HSD). International Journal of Statistics and Applied Mathematics 6(1A): 59–65. <https://doi.org/10.22271/math.2021.v6.i1a.636>

Nezami A, Nabati J and Erwin J (2018) Sprouting, plant establishment, and yield improvement of potato (*Solanum tuberosum* L.) minituber cultivars by foliar application of benzylaminopurine and abscisic acid. Journal of Crop Production 10(4): 75–90. <https://doi.org/10.22069/ejcp.2018.12071.1929>

Pickersgill B (2007) Domestication of plants in the americas: insights from mendelian and molecular genetics. Annals of Botany 100(5): 925–940.

Rehman M, Khan, M, Ahmad M and Ali S (2019) *In vitro* regeneration of *Solanum lycopersicum* L. from different explants. Biomedical Letters 5(2): 67–75.

Saldaña C, Chávez-Galarza J, Cruz G, Jhoncon J, Guerrero-Abad J et al (2022) Revealing the complete chloroplast genome of an andean horticultural crop, sweet cucumber (*Solanum muricatum*), and its comparison with other Solanaceae species. Data 7(9): Article 9. <https://doi.org/10.3390/data7090123>

Shahnawaz Pandey D, Konjengbam M, Dwivedi P, Kaur P et al (2021) Biotechnological interventions of *in vitro* propagation and production of valuable secondary metabolites in *Stevia rebaudiana*. Applied Microbiology and Biotechnology 105(23): 8593–8614. <https://doi.org/10.1007/s00253-021-11580-9>

Sharry S, Adema M and Abedini W (2015) Plantas de probeta. Editorial de la Universidad Nacional de La Plata (EDULP). <https://doi.org/10.35537/10915/46738>

Tacoronte M, Olivo A and Chacín N (2017) Efectos de nitratos y sacarosa en la propagación *in vitro* de tres variedades de papa nativa. Revista Colombiana de Biotecnología 19(2): Article 2. <https://doi.org/10.15446/rev.colomb.biote.v19n2.70160>

Toma R, Faizy W, Tamer Y and Khaza'al W (2021) Auxins and cytokinins involved in micropropagation of pepino plant (*Solanum muricatum* Aiton). Diyala Agricultural Sciences Journal 13(1): Article 1. <https://doi.org/10.52951/dasj.21130103>

Torrent D (2014) Caracterización morfológica y molecular de pepino dulce (*Solanum muricatum*) y especies silvestres relacionadas. <https://riunet.upv.es/server/api/core/bitstreams/a9bd599a-e617-4859-9a2e-4ea1dd2d6089/content>

# Non-destructive estimation of leaf area in hairy fleabane (*Conyza bonariensis*)

Estimación no destructiva del área foliar en rama negra (*Conyza bonariensis*)

<https://doi.org/10.15446/rfnam.v78n3.118970>

Mariana Macedo<sup>1</sup>, Bruno Mussoi Cavichioi<sup>1</sup>, Glauco Pacheco Leães<sup>1</sup>, Lillian Osmari Uhlmann<sup>2</sup>, Ary José Duarte Junior<sup>2</sup>, Tilio Adan Lucas<sup>1</sup> and André da Rosa Ulguim<sup>1\*</sup>

## ABSTRACT

### Keywords:

BIAS index  
Dimensional parameters  
Leaf length  
Leaf width  
Morphometric models

Hairy fleabane (*Conyza bonariensis*) is a widespread and troublesome weed in agricultural systems, and estimating its leaf area (LA) is essential for growth analysis and weed management studies. This study aimed to develop equations to estimate the LA based on the linear dimensions of leaf blades. The relationships between the LA and the dimensional parameters of leaf blade (length and width) were studied in *C. bonariensis* var. *angustifolia* and *C. bonariensis* var. *bonariensis*. Both linear and power regression models were tested, and their performance was assessed using Root Mean Square Error (RMSE), index of agreement (dw), BIAS index, Pearson's linear coefficient (r), and index of confidence or performance (c). The best-performing model used the product of length and width (L×W), yielding the highest r values and the lowest RMSE for both botanical varieties. Specific models provided better estimates than the general model. The linear equations  $LA = 0.6578 \times (L \times W)$  and  $LA = 0.5896 \times (L \times W)$  for *C. bonariensis* var. *angustifolia* and *C. bonariensis* var. *bonariensis*, respectively, were the most accurate for estimating their LA. These equations offer reliable, non-destructive tools for estimating LA in studies involving each variety, contributing to improved precision in weed science research.



## RESUMEN

### Palabras clave:

Índice BIAS  
Parámetros dimensionales  
Longitud de la hoja  
Anchura de la hoja  
Modelos morfométricos

La rama negra (*Conyza bonariensis*) es una maleza extendida y problemática en los sistemas agrícolas, y la estimación de su área foliar (AF) es esencial para el análisis del crecimiento y los estudios de manejo de malezas. El objetivo del estudio fue determinar ecuaciones para estimar el AF con base en dimensiones lineales de las láminas foliares. Se estudiaron las relaciones entre el AF y los parámetros dimensionales del limbo (longitud y anchura) en *C. bonariensis* var. *angustifolia* y *C. bonariensis* var. *bonariensis*. Se evaluaron modelos de regresión lineales y potenciales, y su desempeño se evaluó utilizando el Error cuadrático medio (RMSE), index of agreement (dw), índice BIAS, coeficiente lineal de Pearson (r) y el index of confidence or performance (c). El mejor modelo fue la basada en el producto longitud y anchura (L×A), ya que presentó los valores más altos de r y los más bajos de RMSE para ambas variedades botánicas. Los modelos específicos para cada variedad proporcionaron mejores estimaciones que un modelo general. Las ecuaciones  $AF = 0,6578 \times (L \times A)$  y  $AF = 0,5896 \times (L \times A)$  para *C. bonariensis* var. *angustifolia* y *C. bonariensis* var. *bonariensis*, respectivamente, fueron las más precisas. Estas ecuaciones constituyen herramientas confiables y no destructivas para la estimación del área foliar en estudios que involucran cada variedad, contribuyendo a mejorar la precisión en la investigación en ciencias de malezas.

<sup>1</sup>Department of Crop Protection, Federal University of Santa Maria (UFSM), Santa Maria, Brazil. [mariana\\_dx@hotmail.com](mailto:mariana_dx@hotmail.com) , [cavichiolibruno@yahoo.com.br](mailto:cavichiolibruno@yahoo.com.br) , [glaucoleaes@gmail.com](mailto:glaucoleaes@gmail.com) , [tiliolucasp@gmail.com](mailto:tiliolucasp@gmail.com) , [andre.ulguim@ufsm.br](mailto:andre.ulguim@ufsm.br) 

<sup>2</sup>Department of Plant Sciences, Federal University of Santa Maria (UFSM), Santa Maria, Brazil. [lillian.uhlmann@ufsm.br](mailto:lillian.uhlmann@ufsm.br) , [ary.duarte@gmail.com](mailto:ary.duarte@gmail.com) 

\*Corresponding author



**H**airy fleabane (*Conyza bonariensis* (L.) Cronq.) is responsible for significant yield losses in many crops in Brazil (Yamashita et al. 2011). It is currently an important weed in pastures and crops, especially wheat, soy, and corn (Silva et al. 2020; Oliveira et al. 2021). The species originates in the subtropical regions of South America and belongs to the Asteraceae family, and it has an annual cycle. There are varieties within the same species, which differ in some botanical characteristics, as is the case of *C. bonariensis* var. *bonariensis* with capitulescence corymbiform and frequently flat-topped, while *C. bonariensis* var. *angustifolia* has pyramidal capitulescence which can reach up to 1.20 m in height, with a slightly branched and densely leafy stem (Kalsing et al. 2024). *Conyza bonariensis* var. *angustifolia* often has narrower leaves in the vegetative stage than those observed at *C. bonariensis* var. *bonariensis*.

*Conyza bonariensis* (L.) has a high potential to produce seeds which germinate in autumn/winter and whose cycle ends in spring and summer (Soares et al. 2017). A single plant can produce more than 800,000 viable seeds (Kaspary et al. 2017). The seeds are easily dispersed by the wind and can reach distances greater than 100 m (Constantin et al. 2013). This fact, combined with the high rate of propagule production, favors the formation of a seed bank (Paula et al. 2011). The high number of seeds in the soil and the fact that this species can easily adapt to different environments (Soares et al. 2017; Vargas et al. 2018) contribute to its success in colonizing cultivated areas at high densities (Paula et al. 2011). The occurrence of high densities of hairy fleabane in crop production areas is the fact that the species has been reported to be resistant to different mechanisms of herbicidal action (Heap 2025), which makes the adoption of chemical control difficult.

Because of the difficulties to hairy fleabane control it is an extremely relevant species for agriculture, as it causes significant losses in crop yield (Agostinetto et al. 2018). Understanding the growth and development of weed species helps to recommend management practices. Several research studies are frequently carried out with the growth of hairy fleabane and need, for example, to determine its leaf area (LA) and the leaf area index (LAI). LA determination is important for the evaluation of photosynthetic capacity and light interception in weed-crop competition (Raniero et al. 2023) and in the contact surface

of the herbicide with the leaf. The ratio of the LA to the soil area occupied by the plant can be used to determine the LAI, one of the most used ecophysiological indexes to study leaf growth and development (Schwab et al. 2014).

There are several ways to estimate the LA of plants, but they usually require expensive equipment and, sometimes, destructive methods as well. Then, it can be considered as one of the most difficult growth parameters to be measured. Methods for measurement of the LA can be classified as destructive (direct), in which all the leaves of the plant are usually collected, and non-destructive (indirect), which allows to follow the growth and leaf expansion of the same plant until the end of its productive cycle, i.e., the leaves are not collected (Fang et al. 2019). This way, the leaves are preserved if there is a need for further studies (Olfati et al. 2010). Such a method has been described in cultivated species and weeds, such as *Helianthus annuus* L. (Aquino et al. 2011), *Ipomoea hederifolia* and *Ipomoea nil* (Bianco et al. 2007), based on linear measurements of their leaf blade.

Little is known about non-destructive methods for the determination of the LA of hairy fleabane, and there are no validated equations based on leaf length and width, but this information should be further investigated. Given the lack of reliable non-destructive models for this species, this study aims to determine equations to estimate the LA of two varieties of hairy fleabane according to the linear dimensions of their leaf blades by the non-destructive method.

## MATERIALS AND METHODS

The experiment was conducted at the Federal University of Santa Maria, in Santa Maria, state of Rio Grande do Sul, Brazil (latitude: 29°43'23"; longitude 53°43'15"; altitude: 95 m). Local climate is Cfa, according to the Köppen classification, i.e., humid subtropical with hot summers and without a defined dry season (Beck et al. 2018). The present study focused on two botanical varieties of *Conyza bonariensis*: *C. bonariensis* var. *angustifolia* and *C. bonariensis* var. *bonariensis*. These two varieties were selected because of their differences in leaf width and leaf length.

To estimate the equations that relate the individual leaf area (LA) to the linear dimensions, 25 perfect leaf blades

(without deformations), with an average height of 25 cm, were collected from the basal, intermediate and upper portions of five plants from each of the varieties, immediately before the analysis, when they were growing in the field.

After collection, the length (L) and the largest width (W) of the leaves were measured with the aid of a millimeter ruler, and then each leaf was scanned at 300 dpi. The individual area of each scanned leaf was then calculated using the Quant software, version 1.0.1. Based on the ratio of the LA to the linear dimensions, different types of equations from the linear models were tested: (Equation 1) when using the product of length and width, and predictive power: Equations 2 and 3 when only one of the leaf dimensions was used.

$$LA = a. (L.W) \quad (1)$$

$$LA = a. (L)^b \quad (2)$$

$$LA = a.(L.)^b \quad (3)$$

Where LA is the leaf area (cm<sup>2</sup>), L is the leaf length (cm), W is the largest leaf width (cm), a is the angular coefficient, and b is the predictive power coefficient.

In Equation 1, the angular coefficient (a) was estimated by linear regression, forcing the line to pass through the origin (b=1), which is more advisable, because when the measured area is equal to zero, the calculated area will also be zero. In Equations 2 and 3, the angular coefficient (a) was estimated by non-linear regression; the line tends to pass by the origin, where the coefficient is considered as null.

To test the performance and to validate Equations 1, 2, and 3, another 25 leaf blades (without deformations), with an average height of 25 cm, were collected from the whole parts of the plants to validate the model with leaves of different sizes from 5 plants of each of the varieties found in the field. After collection, the linear dimensions of the leaves were measured, and Equations 1, 2, and 3 were used. The leaves were later scanned, and their area was analyzed using the Quant v software. 1.0.1, as mentioned above.

To evaluate the performance of the Equations, the following statistical indices were used: Root mean square error (RMSE) (Equation 4), index of agreement (dw) (Equation 5), BIAS index (Equation 6), correlation coefficient (r)

(Equation 7), index of confidence or performance (c) (Equation 8), as follows.

$$RMSE = \left[ \sum_{i=1}^N \frac{(Pi - Oi)^2}{N} \right]^{0.5} \quad (4)$$

$$dw = 1 - \frac{\sum_{i=1}^n (Pi - Oi)^2}{\sum_{i=1}^n (|Pi - \bar{O}| + |Oi - \bar{O}|)^2} \quad (5)$$

$$BIAS = \frac{\sum_{i=1}^n Pi - \sum_{i=1}^n Oi}{\sum_{i=0}^n Oi} \quad (6)$$

$$r = \frac{\sum (Oi - \bar{O})(Pi - P)}{\left\{ \left[ \sum (Oi - \bar{O})^2 \right] \left[ \sum (Pi - P)^2 \right] \right\}^{0.5}} \quad (7)$$

$$c = r.dw \quad (8)$$

Where the equations 4, 5, 6, 7, Pi is the estimated LA values (cm<sup>2</sup> per leaf), P is the mean of the estimated LA values (cm<sup>2</sup> per leaf), Oi is the observed LA values (cm<sup>2</sup> per leaf),  $\bar{O}$  is the observed mean LA values (cm<sup>2</sup> per leaf) and N is the number of observations.

RMSE expresses the mean magnitude of errors estimated by the model (accuracy of interpolation), and the quality of the measured or estimated values is determined through positive numbers and numbers closer to zero (Alves et al. 2011). The BIAS index expresses the mean deviation of the estimated values in comparison to the observed values, thus indicating how much the model is being underestimated (negative value) or overestimated (positive value). Ideally, the value of the study model tends to be zero (De Leite and Andrade 2002). The correlation coefficient (r) measures the degree of linear correlation between two quantitative variables; in this case, if the association of the simulated data in comparison to the observed data is close to one, there will be a greater correlation between the simulated and the observed data, while the values close to 0 indicate absence of linear correlation (Figueiredo and Silva 2010). The confidence or performance index (c) indicates the performance of the methods; the values of this index range from 0.0 for no agreement to 1.0 for perfect agreement between the data (Camargo et al. 1997).

In addition to these statistics, the relationship between data on measured and calculated LA underwent simple regression analysis (Equation 9):

$$Y = a + bx \quad (9)$$

Where  $a$  is the linear coefficient (considered as zero in the analysis, to force the model to pass through the origin) and  $b$  is the angular coefficient, which must be as close as possible to the unit. The final model that was selected was the one with the highest  $R^2$  in the simple

linear regression between the values observed and those estimated by the models, which were chosen based on the criteria mentioned above.

## RESULTS AND DISCUSSION

The tests with the three equations used the linear dimensions of the leaves showed a good relationship with the leaf area (LA), with a coefficient ( $R^2$ ) above 0.90. This result indicates that the data fitted the tested models, which were adequate to calculate the LA of hairy fleabane (Figure 1).

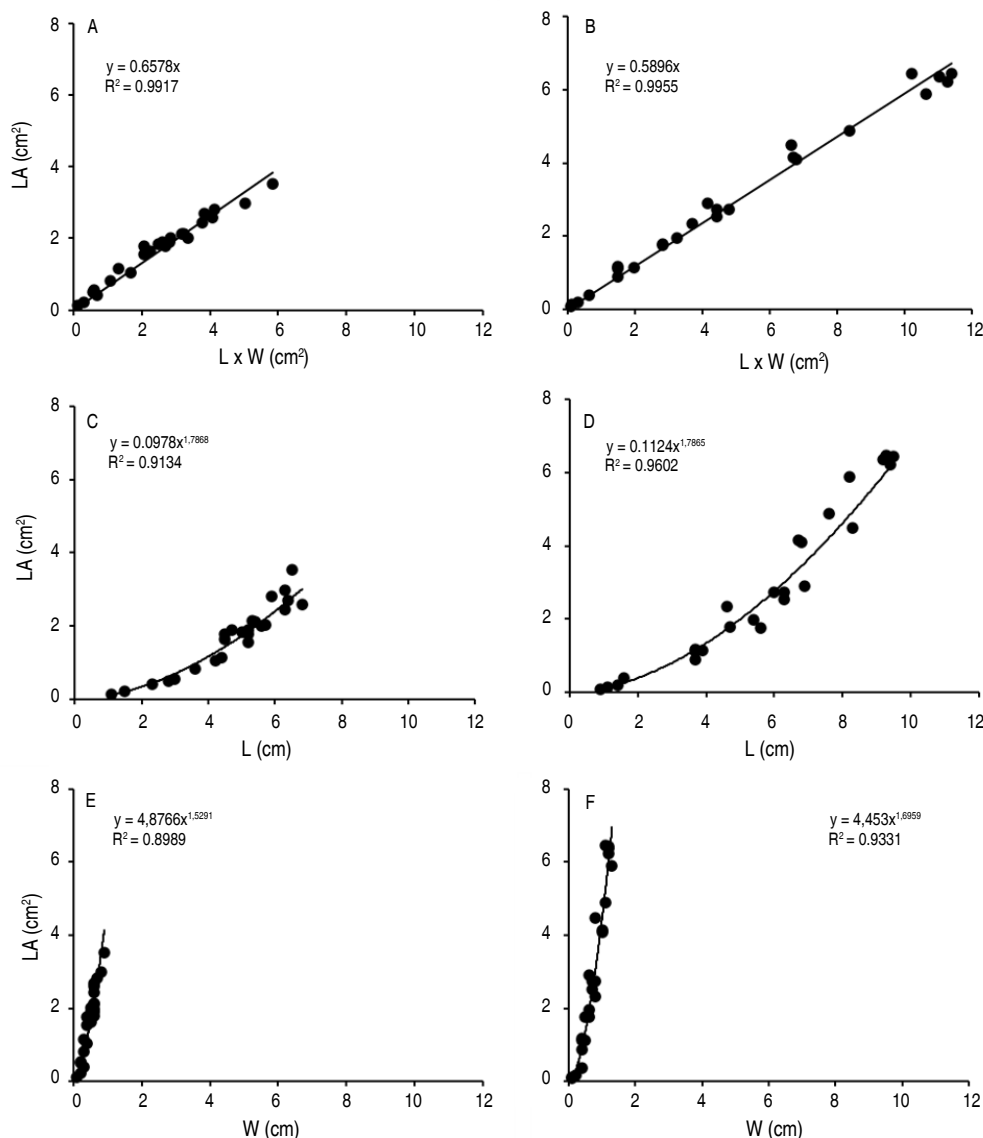


**Figure 1.** Relationship between measured leaf area (cm<sup>2</sup>) versus the product of length and width (L×W), length (L), and its width (W), for *Conyza bonariensis* var. *angustifolia* (A, C, E) and *Conyza bonariensis* var. *bonariensis* (B, D, F); the curve and the fitted equation in each panel are models indicated in Equations 1, 2, and 3, respectively.

For *Conyza bonariensis* var. *bonariensis*, the equations that used only one linear measure (W or L) were those that presented the lowest values of  $R^2$ , when compared to the product of its linear dimensions ( $L \times W$ ) (Figure 1). For *C. bonariensis* var. *angustifolia* the highest value of  $R^2$  was in the equation that used only the linear measurement of leaf length. It should be noted that in situations where only one of the linear dimensions is used as a predictor, coefficient b is greater than 1, which represents a non-linear relationship between the two variables (Schwab et al. 2014). Considering the principle of parsimony and the goodness of fit of simpler models, a univariate model with a linear leaf measurement is particularly valuable, as it can describe the LA of both species simultaneously.

When a simple linear Equation is used with the line passing through the origin, a single correction factor may be established; therefore, the use of such a factor is facilitated from a practical point of view (Bianco et al. 2007). For estimation of the LA of the hairy fleabane varieties, the relation of the product width and length (Equation 1) should be used with the linear equation. The linear model between LA and the product of L and W was also the one that showed the best estimate of the leaf area of gladiolus (Schwab et al. 2014).

Between the two hairy fleabane varieties, coefficient a of the simple linear regression of Equation 1, which represents the correction factor for estimating the LA, ranged from 0.589 to 0.657 (Figure 1). This small difference (0.068) indicates that the leaves of *Conyza bonariensis* var. *angustifolia* and *Conyza bonariensis* var. *bonariensis* are similar in shape, and a general equation can be used. As a result, a general equation covering the two botanical varieties was fitted:  $LA = 0.6022 \times (L \times W)$ , with  $R^2 = 0.98$ , indicating that 60.22% of the area is given by the product of length and width. This general equation was then tested with independent data for each variety, and its performance was assessed using statistical measures of predictive power (Table 1).

A comparison between the statistics (RMSE, dw, BIAS, and c) of performance of the specific variety equations ( $LA \text{ Model} = a \cdot (L \times W)$ ) and the same statistics but using the general equation ( $LA \text{ Model} = 0.6022 \cdot (L \times W)$ ) showed that, for *Conyza bonariensis* var. *angustifolia* and *Conyza bonariensis* var. *bonariensis*, the best performance was found when the specific variety equations were used (Table 1). More accurate estimates of the LA were found for *Ipomoea hederifolia* and *Ipomoea nil* using specific Equations (Bianco et al. 2007).

**Table 1.** Statistical measures of predictive power of the equations for estimating the leaf area (LA) of hairy fleabane based on its linear dimensions - length  $\times$  width ( $L \times W$ ), length (L), and width (W) with independent data.

Hairy fleabane	Statistical measure				
	RMSE	dw	BIAS	r	c
<b>Model <math>LA = a \cdot (L \times W)</math></b>					
<i>C. bonariensis</i> var. <i>angustifolia</i>	0.1599	0.9891	-0.0557	0.9832	0.9725
<i>C. bonariensis</i> var. <i>bonariensis</i>	0.3220	0.9947	0.0215	0.9935	0.9883
<b>Model <math>LA = a \cdot (L)^b</math></b>					
<i>C. bonariensis</i> var. <i>angustifolia</i>	0.2981	0.9565	-0.0001	0.9204	0.8803
<i>C. bonariensis</i> var. <i>bonariensis</i>	0.3970	0.9906	0.0451	0.9857	0.9764
<b>Model <math>LA = a \cdot (W)^b</math></b>					
<i>C. bonariensis</i> var. <i>angustifolia</i>	0.2978	0.9621	0.0299	0.9287	0.8935
<i>C. bonariensis</i> var. <i>bonariensis</i>	0.5085	0.9857	0.0022	0.9718	0.9578
<b>Model <math>LA = 0.6022 \cdot (L \times W)</math></b>					
<i>C. bonariensis</i> var. <i>angustifolia</i>	0.2318	0.9754	-0.1355	0.9832	0.9590
<i>C. bonariensis</i> var. <i>bonariensis</i>	0.3690	0.9932	0.0433	0.9935	0.9868

RMSE = Root mean square error; dw: agreement index; BIAS = BIAS index; r = Pearson's correlation coefficient; and c = confidence index.

Figure 2 shows the validation of the specific equations for each botanical variety. The analysis of data dispersion in the graphs shows good predictive power of the leaf area of hairy fleabane by measuring the linear dimensions of the product of length and width ( $L \times W$ ) of the leaf; higher RMSE was found for the two botanical varieties (Table 1). This can be inferred because the points are close to the

hypothetical 1:1 line, indicating that the measured area is close to the calculated area, and the angular coefficients of determination ( $R^2$ ) are closer to 1 (Figures 2A, D). It should be noted that there were small dispersions of the data in relation to the lines, which suggests that the specific equations may satisfactorily represent the actual LA.

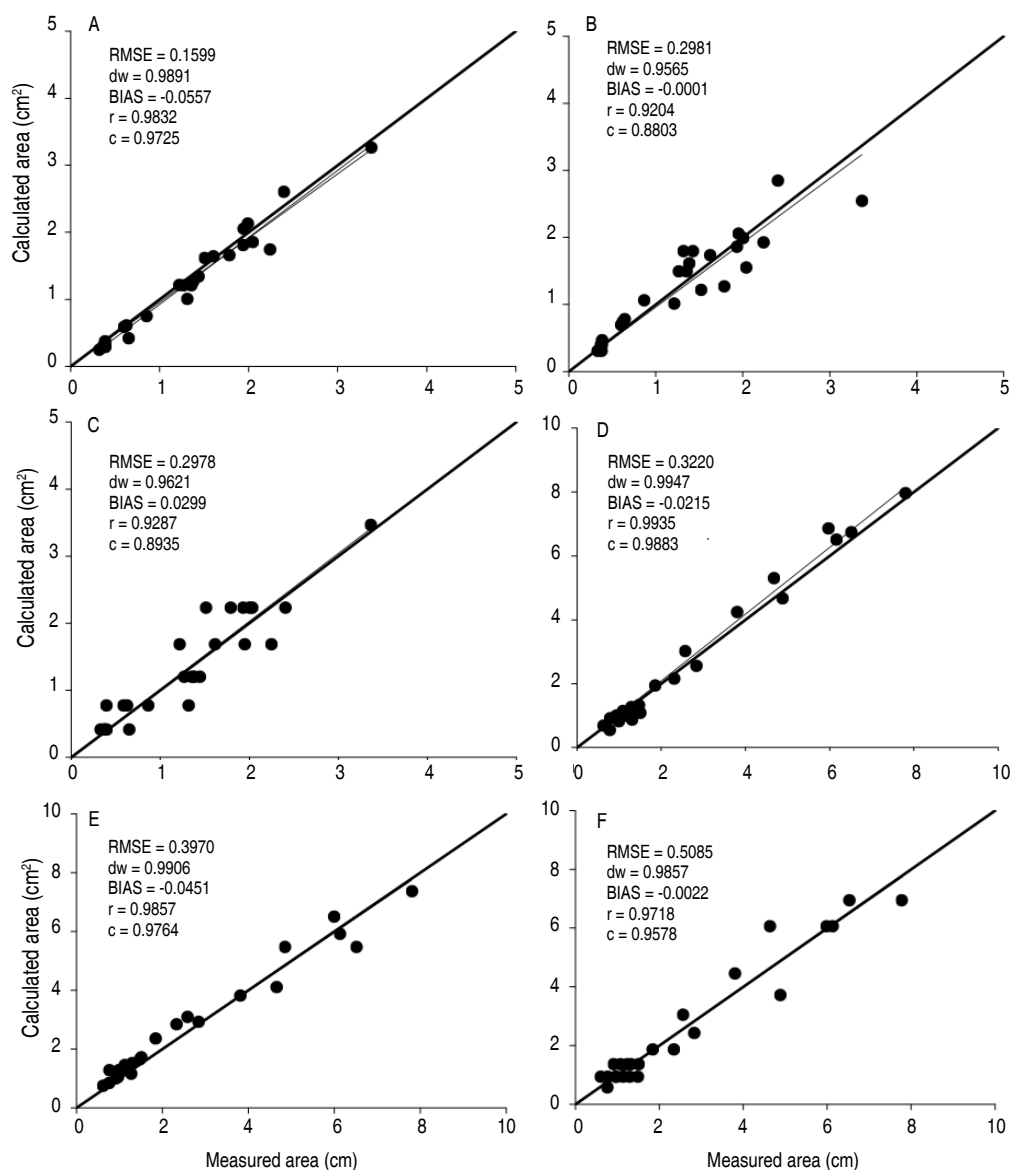


**Figure 2.** Leaf area calculated by the specific equations, based on the linear dimensions of the product of length and width ( $L \times W$ ) (A and D), length (L) (B and E), and width (W) (C and F) for *Conyza bonariensis* var. *angustifolia* (A, B, C) and *Conyza bonariensis* var. *bonariensis* (D, E, F), versus the area of the measured leaf ( $\text{cm}^2$ ).



It can usually be assumed that in the generation and performance of the model, the best result was found with the linear model, and both the specific equations and the general equation obtained in the present study can be used to estimate the LA of *Conyza bonariensis*. However, the most accurate estimates will be obtained by using the specific equations:  $LA = 0.6578 \times (L \times W)$ , for *Conyza bonariensis* var. *angustifolia* and  $LA = 0.5896 \times (L \times W)$ , for *Conyza bonariensis* var. *bonariensis*. The value of the shape coefficient  $a$  (Equation 1) obtained for *Conyza* spp is lower than that values for *Ipomea hederifolia* (Bianco et al. 2007), and *Sida rhombifolia* (Bianco et al. 2008).

The Equations obtained in the present study are important tools in studies on plant morphology. They can be used to investigate ecological adaptation, competition with other species, and management effects. Based on the present findings, further research can be conducted with weeds of the genus *Conyza*, without the need for destructive methods. Accordingly, LA and LAI in hairy fleabane botanical varieties can be reliably estimated through specific equations based on the length and width measurements of all plant leaves. In practice, measuring the length and width of the leaf is sufficient to accurately estimate the LA throughout the entire crop cycle.

## CONCLUSION

The non-destructive method, using the linear dimensions of the leaf blades, is appropriate for estimating the LA of hairy fleabane. The equations for specific varieties  $LA = 0.6578 \times (L \times W)$  and  $LA = 0.5896 \times (L \times W)$  for *Conyza bonariensis* var. *angustifolia* and *Conyza bonariensis* var. *bonariensis*, respectively, were the most accurate for estimating their LA. The equations can be used separately for studies estimating the LA of hairy fleabane in order to accurately and appropriately estimate the parameter for each botanical variety. This is important for improving experimental methods for these important weeds. Future studies could validate these models under field conditions or test their application in other *Conyza* species, thereby expanding the scientific understanding and practical use of LA estimation in weed ecology.

## ACKNOWLEDGMENTS

The authors would like to thank the Federal University of Santa Maria (UFSM) and the Departments of Crop

Protection and Plant Science for the infrastructure. They are also thankful to the Agrometeorology Group, UFSM, for their assistance in all stages of the research.

## CONFLICT OF INTERESTS

No conflicts of interest have been declared.

## REFERENCES

- Agostinetto D, Vargas AAM, Ruchel Q, Da Silva JDG and Vargas L (2018) Germination, viability and longevity of horseweed (*Conyza* spp.) seeds as a function of temperature and evaluation periods. *Ciência Rural* 48(9): e20170687. <https://doi.org/10.1590/0103-8478cr20170687>
- Alves EDL and Vecchia FAZ (2011) Análise de diferentes métodos de interpolação para a precipitação pluvial no Estado de Goiás. *Acta Scientiarum* 33(2): 193–7. <http://www.redalyc.org/articulo.oa?id=307325341009>
- Aquino LA, Júnior VCS, Guerra JVS and Costa MM (2011) Estimates of sunflower leaf area by a non-destructive method. *Bragantia* 70(4): 832–836. <https://doi.org/10.1590/S0006-87052011000400015>
- Beck HE, Zimmermann NE, McVicar TR, Vergopolan N, Berg A and Wood EF (2018) Present and future Köppen-Geiger climate classification maps at 1-km resolution. *Scientific Data* 5(1): 180214. <https://doi.org/10.1038/sdata.2018.214>
- Bianco S, Bianco MS, Pavani MCMD and Duarte DJ (2007) Leaf area estimate in *Ipomoea hederifolia* and *Ipomoea nil* Roth: using linear dimensions of the leaf blade. *Planta Daninha* 25: 325-329. <https://doi.org/10.1590/S0100-83582007000200012>
- Bianco S, Carvalho LB and Bianco MS (2008) Estimate of *Sida cordifolia* and *Sida rhombifolia* leaf area using leaf blade linear dimensions. *Planta daninha* 26(4): 807-813. <https://doi.org/10.1590/S0100-83582008000400012>
- Camargo AP and Sentelhas PC (1997) Avaliação do desempenho de diferentes métodos de estimativa da evapotranspiração potencial no estado de São Paulo, Brasil. *Revista Brasileira de Agrometeorologia* 5(1): 89–97.
- Constantin J, Oliveira JRRS and Oliveira Neto AM (2013) Buva: Fundamentos e recomendações para manejo. Omnipax. Curitiba. 104 p.
- De Leite HG and Andrade VCL (2002) A method for conducting forest inventories without using volumetric equations. *Revista Árvore* 26(3): 321–328. <https://doi.org/10.1590/S0100-67622002000300007>
- Figueiredo Filho DB and Silva Júnior JÁ (2010) Desvendando os Mistérios do Coeficiente de Correlação de Pearson (r). *Revista Política Hoje* 18(1): 115–146. <https://periodicos.ufpe.br/revistas/index.php/politica/hoje/article/view/3852/3156>
- Heap I (2025) In: The international survey of herbicide resistant weeds.
- Fang H, Baret F, Plummer S and Schaepman-Strub G (2019) An Overview of Global Leaf Area Index (LAI): Methods, Products, Validation, and Applications. *Reviews of Geophysics* 57(3): 739–799. <https://doi.org/10.1029/2018RG000608>
- Kalsing A, Nunes FA, Gotardi GA, Campos JB, Schneider AA et al (2024) Taxonomic resolution of fleabane species (*Conyza* spp.) based on morphological and molecular markers and their dispersion across soybean-cropping macroregions and seasons in Brazil. *Weed Science* 72(2): 192–204. <https://doi.org/10.1017/wsc.2024.3>
- Kaspary TE, Lamego FP, Cutti L, Aguiar ACdM, Rigon CAG and



- Basso CJ (2017) Growth, phenology, and seed viability between glyphosate-resistant and glyphosate-susceptible hairy fleabane. *Bragantia* 76(1): 92–101. <https://doi.org/10.1590/1678-4499.542>
- Olfati JA, Peyvast GH, Shabanl H and Nosratie-rad Z (2010) An estimation of individual leaf area in cabbage and broccoli using non-destructive methods. *Journal of Agricultural Science and Technology* 12: 627–632. <http://jast.modares.ac.ir/article-23-4883-en.html>
- Oliveira MC, Lencina A, Ulguim AR and Werle R (2021) Assessment of crop and weed management strategies prior to introduction of auxin-resistant crops in Brazil. *Weed Technology* 35(1): 155–165. <https://doi.org/10.1017/wet.2020.96>
- Paula JM, Vargas L, Agostinetto D and Nohatto MA (2011) Management of Glyphosate-resistant *Conyza bonariensis*. *Planta Daninha* 29(1): 217–227. <https://doi.org/10.1590/S0100-83582011000100024>
- Raniro HR, Oliveira F, Araujo JO and Christoffoleti PJ (2023) Broadcast nitrogen application can negatively affect maize leaf area index and grain yield components under weed competition. *Farming System* 1(3): 100047. <https://doi.org/10.1016/j.farsys.2023.100047>
- Schwab NT, Streck NA, Rehbein A, Ribeiro BSMR, Uhlmann LO, Langner JA and Becker CC (2014) Linear dimensions of leaves and its use for estimating the vertical profile of leaf area in gladiolus. *Bragantia* 73(2): 97–105. <https://doi.org/10.1590/brag.2014.014>
- Silva AL, Streck NA, Avila Neto R, Pigatto CS, Macedo M, Pereira VF and Ulguim AR (2020) Fitossociologia de plantas daninhas em arroz irrigado no sistema de cultivo Clearfield®. *Revista Brasileira de Herbicidas*. 19(3): 1–9. <https://doi.org/10.7824/rbh.v19i3.724>
- Soares DJ, De Oliveira WS, Uzuele EL, Carvalho SJP, Lopez-Ovejero RF and Christoffoleti PJ (2017) Growth and development of *Conyza bonariensis* based on days or thermal units. *Pesquisa Agropecuária Brasileira* 52(1): 45–53. <https://doi.org/10.1590/S0100-204X2017000100006>
- Vargas AAM, Agostinetto D, Zandoná RR, Fraga DS and Avila Neto RC (2018) Longevity of Horseweed seed bank depending on the burial depth. *Planta Daninha* 36: e0182073. <https://doi.org/10.1590/S0100-83582018360100050>
- Yamashita OM and Guimaraes SC (2011) Germination of *Conyza canadensis* and *Conyza bonariensis* seeds under different conditions of temperature and light. *Planta Daninha* 29(2): 333–342. <https://doi.org/10.1590/S0100-83582011000200011>

# Hydrogen production by dark fermentation from by-products of coffee wet processing and other organic wastes

Producción de hidrógeno por fermentación oscura a partir de subproductos del beneficio húmedo del café y otros residuos orgánicos

<https://doi.org/10.15446/rfnam.v78n3.116340>

Iván Andrés Quiñones Navia<sup>1</sup>, Víctor Manuel Martínez Castro<sup>2</sup> and Edilson León Moreno Cárdenas<sup>3\*</sup>

## ABSTRACT

### Keywords:

Biohydrogen  
Co-digestion  
Coffee pulp  
Sustainable energy  
Waste coffee water

Wet coffee processing generates liquid and solid residues with a high organic load, which constitute a significant environmental problem in producing regions such as Pitalito, Huila (Colombia). This study evaluated hydrogen production by dark fermentation (DF) from first coffee wash water (FWCW) in co-digestion with vegetable waste (VW), sugarcane juice (SCJ), and coffee pulp (CP), without thermal pretreatments or external inoculation. The assays were carried out in a 35 L batch bioreactor under three treatments with different proportions (% v/v): L1 (18:25:5:5:14), L2 (18:48:0:0:35), and L3 (18:68:0:0:14), corresponding to VW, FWCW, CP, SCJ, and water, respectively. Treatment L1 reached the highest cumulative  $H_2$  production ( $70.03 \pm 2.65$  L), as well as the best substrate volume yield ( $2.00 \pm 0.08$  L  $H_2$  L<sub>substrate</sub><sup>-1</sup>) and  $H_2$  content ( $43.99 \pm 3.89\%$ ). According to the modified Gompertz model, L1 also presented the highest average production rate ( $2.70 \pm 0.82$  L  $H_2$  h<sup>-1</sup>) and lag phase time of  $24 \pm 6.93$  h. The Wilcoxon test evidenced significant differences ( $P=0.05$ ) in cumulative hydrogen production between L1 and L3, confirming the influence of substrate composition on the process. These results highlight that co-digestion of FWCW and VW represents a viable alternative for valorizing the byproducts generated in the wet coffee processing through hydrogen production.


## RESUMEN

### Palabras clave:

Biohidrógeno  
Co-digestión  
Pulpa de café  
Energía sostenible  
Aguas residuales de café

El procesamiento húmedo del café genera residuos líquidos y sólidos con alta carga orgánica, los cuales constituyen una problemática ambiental significativa en regiones productoras como Pitalito, Huila (Colombia). Este estudio evaluó la producción de hidrógeno por fermentación oscura (DF) a partir de aguas del primer lavado de café (FWCW) en co-digestión con residuos vegetales (VW), jugo de caña (SCJ) y pulpa de café (CP), sin pretratamientos térmicos ni inoculación externa. Los ensayos se realizaron en un biorreactor batch de 35 L, bajo tres tratamientos con diferentes proporciones (% v/v): L1 (18:25:5:5:14), L2 (18:48:0:0:35) y L3 (18:68:0:0:14), correspondientes a VW, FWCW, CP, SCJ y agua, respectivamente. El tratamiento L1 alcanzó la mayor producción acumulada de  $H_2$  ( $70,03 \pm 2,65$  L), así como el mejor rendimiento por volumen de sustrato ( $2,00 \pm 0,08$  L  $H_2$  L<sub>sustrato</sub><sup>-1</sup>) y un contenido de  $H_2$  ( $43,99 \pm 3,89\%$ ). De acuerdo con el modelo de Gompertz modificado, L1 también presentó la mayor tasa media de producción ( $2,70 \pm 0,82$  L  $H_2$  h<sup>-1</sup>) y un tiempo de fase Lag de  $24 \pm 6,93$  h. La prueba de Wilcoxon evidenció diferencias significativas ( $P=0,05$ ) en la producción acumulada de hidrógeno entre L1 y L3, confirmando la influencia de la composición del sustrato en el proceso. Estos resultados destacan que la co-digestión de las FWCW y VW representa una alternativa viable para valorizar los subproductos generados en la vía húmeda del café mediante la generación de hidrógeno.

<sup>1</sup>Programa de Ingeniería Agrícola. Universidad Surcolombiana Sede Pitalito, Huila, Colombia. [ivanandress123@gmail.com](mailto:ivanandress123@gmail.com) 

<sup>2</sup>Docente Ocasional, Programa de Ingeniería Agrícola. Universidad Surcolombiana Sede Pitalito, Huila, Colombia. [victor.martinez@usco.edu.co](mailto:victor.martinez@usco.edu.co) 

<sup>3</sup>Profesor Asociado Departamento de Ingeniería Agrícola y Alimentos, Universidad Nacional de Colombia Sede Medellín, Colombia. [elmorenoc@unal.edu.co](mailto:elmorenoc@unal.edu.co) 

\*Corresponding author

The energy matrix continues to be dominated by fossil fuels, which account for around 80% of the supplied energy. However, its impact on the environment and depletion raises concerns about energy supply because global coal, oil, and gas reserves are estimated to last 60, 200, and 40 years, respectively (Aravindan and Praveen 2023). Hydrogen ( $H_2$ ) is considered an alternative energy option to fossil fuels when obtained from renewable and sustainable energy sources, standing out for its high net calorific value of  $120 \text{ MJ kg}^{-1}$  (Al-Haddad et al. 2023).

Hydrogen can also be obtained from biomass through three techniques: biological processes, such as biofermentation (including dark fermentation (DF) and photo fermentation), and biophotolysis. Biological production from sources like organic waste is very promising (Al-Haddad et al. 2023). DF has received significant attention due to its use of carbohydrate-rich waste and *in situ* energy production. This approach reduces costs and energy expenses while maintaining the lowest global warming potential ( $<1 \text{ kg CO}_2 \text{ kg}^{-1} H_2^{-1}$ ).

This is especially relevant in regions with high agro-industrial waste. Coffee is Colombia's main agricultural product due to its impact on the economy and rural employment; in Huila, it accounts for the largest share of the agricultural Gross Domestic Product (GDP), with the highest production concentrated in Pitalito, Huila (Cerquera Losada et al. 2020). However, the wet processing of coffee generates large volumes of solid and liquid waste. Wastewater from the demucilaging process shows chemical oxygen demand (COD) concentrations ranging from 18,600 to 29,500  $\text{mg L}^{-1}$ , biochemical oxygen demand ( $BOD_5$ ) between 10,500 and 14,340  $\text{mg L}^{-1}$ , and total solids ranging from 14,000 to 18,500  $\text{mg L}^{-1}$ , with a pH ranging from 3.5 to 4.5 (Campos et al. 2021). These effluents pose health risks to people in contact with them (Ijanu et al. 2020).

In this context, combining organic residues offers a feasible alternative. Co-digestion enhances anaerobic digestion performance by balancing the nutritional supply for microorganisms. Wastewater and agricultural residues are considered viable options due to their availability and organic content. To increase hydrogen production, it is essential to co-ferment with by-products that optimize

process conditions. Co-digestion, which involves mixing wastes in different proportions and maintaining an appropriate C/N ratio, has been shown to improve yields and reduce common issues associated with mono-digestion, such as nutrient imbalances and the presence of toxic or recalcitrant compounds (Mumtha and Mahalingam 2024). Previous studies support its effectiveness. The co-digestion of sugarcane bagasse and whey using a bacterial consortium achieved a hydrogen production of  $1,098 \text{ mL H}_2 \text{ L}^{-1}$ , surpassing the values obtained with pure cultures (Mumtha and Mahalingam 2024). Likewise, 605.75  $\text{mL H}_2$  and a hydrogen concentration of 39.75% in the biogas were obtained using a mixture of coffee wastewater (53%), liquid swine manure (47%), and dehydrated coffee pulp (3  $\text{g L}^{-1}$ ), with thermal pretreatment (Lourenço et al. 2025). Similarly, using a substrate composed of coffee mucilage, cocoa mucilage, and pig manure, a hydrogen production rate of 90  $\text{mL H}_2$  per day was reported under thermophilic conditions ( $55^\circ \text{C}$ ) and a C/N ratio of 35 (Rangel et al. 2021).

Additionally, some coffee residues have been utilized to generate hydrogen ( $H_2$ ). For instance, the production of 82  $\text{mL H}_2$  from coffee pulp, husk, and coffee wastewater with a pH of 7.0 and a temperature of  $30^\circ \text{C}$  is reported (Villa Montoya et al. 2019). Miñón-Fuentes and Aguilar-Juárez (2019) reached  $4.18 \text{ L H}_2 \text{ kg}^{-1}$  from coffee pulp and a vinasse inoculum. Other authors reported  $284.02 \text{ mL H}_2 \text{ g}^{-1} \text{ COD}^{-1}$  using coffee and cocoa mucilage as substrates, with inoculum from an anaerobic digester (Rangel et al. 2021). Although these studies provide valuable information, there is no robust data on the potential of wastewater from the first coffee wash (FWCW) for hydrogen production through DF. In this context, co-digestion emerges as a viable alternative to overcome its microbiological and nutritional limitations and thus improve production yields (Mumtha and Mahalingam 2024).

This study aimed to evaluate hydrogen production through DF using co-digestion of different proportions of water from the first coffee wash, vegetable waste (lettuce, cabbage, parsley, celery, and broccoli), cane juice, and coffee pulp as a substrate without inoculating microorganisms.

## MATERIALS AND METHODS

### Substrate

A mixture of VW, FWCW, CP, SCJ, and water was

used as the substrate. The selection of VW and FWCW was based on their availability as carbon sources and the presence of microorganisms with high potential for hydrogen production through DF, as reported by Cárdenas et al. (2020). The FWCW, obtained from the traditional processing method (fermentation for 24 hours), and coffee pulp (CP) were collected at Los Naranjos farm, located in the municipality of Pitalito (Huila) at 1,641 meters above sea level (masl) with an average temperature of 19 °C. The vegetable waste (VW) was obtained from the Pitalito marketplace, containing residues of lettuce, chard, cabbage, parsley, celery, and broccoli, residues in equal proportions, which were

not suitable for human consumption. Meanwhile, sugar cane juice (SCJ) was obtained from a panela processing plant located in the municipality of Palestina, Huila. Prior to the experimental stage, preliminary fermentation trials (data not included in this document) were conducted to determine the proportions of the raw materials. From the trial with the highest hydrogen production, 2 L of residual sludge were collected and used as untreated inoculum, which was added to each treatment. The solid waste was crushed using a commercial blender (Oster® BLSTTDG-NBG) to obtain a homogeneous sample (Figure 1). Only the pH of the substrate was recorded (pH<sub>i</sub>); no initial physicochemical characterization was performed.



**Figure 1.** Substrate and raw materials: **A.** Wastewater from the first coffee wash (FWCW); **B.** Coffee pulp (CP); **C.** Vegetable waste (VW); **D.** Sugar cane juice (SCJ); and **E.** Mixed Substrate (FWCW, CP, VW, and SCJ).

### Bioreactor

It consisted of a 50 L high-density polyethylene container with a useful volume for 35 L substrate, which was placed inside another container with a capacity of 200 L and an opening at the top. The space between the two containers was filled with water, which was heated by three electrical resistors of 800 W (127 V), until reaching a temperature of 35 °C in the bioreactor. Water and substrate temperature were recorded with six sensors; four were DS18B20 and two PT100 thermocouples. The stirring system consisted of oblique blades driven by an electric motor (XD-153) at 1,600 rpm (115 V). The pressure in the bioreactor was measured with a Rockage® analogue pressure gauge (0-413.68 kPa). An industrial pressure sensor (0-1.2 MPa) allowed the operation of a 2 w-160-15 solenoid valve (Air control, 110 V), releasing the gas when a value of 68.94 kPa is reached. For the control, an Arduino Uno R3® board was implemented, programmed in C++ language. The pressure and temperature were shown on an LCD

display, screen 1602 (16x2) (Figure 2). A gas meter was coupled to the bioreactor (Humcar® G1.6, minimum flow 0.016 m<sup>3</sup>h<sup>-1</sup> and maximum pressure of 50 kPa), recording the total volume of gas generated. The bioreactor was installed at the Chemistry of Basic Sciences laboratory of the Universidad Surcolombiana (USCO) at Pitalito, where the tests were carried out.

### Experimental design

Batch fermentations were made under a completely randomized experimental design to evaluate the effect of the proportions (% v/v) of the raw materials on the substrate. Three treatments were set with different amounts of VW, FWCW, CP, SCJ, and water, with three replicates per treatment. The temperature, agitation, acidification time ( $t_a$ ) and operating pH (pH<sub>o</sub>) in the fermentations (Table 1) were measured according to the invention patent 31671 granted to Universidad Nacional de Colombia by the Superintendencia de Industria y Comercio, conditions favorable for hydrogen

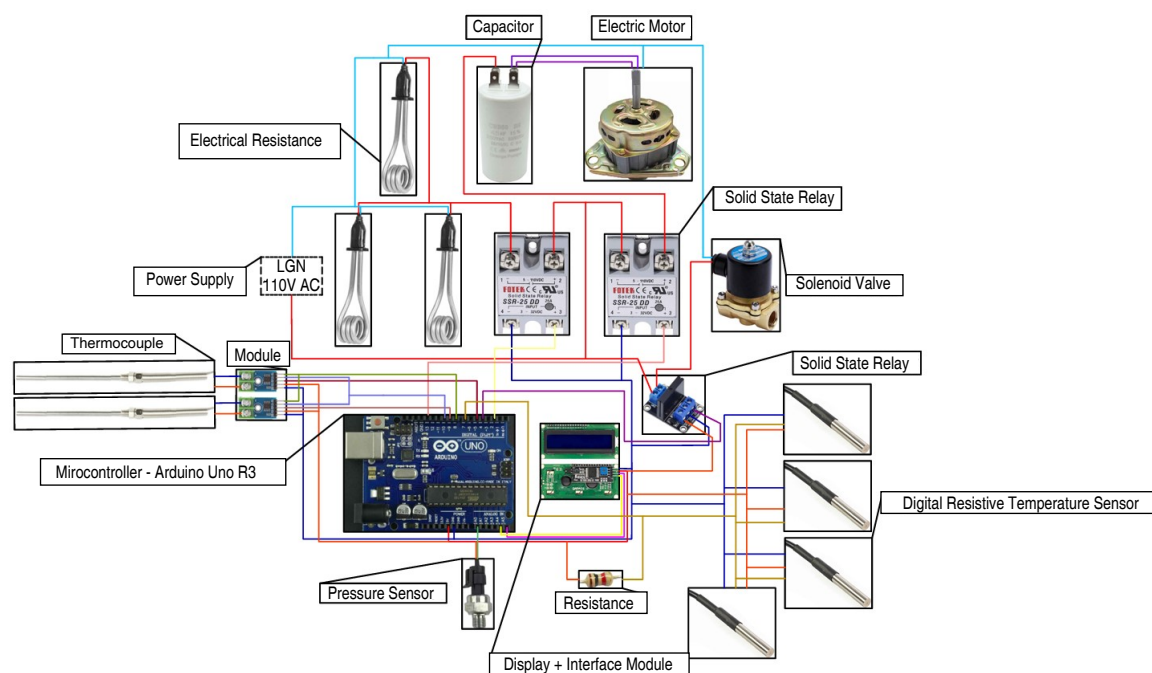


**Figure 2.** Control and automation system.

production. All fermentations began with the grinding of solid residues (VW and CP) to a particle size of <2 cm. Subsequently, FWCP, SCJ, and treated water suitable for human consumption were added in the proportions established by the experimental design. The substrate was transferred to the bioreactor and left to rest for 72 hours, without agitation and at room temperature, to promote lactic acidification. After this period, the pH ( $pH_0$ ) was adjusted to 6.5 using sodium carbonate ( $Na_2CO_3$ ) to initiate hydrogen production.

The pH was monitored with a HI 98107 Hanna Instruments® pH-meter, with 0.1 resolution and  $\pm 0.1$  accuracy. The response variables were hydrogen production rate for the day of maximum production ( $HP$ ,  $L\ H_2\ h^{-1}\ d_{max}^{-1}$ ), cumulative hydrogen production ( $CHP$ ,  $L\ H_2$ ), maximum hydrogen content in the gas ( $MCH$ ,  $\%H_2$ ), substrate yield ( $Y_s$ ,  $L\ H_2\ L_{Substrate}^{-1}$ ), average maximum hydrogen production rate ( $R_{max-avg}$ ,  $L\ H_2\ h^{-1}$ ), and specific hydrogen production rate per biomass ( $SYPB$ ,  $L\ H_2\ h^{-1}\ L^{-1}$ ).

**Table 1.** Substrate proportion and operation conditions.

Treatment	Proportion (% V/V)	Temperatures (°C)	$pH_0$	W (rpm)	$t_a$ (h)
L1	18:25:5:5:47				
L2	18:48:0:0:35	$35 \pm 0.5$	$6.5-7.0 \pm 0.1$	100	72
L3	18:68:0:0:14				

Proportion = VW, FWCP, CP, SCJ, and water, respectively. Temperature = substrate,  $pH_0$  = operating pH, W = stirring (2 minutes per hour),  $t_a$  = hours from fermentation to base add.

### Kinetic and statistical analysis

The cumulative production of  $H_2$  was adjusted to the modified Gompertz model (Equation 1). The model was

applied using Visual Studio Code (version 1.87.2) and Python programming language (version 3.12.2), where H is the cumulative hydrogen production (mL),  $\lambda$  the lag



phase time (h),  $P$  the potential hydrogen production (mL),  $R_{\max}$  the maximum hydrogen production rate (mL h<sup>-1</sup>),  $t$  corresponds to the elapsed time in hours, and  $e$  is 2.718281828.

$$H = P \cdot \exp \left\{ -\exp \left[ \frac{R_{\max} \cdot e}{p} \cdot (\lambda - t) + 1 \right] \right\} \quad (1)$$

The results of  $H$  and  $R_{\max}$  were subjected to a non-parametric Wilcoxon signed-rank test ( $\alpha=0.05$ ) to determine differences between treatments using VS Code and the Python programming language.

### Chromatographic analysis

To determine the production of  $H_2$ , gas samples were taken every 16 h using 1 L Tedlar bags. Concentrations of hydrogen ( $H_2$ ), methane ( $CH_4$ ), carbon monoxide (CO), carbon dioxide ( $CO_2$ ), and nitrogen ( $N_2$ ) were identified and quantified using gas chromatography with a MicroGC 3000 Agilent equipped with a thermal conductivity detector (TCD). This GC-TCD was coupled to the Molsieve and PLOTU columns, using argon and helium as carrier gases, respectively. The temperature for the injector and column was set at 60 °C, the pressure was 206.8 kPa, and injection flow was 0.83 mL s<sup>-1</sup>. The analyses were conducted at the Energy Sciences laboratory at Universidad Nacional de Colombia Medellín Headquarters.

## RESULTS AND DISCUSSION

### Gas Composition

The highest  $H_2$  content was recorded for treatment L1 (43.99±3.89%), with a maximum value of 48.34% observed in trial L1-R2 (treatment 1, repeat 2). Al-Haddad et al. (2023), using glucose as the substrate, reported  $H_2$  concentrations of 28.70% with untreated inoculum, 30.70% with thermal pretreatment at 115 °C for 20 min, and 27.40%  $H_2$  with acid-treated inoculum. In this study, without substrate pretreatment, significantly higher  $H_2$  values were obtained. The highest  $CH_4$  concentration was 1.04% (L1-R2), a favorable outcome indicating that no significant  $H_2$  consumption occurred for methane formation. The mean value for L1 was 0.93±0.35%, the highest among all treatments. The highest average CO content was observed in treatment L1 (9.85±3.93%), with a maximum value of 17.20% in trial L1-R2 (Figure 3).

The formation of CO is attributed to homoacetogenic bacteria, which can grow using  $H_2$  and  $CO_2$  as energy sources (Mehi et al. 2024). The highest  $CO_2$  content in this study was 33.59±12.16% for treatment L1. However, considering the remarkable results in  $H_2$  production, in this work, CO could be more associated with metabolic pathways that do not consume  $H_2$ .

The highest  $N_2$  mean was obtained in treatment L3 (33.93±7.89%), with a maximum value of 50.01% in trial L3-R3. Rojas-Sossa et al. (2017) studied the production of  $H_2$  using coffee wastewater and indicated that the Comamonadaceae family was the most abundant group of proteobacteria. This genus performs the denitrification and decomposition of organic acids through the enzyme nitrate reductase, whose final product is  $N_2$ . Some researchers report that  $H_2$ ,  $CH_4$ ,  $CO_2$ , and  $N_2$  have concentrations of 18.08, 0.20, 8.96, and 51.30%, respectively, using fruits and vegetables as substrates (Moreno Cárdenas et al. 2013). Mixed cultures from environmental sources may contain  $H_2$ -consuming microorganisms, such as methanogenic bacteria, which produce nitrate and iron, propionate, lactate and caproate; in these,  $H_2$  can be consumed as reducing equivalent ( $NADH_2$ ; potential  $H_2$ ) or as molecular  $H_2$  (Saady 2013). These results demonstrate that untreated substrates maximize  $H_2$  production, minimizing unwanted byproducts such as methane while maintaining low levels of CO, suggesting an efficient and sustainable alternative for clean energy generation.

### Bio-Hydrogen production and yield

Hydrogen production varied between 1.37±1.37 and 1.87±0.38 L  $H_2$  h<sup>-1</sup> d<sub>max</sub><sup>-1</sup>, the MCH ranged between 34.37±9.45 and 43.99±3.89%, and the CHP between 43.63±17.39 and 70.03±2.65 L (Table 2). The maximum  $H_2$  yield was found in trial L1-R2 with 2.30 L  $H_2$  h<sup>-1</sup> d<sub>max</sub><sup>-1</sup>. Additionally, a cumulative  $H_2$  production of 25.94 L  $H_2$ , with an  $H_2$  content of 35.85%, has been reported after one day of acidification at a temperature of 30 °C, pH of 6.5, and a chemical oxygen demand (COD) of 60 g O<sub>2</sub> L<sup>-1</sup> of coffee mucilage and organic waste (Cárdenas et al. 2020). Likewise, an average  $H_2$  production rate of 1,398.3 NmL L<sub>substrate</sub><sup>-1</sup> d<sup>-1</sup> has been found, and an average concentration of 39% of  $H_2$  using coffee mucilage and swine manure at a pH of 5.5 and a temperature of 55 °C (Hernández et al. 2014). García-Depraect and León-Becerril (2023)

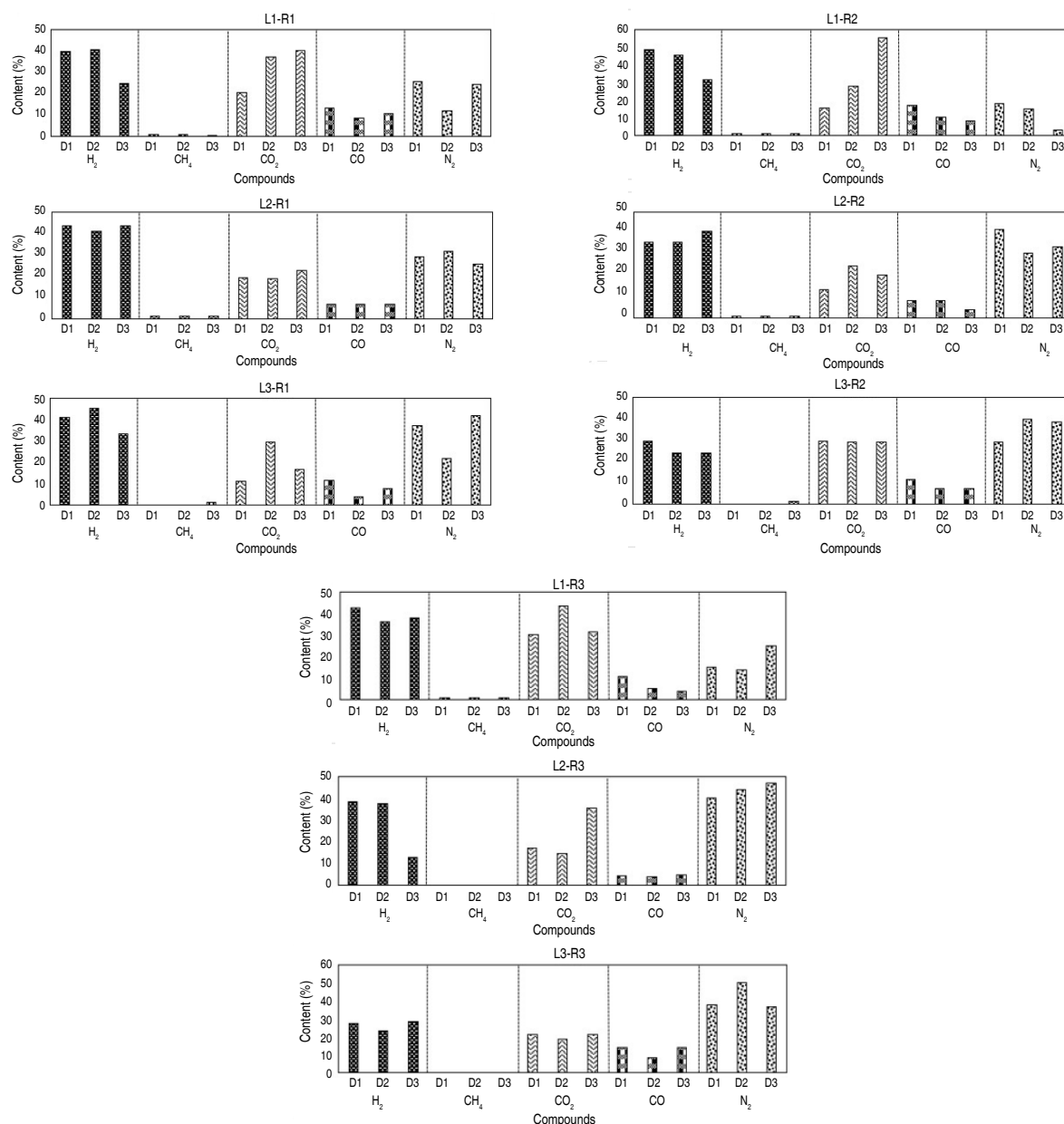


**Figure 3.** Gas composition across three treatments (L1, L2, L3), each with three repeats (R1, R2, R3), assessed on their respective sampling days (D).

investigated the use of a specialized biocatalyst to produce hydrogen, lactate, and butyrate, reporting  $0.2 \text{ NL H}_2 \text{ L}^{-1}$ , low butyrate production ( $3.3 \text{ g L}^{-1}$ ), and rapid decreases in lactate, from coffee industry wastewater (20% v/v from the fermentation stage; 80% v/v from the demucilagization stage). The authors suggest that co-fermentation with other substrates, such as fruit and vegetable waste, could improve process efficiency.

The best yield obtained in the present study ( $Y_s$ ) was  $2.00 \pm 0.08 \text{ L H}_2 \text{ L}_{\text{substrate}}^{-1}$  for L1 under non-sterile conditions and without inoculation. Researchers have reported  $1.29 \text{ L H}_2 \text{ L}_{\text{substrate}}^{-1}$  and a yield of  $1.65 \text{ mol H}_2 \text{ mol}_{\text{hexose}}^{-1}$  with coffee mucilage combined with organic residues, no inoculation, and an organic load of  $60 \text{ g O}_2 \text{ L}^{-1}$  (COD), and a pH of 6.5 (Cárdenas et al. 2020). Previous studies report  $1.29 \text{ mol H}_2 \text{ mol}_{\text{hexose}}^{-1}$  from wastewater generated during beverage

manufacturing, subjected to heat treatment at 90 °C for 20 minutes (Jung et al. 2010). A yield of 49.2 mL H<sub>2</sub> g<sup>-1</sup> COD<sup>-1</sup> has been found using coffee pulp as a substrate, with inoculation (Miñón-Fuentes and Aguilar-Juárez 2019). Yields of 1.90 L H<sub>2</sub> L<sub>substrate</sub><sup>-1</sup> have been achieved with urban

organic waste in a bioreactor with pulsed stirring, without inoculation (Cano Quintero and Moreno-Cárdenas 2019). In addition, Hernández et al. (2014) reported that using coffee mucilage with inoculum and an organic load of 12.1 kg COD m<sup>-3</sup> d<sup>-1</sup>, the yield was 2.5 mol H<sub>2</sub> mol<sub>glucose</sub><sup>-1</sup>.

**Table 2.** Production yield indicators.

Trial	MCH (%H <sub>2</sub> )	MCH (%H <sub>2</sub> )±SD*	HP (L H <sub>2</sub> h <sup>-1</sup> d <sub>max</sub> <sup>-1</sup> )	HP (L H <sub>2</sub> h <sup>-1</sup> d <sub>max</sub> <sup>-1</sup> )±SD*	CPH (L H <sub>2</sub> )	CPH (L H <sub>2</sub> )±SD*	Y <sub>s</sub> (L H <sub>2</sub> L <sub>substrate</sub> <sup>-1</sup> )	Y <sub>s</sub> (L H <sub>2</sub> L <sub>substrate</sub> <sup>-1</sup> )±SD*
L1-R1	40.87		1.71		70.01		2.00	
L1-R2	48.35	43.99±3.89	2.30	1.87±0.38	72.69	70.03±2.65	2.08	2.00±0.08
L1-R3	42.74		1.59		67.39		1.93	
L2-R1	43.88		2.16		75.56		2.16	
L2-R2	41.02	41.08±2.77	1.38	1.61±1.61	56.80	56.79±18.78	1.62	1.62±0.54
L2-R3	38.35		1.28		38.00		1.09	
L3-R1	45.26		1.84		63.57		1.82	
L3-R2	29.56	34.37±9.45	1.05	1.37±1.37	31.62	43.63±17.39	0.90	1.25±0.50
L3-R3	28.29		1.22		35.69		1.02	

MCH=maximum hydrogen content in the gas, HP=hydrogen production rate for the day of maximum production, CPH=cumulative hydrogen production, Y<sub>s</sub>=substrate yield, ±SD=standard deviation, \*=average value.

During hydrogen production, various organic acids and alcohols have been identified, including lactic acid (pH=3.2–4.5), butyric acid (pH=4.7–5.0), acetic acid (pH=4.5), valeric acid (pH=6.0), propionic acid (pH=6.0), butanol (pH=4.7–4.9), and ethanol. Their presence varies depending on the microbial community in non-sterilized substrates (Villa Montoya et al. 2020a). This confirms that, in non-sterilized substrates, the microbial community

influences the variability of compounds and metabolic pathways for hydrogen production. It has been reported that at pH=5.5, volatile fatty acids (VFAs) such as acetic, propionic, and isocaproic are accumulated, which could influence hydrogen production (Tiegam Tagne et al. 2024). Although this study did not evaluate VFA production, it is possible that favorable VFA formation pathways occurred, contributing to hydrogen production (Table 3).

**Table 3.** Temperature and pH values in the trials.

Trial	T (°C)	pH <sub>i</sub>	pH <sub>o</sub>	pH <sub>f</sub>
L1-R1	35±0.5	4.10	6.30	7.20
L1-R2	35±0.5	4.30	6.00	6.80
L1-R3	35±0.5	4.40	6.50	7.00
L2-R1	35±0.5	4.20	5.60	6.80
L2-R2	35±0.5	4.00	5.80	6.80
L2-R3	35±0.5	4.30	6.00	7.30
L3-R1	35±0.5	3.80	5.80	6.10
L3-R2	35±0.5	3.90	6.30	5.80
L3-R3	35±0.5	3.90	5.90	5.90

T=substrate temperature, pH<sub>i</sub>=initial pH of the substrate, pH<sub>o</sub>=operating pH, pH<sub>f</sub>=final pH of the substrate.

Figure 4 shows that the maximum production was not recorded on the same day for all the trials. Previous studies have demonstrated that  $H_2$  production is influenced by microbial diversity and that processes may be affected by operating conditions; hence, bacteria can adapt to dynamic conditions and alter the speed and efficiency of  $H_2$  production (Mehi et al. 2024). The results show that production lasted between three and five days, reaching

its maximum between the first and second day, while on days four and five it was marginal, according to the batch operation. The use of native communities has been found to favor hydrogen production pathways. A yield of  $596.3 \text{ mL } H_2 \text{ L}^{-1}$  and  $25 \text{ g L}^{-1}$  of lactic acid were reported from native communities of organic substrates, as they are well adapted to the substrates, efficiently converting lactic acid into hydrogen (Villanueva-Galindo et al. 2024).

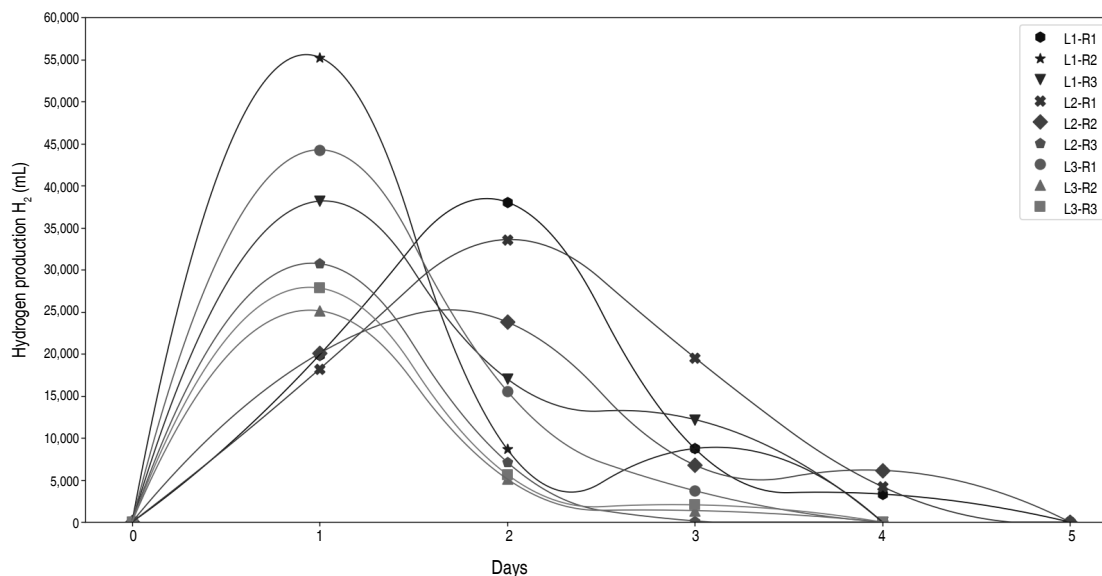


**Figure 4.** Hydrogen production across three treatments (L1, L2, L3), each with three repeats (R1, R2, R3).

#### Modified Gompertz model applied to cumulative hydrogen production (CPH)

The kinetics of product formation ( $H_2$ ) using the modified Gompertz model showed that the highest volume of  $H_2$  was found in trial L2-R1 with  $75,556.69 \text{ mL}$  (Figure 5). The lag phase did not have the same duration in all the trials, since after the acidification time, the reaction rate of the base was not the same in all of them. The multiple correlation coefficient in relation to the Gompertz logistic model was 0.99 for all the tests (Table 4). The maximum  $H_2$  production rate ( $R_{\max}$ ) was observed in trial L1-R2 with  $3,638.34 \text{ mL } H_2 \text{ h}^{-1}$ , with lag phase time of 28 h. The best  $R_{\max\text{-avg}}$  and the best SYPB were obtained in L1, with  $2.70 \pm 0.82 \text{ L } H_2 \text{ h}^{-1}$  and  $0.08 \pm 0.02 \text{ L } H_2 \text{ h}^{-1} \text{ L}^{-1}$ , respectively (Table 4). However, all the parameters shown by the Gompertz model must be analyzed simultaneously since high values in the production rate and yield do not always imply high production, such was the case of trial L3-R3

that obtained outstanding values of  $R_{\max\text{-avg}}$  and SYPB but showed the second lowest production ( $H_{\max}$ ).

Villa Montoya et al. (2020a) report  $H_{\max}$  values of  $244 \text{ mL}$ ,  $R_{\max}$  of  $11.40 \text{ mL h}^{-1}$ ,  $\lambda$  of  $17.10 \text{ h}$  at pH of 5.5 and temperature of  $30^\circ \text{C}$ , using pulp and coffee husk as a substrate with hydrothermal pretreatment at  $150^\circ \text{C}$ . For additional studies using pulp and coffee wastewater pretreated at  $180^\circ \text{C}$  for 15 minutes, the  $H_{\max}$  results were  $8 \text{ mL}$ ,  $R_{\max}$  of  $0.80 \text{ mL h}^{-1}$ , and  $\lambda$  of  $14.70 \text{ h}$  (Villa Montoya et al. 2020b). Meanwhile, using a synthetic substrate, an  $R_{\max}$  of  $59.6 \text{ mL h}^{-1}$ ,  $H_{\max}$  of  $758.70 \text{ mL}$ , and  $\lambda$  of  $27.30 \text{ h}$  were recorded, thus establishing that high organic loads cause inhibition and affect production (Laathanachareon et al. 2014). Similar results are reported by Moreno Cárdenas and Zapata Zapata (2019) for  $H_2$  production using fruit and vegetable waste in co-digestion with fresh coffee mucilage; they found that  $H_2$  production

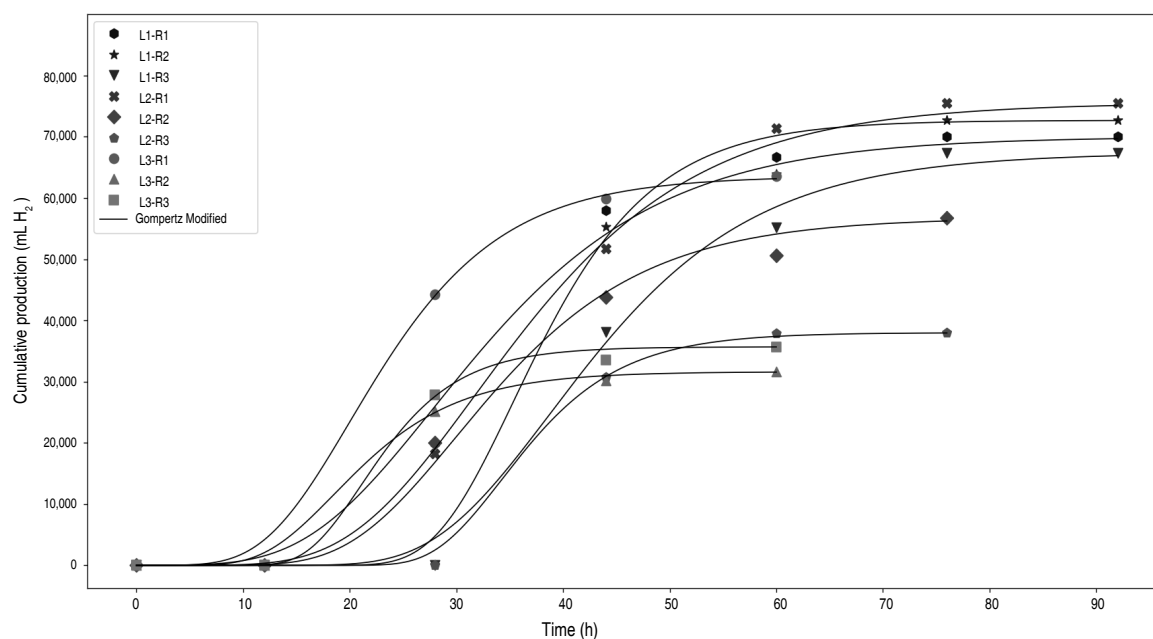


**Figure 5.** Accumulated hydrogen production fitted to the modified Gompertz model across three treatments (L1, L2, L3), each with three repeats (R1, R2, R3).

decreased with organic loads greater than 70,000 mg of  $O_2 L^{-1}$ . Additionally, Abreu et al. (2009) reported  $H_{max}$  of 137.20 mL,  $R_{max}$  of 1.70 mL  $h^{-1}$ , and  $\lambda$  of 13.70 h using hemicellulosic biopolymers (L-arabinose) at 30 g  $L^{-1}$  and 37 °C, demonstrating the impact of substrate type and operational conditions on hydrogen production. Muri et al. (2016) documented  $H_{max}$  of 346 N mL,  $R_{max}$  of 91 N mL  $h^{-1}$ ,  $\lambda$  of 6.50 h,

and  $Y_s$  of 1.55 mol  $H_2$  per mol glucose using glucose (5 g  $L^{-1}$ ) at 37 °C and pH=6.4, noting that low pH suppresses hydrogenase activity, reducing  $H_{max}$  and  $R_{max}$ . This trend is consistent with the results achieved in this research, where the lowest  $H_{max}$  values were presented in treatment 3, which had the lowest proportion of water (18:68:0:0:14) with 14%, which implied a lower dilution and greater organic load.

**Table 4.** Parameters of the Gompertz modified model.

Trial	$H_{max}$ (mL $H_2$ )	$R_{max}$ (mL $H_2 h^{-1}$ )	$\lambda$ (h)	$R^2$	$\lambda$ (h)±SD*	$R_{max-avg}$ (L $H_2 h^{-1}$ )±SD*	SYPB (L $H_2 h^{-1} L^{-1}$ )±SD*
L1-R1	70,012.44	2,164.95	16	0.99			
L1-R2	72,687.41	3,638.34	28	0.99	24.00±6.93	2.70±0.82	0.08±0.02
L1-R3	67,393.51	2,295.57	28	0.99			
L2-R1	75,556.69	2,364.38	20	0.99			
L2-R2	56,795.13	2,103.30	20	0.99	22.67±4.62	2.24±0.13	0.06±0.00
L2-R3	38,003.92	2,239.15	28	0.99			
L3-R1	63,572.64	2,927.82	12	0.99			
L3-R2	31,620.35	1,776.15	12	0.99	13.33±2.31	2.43±0.59	0.07±0.02
L3-R3	35,689.79	2,581.25	16	0.99			

$H_{max}$ =maximum  $H_2$  production rate,  $R_{max}$ =maximum hydrogen production rate,  $\lambda$ =lag phase time,  $R_{max-avg}$ =average maximum hydrogen production rate, SYPB=specific hydrogen production rate per biomass, ±SD=standard deviation, \*=average value.



### Comparing medians: Statistical analysis for cumulative hydrogen production (CPH)

The results for the CPH variable indicate that the data are normal ( $P$ -value=0.10) according to the Shapiro-Wilk test and homogeneity of variance

( $P$ -value= 0.10), according to the Levene test. However, given the number of data available in the study, a non-parametric Wilcoxon test was preferred for comparing medians for the variables CHP and  $R_{\max}$  (Figure 6).

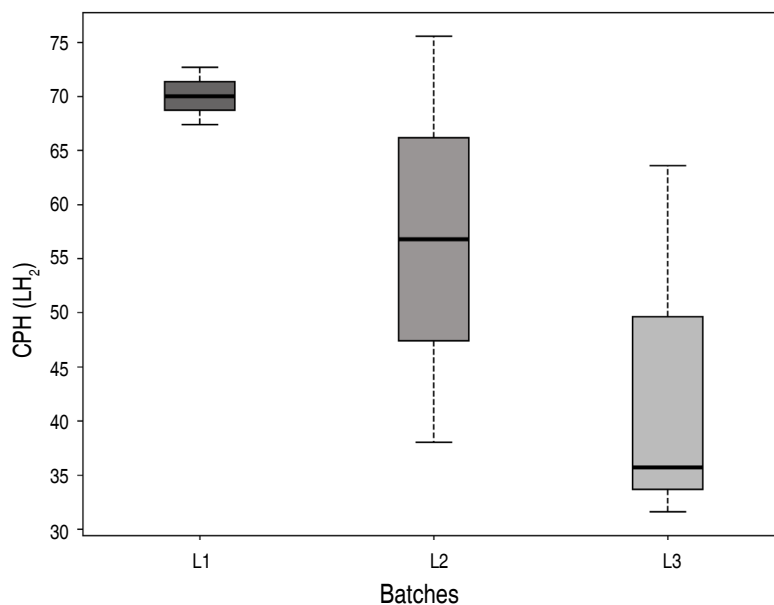


**Figure 6.** Mean and interval for cumulative hydrogen production (CHP) variable in the treatments.

After applying the Wilcoxon test (Table 5), significant differences were observed between L1 and L3 in the variable CHP. In contrast, when comparing the medians between treatments L2 and L3 and between L1 and L2, no significant differences were found.

Since there were no statistical differences in the variable CHP between the treatments L1 (composition of 18:25:5:5:47, in its order VW, FWCW, CP, SCJ and water) and L2 (composition of 18:48:0:0:35, in its order

VW, FWCW and water), the substrate can be simplified to VW and FWCW, which opens a door for such residues to be used as main substrates without significantly affecting the H<sub>2</sub> production. Moreover, given that there are significant differences between the L1 treatment (with 47% water) and the L3 treatment (water was reduced to 14%), and that in the latter the production of H<sub>2</sub> was the lowest, there could have been an inhibitory effect due to organic overload. The rate of organic load is an essential factor in the DF, it represents the availability of substrate for

**Table 5.** Wilcoxon test results for cumulative hydrogen production (CHP) and maximum hydrogen production rate ( $R_{\max}$ ).

Treatment comparison	Wilcoxon W (CHP)	P-value (CHP)	Wilcoxon W ( $R_{\max}$ )	P-value ( $R_{\max}$ )
L1 vs L2	6	0.35	6	0.35
L2 vs L3	7	0.20	3	0.80
L1 vs L3	9	0.05	5	0.50

CHP=cumulative hydrogen production,  $R_{\max}$ =maximum hydrogen production rate, Wilcoxon W=Wilcoxon test statistic value, P-value=statistical significance value ( $P \leq 0.05$ ).

H<sub>2</sub>-producing microorganisms, allowing higher productions as long as the process is not inhibited by substrate overload (García-Depraect et al. 2021). High organic loads favor the production of undesirable by-products such as propionate and isocaproic acid negatively affecting the process (García-Depraect and León-Becerril 2023; Tiegam Tagne et al. 2024). Previous studies have reported a decrease in H<sub>2</sub> production due to organic overload when using different substrates, including mixtures of pig manure, coffee mucilage, and cocoa at concentrations between 40 and 50 g VS L<sup>-1</sup> (Rangel et al. 2020).

The Wilcoxon test results indicate no significant differences between the evaluated treatments for R<sub>max</sub>. Although the limited number of replicates and the variability in the data suggest that these findings should be interpreted with some caution, the results support that, under the conditions evaluated, variations in substrate composition do not substantially affect R<sub>max</sub>.

## CONCLUSION

Dark fermentation of FWCW in co-digestion with VW, SCJ or CP allowed achieving a maximum hydrogen content of 43.99±3.89%, a substrate yield of 2.00±0.08 L H<sub>2</sub> L<sup>-1</sup> Substrate<sup>-1</sup>, and a maximum average production rate of 2.70±0.82 L H<sub>2</sub> h<sup>-1</sup>, with a microbial adaptation period of 24±6.93 hours, without the need for thermal pretreatment, following the operational conditions established in patent 31671. The Wilcoxon test revealed a significant effect of substrate composition on cumulative hydrogen production, with statistically significant differences observed between treatments L1 and L3 (*P*=0.05). These results highlight the potential of FWCW and co-substrates in hydrogen production processes. Further studies are recommended to characterize the substrates in terms of carbohydrate and volatile fatty acids by high-performance liquid chromatography, as well as to conduct metagenomic analysis of microbial communities to identify hydrogen-producing microorganisms and key metabolic pathways, to optimize the process at an industrial scale.

## ACKNOWLEDGEMENTS

We thank the Universidad Surcolombiana and its Faculty of Engineering, Dean Rómulo Medina Collazos, for the financing, and Roger Iván Quiñones and Lady Marcela Navia for the additional financial support. Likewise, to the Universidad Nacional de Colombia Medellín Headquarters for allowing us to work with their patent.

## CONFLICT OF INTERESTS

The authors declare that they have no conflicts of interest.

## REFERENCES

- Abreu AA, Danko AS, Costa JC et al (2009) Inoculum type response to different pHs on biohydrogen production from l-arabinose, a component of hemicellulosic biopolymers. *International Journal of Hydrogen Energy* 34:1744–1751. <https://doi.org/10.1016/j.ijhydene.2008.12.020>
- Al-Haddad S, Okoro-Shekwa CK, Fletcher L et al (2023) Assessing different inoculum treatments for improved production of hydrogen through dark fermentation. *Energies (Basel)* 16:1–15. <https://doi.org/10.3390/en16031233>
- Aravindan M and Praveen G (2023) Hydrogen towards sustainable transition: A review of production, economic, environmental impact and scaling factors. *Results in Engineering* 20: 1–21. <https://doi.org/10.1016/j.rineng.2023.101456>
- Campos RC, Pinto VRA, Melo LF et al (2021) New sustainable perspectives for “Coffee Wastewater” and other by-products: A critical review. *Future Foods* 4. <https://doi.org/10.1016/j.fufo.2021.100058>
- Cano Quintero DY and Moreno-Cárdenas EL (2019) Incidence of operative parameters in the production of biohydrogen generated from urban organic waste. *Revista Facultad Nacional de Agronomía Medellín* 72: 8841–8853. <https://doi.org/10.15446/rfnam.v72n2.73138>
- Cárdenas ELM, Zapata-Zapata AD and Kim D (2020) Modeling dark fermentation of coffee mucilage wastes for hydrogen production: Artificial neural network model vs. fuzzy logic model. *Energies (Basel)* 13: 1–13. <https://doi.org/10.3390/en13071663>
- Cerquera Losada OH, Pérez Gómez VH and Sierra Chavarro J (2020) Análisis de la competitividad de las exportaciones del café del Huila. *Tendencias* 21: 19–44. <https://doi.org/10.22267/rtend.202102.139>
- García-Depraect O, Castro-Muñoz R, Muñoz R et al (2021) A review on the factors influencing biohydrogen production from lactate: The key to unlocking enhanced dark fermentative processes. *Bioresour Technology* 324: 1–14. <https://doi.org/10.1016/j.biortech.2020.124595>
- García-Depraect O and León-Becerril E (2023) Use of a highly specialized biocatalyst to produce lactate or biohydrogen and butyrate from agro-industrial resources in a dual-phase dark fermentation. *Fermentation* 9. <https://doi.org/10.3390/fermentation9090787>
- Hernández MA, Rodríguez Susa M and Andres Y (2014) Use of coffee mucilage as a new substrate for hydrogen production in anaerobic co-digestion with swine manure. *Bioresour Technology* 168: 112–118. <https://doi.org/10.1016/j.biortech.2014.02.101>
- Ijanu EM, Kamaruddin MA and Norashiddin FA (2020) Coffee processing wastewater treatment: a critical review on current treatment technologies with a proposed alternative. *Applied Water Science* 10: 1–11. <https://doi.org/10.1007/s13201-019-1091-9>
- Jung KW, Kim DH and Shin HS (2010) Continuous fermentative hydrogen production from coffee drink manufacturing wastewater by applying UASB reactor. *International Journal of Hydrogen Energy* 35: 13370–13378. <https://doi.org/10.1016/j.ijhydene.2009.11.120>
- Laathanachareon T, Kanchanasuta S, Mhuanthong W et al (2014) Analysis of microbial community adaptation in mesophilic hydrogen fermentation from food waste by tagged 16S rRNA gene pyrosequencing. *Journal of Environmental Management* 144: 143–151. <https://doi.org/10.1016/j.jenvman.2014.05.019>

- Lourenço VA, Camargo FP, Sakamoto IK et al (2025) Influence of substrates proportion and concentration on biogas composition and yield in the co-digestion of solid and liquid waste from coffee and swine farms. *Renew Energy* 249: 1–19. <https://doi.org/10.1016/j.renene.2025.123191>
- Mehi Gaspari Augusto I, Zampol Lazaro C, Albanez R et al (2024) H<sub>2</sub> production via dark fermentation of soybean molasses: Elucidating the role of homoacetogenesis and endogenous substrate microorganisms by kinetic and microbial analysis. *Energy* 298: 1–18. <https://doi.org/10.1016/j.energy.2024.131301>
- Miñón-Fuentes R and Aguilar-Juárez O (2019) Hydrogen production from coffee pulp by dark fermentation. *Water Science and Technology* 80: 1692–1701. <https://doi.org/10.2166/wst.2019.416>
- Moreno Cárdenas EL, Cano Quintero DJ and Elkin Alonso CM (2013) Generation of biohydrogen by anaerobic fermentation of organics wastes in Colombia. In: *Liquid, Gaseous and Solid Biofuels - Conversion Techniques*. InTech pp 377–400.
- Moreno Cárdenas EL and Zapata Zapata AD (2019) Biohydrogen production by co-digestion of fruits and vegetable waste and coffee mucilage. *Rev Facultad Nacional de Agronomía Medellín* 72: 9007–9018. <https://doi.org/10.15446/rfnam.v72n3.73140>
- Mumtha C and Mahalingam PU (2024) Biohydrogen production from co-substrates through dark fermentation by bacterial consortium. *3 Biotech* 14: 1–9. <https://doi.org/10.1007/s13205-024-04106-3>
- Muri P, Črnivec IGO, Djinović P and Pintar A (2016) Biohydrogen production from simple carbohydrates with optimization of operating parameters. *Acta Chimica Slovenica* 63: 154–164. <https://doi.org/10.17344/acsi.2015.2085>
- Rangel C, Sastoque J, Calderon J et al (2020) Hydrogen production by dark fermentation process: Effect of initial organic load. *Chemical Engineering Transactions* 79: 133–138. <https://doi.org/10.3303/CET2079023>
- Rangel CJ, Hernández MA, Mosquera JD et al (2021) Hydrogen production by dark fermentation process from pig manure, cocoa mucilage, and coffee mucilage. *Biomass Convers Biorefin* 11: 241–250. <https://doi.org/10.1007/s13399-020-00618-z>
- Rojas-Sossa JP, Murillo-Roos M, Uribe L et al (2017) Effects of coffee processing residues on anaerobic microorganisms and corresponding digestion performance. *Bioresour Technology* 245: 714–723. <https://doi.org/10.1016/j.biortech.2017.08.098>
- Saady NMC (2013) Homoacetogenesis during hydrogen production by mixed cultures dark fermentation: Unresolved challenge. *International Journal of Hydrogen Energy* 38: 13172–13191. <https://doi.org/10.1016/j.ijhydene.2013.07.122>
- Tiegam Tagne RF, Costa P, Gupte AP et al (2024) Efficient production of biohydrogen from African lignocellulosic residues. *Sustainable Energy Technologies and Assessments* 72. <https://doi.org/10.1016/j.seta.2024.104060>
- Villa Montoya AC, Cristina da Silva Mazareli R, Delforno TP et al (2019) Hydrogen, alcohols and volatile fatty acids from the co-digestion of coffee waste (coffee pulp, husk, and processing wastewater) by applying autochthonous microorganisms. *International Journal of Hydrogen Energy* 44: 21434–21450. <https://doi.org/10.1016/j.ijhydene.2019.06.115>
- Villa Montoya AC, Cristina da Silva Mazareli R, Silva EL and Varesche MBA (2020a) Improving the hydrogen production from coffee waste through hydrothermal pretreatment, co-digestion and microbial consortium bioaugmentation. *Biomass Bioenergy* 137: 1–11. <https://doi.org/10.1016/j.biombioe.2020.105551>
- Villa Montoya AC, da Silva Mazareli RC, Delforno TP et al (2020b) Optimization of key factors affecting hydrogen production from coffee waste using factorial design and metagenomic analysis of the microbial community. *International Journal of Hydrogen Energy* 45: 4205–4222. <https://doi.org/10.1016/j.ijhydene.2019.12.062>
- Villanueva-Galindo E, Pérez-Rangel M and Moreno-Andrade I (2024) Biohydrogen production from lactic acid: Use of food waste as substrate and evaluation of pretreated sludge and native microbial community as inoculum. *International Journal of Hydrogen Energy*. <https://doi.org/10.1016/j.ijhydene.2023.12.202>

# Global trends in sustainable cocoa (*Theobroma cacao* L.) production: A bibliometric analysis (2019–2025)



Tendencias globales en la producción sostenible de cacao (*Theobroma cacao* L.): un análisis bibliométrico (2019–2025)

<https://doi.org/10.15446/rfnam.v78n3.119620>

Alfredo Enrique Sanabria Ospino<sup>1\*</sup>, Alix Estela Yusara Contreras Gómez<sup>1</sup> and Mary Yaneth Rodríguez Villamizar<sup>2</sup>

## ABSTRACT

### Keywords:

Agroindustry  
Circular economy  
Fair-trade  
Green practices



Currently, there is global concern about rising temperatures, which, together with the food risk, is causing climate change. In addition, cocoa (*Theobroma cacao* L.) production is questioned because of its production method, which generates deforestation and high energy and water consumption in the process. These environmental problems cause a bad image in the sector, and uncertainty in the overall production of the cocoa industry, which has been striving to implement sustainable practices to mitigate the effects of climate change. However, solutions to this environmental issue have received little attention from the scientific community, and the need has arisen to investigate sustainable solutions for the cocoa industry. This study aims to conduct a bibliometric analysis to identify global sustainable trends that have been researched in the cocoa industry. For this purpose, a search strategy was designed and applied in the Scopus and Web of Science (WoS) databases, to collect information, filtering the results, in the categories of articles related to the agriculture and business groups in the 2019-2025 period, published in journals cataloged in quartiles one and two. Using the R programming language for information processing, 56 documents were found. Eleven sustainable practices were identified in the industry to improve social, economic, and environmental performance, through waste valorization, soil improvement, reduction of water and energy consumption, and the adoption of green certifications. Finally, a framework is proposed for integrating the links in the supply chain with the practices for making them most sustainable.

## RESUMEN

### Palabras clave:

Agroindustria  
Economía circular  
Comercio justo  
Prácticas verdes

En la actualidad, existe preocupación mundial por el aumento de las temperaturas que, junto con el riesgo alimentario, provoca el cambio climático. Además, la producción de cacao (*Theobroma cacao* L.) se cuestiona por su método de producción, que genera deforestación y un elevado consumo de energía y agua en el proceso. Estos problemas medioambientales causan mala imagen en el sector e incertidumbre en la producción global de la industria del cacao, que se ha esforzado por aplicar prácticas sostenibles para mitigar los efectos del cambio climático. Sin embargo, las soluciones a este problema ambiental han recibido poca atención por parte de la comunidad científica y ha surgido la necesidad de investigar soluciones sostenibles para la industria. Este estudio tiene como objetivo realizar un análisis bibliométrico para identificar tendencias globales sostenibles que se han investigado en la industria del cacao. Para ello, se diseñó una estrategia de búsqueda aplicada en las bases de datos Scopus y Web of Science (WoS), con el propósito de recopilar información, filtrando los resultados, en las categorías de artículos relacionados con los grupos de agricultura y negocios en el periodo 2019-2025 publicados en revistas catalogadas en los cuartiles uno y dos. Utilizando el lenguaje de programación R para el tratamiento de la información, hallando 56 documentos. Se identificaron 11 prácticas sostenibles en la industria, con el objetivo de mejorar el rendimiento social, económico y medioambiental, mediante la valorización de los residuos, la mejora del suelo, la reducción del consumo de agua y energía y la adopción de certificaciones verdes. Por último, se propone un marco para integrar los eslabones de la cadena de suministro con las prácticas para hacerla sostenible.

<sup>1</sup>Docente-investigador, Universidad Santo Tomás seccional Bucaramanga, Colombia. [alfredoenrique.sanabria@ustabuca.edu.co](mailto:alfredoenrique.sanabria@ustabuca.edu.co) , [alix.contreras@ustabuca.edu.co](mailto:alix.contreras@ustabuca.edu.co) 

<sup>2</sup>Docente-Investigador, Universidad de Santander, Colombia. [mary.rodriguez@mail.udes.edu.co](mailto:mary.rodriguez@mail.udes.edu.co) 

\*Corresponding author



There is currently a drop in world cocoa bean harvests, according to figures reported according to data presented by the International Cocoa Organization (ICCO 2025a). The 2023-2024 production is estimated at 4.3 million tons, with a 14% decrease over the previous year, in which production was 5 million tons. This is a consequence of the 16% drop in the African continent, which produces 70% on average worldwide, the most affected African country was Ivory Coast with a 25% decrease (ICCO 2025a). This problem in production has not been alien to the American context, where the drop in production was 6%, going from a production of 1,046 million tons in the 2022-2023 period to 980 million tons in the 2022-2023 period (ICCO 2025a). In addition, a 5% drop in cocoa beans grindings worldwide in the same period (2023-2024) compared to the previous year, with reported figures of 1,792 million tons, with the European continent being the major player with the processing of 36% of the world's grindings, Africa saw a 10% drop in milling, with Côte d'Ivoire being the most affected country with a 6% drop, between these two continents, approximately 60% of world production is milled in the Americas the drop in the grindings of cocoa beans was 14% from reported figures in the 2022/2023 timeframe of 979 million tons to 891 million tons. (ICCO 2025a).

On the other hand, the food industry is one of the main sectors that pollutes the environment, negatively impacting society (Keller et al. 2022). This has led to the rise of environmentally friendly agriculture in the food industry in order to promote sustainable development (Silva et al. 2017). The cocoa industry is adding to this global cleaner production approach (López del Amo and Akizu-Gardoki 2024). Also, the decision-making power of the demand focused on the acquisition of healthy and environmentally friendly products has generated pressure on cocoa farmers to incorporate green practices in their production processes in order to meet market requirements (Fayaz et al. 2024), with the transformation of cocoa waste into secondary raw materials for applications becoming a challenge (Puyana-Romero et al. 2022). Therefore, cocoa agro-industrial companies that incorporate green practices in their processes can reduce costs and ecosystem impacts to achieve the sustainability of the industry (Girón-Hernández et al. 2024). Also, environmental regulations are public

mechanisms applied by governments in order to control environmental pollution, becoming an important issue for different stakeholders and especially for industrialists and their production (Chen and Haoa 2025) Europe has implemented strong regulations for the care of the environment, such as the regulation against deforestation (EUDR) (EU 2023/1115), which aims to counteract the deforestation of imported products, especially cocoa. This regulation generates global policy innovation for the management of global chains (Urugo et al. 2025), therefore, understanding and complying with the new EU regulations has become a challenge for the cocoa industry, especially for smallholder farmers (Moluh Njoya et al. 2025). Voluntary sustainability standards, which are also called certifications, are non-governmental tools aimed at reducing the environmental, economic, and social impacts of the production of crops such as cocoa (Dröge et al. 2025), most of the cocoa exported is Fairtrade or Rainforest Alliance certified (RA) (Steinke et al. 2024). Fair trade is a global trend that promotes sustainability and fair trade for farmers, prohibits the use of toxic pesticides and trains farmers in the management of agrochemicals, creating more balanced forms of economic and social development (Quach et al. 2025). RA was designed to certify farms that comply with social and environmental standards, which must take care of the soil and water sources as well as treat workers with dignity, without neglecting financial profitability (Tischner et al. 2017).

However, the indiscriminate use of chemical fertilizers to improve production, and the increase of inadequately treated waste that negatively impacts the environment, the economy and society, place the concept of sustainability in the cocoa sector in question (Mariatti et al. 2021; Perez et al. 2022), generating concern in cocoa production processes, which leads to questioning the impacts on the economic, environmental and social dimensions (García-Herrero et al. 2019). Moreover, climate change, the fall in production and the global increase in cocoa prices (which have reached historic highs) has caused farmers to abandon their crops and has led to alarm in the sector, by jeopardizing the sustainability of the industry (Bandanaa et al. 2025). Nonetheless, important research has been conducted previously, relating cocoa to sustainable practices, using the review of literature in the last five years as a research method, with the following being found.



Rathgens et al. (2020) presented the problem of child labor in the cocoa sector, which is a deepening in the assessment of the impact of the certifications, the main challenge for academics. Mariatti et al. (2021) identified the processes successfully implemented in the management of cocoa husk and corn cob residues, in addition to the contribution of technologies associated with Industry 4.0 as an input to circular economy practices, so that this constructive collaboration between technologies and practice strengthens economic and environmental performance.

Ribeiro-Duthie et al. (2021) found the relevant literature on fair trade certification of staple foods, including cocoa. The importance of this certification is that it informs the consumer about the fairness of producers' wages and the democratization of production and sustainability. Perez et al. (2022) identified the main challenges related to the sustainability of the chocolate industry, such as the complexity of monitoring the cocoa and chocolate supply chain, the limited training of farmers in good environmental practices, the slow adaptation to the certification process required by European markets for the export of the product from 2020, and the environmental costs associated with packaging.

Fernández-Ríos et al. (2022) found 15 superfoods with environmental performance measurements, with the existing literature on cocoa being the most cultivated, processed, and consumed superfood, and its supply chain being the most studied. Barrios-Rodríguez et al. (2022) studied the process of transforming cocoa pods into biomass as a circular economy strategy that minimizes environmental impact and refines energy costs and extraction time. Suri and Basu (2022), through a literature review, found the fundamental variables that impact the resistance of chocolate to heat, the difficulties presented in the texture, and the obstacles presented in storage, which have generated an important opportunity for research in sustainability. Previous research has made relevant contributions to cocoa and sustainability. However, there are no studies that propose an integrative route between sustainable cocoa practices and the supply chain to achieve a balance between the three pillars of sustainability (environmental, social, and economic). Also, previous studies did not address the thematic evolution of knowledge to know the next research agenda, hence the importance of this research.

This work aims to perform a bibliometric analysis to identify global trends in the world cocoa industry related to sustainability practices in scientific literature. The above process will be a fundamental input to answer the following research questions: Which are the leading countries in research on cocoa and sustainability? Which are the high-impact journals of scientific publication? What are the global research trends in established cocoa and sustainability issues? What are the main sustainable practices in the cocoa industry? This paper has been divided into four parts: 1) deals with the introduction, including the challenges of the cocoa industry in relation to sustainability. 2) concerned with the methodology used for this study, Preferred Reporting Items for Systematic reviews and Meta-Analyses (PRISMA) approach. 3) deals with the results of the scientific data mining that will provide answers to the questions posed in the introduction, and 4) deals with the discussion from the metaphorical approach of the tree of knowledge.

## MATERIALS AND METHODS

### Type of research

Bibliometrics provides insight into the important factors of the academic dimensions of research on a large scale by studying them at the national level or by individual academic discipline (Siao et al. 2022). The resources applied in bibliometric studies make it possible to estimate publications and citations by relating productivity to the influence and quality of scientific papers (Madeira et al. 2023), allowing the identification of research scopes and existing gaps by reducing scientific subjectivity (Salihu et al. 2022). The R open-source software, with its R Studio extensions, the Bibliometrix library and related Bibloshyne interface were used. The importance of programming languages and their tools is recognized by the scientific community (Aziz et al. 2024). The databases used for the analysis process were Scopus and Web of Science (WoS), because these are databases with an enormous collection of material and quality scientific analysis tools (Tsilika 2023).

### Data analysis

Keywords and similar terms were explored in topics delimited by the research, classifying the level of importance according to the number of records. The first one was called Cocoa, a topic that covers the terminology on this crop, in which the term with the highest result was "cocoa" with

15,873 records in Scopus, and 8,936 in WoS, for a total of 38,315 and 15,875 in the respective databases. Secondly, the dimension of green practices was explored, where the term sustainability is the most used by the scientific community, with 1,410,997 and 776,214. This group is the most influential in the research, with a total result of 1,413,913 and 777,875, which integrates all the terminology associated with this group. Finally, in the integration using the selection mechanisms represented in the Boolean

operators for the design of a search strategy to capture data with the topics related to the research ("Green label") OR ("green certification") OR ("Sustaina\*\*") OR ("green practi\*\*") AND ("Theobroma cacao") OR ("Cocoa") OR ("Cacao"). On July 10, 2025, 1,591 and 1,060 documents were identified documents related to cocoa integrating green practices. This exploration was performed on the main structure of the documents (title, abstract, and keywords). Table 1 presents the results of the two databases.

**Table 1.** Keyword research.

Topic	Scopus	WoS
"Theobroma cacao"	7,693	2,745
"Cocoa"	15,873	8,936
"cacao"	14,749	4,176
Total, topic cacao	38,315	15,875
"Sustaina**"	1,410,997	776,214
"Green label"	286	101
"Green certification"	368	168
"Green practi**"	2,262	1,402
Total, Topic Green	1,413,913	777,875
Final cross-checking of information	1,591	1,060

The PRISMA method was used as input for the research approach to provide a clear and concise systematic approach to data mining (Agyei et al. 2024). The following classification parameters were used to classify information search focused only on articles in areas related to research, such as agriculture and business, in Scopus. The following subject areas were selected: Agricultural and Biological Sciences, Environmental, Social Sciences, Economics, Econometrics, and Finance. Also, in WoS, the selected research areas were Environmental Sciences, Ecology, Agriculture, and Science Technology. Other topics were Food Science Technology, Forestry, Business Economics, and Biodiversity Conservation, to identify global scientific trends. The search was limited to the production of the last six years only (2019-2025). For greater quality in the processing of the information, only articles belonging to quartiles one and two (Q1 and Q2) were selected for a final result in the two databases of 48 and 42 (Figure 1). Finally, to end duplicates, processes were conducted to verify the information, in the R open-source software, R Studio version 4.3.2, in BibTex format, in the two databases. The result was 34 duplicate documents eliminated for a net resulting of the unification of 56. This research did not

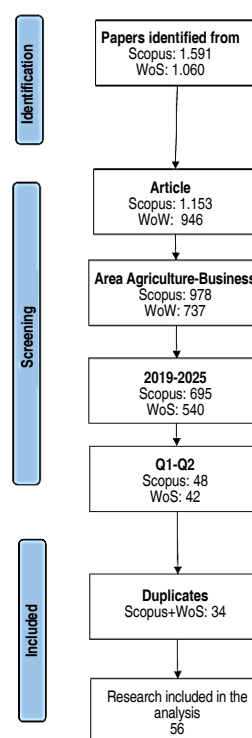


**Figure 1.** Prism method.

include articles classified in quartiles 3 and 4 (Q3-Q4), and databases other than Scopus and WoS were not used, which may introduce limitations in the results.

Figure 2 illustrates the geographical dissemination of research papers. The methodology used to determine geographical representation was the location of the research institutions to which the authors belong. On the other hand, the intensification of the color blue shows the scientific strength of the country according to the number of records, for graphic analysis, the five main countries

will be studied, which in their respective order are: Spain and United Kingdom (17), Ghana and (16) Italy, finally, Ecuador with (15) records. This research has been carried out in partnership with different countries. The strongest collaborations, according to the number of frequencies represented in Figure 3 by the weight of the line, there is a triangulation of collaboration between Finland with China, and the United States, as well as a reported network between China and the USA. Finally, there is a strong collaboration between China and Ghana (Figure 3).

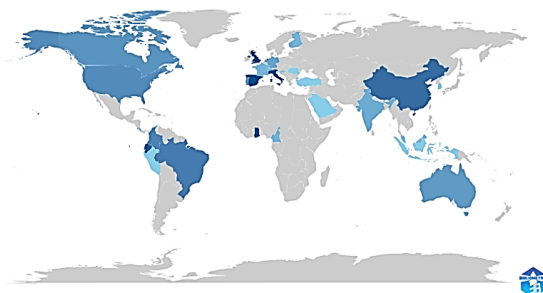


Figure 2. Countries' scientific production.

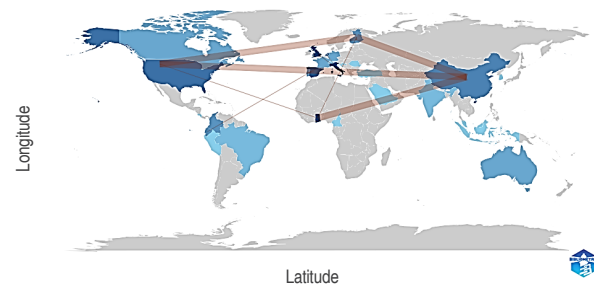


Figure 3. Countries' collaboration.

Figure 4 analyzes citations by country; the top 5, according to total citations, is led by China (177), the United Kingdom

(154), Switzerland (129), and Italy (144). It is worth noting the representation of Colombia in this ranking: (46).

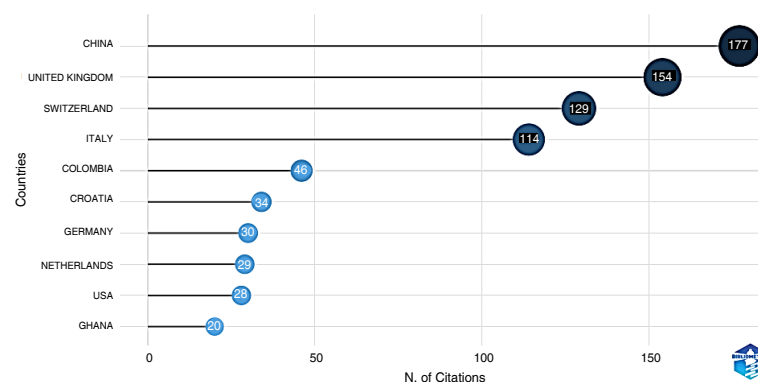


Figure 4. Most cited countries.

Figure 5 presents the ranking according to Multiple Country Publications (MCP) and Single Country Publications (SCP). According to the combination of these variables, the UK leads, followed by Italy and China. In the case of Colombia, research has been carried out only in this

country. Figure 6 shows the historical production by country over the last 5 years, which was initiated by Ghana, the UK, and Italy. Among the new scientific actors, Colombia appears with recent publications in the year 2023 (5) and 2024-2025(10), respectively (Figure 6).

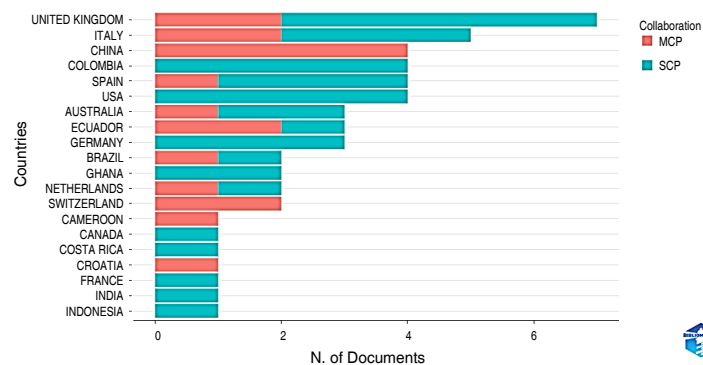


Figure 5. Corresponding author's countries.

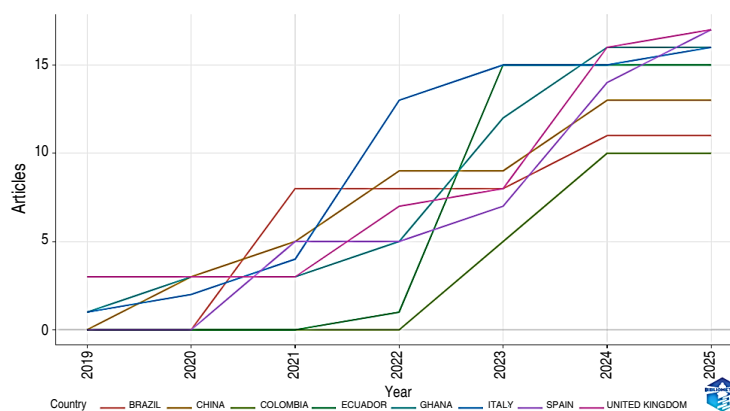


Figure 6. Countries' production over time.

### Preferred journals

Figure 7 shows the top 5 sources according to the number of published articles. Important classifications are highlighted according to the number of records: Journal of Cleaner Production (13); Innovative Food Science (4); Sustainable

Production and Consumption (3). Finally, there are the Applied Geography, Food and Bioprocess Technology, the Journal of International Food and Agribusiness Marketing, and the Supply Chain Management: An International Journal with two registrations, respectively.

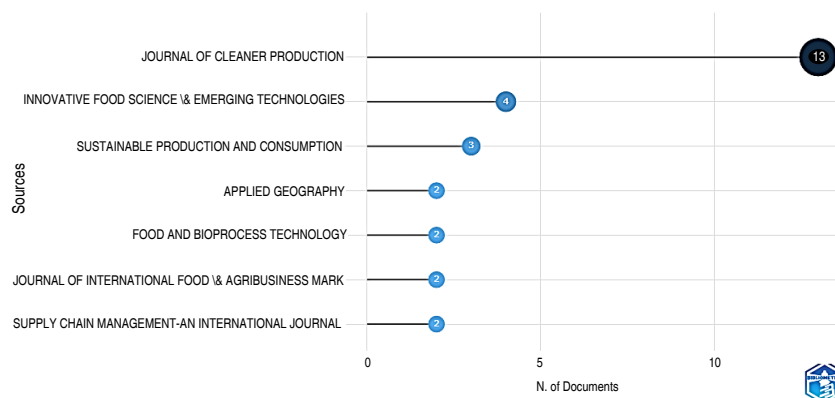


Figure 7. Most relevant sources.

Table 2 shows the main policies of Journals. It should be noted that all of them are of open access, according to the Citi Score bibliometric metrics of the Scopus database, Sustainable Production and Consumption

leads (22.5). However, according to the bibliometric metric, the Impact factor of the WoS database Journal Cleaner Production (10) is the highest among the journals.

**Table 2.** Main bibliometric metrics and journal policies.

Journals	Open access	Article processing charge (USD)	Submission for acceptance	Cite score	Impact factor	Thematic relevance
Cleaner Production	X	4,660	145	20.7	10	Sustainability
Innovative Food Science	X	4,470	85	12.5	6.8	Innovation
Sustainable Production and Consumption	X	3,770	105	22.5	9.6	Technology, consumption and sustainability

**Research trends**

Figure 8 presents the historical distribution of publications, starting in 2019 with 5 papers, reaching historical highs in 2022 with 11 papers, in 2023 there was a 9% decrease in the number of queries. In 2024, there were the same number of papers

as in 2022. In the first half of 2025, the figure is 5 research.

The analysis of references by spectroscopy shows the evolution of citations over time, showing their importance in scientific research (Nica et al. 2024). According to Figure 9,

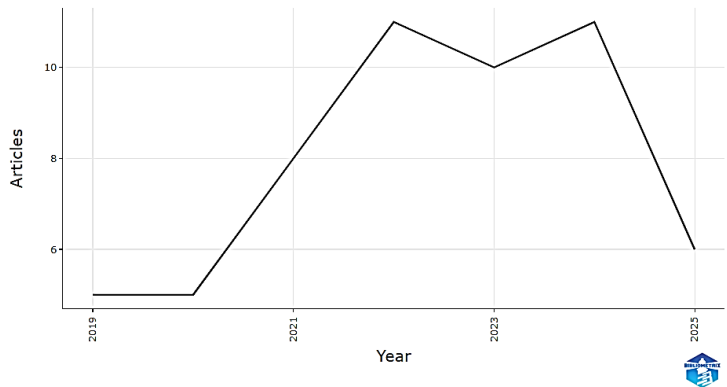


**Figure 8.** Historical evolution of publications.

the first reference found was the research of Nevinson (1906), with one citation. The historical maximum occurred in the 2020s, with 322, taking Adesanya et al. (2020) and LeBaron et al. (2020) as a ranking. According to Google, academic citations for these papers were 120 and 101, respectively (Figure 9).

In this regard, keyword analysis represents the study of the most important words of the authors, revealing important fields in the scientific community (Pesta et al. 2018). In this order of ideas, Figure 10 shows the thematic map

of research, this figure allows to identify the important topics of study according to the keywords of the authors, presenting the weight of the internal importance reflected in the growth of the dimensions and the external importance that is the relationship of the research in a specific field grouped in four segments (Bagdi et al. 2023). Driving topics are relevant topics and have a significant impact on other topics; they are considered topics with restricted progress, niche topics may lack weight and importance, and core topics are fundamental topics but need further research (Serter and Gumusburun 2024).



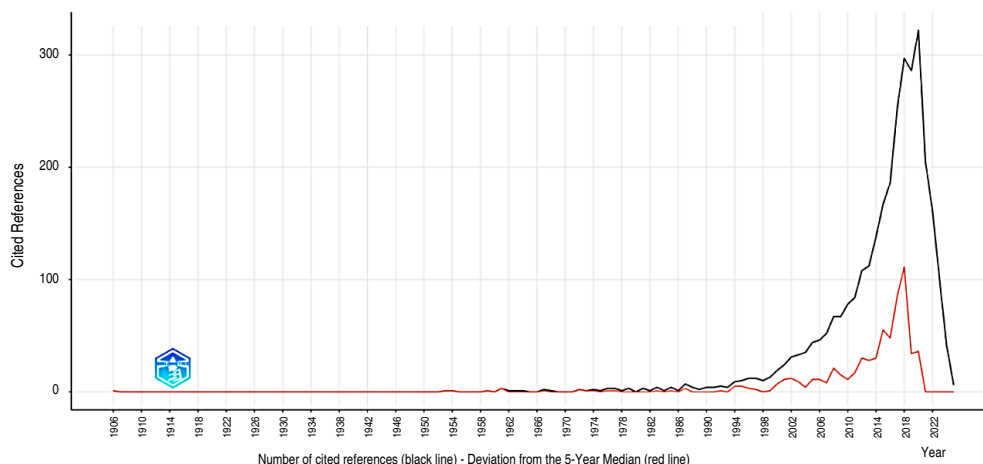


**Figure 9.** Historical evolution of citation.

The following parameters were used to configure the analysis: Number of words: 70, Minimum frequency of clusters (per thousand documents): 5, Number of labels: 3, Label size: 0.3, Community repulsion, and Clustering algorithm Walktrap. The research agenda can be approached from four quadrants: 1) Basic: issues with work that relates to circular economy, cocoa byproducts and

agritourism; 2) Emerging themes: bioactive compounds, polyphenols pretreatment, biochar, cocoa beans, cocoa pod husk; 3) Niche topics are studies related to adoption, agroforestry, agroforestry systems and competitive advantages and 4) Motor topics: sustainability, cocoa, agriculture, life cycle assessment, food and sustainable development.

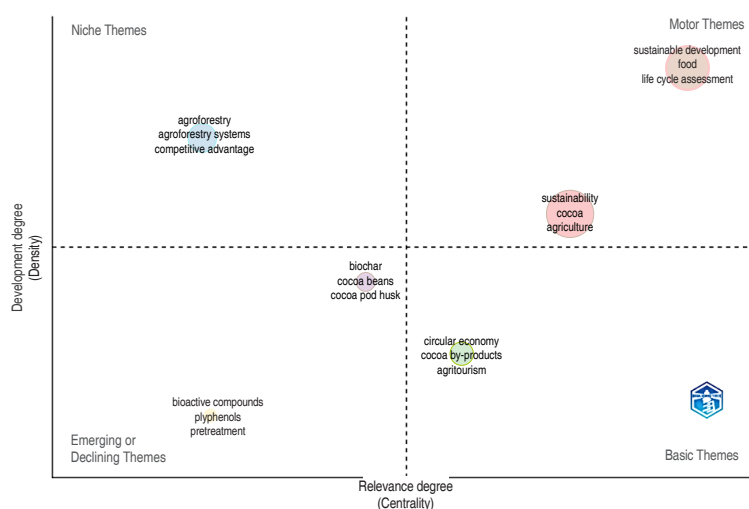


**Figure 10.** Thematic map.

The factorial reduction technique is applied to reduce dimensions and group similarities in scientific topics (Talero-Sarmiento et al. 2025). In this context, by using the multiple correspondence analysis technique (MCA), which represents the data as a point in a low-dimensional

Euclidean space (Abafe et al. 2022). The K-means method was applied to study the association of the co-citation matrix with K=3; the variance of the information in the two dimensions was 86.05%. The first research trend in the green group is related to life cycle assessment in

food. The second blue trend focuses on the sustainable development of supply chains. Finally, the third red trend

is related to cocoa, certifications, sustainability, and supply chain management (Figure 11).

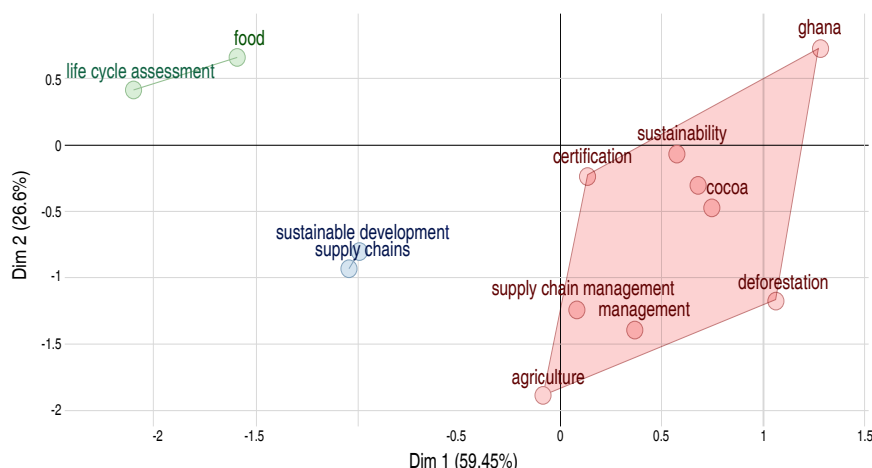


Figure 11. Factorial analysis map.

The keyword clouds figure are a visual scheme of the most relevant words in the research, represented by the size of the word (Turki and Roy 2022). In this line, and

according to Figure 12, taking as a reference the five most relevant according to the records in their respective order, the following were found:



Figure 12. Keywords cloud.

Sustainability (18), Cocoa (11), sustainable development (10), life cycle assessment (7), agriculture, environmental impact, food and management (6), respectively. Figure 13 shows the rectangle diagram, where the size of the geometrical figure represents the importance of the Word (Purna Prakash et al. 2024) and their percentage of use frequency. The following stand out in the same classification, with 40% of the total number of records: Sustainability (10), Cocoa, sustainable

development, life cycle assessment, agriculture, environmental impact and food and management (6), respectively (Figure 13).

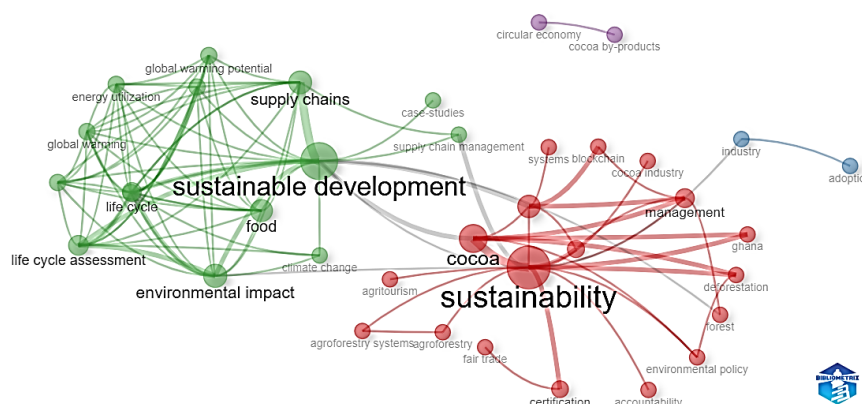
The co-occurrence analysis studies the relationship between keywords. The size of the node and closeness between words allow it to determine the degree of association between them (Det Udomsap and Hallinger 2020). The Walktrap algorithm is recognized for its



**Figure 13.** Keywords tree map.

efficiency in the clustering of key terms and the design of the visualization of the mapping of fields (Pons and Latapy 2005). According to Figure 14, three important word clusters were identified. The first red cluster focused more on sustainability and was related to agro-tourism, agro-forestry, forestry, and certifications, especially fair trade, the cocoa industry, and emerging technologies such as the blockchain. The second, the green color, is more focused on sustainable development related to climate change, global warming, supply chain, life cycle assessment, and environmental

impacts. Finally, the purple cluster focuses more on the circular economy and cocoa byproducts. In order to identify the research trends, a density map was used, where the intensity of red color represents the most important scientific currents. According to the above, in the cluster focused on sustainability, most of the research is done in environmental policies, deforestation, and management, and the cluster led by sustainable development, environmental impacts, climate change, and life cycle assessment (Figure 15) (Sun et al. 2023).



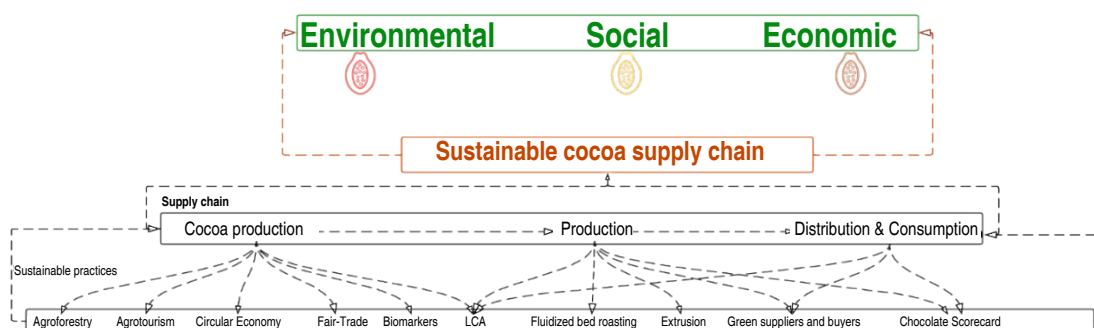
**Figure 14. Keywords co-occurrence.**

Figure 16 shows an integrative conceptual framework, using the metaphorical figure of a cocoa tree for the relevance of the research. The roots are the 10 identified

sustainable practices: Agroforestry, Agrotourism, Circular Economy, Fair Trade, Biomarkers, LCA, Fluidized Bed Roasting, Extrusion, Green Suppliers and Buyers, and



**Figure 15.** Keywords: density map.



**Figure 16.** Framework on sustainable cocoa industry practices.

Chocolate Scorecard, which connect to the supply chain. The above provides support represented in the trunk to the sustainable supply chain. These previously presented relationships will bear fruit, illustrated as three cocoa pods in the balance of the three pillars of sustainability (environmental, social, and economic).

The following are the most relevant results of this research, reflecting on the conceptual and methodological assumptions that underpin the review. From the definition of sustainability by the Brundtland Commission, as the coverage of current needs without sacrificing the coverage of future needs (Brundtland and Khalid 1987), along with the triple bottom line sustainability model developed by John Elkington defined as the balance between profit, social welfare, and environmental impact (Elkington and Rowlands 1999). As it analyzes the concept of sustainable cocoa, it can be defined as the production chain that

generates economic and social benefits while reducing the impact on ecosystems related to the cocoa industry. The definition above is consistent with that (ICCO 2025b). However, according to the same organization, there are problems in the sustainability of the cocoa industry, such as farmers with low economic returns, in addition to the precision exercised by the different stakeholders concerning environmental and social care. Concerning the first topic, the review also revealed the leading research countries as European, which demand high standards for exports related to sustainability and environmental matters. Additionally, Europe plays an important role in the world cocoa trade (Siddiqui et al. 2024). An interesting fact is that as it analyzed the origin of the main journals, these are also European, which ratifies the greater scientific influence of this region, leading the scientific agenda around the sustainability of the cocoa industry. Also, the main papers are open access, which allows a democratization

of knowledge, reaching important studies to groups and interests of little economic development, such as small and medium enterprises (SME), as well as small farmers in the cocoa industry. With respect to research trends, the central topics are certifications, environmental impacts, and dynamic agricultural systems, among which agroforestry systems were identified. This finding is consistent with Olarte and Muñoz (2025).

This research identifies the main sustainable practices in the cocoa industry. The green labels generate benefits for the cocoa supply chain. Farmers can sell their products in European markets, which have the purchase of only sustainably certified cocoa as a restriction since 2020, which motivates exporting companies to certify farmers, generating greater sustainability in their processes. Input purchasing companies guarantee the green traceability of the product, and finally, consumers can enjoy chocolate without remorse of negative impacts on tropical ecosystems (Perez et al. 2022). An important finding was that fair-trade certification generates direct income to farmers by eliminating intermediaries between raw materials and globalized markets, generating higher profits, gender equity, and climate resilience (FairTrade 2025).

Agroforestry emerges as a sustainable system that allows generating benefits to cocoa cultivation, such as planting shade trees to improve production performance and pest control, also minimizing environmental impacts by eliminating the use of chemical insecticides. Also, biomass produced by trees increases the stock of carbon and nutrients in the soil, which improves production yields, which can be transformed into income in carbon payment systems (Krause et al. 2025). However, these agroforestry

systems compete with the resources of cocoa monocrops, with the analysis of the compensation system between the consumption of water, space, and light of the trees versus the performance in cocoa production being important (Abdulai et al. 2025; Ariza-Salamanca et al. 2024).

Life Cycle Assessment (LCA) allows for the analysis of the environmental impacts of a production system along the supply chain (Dominguez et al. 2023). In a global context, the cocoa industry presents high consumption of resources, such as water, electricity, and energy in the production, manufacturing, and transportation stages, generating toxic effects on sources of seawater and human consumption, as a result of wastewater and material waste. In the stage of international transportation from factories to distribution points, fuel consumption produces polluting metals such as mercury and chromium, generating negative impacts on ecosystems (Wang and Dong 2025). Nevertheless, the environmental impact can be mitigated with the following system improvement options: In production, with the use of organic fertilizers and the reduction of pesticides in processing, by switching from diesel to natural gas systems (Ntiamoah and Afrane 2008). Finally, the circular economy has been used in the waste generated by cocoa, such as the cocoa pod, which can be transformed into a reassessment of this waste, such as compost to produce organic fertilizers and pectin for potential use in the biomedical industry (Dachs et al. 2025).

Table 3 presents six authors who investigated the reassessment of cocoa byproducts: Cocoa bean shells (CBS) and pod husks (CPH), from which biochar, polyphenols, advanced materials, improved fertilizers, compost, and hydrocarbons can be obtained.

**Table 3.** Circular economy research.

Authors	Result
Mariatti et al. (2021)	Analyzed the reassessment of waste CBS, CPH, identifying the extraction of polyphenols relevant compound for the biomedical industry.
Mwafurirwa et al. (2024)	Applying the circular economy to identify the extraction of biochar and compost from the CPH.
Girón-Hernández et al. (2024)	Biomass extraction from CPH, studied to extract advanced materials to improve human health.
Hoof et al. (2024)	Biomass reduction of CPH with applied vermicomposting was studied.
Andoh-Mensah et al. (2023)	CBS and NPK fertilizer blend investigated to improve performance in coconut crops.
Landázuri et al. (2023)	Investigated the hydrothermal carbonization of lignocellulosic wastes to produce hydrocarbon from CPH. Materials produced by this process are highly insulating, and can be used by the electrical industry.



Table 4 presents three authors who did research on LCA, which is more focused on studying energy consumption on farms.

Table 5 presents two authors' research on the Sustainable supply chain, which relies on the blockchain to map the supply chain, guaranteeing its sustainability and transparency.

Table 4. LCA Research.

Authors	Result
Caicedo-Vargas et al. (2023)	Identified the volume of cocoa production by smallholder farmers under 10 hectares, the non-cumulative demand for non-renewable energy, carbon footprint, and the net margin.
Armengot et al. (2021)	Studied the relationship between food production and energy, and water consumption using LCA in cocoa farms.
Tagne et al. (2022)	CPH analysis for biomass and bioethanol production.

Table 5. Research Sustainable supply chain.

Authors	Result
Quayson et al. (2021)	Applied technologies, such as blockchains, to improve the vulnerability resistance of small producers in the supply chain and make it more sustainable.
Bai et al. (2022)	Analyzed the application of emerging technologies, such as blockchain, to improve supply chain transparency and solve problems, such as a lack of social responsibility and decreasing environmental performance.
Quayson et al. (2024)	Analyzed the barriers that occur in emerging economies in the implementation of blockchain technology in supply chain sustainability.

Table 6 features the works related to green labels, which focus on Fair-Trade certification, which combines the social and environmental approach on farms.

Seven research projects were carried out studying non-conventional sustainable practices such as Biomarkers, Fluidized bed roasting, Extrusion, Green suppliers and buyers, Chocolate Scorecard, and Agrotourism (Table 7).

Table 6. Green Labels.

Authors	Result
Miglietta et al. (2022)	Studied the discussion of the scope of Fair Trade in ecological sustainability in the economic productivity of the water obtained by the Fair-Trade premium.
Knöbelsdorfer et al. (2021)	Investigated the impact of Fair-Trade certification on food security, concluding that it has an improvement in the standard of living of cocoa farmers and a negative impact on food security.

Table 7. Agroforestry.

Authors	Result
Krause et al. (2025)	Studied how to improve the sequestration of soil carbon dioxide gas reserves by generating tree biomass.
Ariza-Salamanca et al. (2024)	Investigates the variables that drive performance in young cocoa crops compared to agroforestry, where increasing the height of the trees in the agroforestry system may have a decreasing effect on cocoa performance.
Abdulai et al. (2025)	Analyzed how the phenology of leaves in agroforestry systems influences the climate resilience and yield of cocoa.

Table 8 presents studies that explored additional types of sustainable practices.

The practical implications of this work are the identification of a set of sustainable practices in the cocoa industry, along with the design of an integrative framework that allows the different links in the supply chain to generate strategies for

the implementation of practices to achieve sustainability. For example, the government can generate public policies and programs to encourage the implementation of the practices in industry. Additionally, the farmers' cooperatives will have a portfolio of sustainable practices, which will allow them to improve their sustainability strategies and generate green income.

**Table 8.** Research that addressed other types of sustainable practices.

Authors	Practices	Result
Lafargue et al. (2022)	Biomarkers	Created a biomarkers library, which allows sustainable traceability of the cocoa supply chain, enabling audits for compliance with standards.
Peña-Correa et al. (2022)	Fluidized bed roasting	Study of cocoa roasting techniques, oven roasting, and fluidized bed roasting. The latter method is more productive, generating efficiency in energy and water consumption.
Valverde et al. (2021)	Extrusion	Investigated extrusion, which is a more sustainable processing method compared to the traditional alkalization method, where extrusion allows generating an alkalized product with high sensory properties more efficiently and sustainably.
Amoako et al. (2023)	Green suppliers and buyers	Investigated how a strong relationship between green buyers and suppliers improves sustainability through recruitment strategies and rewards.
Perkiss et al. (2025)	Chocolate Scorecard	Used the Chocolate Scorecard sustainability accounting tool to improve sustainability in the company.
Little and Blau (2020)	Agrotourism	Investigated how agrotourism can improve the standard of living of communities and strengthen them in the face of climate change.

For this research, the authors conducted a rigorous search of scientific literature. However, the following limitations are presented: only English language documents from Scopus and WoS databases classified in Q1 and Q2 in the period 2019- 2024 were analyzed. This may lead to the exclusion of relevant documents published in other databases, outside the analyzed period, and journals of minor categories in languages other than English.

## CONCLUSION

According to the literature, the recent increase in global temperatures, surpassing levels recorded in the 19th century, is expected to cause more frequent droughts, food shortages, and a decline in the nutritional quality of food. By defining sustainable cocoa production as an environmentally friendly agricultural process that generates economic gains and benefits families, the above corresponds to only one link in the sustainable supply chain, which covers production, manufacturing,

and marketing, in which balance must be maintained in the three pillars (Environmental, Economic, and Social) for sustainable supply chain holders.

Geographical analysis showed Spain, the UK, and Ghana, together with Ecuador, lead the research; the strongest scientific clusters are those related to the China-US network, and finally, there is a strong collaboration between China and Ghana. Research on sustainable cocoa production is concentrated in Europe. This leadership arises because of the restrictive measures imposed on cocoa exports to this region.

Analyzing the submission policies and trends of the journals (high-impact journals), all of which are Open Access, generates greater visibility of the research, as there is no charge for accessing the document. This allows the development of a democratization of knowledge by providing access to information to various

stakeholders, including cocoa cooperatives and small and medium-sized enterprises, which face budgetary constraints.

About the global research trends in the established topics in cocoa and sustainability, the thematic analysis was able to demonstrate that the trend in research revolves around certifications in sustainability and environmental impacts, together with dynamic farming systems, in addition to the decrease of the environmental impacts through the assessment of the residues of the cocoa production process, in this case the cocoa pod. Regarding the supply chain, to guarantee sustainability in all the links of the production, manufacturing and commercialization chain.

Finally, according to the bibliometric analysis, sustainable agroforestry systems provide an important opportunity to enhance sustainability in the cocoa production process by reducing environmental impacts through carbon sequestration, which can be translated into income for producers. However, a cost–benefit relationship was identified between the profitability of the system and resource consumption, so farmers should assess whether the benefits of adopting sustainable agroforestry systems outweigh the resources used. Sustainable certifications, such as those identified in the Fair-Trade study, also serve as a competitive advantage when entering European markets and generate direct income for farmers by reducing the influence of intermediaries. Life Cycle Assessment (LCA) analysis enables producers to implement improvement measures aimed at reducing environmental impacts related to energy and water use, as well as enhancing environmentally friendly transportation systems to prevent the discharge of heavy metals into water sources for both marine and human consumption. Additionally, residues from cocoa production, such as cocoa pods, can be converted into compost through circular economy practices, replacing chemical fertilizers, improving profitability, and making production more environmentally friendly. Moreover, these residues can be processed into pectin, a key component in the biomedical industry. Future research could further explore the relationship between sustainability, Industry 4.0 technologies, and cocoa—an area that remains underexplored—such as the use of precision agriculture tools and blockchain traceability.

It could also address how technology adoption in the cocoa industry can improve enterprise sustainability and contribute to sustainable development, as well as expand geographical studies to regions such as Central Africa and Southeast Asia, where cocoa production is significant but underrepresented in the literature.

## ACKNOWLEDGMENTS

The researchers would like to thank the UNIRED Activa2 call, the Santo Tomás University, Bucaramanga branch, and the University of Santander for the resources provided for this research.

## CONFLICT OF INTERESTS

Researchers state that they have no conflict of interest.

## REFERENCES

- Abafe EA, Bahta YT and Jordaan H (2022) Exploring biblioshiny for historical assessment of global research on sustainable use of water in agriculture. *Sustainability* 14: 10651. <https://doi.org/10.3390/su141710651>
- Abdulai I, Hoffmann M, Kahiluoto H et al (2025) Functional groups of leaf phenology are key to build climate-resilience in cocoa agroforestry systems. *Agric Ecosyst Environ* 379: 109363. <https://doi.org/10.1016/j.agee.2024.109363>
- Adesanya A, Yang B, Bin Iqdara FW and Yang Y (2020) Improving sustainability performance through supplier relationship management in the tobacco industry. *Supply Chain Management: An International Journal* 25: 413–426. <https://doi.org/10.1108/SCM-01-2018-0034>
- Agyei V, Adom-Asamoah G and Poku-Boansi M (2024) Sustainable transportation in Africa: A bibliometric, visualisation and thematic analysis. *Journal of Cleaner Production* 462: 142727. <https://doi.org/10.1016/j.jclepro.2024.142727>
- Amoako DK, Zakuan MN, Okyere-Kwakye E and Tetteh FK (2023) Effect of Training and Reward on Social Sustainability in Ghana's Cocoa Supply Chain: The Role of Green Buyer-Supplier Relationship. *Journal of International Food & Agribusiness Marketing* 35: 212–243. <https://doi.org/10.1080/08974438.2021.1981511>
- Andoh-Mensah E, Anthonio CK, Sossah FL et al (2023) Integrated soil fertility management using cocoa bean shells improves soil chemical properties, coconut yield and mitigates environmental pollution. *Journal of Cleaner Production* 428: 139418. <https://doi.org/10.1016/j.jclepro.2023.139418>
- Ariza-Salamanca AJ, Navarro-Cerrillo RM, Crozier J et al (2024) Drivers of cocoa yield and growth in young monoculture and agroforestry systems. *Agric Syst* 219: 104044. <https://doi.org/10.1016/j.agsy.2024.104044>
- Armengot L, Beltrán MJ, Schneider M et al (2021) Food-energy-water nexus of different cacao production systems from a LCA approach. *Journal of Cleaner Production* 304: 126941. <https://doi.org/10.1016/j.jclepro.2021.126941>
- Aziz F, Li C, Khan AU and Khan A (2024) Emerging trends and insights in sustainable innovation performance: A two decade literature review (2002–2022). *Journal of Cleaner Production* 467: 142805.

<https://doi.org/10.1016/j.jclepro.2024.142805>

Bagdi T, Ghosh S, Sarkar A et al (2023) Evaluation of research progress and trends on gender and renewable energy: A bibliometric analysis. *Journal of Cleaner Production* 423: 138654. <https://doi.org/10.1016/j.jclepro.2023.138654>

Bai C, Quayson M and Sarkis J (2022) Analysis of Blockchain's enablers for improving sustainable supply chain transparency in Africa cocoa industry. *Journal of Cleaner Production* 358: 131896. <https://doi.org/10.1016/j.jclepro.2022.131896>

Bandanaa J, Asante IK, Annang TY et al (2025) Social and environmental trade-offs and synergies in cocoa production: Does the farming system matter? *Sustainability* 17: 1674. <https://doi.org/10.3390/su17041674>

Barrios-Rodríguez YF, Salas-Calderón KT, Orozco-Blanco DA et al (2022) Cocoa pod husk: a high-pectin source with applications in the food and biomedical fields. *ChemBioEng Reviews* 9: 462–474. <https://doi.org/10.1002/cben.202100061>

Brundtland GH and Khalid M (1987) *Our common future*. Oxford University Press, Oxford, GB.

Caicedo-Vargas C, Pérez-Neira D, Abad-González J and Gallar D (2023) Agroecology as a means to improve energy metabolism and economic management in smallholder cocoa farmers in the Ecuadorian Amazon. *Sustainable Production and Consumption* 41: 201–212. <https://doi.org/10.1016/j.spc.2023.08.005>

Chen W and Hao H (2025) Environmental regulation and Outward FDI of Chinese listed companies: The role of technological innovations. *Economic Analysis and Policy*. <https://doi.org/10.1016/j.eap.2025.07.023>

Dachs I, Rülke J and Franz M (2025) Bringing a circular economy perspective into global production networks: Cocoa pod husk-based compost production in Ghana. *Journal of Cleaner Production* 519: 145955. <https://doi.org/10.1016/j.jclepro.2025.145955>

Det Udomsap A and Hallinger P (2020) A bibliometric review of research on sustainable construction, 1994–2018. *Journal of Cleaner Production* 254: 120073. <https://doi.org/10.1016/j.jclepro.2020.120073>

Dominguez Aldama D, Grassauer F, Zhu Y et al (2023) Allocation methods in life cycle assessments (LCAs) of agri-food co-products and food waste valorization systems: Systematic review and recommendations. *Journal of Cleaner Production* 421: 138488. <https://doi.org/10.1016/j.jclepro.2023.138488>

Dröge S, Makmun Jusrin MJ, Verbist B et al (2025) No effect of rainforest alliance cocoa certification on shade cover and bird species richness in Sulawesi, Indonesia. *Journal for Nature Conservation* 84: 126849. <https://doi.org/10.1016/j.jnc.2025.126849>

Elkington J and Rowlands IH (1999) Cannibals with forks: The triple bottom line of 21st century business. *Alternatives Journal* 25: 42.

FairTrade (2025) Cocoa. [https://www.fairtrade.net/en/products/Fairtrade\\_products/cocoa.html](https://www.fairtrade.net/en/products/Fairtrade_products/cocoa.html)

Fayaz G, Mhamadi M, Rodrigue D et al (2024) Mapping approach for selecting promising agro-waste dietary fibers as sustainable and functional food ingredients. *Food and Bioprocess Technology* 17: 1797–1813. <https://doi.org/10.1007/s11947-023-03223-w>

Fernández-Ríos A, Laso J, Hoehn D et al (2022) A critical review of superfoods from a holistic nutritional and environmental approach. *Journal of Cleaner Production* 379: 134491. <https://doi.org/10.1016/j.jclepro.2022.134491>

García-Herrero L, Menna F De and Vittuari M (2019) Sustainability concerns and practices in the chocolate life cycle: Integrating consumers'

perceptions and experts' knowledge. *Sustainable Production and Consumption* 20: 117–127. <https://doi.org/10.1016/j.spc.2019.06.003>

Girón-Hernández J, Rodríguez YB, Corbezzolo N et al (2024) Exploiting residual cocoa biomass to extract advanced materials as building blocks for manufacturing nanoparticles aimed at alleviating formation-induced oxidative stress on human dermal fibroblasts. *Nanoscale Advances* 6: 3809–3824. <https://doi.org/10.1039/D4NA00248B>

Hoof B Van, Solano A, Riaño J et al (2024) Decision-making for circular economy implementation in agri-food systems: A transdisciplinary case study of cacao in Colombia. *Journal of Cleaner Production* 434: 140307. <https://doi.org/10.1016/j.jclepro.2023.140307>

ICCO (2025a) Data on production and grindings of cocoa beans. <https://www.icco.org/statistics/>

ICCO (2025b) Sustainability of the world cocoa economy. <https://www.icco.org/economy/#sustainability>

Keller J, Jung M and Lasch R (2022) Sustainability Governance: Insights from a cocoa supply chain. *Sustainability* 14: 10763. <https://doi.org/10.3390/su141710763>

Knöbelsdorfer I, Sellare J and Qaim M (2021) Effects of Fairtrade on farm household food security and living standards: Insights from Côte d'Ivoire. *Global Food Security* 29: 100535. <https://doi.org/10.1016/j.gfs.2021.100535>

Krause H-M, Saj S, Rüegg J et al (2025) Successional agroforestry promotes biomass carbon storage in cocoa production systems: results from a long-term system comparison experiment on organic and conventional systems. *Agriculture, Ecosystems & Environment* 393: 109820. <https://doi.org/10.1016/j.agee.2025.109820>

Lafargue P, Rogerson M, Parry GC and Allaingillaume J (2022) Broken chocolate: Biomarkers as a method for delivering cocoa supply chain visibility. *Supply Chain Management: An International Journal* 27: 728–741. <https://doi.org/10.1108/SCM-11-2020-0583>

Landázuri AC, Pröcel LM, Caisaluisa O et al (2023) Valorization of ripe banana peels and cocoa pod husk hydrochars as green sustainable "low loss" dielectric materials. *Journal of Cleaner Production* 426: 139044. <https://doi.org/10.1016/j.jclepro.2023.139044>

LeBaron T, Singh R, Fatima G et al (2020) The effects of 24-week, high-concentration hydrogen-rich water on body composition, blood lipid profiles and inflammation biomarkers in men and women with metabolic syndrome: A randomized controlled trial. *Diabetes, Metabolic Syndrome and Obesity Volume* 13: 889–896. <https://doi.org/10.2147/DMSO.S240122>

Little ME and Blau E (2020) Social adaptation and climate mitigation through agrotourism: A case study of tourism in Mastatal, Costa Rica. *Journal of Ecotourism* 19: 97–112. <https://doi.org/10.1080/14724049.2019.1652305>

López del Amo B and Akizu-Gardoki O (2024) Derived environmental impacts of organic fairtrade cocoa (Peru) compared to its conventional equivalent (Ivory Coast) through life-cycle assessment in the basque country. *Sustainability* 16: 493. <https://doi.org/10.3390/su16020493>

Madeira C, Rodrigues P and Gomez-Suarez M (2023) A bibliometric and content analysis of sustainability and smart tourism. *Urban Science* 7: 33. <https://doi.org/10.3390/urbansci7020033>

Mariatti F, Gunjević V, Boffa L and Cravotto G (2021) Process intensification technologies for the recovery of valuable compounds from cocoa by-products. *Innovative Food Science & Emerging Technologies* 68: 102601. <https://doi.org/10.1016/j.ifset.2021.102601>



- Miglietta PP, Fischer C and De Leo F (2022) Virtual water flows and economic water productivity of Italian fair-trade: The case of bananas, cocoa and coffee. *British Food Journal* 124: 4009–4023. <https://doi.org/10.1108/BFJ-03-2020-0265>
- Moluh Njoya H, Cristóbal Reyes S, Hien KA et al (2025) Can cooperative membership foster compliance with New European Union regulations on deforestation-free production? Evidence from cocoa farmers in Western Côte d'Ivoire. *Trees, Forests and People* 20: 100897. <https://doi.org/10.1016/j.tfp.2025.100897>
- Mwafurirwa L, Sizmur T, Daymond A et al (2024) Cocoa pod husk-derived organic soil amendments differentially affect soil fertility, nutrient leaching, and greenhouse gas emissions in cocoa soils. *Journal of Cleaner Production* 479: 144065. <https://doi.org/10.1016/j.jclepro.2024.144065>
- Nevinson HW (1906) *A modern slavery*. Harper & Brothers, United Kingdom.
- Nica I, Georgescu I and Chiriță N (2024) Simulation and Modelling as Catalysts for Renewable Energy: A bibliometric analysis of global research trends. *Energies (Basel)* 17: 3090.
- Ntiamoah A and Afrane G (2008) Environmental impacts of cocoa production and processing in Ghana: Life cycle assessment approach. *Journal of Cleaner Production* 16: 1735–1740. <https://doi.org/10.1016/j.jclepro.2007.11.004>
- Olarte Libreros MM and Muñoz Maya CM (2025) Sustainable practices in the cocoa value chain: A systematic literature review. *Tendencias* 26: 191–215. <https://doi.org/10.22267/trend.252601.270>
- Peña-Correa RF, Ataç Mogol B, van Boekel MAJS and Fogliano V (2022) Fluidized bed roasting of cocoa nibs speeds up processing and favors the formation of pyrazines. *Innovative Food Science & Emerging Technologies* 79: 103062. <https://doi.org/10.1016/j.ifset.2022.103062>
- Perez M, Lopez-Yerena A and Vallverdú-Queralt A (2022) Traceability, authenticity and sustainability of cocoa and chocolate products: a challenge for the chocolate industry. *Critical Reviews in Food Science and Nutrition* 62: 475–489. <https://doi.org/10.1080/10408398.2020.1819769>
- Perkiss S, Dumay J, Bernardi C et al (2025) Accountability to tackle sustainability challenges in the cocoa supply chain. *Accounting, Auditing & Accountability Journal*. <https://doi.org/10.1108/AAAJ-05-2024-7069>
- Pesta B, Fuerst J and Kirkegaard E (2018) Bibliometric Keyword Analysis across Seventeen Years (2000–2016) of Intelligence Articles. *Journal of Intelligence* 6: 46. <https://doi.org/10.3390/jintelligence6040046>
- Pons P and Latapy M (2005) Computing communities in large networks using random walks. pp 284–293. [https://doi.org/10.1007/11569596\\_31](https://doi.org/10.1007/11569596_31)
- Purna Prakash K, Venkata Pavan Kumar Y, Himajyothi K and Pradeep Reddy G (2024) Comprehensive bibliometric analysis on smart grids: Key concepts and research trends. *Electricity* 5: 75–92. <https://doi.org/10.3390/electricity5010005>
- Puyana-Romero V, Iannace G, Cajas-Camacho LG et al (2022) Acoustic characterization and modeling of silicone-bonded cocoa crop waste using a model based on the gaussian support vector machine. *Fibers* 10: 25. <https://doi.org/10.3390/fib10030025>
- Quach S, Roberts RE, Dang S et al (2025) The interaction between values and self-identity on fairtrade consumption: The value-identity-behavior model. *Appetite* 206: 107826. <https://doi.org/10.1016/j.appet.2024.107826>
- Quayson M, Bai C and Sarkis J (2021) Technology for social good foundations: A perspective from the smallholder farmer in sustainable supply chains. *IEEE Transactions on Engineering Management* 68: 894–898. <https://www.semanticscholar.org/paper/Technology-for-Social-Good-Foundations%3A-A-From-the-Quayson-Bai/f71de9e08fc48d8bdebf569c1cdf0072c230d7ad>
- Quayson M, Bai C, Sarkis J and Hossin MA (2024) Evaluating barriers to blockchain technology for sustainable agricultural supply chain: A fuzzy hierarchical group DEMATEL approach. *Operations Management Research* 17: 728–753. <https://doi.org/10.1007/s12063-024-00443-x>
- Rathgens J, Gröschner S and von Wehrden H (2020) Going beyond certificates: A systematic review of alternative trade arrangements in the global food sector. *Journal of Cleaner Production* 276: 123208. <https://doi.org/10.1016/j.jclepro.2020.123208>
- Ribeiro-Duthie AC, Gale F and Murphy-Gregory H (2021) Fair trade and staple foods: A systematic review. *Journal of Cleaner Production* 279: 123586. <https://doi.org/10.1016/j.jclepro.2020.123586>
- Salihi C, Hussein M, Mohandes SR and Zayed T (2022) Towards a comprehensive review of the deterioration factors and modeling for sewer pipelines: A hybrid of bibliometric, scientometric, and meta-analysis approach. *Journal of Cleaner Production* 351: 131460. <https://doi.org/10.1016/j.jclepro.2022.131460>
- Serter M and Gumusburun Ayalp G (2024) A Holistic analysis on risks of post-disaster reconstruction using RStudio Bibliometrix. *Sustainability* 16: 9463. <https://doi.org/10.3390/su16219463>
- Siao H-J, Gau S-H, Kuo J-H et al (2022) Bibliometric analysis of environmental, social, and governance management research from 2002 to 2021. *Sustainability* 14: 16121. <https://doi.org/10.3390/su142316121>
- Siddiqui SA, Karim I, Shahiya C et al (2024) A critical review of consumer responsibility in promoting sustainable cocoa production. *Current Research in Food Science* 9: 100818. <https://doi.org/10.1016/j.crf.2024.100818>
- Silva AR de A, Bioto AS, Efraim P and Queiroz G de C (2017) Impact of sustainability labeling in the perception of sensory quality and purchase intention of chocolate consumers. *Journal of Cleaner Production* 141: 11–21. <https://doi.org/10.1016/j.jclepro.2016.09.024>
- Steinke J, Ivanova Y, Jones SK et al (2024) Digital sustainability tracing in smallholder context: Ex-ante insights from the Peruvian cocoa supply chain. *World Development Sustainability* 5: 100185. <https://doi.org/10.1016/j.wds.2024.100185>
- Sun J, Zhang D, Peng S et al (2023) Insights of the fate of antibiotic resistance genes during organic solid wastes composting based on bibliometric analysis: Development, hotspots, and trend directions. *Journal of Cleaner Production* 425: 138781. <https://doi.org/10.1016/j.jclepro.2023.138781>
- Suri T and Basu S (2022) Heat resistant chocolate development for subtropical and tropical climates: A review. *Critical Reviews in Food Science and Nutrition* 62: 5603–5622. <https://doi.org/10.1080/10408398.2021.1888690>
- Tagne RFT, Santagata R, Tchuiwon Tchuiwon DR et al (2022) Environmental impact of second-generation biofuels production from agricultural residues in Cameroon: A life-cycle assessment study. *Journal of Cleaner Production* 378: 134630. <https://doi.org/10.1016/j.jclepro.2022.134630>
- Talero-Sarmiento LH, Parra-Sanchez DT and Lamos-Diaz H (2025) A bibliometric analysis of computational and mathematical techniques in the cocoa sustainable food value chain. *Heliyon* 11: e43015. <https://doi.org/10.1016/j.heliyon.2025.e43015>



doi.org/10.1016/j.heliyon.2025.e43015

Tischner U, Stø E, Kjærnes U and Tukker A (2017) System innovation for sustainability 3: Case studies in sustainable consumption and production—food and agriculture. Routledge.

Tsilika K (2023) Exploring the contributions to mathematical economics: A bibliometric analysis using bibliometrix and VOSviewer. *Mathematics* 11: 4703. <https://doi.org/10.3390/math11224703>

Turki T and Roy SS (2022) Novel hate speech detection using word cloud visualization and ensemble learning coupled with count vectorizer. *Applied Sciences* 12: 6611. <https://doi.org/10.3390/app12136611>

Urugo MM, Worku M, Tola YB and Gemele HF (2025) Ethiopian

coffee: Production systems, geographical origin traceability, and European Union deforestation regulation directive compliance. *Journal of Agriculture and Food Research* 19: 101695. <https://doi.org/10.1016/j.jafr.2025.101695>

Valverde D, Sánchez-Jiménez V, Barat JM and Pérez-Esteve É (2021) The effect of extrusion on the physical and chemical properties of alkalized cocoa. *Innovative Food Science & Emerging Technologies* 73: 102768. <https://doi.org/10.1016/j.ifset.2021.102768>

Wang S and Dong Y (2025) Analyzing the environmental footprint of the chocolate industry using a hybrid life cycle assessment method. *Cleaner Engineering and Technology* 25: 100912. <https://doi.org/10.1016/j.clet.2025.100912>

# Gluten-free cookies made with white carrot (*Arracacia xanthorrhiza* Bancr) and rice (*Oryza sativa*) flour



Galletas sin gluten elaboradas con zanahoria blanca (*Arracacia xanthorrhiza* Bancr) y arroz (*Oryza sativa*)

<https://doi.org/10.15446/rfnam.v78n3.115838>

Gina Mariuxi Guapi Álava<sup>1\*</sup>, Vicente Alberto Guerrón Troya<sup>1</sup>, Milena Mayerli Alvarado Moran<sup>1</sup>, Jhonnatan Placido Aldas Morejon<sup>2,3</sup> and Karol Yannela Revilla Escobar<sup>4</sup>

## ABSTRACT

### Keywords:

Gluten-free diet  
Food safety  
Nutritional value  
Rice-based products  
Sensory analysis  
White carrot

White carrot (*Arracacia xanthorrhiza* Bancr) flour is a rich source of nutrients, dietary fiber, and antioxidants such as polyphenols, while rice (*Oryza sativa*) flour is valued for its flavor and emulsifying properties. This study aimed to develop gluten-free cookies by combining white carrot flour and rice flour. A completely randomized design with a factorial arrangement A×B was used, where factor A was the flour ratio and factor B was the dough resting time, resulting in six treatments with three replicates (18 experimental units). Physicochemical, sensory, and microbiological analyses were conducted. Statistical differences were determined using the Tukey test ( $P<0.05$ ) with InfoStat software. The results of the physicochemical analysis showed that treatment T1 (90% carrot flour/10% rice flour + 10 min rest) had the highest values of protein (5.39%), fat (20.01%), and fiber (18.66%). In sensory evaluation, T1 also obtained the highest scores for odor (4.4), flavor (4.2), and texture (4.0). Microbiological results confirmed that counts for molds, yeasts, and mesophilic aerobic bacteria were below the permissible limits established by INEN 1529-10 and NTE INEN 1529-5 standards. In conclusion, the proportion of white carrot and rice flour significantly influenced the physicochemical and sensory qualities of the gluten-free cookies, demonstrating the potential of these ingredients in functional food formulations.

## RESUMEN

### Palabras clave:

Dieta sin gluten  
Seguridad alimentaria  
Valor nutricional  
Productos a base de arroz  
Análisis sensorial  
Zanahoria blanca

La harina de zanahoria blanca (*Arracacia xanthorrhiza*) es una fuente rica en nutrientes, fibra dietética y compuestos antioxidantes como los polifenoles, mientras que la harina de arroz (*Oryza sativa*) se caracteriza por su sabor y capacidad emulsionante. El objetivo de este estudio fue elaborar galletas libres de gluten a partir de la combinación de harina de zanahoria blanca y harina de arroz. Se utilizó un diseño completamente al azar con un arreglo factorial A×B, donde el factor A fue la proporción de harinas y el factor B el tiempo de reposo de la masa, obteniendo seis tratamientos con tres repeticiones (18 unidades experimentales). Se realizaron análisis fisicoquímicos, sensoriales y microbiológicos. Las diferencias estadísticas se evaluaron mediante la prueba de Tukey ( $P<0,05$ ) utilizando el software InfoStat. Los resultados del análisis fisicoquímico indicaron que el tratamiento T1 (90% harina de zanahoria/10% harina de arroz + 10 min de reposo) presentó los mayores valores de proteína (5,39%), grasa (20,01%) y fibra (18,66%). En la evaluación sensorial, T1 también destacó con puntajes más altos en olor (4,4), sabor (4,2) y textura (4,0). El análisis microbiológico mostró que los conteos de mohos, levaduras y aerobios mesófilos estuvieron por debajo de los límites permitidos según las normas INEN 1529-10 y NTE INEN 1529-5. En conclusión, la proporción de harinas influyó significativamente en las características fisicoquímicas y sensoriales de las galletas, demostrando el potencial de estos ingredientes en formulaciones de alimentos funcionales.

<sup>1</sup>Facultad de Ciencias de la Industria y Producción, Universidad Técnica Estatal de Quevedo, Quevedo, Ecuador. [gguapi@uteq.edu.ec](mailto:gguapi@uteq.edu.ec) , [vguerron@uteq.edu.ec](mailto:vguerron@uteq.edu.ec) , [milena.alvarado2016@uteq.edu.ec](mailto:milena.alvarado2016@uteq.edu.ec)

<sup>2</sup>Pontificia Universidad Católica del Ecuador Sede Esmeraldas, Esmeraldas, Ecuador. [jpaldasmorejón@puces.edu.ec](mailto:jpaldasmorejón@puces.edu.ec)

<sup>3</sup>Facultad de Ciencias Aplicadas a la Industria, Universidad Nacional de Cuyo, San Rafael, M5600APG, Argentina.

<sup>4</sup>Universidad Pública de Santo Domingo de los Tsáchilas - UPSDT, km 28, vía Santo Domingo - Quevedo, Ecuador. [krevillaescobar@upsdt.edu.ec](mailto:krevillaescobar@upsdt.edu.ec)

\* Corresponding author



For a long time, wheat flour has been widely used in the manufacture of various bakery products due to its gluten content. However, gluten consumption is associated with celiac disease (Ahmad et al. 2016), which has driven the need to develop safe, gluten-free alternatives, including cookies (Nieto-Mazzocco et al. 2018). One promising approach involves the use of unconventional flours such as white carrot (*Arracacia xanthorrhiza* Bancr.) flour and rice (*Oryza sativa* L.) flour for gluten-free product development.

White carrot (*Arracacia xanthorrhiza* Bancr.) is a tuberous root cultivated along the Andean Mountain range from Venezuela to northern Chile, notable for its geographic adaptability and classified into three varieties: white, yellow, and purple. In Ecuador, yields of up to 5,000 kg per hectare have been reported, with annual production reaching between 12,000 and 24,000 tons (Nayghit Carrero et al. 2018). Rich in starch, calcium, vitamin A, niacin, ascorbic acid, and phosphorus, white carrot flour is utilized in the production of breads, snacks, instant soups, desserts, beer, dog food, cookies, porridges, and functional foods for children (Mandrich et al. 2023).

The incorporation of fruits and vegetables into the food industry is increasingly valued for their content of dietary fiber, minerals, vitamins, antioxidants, and bioactive compounds (Bas-Bellver et al. 2024). Specifically, white carrot flour has been identified as a promising source of carbohydrates, bioactive compounds, and antioxidants such as polyphenols and carotenoids, which may confer functional properties (Jordán Villamar 2018).

In recent years, cereals have gained attention in the food industry due to their functional properties, including water absorption and retention, emulsification, and stability. Additionally, their high protein content enhances the nutritional value of food products (Pérez Ramos et al. 2017). Rice (*Oryza sativa* L.) flour, recognized for its neutral flavor and dough-forming capacity, is widely used in gluten-free products. It also serves as a suitable source of starch and quality protein, making it ideal for baked goods such as cookies (Almora-Hernández et al. 2023).

Cookies are among the most popular bakery products worldwide, with their diverse flavors and shelf life fostering continuous product development. The use of novel flours

in cookie production has gained popularity due to their potential nutritional benefits (Ranasinhe et al. 2022).

Despite the growing interest in gluten-free bakery products, there is limited research on the combined use of white carrot and rice flours for cookie production. Therefore, this study aims to develop gluten-free cookies using white carrot (*Arracacia xanthorrhiza* Bancr.) flour and rice (*Oryza sativa* L.) flour, evaluating their potential to deliver nutritionally enhanced and functional bakery products that meet the increasing demand for gluten-free alternatives.

## MATERIALS AND METHODS

The raw materials used in the study were purchased at the local market in the Quevedo canton, located in the Los Ríos province of Ecuador. The physicochemical and microbiological analysis were performed in the Biotechnology Laboratory of the "La María" experimental farm, part of the Quevedo State Technical University (UTEQ), located in the city of Quevedo (1.0285° S, 79.4603° W).

### Experimental design

A complete randomized design with factorial arrangement AxB was applied, where factor A: ratio of white carrot flour-rice flour and factor B: dough rest, thus obtaining a total of six treatments with three replicates resulting in 18 experimental units. To determine statistical differences, a Tukey test ( $P < 0.05$ ) was applied using the InfoStat Software. The treatments are detailed in Table 1.

**Table 1.** Treatments for the development of gluten-free cookies using white carrot flour and rice flour.

Treatments	Description
T1	90% white carrot flour/10% rice flour +10 min.
T2	90% white carrot flour/10% rice flour +20 min.
T3	80% white carrot flour/20% rice flour +10 min.
T4	80% white carrot flour/20% rice flour +20 min.
T5	70% white carrot flour/30% rice flour +10 min.
T6	70% white carrot flour/30% rice flour +20 min.

### Process for the elaboration of white carrot and rice flour-based cookies

The raw materials were received and visually checked to ensure they were free from damage. The white carrots were previously washed to remove impurities, cut into

2 mm pieces, placed in aluminum trays, and dehydrated in an oven for 24 h at 65 °C. This temperature was selected because it is below the gelatinization temperature of starch (typically 68–75 °C), preventing structural changes that could negatively affect the functionality of the flour. Once the white carrot flour was obtained, the following ingredients were mixed and homogenized using a mixer until a consistent dough was formed: vegetable shortening (60 g), egg (50 g), sugar (80 g), baking powder (5 g), coconut essence (2 mL), salt (1 g), white carrot flour (100 g), and rice flour (100 g). The dough was left to rest for 20 min to allow for proper hydration of the flours and to relax the structure, facilitating handling and improving the texture of the final baked product. Afterward, the dough was baked for 30 min at 150 °C and finally stored at room temperature (28 °C).

### Physicochemical analysis of gluten-free cookies

Moisture content was determined according to the Ecuadorian Technical Standard NTE INEN 2 085 (INEN 2005). Ash content was obtained by incineration in a muffle furnace at 100 °C for 30 minutes, following the procedure established in NTE INEN (1981). Protein and fat contents were determined based on the reference methods NTE INEN 0523 (INEN 1980) and AOAC 21st ed. 920.87, respectively. Crude fiber was determined according to NTE INEN 522 (INEN 1981). Carbohydrate content was calculated by difference, subtracting the sum of moisture, ash, protein, fat, and fiber from 100. The energy value was estimated using the Atwater system, applying the following conversion factors: 4 kcal g<sup>-1</sup> for protein, 9 kcal g<sup>-1</sup> for fat, and 4 kcal g<sup>-1</sup> for carbohydrates.

### Sensory analysis

The sensory profiles were evaluated by a panel of 25 semi-trained evaluators, each of whom received a 10 g sample for analysis. The sensory evaluation employed a structured 5-point hedonic scale, where 5 represented “very liked” and 1 indicated “disliked.” The attributes evaluated included color, odor, flavor, and overall acceptability.

### Microbiological analysis

Mold and yeast analyses were performed on the treatment that presented the best sensory characteristics. These were carried out in certified laboratories using the methods described in the Ecuadorian Technical Standard NTE INEN 1529-10 (INEN 2013).

## RESULTS AND DISCUSSION

According to Table 2 there were significant differences in moisture content ( $P<0.05$ ), where T3 had a higher moisture content of 7.30%, while T5-T6 had a lower moisture content of 5.20. These values were lower than those obtained in the present study where cookies made from brown rice with the addition of Stevia obtained moisture values ranging from 4.43 to 3.96% (Almora-Hernández et al. 2023). Bazan-Aliaga et al. (2015) mention that obtaining a moisture content lower than 10%, significantly reduces the risk of spoilage by microorganisms and in turn prolongs the shelf life of the product.

The ash results showed similarity between treatments T2, T5, and T6, with a value of 3.7% where the highest content was observed. On the other hand, treatments

**Table 2.** Physicochemical characterization of cookies.

Treatments	Moisture (%)	Ash (%)	Protein (%)	Fat (%)	Fiber (%)	Energy (kcal)	Carbohydrates (%)
T1	6.24±0.01 <sup>b</sup>	3.5±0.01 <sup>a</sup>	5.39±0.01 <sup>c</sup>	20.01±0.01 <sup>e</sup>	18.66±0.01 <sup>f</sup>	5.13±0.01 <sup>d</sup>	46.17±0.01 <sup>a</sup>
T2	6.37±0.01 <sup>c</sup>	3.7±0.01 <sup>b</sup>	5.72±0.01 <sup>e</sup>	18.99±0.01 <sup>d</sup>	10.20±0.01 <sup>a</sup>	4.46±0.01 <sup>a</sup>	55.06±0.01 <sup>e</sup>
T3	7.30±0.01 <sup>e</sup>	3.5±0.01 <sup>a</sup>	5.44±0.01 <sup>d</sup>	18.07±0.02 <sup>a</sup>	11.29±0.01 <sup>b</sup>	4.46±0.01 <sup>a</sup>	54.44±0.01 <sup>d</sup>
T4	7.27±0.02 <sup>d</sup>	3.5±0.01 <sup>a</sup>	4.36±0.01 <sup>a</sup>	18.25±0.01 <sup>c</sup>	16.96±0.01 <sup>e</sup>	4.96±0.01 <sup>b</sup>	49.62±0.01 <sup>b</sup>
T5	5.20±0.01 <sup>a</sup>	3.7±0.02 <sup>b</sup>	5.44±0.01 <sup>d</sup>	18.89±0.01 <sup>d</sup>	13.64±0.01 <sup>d</sup>	5.01±0.01 <sup>c</sup>	53.11±0.01 <sup>c</sup>
T6	5.20±0.01 <sup>a</sup>	3.7±0.01 <sup>b</sup>	5.25±0.01 <sup>b</sup>	18.19±0.01 <sup>b</sup>	11.50±0.01 <sup>c</sup>	7.21±0.01 <sup>e</sup>	56.18±0.01 <sup>f</sup>

T1, T3, and T4 showed the lowest contents with a value of 3.5%. Elías Silupu et al. (2021) emphasize that ash content is directly correlated with the percentages of minerals present in the raw material. In other

research, values of 1.75 to 2.16% have been reported when replacing 50% with potato flour, indicating that increasing the percentage leads to an increase in ash content (Cerón et al. 2014).

Table 2 shows the protein values, where it was noted that T2 is statistically different ( $P<0.05$ ) from T6, showing a decrease with a value of 5.72 to 5.25%, respectively. In this way, it is highlighted that by using 70% white carrot flour/30% rice flour for a period of 20 min of rest, a greater loss was obtained. In several investigations, values between 3.60 to 6.05% were determined, indicating that the variation is associated with the percentage of carrot flour used (Sanaguano et al. 2017). On the other hand, the Ecuadorian Technical Standard INEN 2085:2005 specifies within the bromatological requirements for cookies a minimum protein content of 3%. This indicates that the cookies made from white carrot flour and rice are within the requirements of the standard.

Regarding fat content, variability was observed among the results of the treatments ( $P<0.05$ ), showing that T1 had the highest value with 20.01%, compared to T3, which obtained a lower result with 18.07%. Aji Sunaryo et al. (2021) reported values from 7.6 to 9.22%, which were lower than those presented in this study. This difference can be attributed to the lower percentage of carrot flour used in their different formulations (10, 20, and 30%) in their research on the elaboration of pumpkin (*Cucurbita moschata Duchesne*) and carrot (*Daucus carota* L.) cookies. In relation to Ecuadorian regulations, according to the Norma Técnica Ecuatoriana NTE INEN 1415: (INEN 2011) ("Galletas y productos de panadería similares – Requisitos"), the maximum fat content recommended for cookies and similar products is 15%. The fat content values found in this study (18.07–20.01%) exceed this limit, classifying these samples as high-fat products. This higher fat content could influence the product's nutritional labeling and consumer acceptance, especially considering the Ministerio de Salud Pública recommendations to limit fat intake to reduce risks of cardiovascular diseases and obesity. Therefore, if these products are intended for commercialization within Ecuador, reformulation to reduce fat content or explicit labeling as high-fat products would be necessary to comply with national standards and protect consumer health.

In relation to fiber content, a significant increase was observed in T1 with 18.66%, being statistically different ( $P<0.05$ ) compared to T3 with 10.20%, which showed a lower content. This suggests that by using a composition

of 90% white carrot flour/10% rice flour, with a resting period of 10 minutes, the amount of fiber present in the sample is remarkably representative. This result was expected, since carrot flour increases the fiber content due to its richness in this nutrient (Santos et al. 2022). According to the literature, the fiber in carrot flour is predominantly insoluble, which contributes mainly to promoting intestinal transit and enhancing satiety. On the other hand, when using 20% carrot peel flour, a fiber content of 3.32% was found (Quitral et al. 2023). Consuming products rich in fiber is not only beneficial for health but also contributes to the feeling of satiety when consumed (Venegas et al. 2022).

Regarding energy content, the highest value was recorded in T6 with 7.21 kcal, which differs significantly ( $P<0.05$ ) from treatments T2 and T3, which presented lower values with 4.96 kcal. This finding indicates that the inclusion of 30% rice flour significantly increases the energy content. According to research on the nutritional characteristics of commercially available cookies, an energy value of 471.86 per 100 g has been observed, mainly attributed to the presence of added sugars (Hoyos et al. 2020). Studies on cookies enriched with flaxseed, they provide an energy value of 383.04–397.59 kcal. It is necessary to mention that researchers mention that proteins should provide between 12–14% of the total of a diet (Benítez 2017).

A statistically significant effect ( $P<0.05$ ) was observed in the percentage of carbohydrates among the evaluated treatments. Treatment T6, with 56.18%, showed a notable increase compared to T3, which registered the lowest percentage with 46.17%, positioning itself as the treatment with the lowest carbohydrate content. This highlights the influence of the treatments on carbohydrate content, underlining the variability observed in each one. On the other hand, in previous research, the incorporation of carrot flour in cookie production values ranging from 52.77 to 63.47% were reported. These values are consistent with those obtained in the present study (Kiin et al. 2021). In addition, carbohydrates play a crucial role in consumer food choice in relation to health. Previous research, such as the study on fig and oat flour-based cookies, highlights the importance of carbohydrates by constituting a significant part (49.79%) of the total product composition (Quelal 2023).



### Sensory characterization

Through the evaluation of the sensory profiles of cookies made from carrot and rice flour (Figure 1), it was determined that T1 (90% carrot flour/10% rice flour +10 min) obtained the best scores for odor 4.4; flavor 4.2 and texture 4.0; while, T6 (70% carrot flour/30% rice flour +20 min) had the lowest scores in the odor and texture profiles 3.7. In general, O'Sullivan (2017) emphasizes that, to achieve success, a product must satisfy the consumer through sensory perceptions. According to the sensory analysis on brown rice-based cookies with moringa (*Moringa oleifera*) and stevia (*Stevia rebaudiana* Bertoni) conducted by Almora-Hernández

et al. (2023) the cookies received moderate criticism in terms of their texture, specifically in terms of their ability to fracture and their level of crunchiness. Castro García et al. (2024) evaluated the sensory profile of cookies made with brown rice (*O. Sativa*), carob (*Prosopis alba*) and pigeon pea (*Cajanus cajan*), obtaining values of 4.2 color, 3.6 odor, 4.0 flavor, and 4.20 for texture, which are comparable to the results reported in this study. On the other hand, in studies of cookies based on carrot peel in concentrations of 5, 10, and 20%, in which a sensory characterization determined that including 20% in the formulation and preparation was significantly preferable (Quitral et al. 2023).

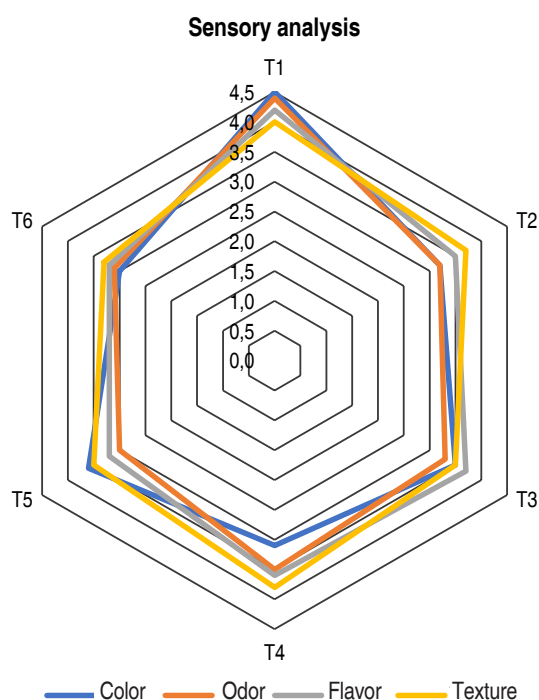


**Figure 1.** Sensory profile of gluten-free cookies made with white carrot flour and rice flour. The values represent the average scores given by the sensory panelists for each attribute (color, odor, flavor, and texture).

### Microbiological analysis

Microbiological analyzes were conducted on treatment T1 (90% carrot flour / 10% rice flour + 10 min), which showed the highest sensory acceptance. The results indicated that mesophilic aerobic bacteria, molds, and yeasts were within the acceptable limits established by the Ecuadorian Technical Standards NTE INEN 1529-10 (INEN 2013) and NTE INEN 1529-5 (INEN 2012) for microbiological control in food products. Specifically, the counts of viable

molds and yeasts, determined by plate count with deep inoculation, were consistent with the regulatory thresholds (Table 3), confirming the microbiological safety of the cookies. Furthermore, according to Smelt and Brul (2014), the low presence of molds and yeasts may be attributed to the thermal treatment applied during baking, as these microorganisms are sensitive to high temperatures (189 °C), which significantly reduces their survival in the final product.

**Table 3.** Microbiological analysis of the best treatment of cookies made with white carrot flour and rice flour.

Treatments	Unit	Results	Method/Ref.
Molds and yeasts	UFC g <sup>-1</sup>	1.2x10 <sup>2</sup>	Ecuadorian Technical Standards NTE INEN 1529-10 (2013) and NTE INEN 1529-5 (2012)
Mesophilic aerobes	UFC g <sup>-1</sup>	30	

## CONCLUSION

The incorporation of 90% white carrot flour and 10% rice flour in the formulation of gluten-free cookies (T1) significantly improved their nutritional composition, increasing protein (5.39%), fat (20.01%), and fiber content (18.66%) compared to other formulations. These values highlight the potential of white carrot flour as a functional ingredient for enhancing the nutritional profile of baked products. Additionally, the sensory analysis indicated high consumer acceptance in terms of odor, taste, and texture for treatment T1, making it the most preferred formulation. Microbiological evaluation confirmed the safety of the cookies, with mold, yeast, and mesophilic counts within acceptable limits according to Ecuadorian regulations. These results demonstrate that white carrot flour can be successfully used to develop nutritionally enhanced, microbiologically safe, and organoleptically acceptable gluten-free cookies. The study contributes to the diversification of gluten-free products using underutilized root crops with functional properties. Future research should focus on evaluating the shelf-life stability of cookies under different storage conditions, analyzing bioactive compound retention, and assessing consumer acceptance in broader demographic groups. Additionally, exploring the use of white carrot flour in other gluten-free baked goods could expand its applicability in the functional food industry.

## CONFLICT OF INTERESTS

The authors declare that they have no conflicts of interest.

## REFERENCES

- Ahmad M, Ahmed-Wani T, Wani SM, Masoodi and Gani A (2016) Incorporation of carrot pomace powder in wheat flour: effect on flour, dough and cookie characteristics. *Journal of Food Science and Technology* 53(10): 3715-3724. <https://doi.org/10.1007/s13197-016-2345-2>
- Aji Sunaryo N, Devi M, Saputri AM, Cahyani R (2021) Proximate analysis of pumpkin and carrot cookies International Conference on Life Sciences and Technology. <https://doi.org/10.1063/5.0052617>
- Almora-Hernández E, Monteagudo-Borges R, Lago-Abascal V et al (2023) Evaluation physicochemical and sensory of enriched integral rice cookies with *Moringa oleifera* and *Stevia rebaudiana*. *Tecnología Química* 43(1):1-20. <https://tecnologiaquimica.uo.edu.cu/index.php/tq/article/view/5309/4770>
- Bas-Bellver C, Barrera C, Betoret N, Seguí L and Harasym J (2024) IV-range carrot waste flour enhances nutritional and functional properties of rice-based gluten-free muffins. *Foods* 13(9). <https://doi.org/10.3390/foods13091312>
- Bazan-Aliaga G, Gabrielli González R, Acosta Chinchayhuara D, Rojas Castillo JA et al (2015) Highly adaptable biscuits made from rice flour (*Oryza sativa*) and potato flour (*Solanum tuberosum*) var.parda pastasa. *Agroindustrial Science* 5(1): 69-75. <https://doi.org/10.17268/agroind.science.2015.01.07>
- Benítez B, Ortega J, Barboza M, Rangel Y, Romero L et al (2017) Formulation and physicochemical, microbiological, and sensory evaluation of biscuits enriched with flaxseed as a functional food. *Venezuelan Archives of Pharmacology and Therapeutics*. 36(4): 106-113. <https://www.redalyc.org/pdf/559/55952806003.pdf>
- Castro García AI, Caicedo Hinojosa LA, Núñez Rodríguez PJ and Peñafiel Zamaro MJ (2024) Sensory and food evaluation of Brown Rice (*Oryza Sativa*), Carob (*Prosopis Alba*) and Pigeon Pea (*Cajanus cajan*) cookies. *Journal of Science and Research* 8(2). <https://revistas.utb.edu.ec/index.php/sr/article/view/3133>
- Cerón Cardenas AF, Bucheli Jurado MA and Osorio Mora O (2014) Production of biscuits using potato flour from the Parda Pastusa variety (*Solanum tuberosum* L.). *Acta Agronomica*. 63(2). <http://doi.org/10.15446/acag.v63n2.39575>
- Elías Silupu JW, García Rivas CE, Pérez Salcedo R and Yauris Silvera CV (2021) Physicochemical characterization of bread with partial replacement of wheat flour by germinated Quinoa (*Chenopodium quinoa* willd) and Kiwicha (*Amaranthus caudatus* L.) flour. *SENDAS* 2(2): 69-83. <https://doi.org/10.47192/rcs.v2i2.64>
- Hoyos Vázquez SM, García Castillo S, Rodríguez Delgado J and Praena Crespo M (2020) Nutritional characteristics and composition of cookies available on the Spanish market and cookies aimed at children. *Primary Care Pediatrics*. 22(86). [https://scielo.isciii.es/scielo.php?script=sci\\_arttext&pid=S1139-76322020000300004](https://scielo.isciii.es/scielo.php?script=sci_arttext&pid=S1139-76322020000300004)
- INEN - Ecuadorian Institute of Standardization (1980) Ecuadorian Technical Standard NTE INEN 0523. Flours of vegetable origin, Fat determination.
- INEN - Ecuadorian Institute for Standardization (1981) Ecuadorian Technical Standard NTE INEN 0520. Flours of vegetable origin. Determination of ash.
- INEN - Ecuadorian Institute for Standardization (1981) Ecuadorian Technical Standard NTE INEN 522. Flours of vegetable origin. Determination of crude fiber.
- INEN - Ecuadorian Institute of Standardization (2005) Ecuadorian Technical Standard NTE INEN 2 085. Cookies. Bramatological Requirements. Quito.
- INEN - Ecuadorian Institute for Standardization (2012) Ecuadorian Technical Standard NTE INEN 1529-5. Microbiological control of food.

- Determination of the quantity of mesophilic aerobic microorganisms. Rep. Quito. <https://es.scribd.com/doc/240179897/1529-5-1-c-Mesofilos-Aerobios>
- INEN - Ecuadorian Institute of Standardization (2013) Ecuadorian Technical Standard NTE INEN 1529-10. Microbiological control of food: viable molds and yeasts, plate counts by deep seeding. Quito. <https://es.scribd.com/document/488093112/1529-10-1R-MOHOS-Y-LEVADURAS-VIABLES-pdf>
- INEN - Ecuadorian Institute for Standardization (2011) Ecuadorian Technical Standard NTE INEN 1415:2011. Cookies and similar bakery products – Requirements. <https://www.normalizacion.gob.ec>
- Jordán Villamar RE (2018) Development of a formula for an instant dessert using white carrot (*Arracacia xanthorrhiza* Bancroft) and pumpkin (*Cucurbita maxima* Duchesne) flours. [Degree thesis]. Catholic University of Santiago de Guayaquil, Guayaquil. Institutional repository. <http://repositorio.ucsg.edu.ec/handle/3317/10198>
- Kiin Kabani D, Uzoamaka MC and Akuso O (2021) Production, nutritional evaluation and acceptability of cookies made from a blend of wheat, african walnut, and carrot flours. Asian Food Science Journal 20(6): 60-76. <https://doi.org/10.9734/afsj/2021/v20i630310>
- Mandrich L, Valeria Esposito A, Costa S and Caputo E (2023) Chemical composition, functional and anticancer properties of carrot. Molecules 28(20). <https://doi.org/10.3390/molecules28207161>
- Nayghit Carrero Y, Acosta M and Dávila M (2018) White carrot (*Arracacia xanthorrhiza* Bancr) potential phytopharmaceutical: mini-review. Clinical Research. 59(1): 109-111. [https://www.researchgate.net/publication/326449587\\_ZANAHORIA\\_BLANCA\\_Arracacia\\_xanthorrhiza\\_bancr\\_POTENCIAL\\_FITOFARMACO\\_MINI\\_REVISION](https://www.researchgate.net/publication/326449587_ZANAHORIA_BLANCA_Arracacia_xanthorrhiza_bancr_POTENCIAL_FITOFARMACO_MINI_REVISION)
- Nieto-Mazzocco E, Rangel Contreras A, Saldaña Robles A, Abraham Juárez and Ozuna C (2018) Characterization of gluten-free flours and their incorporation into bakery products. Research and Development in Food Science and Technology. 3(4): 1-8.
- Pérez Ramos K, Penafiel CE and Delgado Soriano V (2017) High protein snack: an extruded product made from Quinoa (*Chenopodium quinoa* Willd.), Tarwi (*Lupinus mutabilis* Sweet) and sweet potato (*Ipomoea batatas* L.). Scientia Agropecuaria 8(4): 377-388. <http://doi.org/10.17268/sci.agropecu.2017.04.09>
- Quelal Peralta ML (2023) Production of cookies based on fig flour (*Ficus carica*) and oat flour (*Avena sativa*) using three types of sweeteners (brown sugar, white sugar, and erythritol) for young adults aged 18–25 [Undergraduate thesis], Technical University of Ambato, Ambato. Institutional repository: <https://repositorio.uta.edu.ec/bitstream/123456789/37915/1/CAL%20041.pdf>
- Quitral V, Flores M, Plaza K, Quezada F and Arce H (2023) Carrot peel flour as an ingredient in cookie making. Chilean Nutrition Journal. 50(2): 226-232. <http://doi.org/10.4067/s0717-75182023000200226>
- Ranasinhe M, Manikas I, Maqsood S and Stathopoulos C (2022) Date components as promising plant-based materials to be incorporated into baked goods—A review. Sustainability 14(2): 605. <https://doi.org/10.3390/su14020605>
- Sanaguano Salguero H, Tigre León A, Bayas Morejón F and Ruilova B (2017) Nutritional value and sensory properties of cookies prepared from flour mixes of carrot (*Daucus carota*), Lupine (*Lupinus perennis*) and Barley (*Hordeum vulgare*). European Scientific Journal 13(9): 378-391.
- Santos D, Lopes Da Silva J and Pintado M (2022) Fruit and vegetable by-products' flours as ingredients: A review on production process, health benefits and technological functionalities. LWT, 154(15). <https://doi.org/10.1016/j.lwt.2021.112707>
- Smelt J and Brul S (2014) Thermal inactivation of microorganisms. Critical Reviews in Food Science and Nutrition 54(10): 1371-1385. <https://doi.org/10.1080/10408398.2011.637645>
- O'Sullivan MG (2017) A handbook for sensory and consumer-driven new product development: Innovative technologies for the food and beverage industry. <https://doi.org/10.1016/C2014-0-03843-9>
- Venegas C, Farfan Beltrán N, Bucchi C, Martínez Gomis J and Fuentes R (2022) Effect of chewing behavior modification on food intake, appetite and satiety-related hormones: A systematic review. Revista Chilena de Nutrición 49(6): 760-774. <https://doi.org/10.4067/S0717-75182022000700760>



# Assessment of physical properties and biological activity of chitosan beads with *Citrus hystrix* essential oil

Evaluación de las propiedades físicas y la actividad biológica de las perlas de quitosano con aceite esencial de *Citrus hystrix*

<https://doi.org/10.15446/rnam.v78n3.114858>

Do Minh Long<sup>1</sup> and Le Pham Tan Quoc<sup>1\*</sup>

## ABSTRACT

### Keywords:

Biopolymer beads  
Food preservation  
Free radical scavengin  
Swelling ratio  
SEM



The production and application of chitosan (CS) beads containing *Chúc* essential oil (CB-EO) is a new advanced technique to address the growing demand for natural and effective food preservation solutions, offering a sustainable alternative to synthetic preservatives. CB-EO was created at different *Chúc* essential oil (ChEO) concentrations of 0, 0.5, 1, and 2% (v/v). The CB-EO quality indicators were also evaluated in the experiments, such as yield and size, swelling ratio, antioxidant and antibacterial activity, Fourier transform infrared (FTIR) spectroscopy, X-ray diffraction (XRD), and scanning electron microscopy (SEM). Results showed that as ChEO concentration increased, antioxidant capacity rose from 33.5 to 40.8%, and the antibacterial inhibition zone diameter expanded from 3.67 to 8.33 mm. Bead collection efficiency changed insignificantly, from 31 to 34 beads per 2 mL of solution. Sphericity was not truly perfect, only reaching 59.60–66.60%. The swelling ratio did not depend on the presence of ChEO. The CB-EO was observed to be in the shape of a bean, with a smooth and wrinkled surface. FTIR analysis showed no new bonds or differences formed between the samples. Moreover, the crystallization ability of the beads showed a decrease in the diffraction intensity at the 28° position, which changed depending on the ChEO concentration. These findings demonstrate CB-EO's significant potential as a natural, highly effective agent for extending food shelf life and enhancing safety. Further research is needed to optimize encapsulation efficiency and evaluate practical application in various food matrices. Overall, the obtained results are promising and suggest good potential for future development and application.

## RESUMEN

### Palabras clave:

Perlas de biopolímero  
Conservación de alimentos  
Eliminación de radicales libres  
Índice de hinchamiento  
SEM

La producción y aplicación de perlas de quitosano (CS) que contienen aceite esencial de *Chúc* (CB-EO) es una nueva técnica avanzada e innovadora para satisfacer la creciente demanda de soluciones naturales y efectivas en la conservación de alimentos, ofreciendo una alternativa sostenible a los conservantes sintéticos. Para reemplazar gradualmente los conservantes sintéticos actuales, se creó CB-EO en diferentes concentraciones de aceite esencial de *Chúc* (ChEO) de 0, 0.5, 1 y 2% (v/v). En el experimento también se evaluaron los indicadores de calidad del CB-EO, como el rendimiento y el tamaño, la relación de hinchamiento, la actividad antioxidante y antibacteriana, la espectroscopia de infrarrojo por transformada de Fourier (FTIR), la difracción de rayos X (XRD) y la microscopía electrónica de barrido (SEM). Los resultados mostraron que, a medida que aumentaba la concentración de ChEO, la capacidad antioxidante se incrementó del 33,5 al 40,8%, y el diámetro del halo de inhibición antibacteriana se amplió de 3,67 a 8,33 mm. La eficiencia de recolección de perlas cambió de manera insignificante, de 31 a 34 perlas por 50 mL de solución. La esfericidad no fue realmente perfecta, alcanzando solo el 59,60–66,60%. La relación de hinchamiento no dependió de la presencia de ChEO. Se observó que el CB-EO tenía la forma de un frijol, con una superficie lisa y arrugada. El análisis FTIR no mostró nuevos enlaces ni diferencias formadas entre las muestras. Además, la capacidad de cristalización de las perlas mostró una disminución en la intensidad de difracción en la posición 28°, que cambió dependiendo de la concentración de ChEO. Estos hallazgos demuestran el gran potencial del CB-EO como agente natural y altamente efectivo para prolongar la vida útil de los alimentos y mejorar su seguridad. Se necesitan más investigaciones para optimizar la eficiencia de encapsulación y evaluar su aplicación práctica en diferentes matrices alimentarias.

<sup>1</sup>Institute of Biotechnology and Food Technology, Industrial University of Ho Chi Minh City, Ho Chi Minh City, Vietnam. [lephamtanquoc@iuh.edu.vn](mailto:lephamtanquoc@iuh.edu.vn) , [dominhlong1309@gmail.com](mailto:dominhlong1309@gmail.com) 

\*Corresponding author



Food preservation has always been a top priority for researchers. Current preservation methods must not only ensure the safety and quality of food during storage but also be of natural origin, safe for humans, and environmentally friendly. Under these circumstances, the edible coating method is widely employed in fruit preservation (Pham et al. 2022; Pham et al. 2023b) and has also been applied to extend the shelf life of animal products such as eggs (Pham et al. 2023a). Among the materials used for edible coatings, chitosan is regarded as one of the most extensively studied biopolymers due to its broad-spectrum antibacterial, anti-inflammatory, and biofilm-forming properties (Mouhoub et al. 2023); however, its direct antibacterial efficacy remains limited. It is more effective when combined with other bioactive agents, and while not used to directly kill microbes, it can be combined with other agents to increase food preservation effectiveness (Mouhoub et al. 2025). In previous reports, Nguyen et al. (2023) used CS to preserve Hoa Loc mangoes, while Çoban (2021) combined CS and propolis extract to preserve shrimp. In addition, CS is also made into beads combined with lavender EO to help stabilize the color of tilapia fillets during storage (Junca et al. 2019).

*Chúc* EO (ChEO) is extracted from the waste of *Chúc* (peel), which is a valuable natural resource with high biological value, owing to its antibacterial, antioxidant, anti-cancer, anti-inflammatory, and anti-insect properties (Long and Quoc 2023). For example, Lertsatitthanakorn et al. (2006) reported the anti-inflammatory properties of ChEO, demonstrating its ability to inhibit *Propionibacterium acnes* and suppress 5-lipoxygenase activity. Additionally, Othman et al. (2023) found that the essential oil exhibited significant anti-proliferative activity against the HeLa cervical cancer cell line. Additionally, other reports have shown that ChEO at a concentration of 220–300 µg mL<sup>-1</sup>, has potential anti-melanoma effects on three human cell lines, WM793, A375, and HTB140, by inhibiting hyaluronidase and tyrosinase (Kulig et al. 2022). Furthermore, many studies have also indicated that ChEO compounds, such as citronellol, limonene, pinene, sabinene, and terpinene-4-ol, act against bacteria and fungi, including *Saccharomyces cerevisiae*, *Bacillus cereus*, *Staphylococcus aureus*, and *Escherichia coli*. These compounds also have a positive impact, like mosquito repellents and fly repellents. ChEO has

also been shown to have stronger antibacterial activity than EOs from other citrus species (Long and Quoc 2023). Therefore, ChEO is widely used, especially in food preservation. However, EOs are not usually used directly but can be combined with other ingredients, such as CS, starch, etc. The most common application is to create a protective coating. For example, ChEO can be combined with cassava starch to form an edible coating that prolongs the shelf life of fresh beef (Utami et al. 2017). Additionally, ChEO can be combined with fish skin gelatin to enhance its antioxidant capacity (Tongnuanchan et al. 2012). However, creating particles containing EOs is less common but is suitable for products that are not affected by the taste and smell of the EOs (Long and Quoc 2023).

The current food preservation methods often rely on synthetic chemicals, raising concerns about safety and sustainability. There's a growing need for natural, eco-friendly alternatives. While chitosan (CS) and *Chúc* (*Citrus hystrix*) essential oil (ChEO) have been individually studied for their antimicrobial and antioxidant properties, their combination in the form of encapsulated beads has not yet been explored. Most previous studies have focused on film or coating applications, but the development of CS beads loaded with ChEO represents a novel strategy that allows better control of essential oil release, minimizes sensory impact, and enhances preservation efficiency.

Therefore, this study introduces a new approach by formulating chitosan beads incorporated with *Chúc* (*Citrus hystrix*) essential oil and evaluating their physical and biological properties. This formulation not only leverages the synergistic effects of two natural agents but also offers a promising and sustainable alternative to synthetic preservatives in food storage applications. The improved chitosan bead system has the potential to be adapted to a variety of foods, promoting safer and longer-term preservation. Future research may focus on optimizing scalability and exploring controlled release mechanisms to maximize efficacy and consumer acceptance.

## MATERIALS AND METHODS

### Materials

The chitosan (CS) sample, provided by Nha Trang University, is white, scale-shaped, and has a degree of deacetylation of 90%. The raw material for essential oil (EO) extraction was *Chúc* (*Citrus hystrix*) peel,

collected in Tinh Bien District, An Giang Province, Vietnam (coordinates: 10°37'55.6"N, 104°59'34.8"E), and processed via steam distillation. Before extraction, the fruit was washed, air-dried at room temperature, peeled, and chopped into small pieces.

As detailed in the previous work (Long et al. 2023), ChEO was extracted via a 3 h steam distillation process at 100 °C. The characteristics of this ChEO were determined to be an approximate yield of 2.8% per batch (from 50–60 kg peel), with acid, ester, and saponification values of  $0.561 \pm 0.106$ ,  $10.66 \pm 1.405$ , and  $11.22 \pm 1.405$  mg KOH g<sup>-1</sup> EO, respectively. Its refractive index was  $1.4699 \pm 0.0002$ . The primary chemical components of this ChEO as analyzed by gas chromatography-mass spectrometry (GC-MS). The gas chromatography-mass spectrometry analysis method (GC-MS) was used to determine the EO's chemical makeup. First, 1 mL of methanol was created by dissolving 20 µL of the sample in methanol. Next, at an injection temperature of roughly 220 °C, 1 mL of EO was added to an Agilent DB-5MS gas chromatograph equipped with a capillary column (30 m×0.25 mm, 0.25 µm). After 1 minute, the temperature was raised to 70 °C, then by 12 °C each minute to 280 °C and finally maintained for 10 minutes. The range of mass was 29–650 atomic mass units (amu). The carrier gas, helium, had a steady flow rate of 1.2 mL min<sup>-1</sup>. The relative abundance of each compound, expressed as percentage area, was determined and identified as: β-pinene (30.19%), D-limonene (22.15%), sabinene (21.37%), citronellal (6.17%), terpinen-4-ol (4.88%), and α-pinene (3.14%) (Long et al. 2023). The ChEO was then preserved in a dark glass bottle at room temperature.

A total of four bacterial strains were used in this study: two Gram-positive strains, *Staphylococcus aureus* (ATCC 25923) and *Bacillus cereus* (ATCC 11778), and two Gram-negative strains, *Pseudomonas aeruginosa* (ATCC 27853) and *Salmonella typhimurium* (ATCC 13311). All strains were provided by the Institute of Biotechnology and Food Technology at the Industrial University of Ho Chi Minh City. The chemicals used included lactic acid and Tween 20 (Xilong, China), as well as 2,2-diphenyl-1-picrylhydrazyl (DPPH; Sigma, USA). The culture media consisted of Nutrient Broth and Mueller–Hinton Agar (MHA) (HiMedia, Thane, India), along with other analytical-grade reagents.

### Preparation of chitosan beads with *Chúc peel* essential oil

For the production of CB-EO, the procedure of Sangsuwan et al. (2016) was followed with some appropriate modifications. A total of 0.75 g of CS was dissolved in 50 mL of 2% lactic acid solution at 55 °C and stirred for 30 min. The mixture was then mixed with ChEO in the following ratios: 0, 0.5, 1, and 2% of the solution volume (v/v) and Tween 20 (0.2% v/v). The 0% ChEO sample was considered the control sample. Stirring continued for 15 min. Then the solution was dripped through a syringe into 50 mL of 2 M NaOH. The beads were washed with distilled water five times and dried in a drying oven at 45 °C for 5 h. For monitoring and research, the CB-EO samples collected were stored in closed plastic boxes at room temperature and labeled according to the ChEO ratios added: control, CB-EO (0.5), CB-EO (1), and CB-EO (2).

### Determination of bead collection efficiency

This process was performed by counting the number of beads comprising a unit volume of the resulting solution.

### Determination of bead size after drying

Length (L), width (W), and thickness (T) were determined with a specialized stainless hardened digital caliper (Mitutoyo, model 500-182-30, USA). To determine the equivalent diameter (ED) (Equation 1) and sphericity (S) (Equation 2), the following Equations were used (Thakur and Nanda 2018):

$$ED = (L \times W \times T)^{\frac{1}{3}} \text{ (mm)} \quad (1)$$

$$S = \frac{ED}{L} \times 100 \text{ (%) } \quad (2)$$

Where L, W, and T are length (mm), width (mm), and thickness (mm), respectively.

### Determination of the swelling ratio of CB-EO

The swelling ratio was determined by the weight measurement method of Anchisi et al. (2006), which has been adjusted to suit the experimental conditions. Dry bead samples weighing 1 g were soaked in physiological water and stirred at 50 rpm at different time intervals (30, 60, 90, and 120 min). Then, the beads were drained and weighed.

The swelling ratio of the bead samples was calculated using Equation (3):

$$\text{Swelling ratio} = \frac{W_t}{W_0} \quad (3)$$

Where  $W_0$  is the dry bead weight (g) and  $W_t$  is the wet bead weight (g).

#### Determination of the antioxidant activity of CB-EO

Antioxidant activity was measured via DPPH free radical scavenging capacity ( $\text{DPPH}_{\text{RSC}}$ ) (Equation 4). This study evaluated the antioxidant activity according to the research procedure of Su et al. (2020), which has been adjusted to suit the experimental conditions. One gram of CB-EO was continuously stirred in 15 mL of alcohol for 2 h. Then 1 mL of this solution was added to 2 mL of the 0.1 mM DPPH reagent to create a reaction for 30 min; the samples were measured at a wavelength of 517 nm. The results were calculated by the percentage (%) inhibition of DPPH.

$$\text{DPPH}_{\text{RSC}} (\%) = \frac{A_0 - A_i}{A_0} \times 100 \quad (4)$$

Where  $A_0$  represents the absorbance of the blank solution (DPPH solution) and  $A_i$  indicates the absorbance of the sample solution (DPPH solution and extract).

#### Determination of antibacterial activity of CB-EO

The antibacterial activity of CB-EO was determined using the disc diffusion method according to the study of Junca et al. (2019), which has been adjusted to match the experiment. About 0.1 mL of the bacterial solution (concentration of  $1.5 \times 10^8$  CFU  $\text{mL}^{-1}$ , equivalent to 0.5 McFarland) was spread on the surface of MHA in a petri dish. CB-EO was also placed in petri dishes containing a Gentamicin (10  $\mu\text{g}$  per plate) positive control and a dimethyl sulfoxide (DMSO 5%) negative control. The petri dishes were incubated for 24 h at 37 °C, and the resulting diameter of the inhibition zones of CB-EO were read in millimeters (mm).

#### Fourier transform infrared analysis

The Fourier transform infrared (FTIR) analysis aimed to identify the functional groups present in the chitosan beads and detect possible interactions between chitosan and

essential oil components. FTIR analysis was performed on a Bruker Tensor 27 FTIR spectrometer (Bruker Optik GmbH, Germany). Spectra were recorded in the range of 4,000–400  $\text{cm}^{-1}$  with a resolution of 1  $\text{cm}^{-1}$  transmittance mode using a KBr beam splitter. The measurement was conducted in transmittance mode using the KBr pellet method, where approximately 2 mg of sample was finely ground and mixed with 200 mg of dry KBr powder, then pressed into a pellet.

#### X-ray diffraction analysis

X-ray diffraction analysis (XRD) was performed using a Bruker AXS D8 Advance ECO Xray diffractometer (Karlsruhe, Germany). During the analysis, the voltage and current were set to 40 kV and 25 mA, respectively. The analysis involved varying the angle within the 2 $\theta$  range, and the scanning speed was set to 0.2  $\text{rad s}^{-1}$ .

#### Scanning electronic microscopy of CB-EO

Scanning electron microscopy (SEM) analysis was conducted using a JSM-IT200 scanning electron microscope (JEOL, Japan). This versatile instrument allowed for magnifying samples at a range of  $\times 40$  to  $\times 10,000$ , utilizing an accelerating voltage of 5 kV.

Before analysis, the samples underwent natural drying to remove any surface moisture. To enhance their conductivity and enable high-resolution imaging, a thin layer of platinum was applied using an auto-fine coater (JEC-3000FC, JEOL, Japan). This technique ensures clear and detailed images of the sample's surface morphology.

#### Data analysis

The experiment involved three independent measurements, and the results are reported as the mean  $\pm$  standard deviation. Statistical analysis was carried out using Statgraphics Centurion XV software. A one-way analysis of variance (ANOVA) was used to assess overall differences among the groups, followed by Fisher's least significant difference (LSD) test to identify statistically significant pairwise differences. A significance level of  $P < 0.05$  was applied.

## RESULTS AND DISCUSSION

#### Size and yield of CB-EO

Based on the results in Table 1, the yield in the process of creating beads in the same unit volume among the EO

**Table 1.** Size and yield of the beads.

Sample	Control	CB-EO (0.5)	CB-EO (1)	CB-EO (2)	Level of significance
Bead number/2 mL solution	34±1.15 <sup>a</sup>	33±0.58 <sup>ab</sup>	32±2 <sup>b</sup>	31±0.58 <sup>b</sup>	*
Length (mm)	4.37±0.33 <sup>a</sup>	4.24±0.29 <sup>a</sup>	4.45±0.35 <sup>a</sup>	3.77±0.30 <sup>b</sup>	*
Width (mm)	2.67±0.22 <sup>a</sup>	2.58±0.26 <sup>a</sup>	2.51±0.18 <sup>a</sup>	2.49±0.16 <sup>a</sup>	*
Thickness (mm)	1.64±0.03 <sup>a</sup>	1.65±0.02 <sup>a</sup>	1.66±0.02 <sup>ab</sup>	1.68±0.02 <sup>b</sup>	*
Equivalent diameter (mm)	2.67±0.12 <sup>a</sup>	2.62±0.12 <sup>a</sup>	2.64±0.12 <sup>a</sup>	2.50±0.10 <sup>b</sup>	*
Sphericity (%)	61.23±2.56 <sup>a</sup>	61.96±3.53 <sup>a</sup>	59.60±2.79 <sup>a</sup>	66.60±3.76 <sup>b</sup>	*

\* Significant at  $P<0.05$ . Control, CB-EO (0.5), (1), and (2) are the chitosan beads containing *Chúc* essential oil at concentrations of 0, 0.5, 1, and 2% (v/v), respectively. Significant differences ( $P<0.05$ ) between samples are indicated by different letters within a row (a–b).

samples has a negligible deviation; the bead count only fluctuates from 31 to 34 per 2 mL.

Bead size also shows negligible fluctuations. However, the length of the beads tends to decrease at higher EO concentrations (4.37 mm for the control and 3.77 mm for CB-EO (2)), while width (2.49–2.67 mm) and thickness (1.64–1.68 mm) remain relatively constant.

The observed sphericity of the beads, ranging from 59.60 to 66.60%, suggests a non-spherical, bean-shaped morphology for the CB-EO beads. The sphericity in this study is significantly lower than that of other reported materials, such as bee pollen beads (76.55%) (Quoc 2021) or green bean beads (84.1–84.18%) (Thong et al. 2010).

Furthermore, the equivalent diameter of the beads is relatively low, ranging only from 2.50 to 2.67 mm. These results tend to be lower than those observed in other CB-EO studies. For instance, Lich et al. (2018) reported bead diameters ranging from 1.96 to 3.10 mm for CS combined with SiO<sub>2</sub>. Determining the size and production yield of CB-EO can make their packaging in food products more reasonable. The variation in size is likely attributable to the material used, the initial degree of deacetylation in the CS, and the ability of CS to interact with other materials. Notably, prior research has yet to evaluate the sphericity of CB-EO beads.

### Swelling ratio of CB-EO

Analyzing swelling ratio data for chitosan (CS) beads coated with *Chúc* essential oil (ChEO) reveals their water absorption properties (Table 2). Every type of bead,

including the control and ChEO-containing ones, showed a notable ability to absorb water, swelling by 1.3 to 1.6 times their initial weight. This unequivocally demonstrates that the main factor influencing the beads' ability to absorb water and create a hydrogel is chitosan's intrinsic hydrophilic character, which is ascribed to its abundance of hydroxyl and amine groups.

The impact of integrating ChEO leads to a more sophisticated view. At most time intervals, there was a minor tendency of slightly decreased swelling ratios in the ChEO-loaded beads when compared to the control (ChEO 0%), even if the overall swelling capacity stayed high. This implies that even though the essential oil is hydrophobic, its presence may have a subtle effect on the structural dynamics of the hydrogel. One possible mechanism is the pore-filling effect, in which ChEO molecules occupy part of the empty spaces within the chitosan polymer network, thereby reducing the volume available for water molecules to penetrate and bind. This is consistent with previous findings, such as those of Anchisi et al. (2006), who also reported variations in the swelling behavior of chitosan when combined with different essential oils.

These CB-EO particles demonstrate strong structural integrity and stability in aqueous environments, as indicated by the relatively constant swelling ratio throughout the immersion period and the minimal impact of ChEO. This property ensures the effective retention of encapsulated active compounds over time without rapid degradation of the carrier, making them well-suited for applications in controlled release systems or food preservation.

**Table 2.** Swelling ratio of beads versus time.

Time (min)	30	60	90	120	Level of significance
Control	1.52±0.03	1.55±0.06	1.57±0.07	1.57±0.08	NS
CB-EO (0.5)	1.49±0.15	1.53±0.15	1.58±0.09	1.54±0.1	NS
CB-EO (1)	1.34±0.07	1.41±0.07	1.45±0.05	1.43±0.06	NS
CB-EO (2)	1.39±0.11	1.48±0.14	1.53±0.12	1.43±0.13	NS

<sup>NS</sup> Not significant at  $P<0.05$ . Control, CB-EO (0.5), (1), and (2) are the chitosan beads containing *Chúc* essential oil at concentrations of 0, 0.5, 1, and 2% (v/v), respectively.

### Antioxidant activity of CB-EO

The antioxidant activity of CB-EO is presented in Table 3. Results show a clear trend: higher EO content corresponds to increased antioxidant activity, ranging from 33.5% in the control to 40.8% in CB-EO (2). Compared to the control, the antioxidant activity of EO-containing samples was 14–21% higher. These findings indicate that chitosan (CS) possesses inherent antioxidant capacity, which is further enhanced by the presence of EO. This can be illustrated in the study of Su et al. (2020), on CS combined with cinnamon EO, where the antioxidant activity increased from 20.6 to 56.9% when the EO content increased. CB-EO shows strong antioxidant properties, making it a potential candidate for food preservation.

In comparison, sodium alginate gel beads encapsulating curcumin/gum Arabic/gelatin microcapsules exhibited significantly higher antioxidant activity, with DPPH and ABTS radical scavenging capacities of 95.59 and 87.65%, respectively (Lin et al. 2024). While CB-EO's antioxidant activity is lower, the encapsulation of ChEO in chitosan beads enhances stability and controlled release, similar to the hydrogel beads' role in protecting curcumin, thereby minimizing undesirable flavor impacts in food applications (Lin et al. 2024). However, while increasing the concentration of EO enhances its antioxidant effect, it can also introduce undesirable flavors to the food. Therefore, depending on the type of food product, users can adjust the appropriate essential oil concentration to exploit CB-EO properties optimally.

**Table 3.** Antioxidant activity of chitosan beads.

Antioxidant activity	Control	CB-EO (0.5)	CB-EO (1)	CB-EO (2)	Level of significance
DPPH <sub>RSC</sub> (%)	33.54±0.73 <sup>a</sup>	38.34±0.07 <sup>b</sup>	39.43±0.08 <sup>c</sup>	40.86±0.07 <sup>d</sup>	*

\*Significant at  $P<0.05$ . Control, CB-EO (0.5), (1), and (2) are the chitosan beads containing *Chúc* essential oil at concentrations of 0, 0.5, 1, and 2% (v/v), respectively. Significant differences ( $P<0.05$ ) between samples are indicated by different letters within a row (a–d).

### Antibacterial activity of CB-EO

The antibacterial activity of CB-EO was determined based on the ability to inhibit the growth of bacteria, through the diameter of the bacterial inhibition zone, as shown in Table 4 and Figure 1. The negative control, DMSO 5% did not exhibit a bacterial inhibition zone, while the positive control, Gentamicin, had a wide bacterial inhibition zone with all four test strains. Antibacterial activity ranked in the following order: *B. cereus* > *S. typhimurium* > *P. aeruginosa* > *S. aureus*.

has antibacterial activity. When combined with ChEO, the antibacterial activity increased significantly from 5.3 to 8.33 mm. The highest antibacterial effect was shown in the CB-EO (2) sample for the *S. aureus* and *B. cereus* strains, with a diameter of 8.33 mm. All of these results are similar to the results of the study by Junca et al. (2019). The EO kept inside CS beads can inhibit EO's evaporation and improve food storage time. Besides, CB-EO also has less influence on the product's taste than pure EOs.

For CB-EO, the control sample showed low antibacterial activity from 3.67 to 4.33 mm, but it also showed that CS

Similar to the findings with chitosan beads incorporated with *Thymus capitatus* essential oil (CB-TCEO),



**Table 4.** Antibacterial activity of chitosan beads.

Bacteria	Bacterial inhibition zone (mm)					Level of significance
	Control	CB-EO (0.5)	CB-EO (1)	CB-EO (2)	Gentamicin	
<i>P. aeruginosa</i>	3.67±0.58 <sup>aA</sup>	5.67±0.58 <sup>bA</sup>	6.33±0.58 <sup>bA</sup>	6.67±0.58 <sup>bA</sup>	17.00±1.00 <sup>cA</sup>	*
<i>S. aureus</i>	3.67±0.58 <sup>aA</sup>	5.33±0.58 <sup>bA</sup>	6.67±0.58 <sup>cA</sup>	8.33±0.58 <sup>dB</sup>	16.33±0.58 <sup>eA</sup>	*
<i>S. typhimurium</i>	3.67±0.58 <sup>aA</sup>	5.33±0.58 <sup>bA</sup>	6.67±0.58 <sup>cA</sup>	7.67±0.58 <sup>cAB</sup>	17.33±0.58 <sup>dA</sup>	*
<i>B. cereus</i>	4.33±0.58 <sup>aA</sup>	5.33±0.58 <sup>aA</sup>	6.67±0.5 <sup>bA</sup>	8.33±0.58 <sup>cB</sup>	20.67±1.15 <sup>dB</sup>	*

\* Significant at  $P<0.05$ . Control, CB-EO (0.5), (1), and (2) are the chitosan beads containing *Chúc* essential oil at concentrations of 0, 0.5, 1, and 2% (v/v), respectively. Significant differences ( $P<0.05$ ) between samples are indicated by different letters within a row (a–e) or a column (A–B).

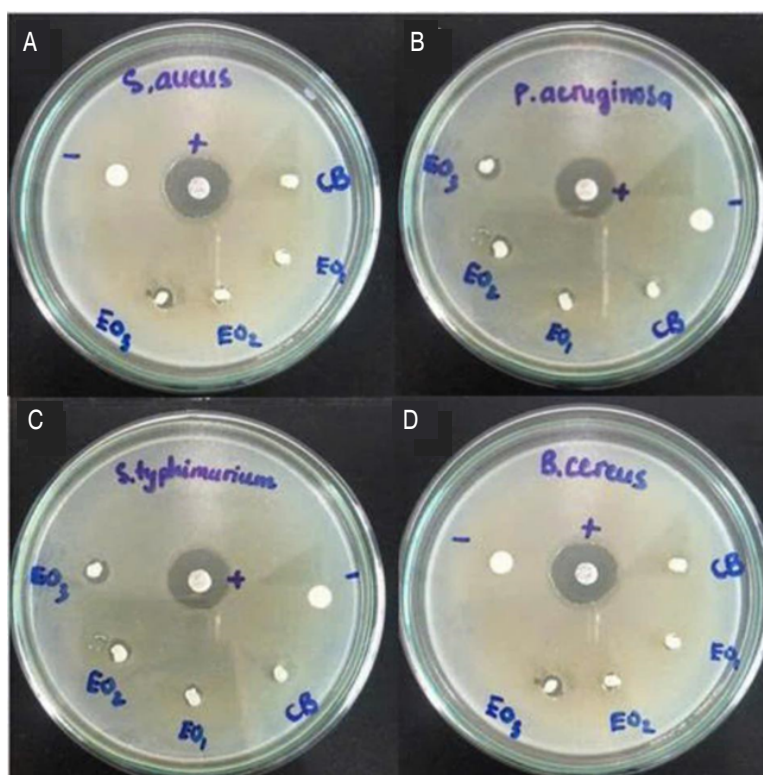


**Figure 1.** Antibacterial activity of CB-EO beads against **A.** *S. aureus*, **B.** *P. aeruginosa*, **C.** *S. typhimurium*, and **D.** *B. cereus*. -, +, CB, EO1, EO2, and EO3 correspond to negative control, positive control, control sample, CB-EO (0.5), CB-EO (1), and CB-EO (2), respectively.

CB-EO exhibited stronger inhibition against Gram-positive bacteria (*B. cereus*) compared to Gram-negative bacteria (*S. typhimurium* and *P. aeruginosa*), likely due to the thinner cell wall of Gram-positive bacteria allowing easier penetration of active compounds, with limonene, one of the key antibacterial components in ChEO, acting as an alkylating agent, binding to nucleophilic groups and

causing protein denaturation and cell lysis (Millezi et al. 2014). Chitosan interacts electrostatically with bacterial cell membranes, disrupting their structure and facilitating the penetration of key components of the essential oil. Chitosan beads combined with *Citrus hystrix* essential oil exhibit antibacterial activity through a synergistic effect between chitosan and the major constituents of the essential oil.

Based on the experimental results, the synergistic combination of CS and ChEO in antibacterial properties will be an alternative method to synthetic antibacterial additives in food preservation as well as other applications in practice.

### SEM analysis of CB-EO

SEM images at  $\times 40$  magnification show that CB-EO

is bean-shaped, with a sphericity of 59.6 to 66.6%. As shown above, the beads have a smooth surface (Figure 2). The small wrinkles on the outer surface may be due to shrinkage during the drying process. This shape is completely similar to that observed in the study of CS combined with sodium tripolyphosphate by Yousefi et al. (2019). When CS is combined with different materials, it may create different shapes.

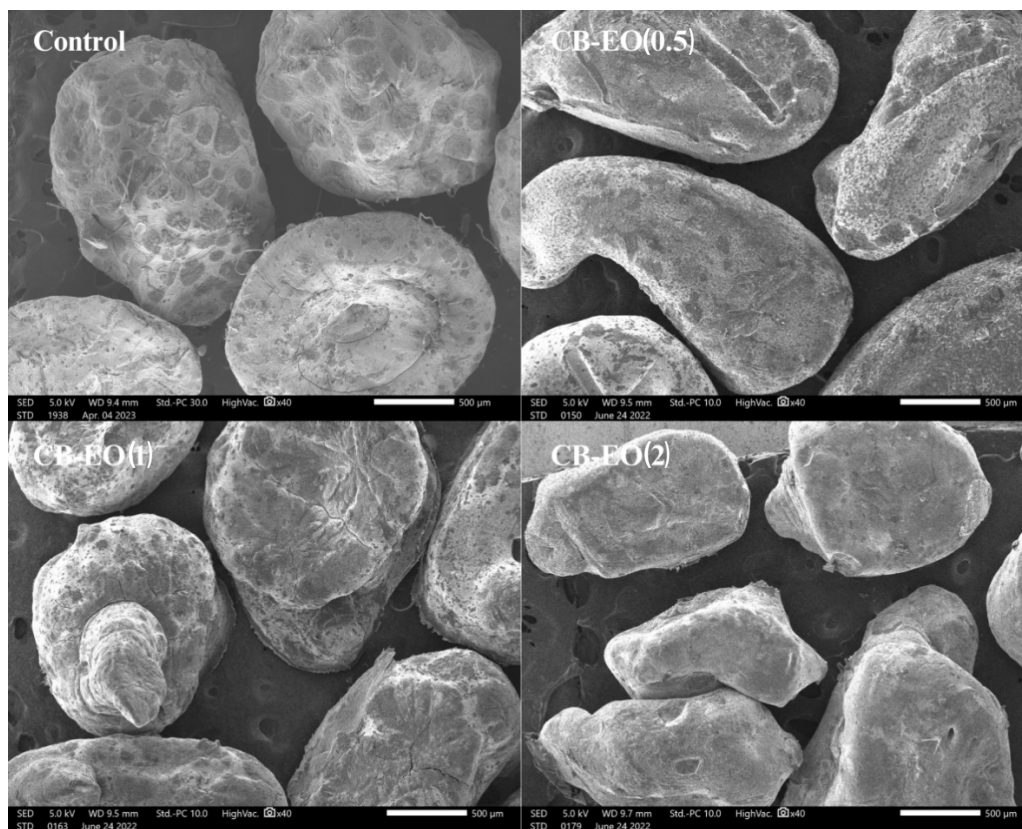


**Figure 2.** Morphological structure analysis of the beads at  $\times 40$  magnification. Control, CB-EO (0.5), (1), and (2) are the chitosan beads containing *Chúc* essential oil at concentrations of 0, 0.5, 1, and 2% (v/v), respectively.

At high magnification, the microstructure of the samples and its changes with different essential oil concentrations can be observed. At  $\times 10,000$  magnification, the surface of the control sample appeared rough and had fewer wrinkles compared to the EO-containing samples (Figure 3). This may be due to the tendency of ChEO to aggregate during the drying process. This study is also similar to that by Lich et al. (2018), where CS was combined with  $\text{SiO}_2$  to create a smooth surface with numerous pores. Compared with the sodium caseinate-sorbitol biofilm containing citral

microparticles, CB-EO did not show obvious micropores, possibly due to the lower efficiency of air bubble removal by sonicating probe than by ultrasonic bath (Yoplac et al. 2022). The results show that differences in shape, size, and surface state can affect the release of EOs during processing and preservation.

However, beyond structural description, it is important to emphasize why morphology matters: in food preservation applications, the surface characteristics of the

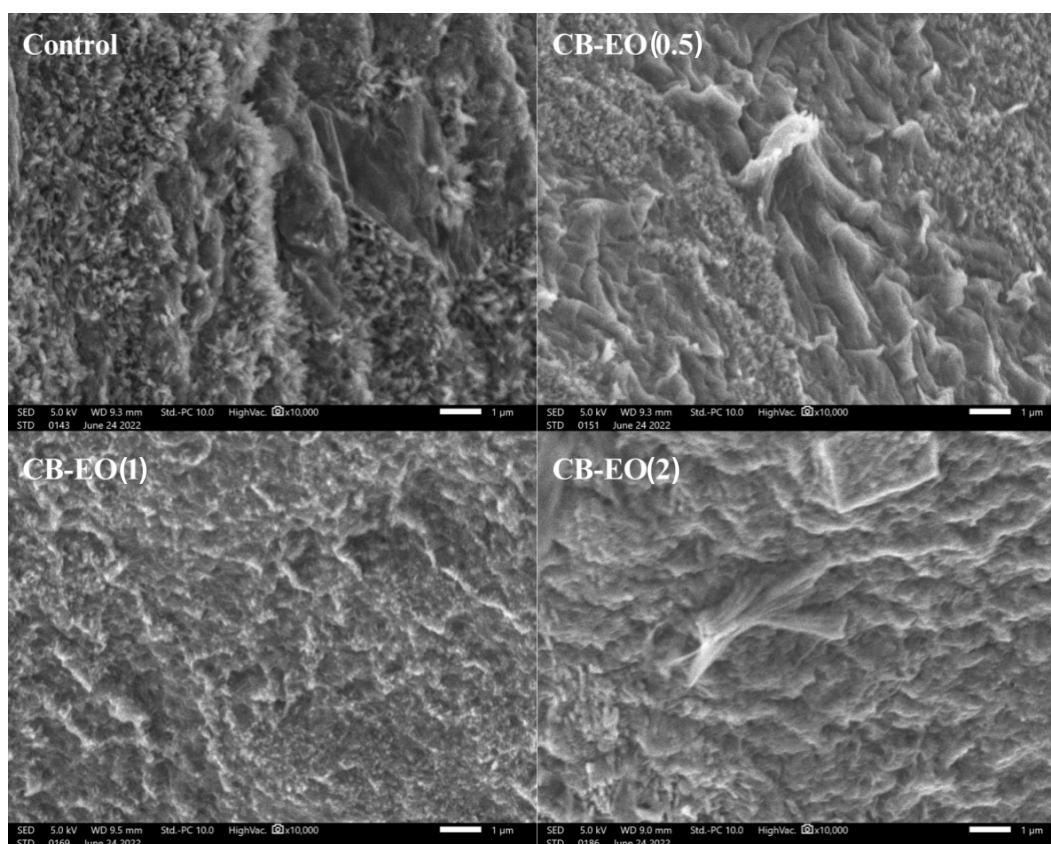


**Figure 3.** Morphological structure analysis of the beads at  $\times 10,000$  magnification. Control, CB-EO (0.5), (1), and (2) are the chitosan beads containing *Chúc* essential oil at concentrations of 0, 0.5, 1, and 2% (v/v), respectively.

beads—such as smoothness, presence of pores, or wrinkles—play a crucial role in the release kinetics of active compounds. A smoother surface may reduce premature diffusion of essential oils, thereby enabling a more controlled and prolonged release, which is beneficial for extending the shelf-life of food products. On the other hand, excessive wrinkles or porosity could lead to rapid initial release, reducing long-term effectiveness. Therefore, analyzing SEM images is not merely for morphological documentation but to help optimize bead structures for practical use in food packaging or coating systems (Yoplac et al. 2021).

#### FTIR analysis of CB-EO

FTIR analysis is one of the preliminary evaluation methods for the presence of compounds and functional groups in the sample, and this evaluation has been carried out in many previous studies on EOs combined with other types of coatings, such as CS combined with *Thymus capitatus* EO (Junca et al. 2019) and CS combined with

*Cinnamomum* EO (Su et al. 2020). As shown in Figure 4, all four samples exhibit the presence of several similar functional groups. Specifically, absorption bands were observed at  $3,450$ ;  $1,640$ ;  $1,380$ ; and  $1,076$   $\text{cm}^{-1}$ , corresponding to OH- groups, C=O groups, S=O groups, and pyranose C–O–C groups, respectively. In addition, at the wavelength of  $2,928$   $\text{cm}^{-1}$ , it shows the presence of the C–H group, which is similar to the results of Su et al. (2020), who previously researched *Cinnamomum* EO encapsulated in CS nanoparticles. At the wavelength of  $1,586$   $\text{cm}^{-1}$ , it proves the presence of the N–H group, similarly to the study of Hosseini et al. (2013), who studied oregano EO in CS nanoparticles.

Following the results, there is an interaction of some compounds in ChEO with CS. Specifically, compared to the control sample, the sample containing ChEO can interact with CS to reduce the intensity of wavelengths such as  $3,450$ ;  $1,640$ ; and  $1,380$   $\text{cm}^{-1}$ . Some other wavelengths do not change significantly, such as  $1,586$ ;



2,928; and 1,076  $\text{cm}^{-1}$ . The presence of biologically active compounds with different EO content can interact with CS to create different properties of CB-EO product.

These interactions are vital for the stability and integrity of the encapsulated essential oil within the chitosan matrix,

directly influencing its release profile and ultimately its effectiveness as an antibacterial and antioxidant agent in food. Stronger interactions suggest better retention of the active compounds, leading to prolonged antimicrobial and antioxidant activity and thus extended shelf life of the food product (Yoplać et al. 2022).

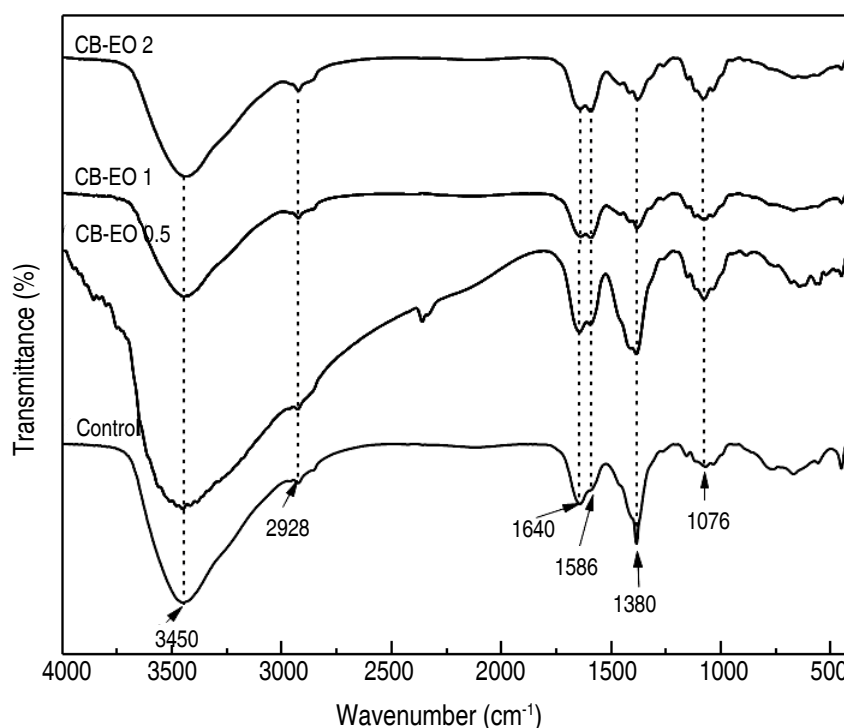


**Figure 4.** Fourier transform infrared (FTIR) spectra of the beads. Control, CB-EO (0.5), (1), and (2) are the chitosan beads containing *Chúc* essential oil at concentrations of 0, 0.5, 1, and 2% (v/v), respectively.

### X-ray diffraction analysis of CB-EO

CS particles combined with EO can change crystallinity, as shown in the study of Yoncheva et al. (2021), in which there were two strong diffraction peaks at 20 and 42° when CS particles were combined with oregano EO. This contrasts with the results of this study, in which the control, CB-EO (0.5), CB-EO (1), and CB-EO (2) samples have the appearance of forming peaks mainly at two positions of 20 and 29° (Figure 5). The diffraction peaks of the samples with ChEO are lower than those of the control, typically at an angle of 29°. The addition of EO may change the interaction between CS and ChEO, leading to a decrease in the crystallinity of the samples. This also shows that the change in crystallinity is related

to the nature of CS, such as origin, deacetylation level, and the compounds present in different EOs. At the same time, the interaction between CS and different types of EO contributes to influencing XRD diffraction peaks.

These results suggest that the developed CB-EO system holds strong potential for real food preservation applications. Similar approaches have been successfully employed by Junca et al. (2019), who demonstrated extended shelf life of red tilapia fillets using chitosan beads loaded with *Thymus capitatus* essential oil, and by Sangsuwan et al. (2016), who effectively inhibited *Botrytis cinerea* and reduced fruit decay in strawberries

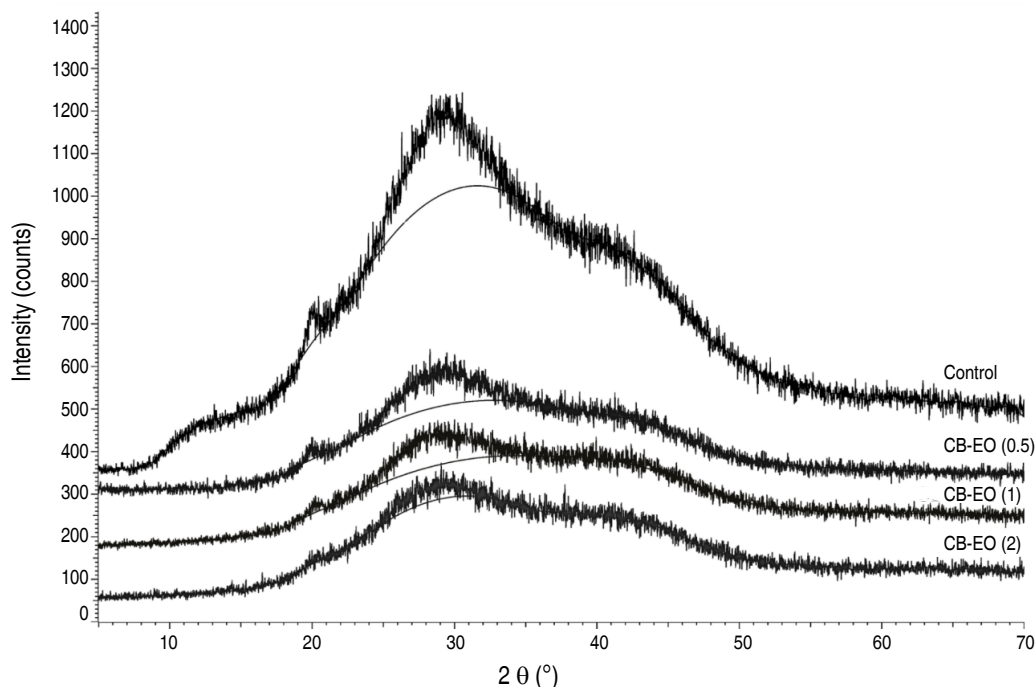


**Figure 5.** X-ray diffraction (XRD) patterns of the beads. Control, CB-EO (0.5), (1), and (2) are the chitosan beads containing *Chúc* essential oil at concentrations of 0, 0.5, 1, and 2% (v/v), respectively.

using chitosan beads combined with lavender or red thyme oils. In this context, the present study reinforces the practical feasibility of using CB-EO as a safe, natural, and biodegradable alternative to synthetic preservatives—particularly in perishable food systems—aligning with current demands in the food industry for green, sustainable technologies. These findings are further supported by the work of Mouhoub et al. (2024), in which chitosan coatings enriched with essential oils significantly extended the postharvest life of strawberries while maintaining sensory and physicochemical quality.

## CONCLUSION

This study successfully developed chitosan beads (CB-EO) by combining chitosan (CS) and *Citrus hystrix* essential oil (ChEO), both sourced from manufacturing waste. The formulation enhanced antioxidant activity by 14–21% and significantly improved antimicrobial properties compared to the control, demonstrating strong potential for food preservation. Its natural origin

ensures safety for human health and environmental compatibility, making it a promising alternative to synthetic preservatives. Despite these promising results, the study was primarily limited to in vitro physicochemical characterization, without validation in real food systems. Therefore, CB-EO may be most suitable for products with an outer layer that is typically removed before consumption, such as many fruits, or where the essential oil's aroma is acceptable. Future studies should evaluate its performance in real food products, conduct sensory assessments, and explore scalability and economic feasibility to support industrial application.

## ACKNOWLEDGMENTS

The present study was supported by Industrial University of Ho Chi Minh City. The authors thank Nguyen Ngoc Phuong Dan, Tran Thi Diem Tien, and Chau Thi Kha Tu for their helpful advice on various technical issues examined in this paper.



## CONFLICT OF INTERESTS

The authors declare no potential conflicts of interest.

## REFERENCES

- Anchisi C, Meloni MC and Maccioni AM (2006) Chitosan beads loaded with essential oils in cosmetic formulations. *Journal of Cosmetic Science* 57(3): 205-214. <https://doi.org/10.1111/j.1468-2494.2007.00371.1.x>
- Çoban MZ (2021) Effectiveness of chitosan/propolis extract emulsion coating on refrigerated storage quality of crayfish meat (*Astacus leptodactylus*). *CyTA - Journal of Food* 19(1): 212-219. <https://doi.org/10.1080/19476337.2021.1882580>
- Hosseini SF, Zandi M, Rezaei M and Farahmandghavi F (2013) Two-step method for encapsulation of oregano essential oil in chitosan nanoparticles: Preparation, characterization and *in vitro* release study. *Carbohydrate Polymers* 95(1): 50-56. <https://doi.org/10.1016/j.carbpol.2013.02.031>
- Junca MAV, Valencia C, López EF et al (2019) Chitosan beads incorporated with essential oil of *Thymus capitatus*: Stability studies on red *Tilapia* filets. *Biomolecules* 9(9): 458. <https://doi.org/10.3390/biom9090458>
- Kulig M, Galanty A, Grabowska K and Podolak I (2022) Assessment of safety and health-benefits of *Citrus hystrix* DC. peel essential oil, with regard to its bioactive constituents in an *in vitro* model of physiological and pathological skin conditions. *Biomedicine and Pharmacotherapy* 151: 113151. <https://doi.org/10.1016/j.biopha.2022.113151>
- Lertsatitthanakorn P, Taweekaisupapong S, Aromdee C and Khunkitti W (2006) *In vitro* bioactivities of essential oils used for acne control. *International Journal of Aromatherapy* 16(1): 43-49. <https://doi.org/10.1016/j.ijat.2006.01.006>
- Lich NQ, Linh VQ, Hanh TD and Duc LM (2018) Effect of the chitosan concentration on the structure of chitosan beads formed in naoh and NaOH.SiO<sub>2</sub>. In: The 1<sup>st</sup> Rajamangala Surin International Conference: "Academic Network Bridge through Research". Surin, Thailand. 10 p.
- Lin Y, Xu J and Gao X (2024) Development of antioxidant sodium alginate gel beads encapsulating curcumin/gum Arabic/gelatin microcapsules. *Food Hydrocoll*, 152: 109901. <https://doi.org/10.1016/j.foodhyd.2024.109901>
- Long DM and Quoc LPT (2023) Essential oil of *Citrus hystrix* DC.: A mini-review on chemical composition, extraction method, bioactivities, and potential applications in food and pharmaceuticals. *Plant Science Today* 10(2): 112-117. <https://doi.org/10.14719/pst.2508>
- Long DM, Quoc LPT, Nhung TTP et al (2023) Chemical profiles and biological activities of essential oil of *Citrus hystrix* DC. peels. *Korean Journal of Food Preservation* 30(3): 395-404. <https://doi.org/10.11002/kjfp.2023.30.3.395>
- Millezi AF, Baptista NN, Caixeta DS et al (2014) Caracterização química e atividade antibacteriana de óleos essenciais de plantas condimentares e medicinais contra *Staphylococcus aureus* e *Escherichia coli*. *Revista Brasileira de Plantas Medicinais* 16: 18-24. <https://doi.org/10.1590/S1516-05722014000100003>
- Mouhoub A, Boutachfaiti RE, Petit E et al (2023) Chemical extraction, characterization, and inspection of the antimicrobial and antibiofilm activities of shrimp chitosan against foodborne fungi and bacteria. *World Journal of Microbiology and Biotechnology* 39(12): 338. <https://doi.org/10.1007/s11274-023-03798-8>
- Mouhoub A, Guendouz A, Alaoui-Talibi ZE et al (2024) Utilization of chitosan-based coating enriched with *Syzygium aromaticum*, *Cinnamomum zeylanicum*, and *Thymus satureioides* essential oils mixture for strawberries with extended shelf life. *Food Measure* 18: 3315-3325. <https://doi.org/10.1007/s11694-024-02405-0>
- Mouhoub A, Guendouz A, Alaoui-Talibi ZE et al (2025) Optimization of chitosan-based film performance by the incorporation of *Cinnamomum Zeylanicum* essential oil. *Food Biophysics* 20, 48. <https://doi.org/10.1007/s11483-025-09943-0>
- Nguyen HDT, Nguyen LPL, Nguyen VD et al (2023) Quality changes of Hoa Loc mangoes (*Mangifera indica* L.) during storage: Effect of chitosan-based nano-silver film coating. *Acta Alimentaria* 52(3): 352-365. <https://doi.org/10.1556/066.2021.00163>
- Othman HIA, Alkatib HH, Zaid A et al (2023) Phytochemical composition, antioxidant and antiproliferative activities of *Citrus hystrix*, *Citrus limon*, *Citrus pyriformis*, and *Citrus microcarpa* leaf essential oils against human cervical cancer cell line. *Plants* 12(1): 134. <https://doi.org/10.3390/plants12010134>
- Pham TT, Baranyai L, Dam MS et al (2023a) Evaluation of shelf life of egg treated with edible coating by means of NIR spectroscopy and laser induced diffuse reflectance imaging. *Journal of Food Engineering* 358: 111688. <https://doi.org/10.1016/j.jfoodeng.2023.111688>
- Pham TT, Nguyen LLP, Dam MS and Baranyai L (2023b) Application of edible coating in extension of fruit shelf life: Review. *AgriEngineering* 5(1): 520-536. <https://doi.org/10.3390/agriengineering5010034>
- Pham TT, Nguyen LPL, Baranyai L et al (2022) Effect of electrolyzed cassava starch-gelatin coating on biochemical properties and ripening of banana (*Musa acuminata* L.) fruits. *Polish Journal of Food and Nutrition Sciences* 72(3): 263-272. <https://doi.org/10.31883/pjfn/152667>
- Quoc LPT (2021) Chemical composition and physical properties of coffee (*Coffea robusta*) bee pollen in Daklak province, Vietnam. *Acta Alimentaria* 50(3): 453-463. <https://doi.org/10.1556/066.2021.00092>
- Sangsuwan J, Pongsapakworawat T, Bangmo P and Sutthasupa S (2016) Effect of chitosan beads incorporated with lavender or red thyme essential oils in inhibiting *Botrytis cinerea* and their application in strawberry packaging system. *LWT – Food Science and Technology* 74: 14-20. <https://doi.org/10.1016/j.lwt.2016.07.021>
- Su H, Huang C, Liu Y et al (2020) Preparation and characterization of cinnamomum essential oil–chitosan nanocomposites: Physical, structural, and antioxidant activities. *Processes* 8(7): 834. <https://doi.org/10.3390/pr8070834>
- Thakur M and Nanda V (2018) Exploring the physical, functional, thermal, and textural properties of bee pollen from different botanical origins of India. *Journal of Food Process Engineering* 43(1): 12935. <https://doi.org/10.1111/jfpe.12935>
- Thong PT, Hong NKD and Surbkar S (2010) Physical properties of green bean (*Vigna radiata* L.). In: *Proceedings of the 5<sup>th</sup> "International Conference on Innovations in Food and Bioprocess Technology"*. Bangkok, Thailand. 13 p.
- Tongnuanchan P, Benjakul S and Prodpran T (2012) Properties and antioxidant activity of fish skin gelatin film incorporated with citrus essential oils. *Food Chemistry* 134(3): 1571-1579. <https://doi.org/10.1016/j.foodchem.2012.03.094>
- Utami R, Kawiji, Khasanah LU and Nasution MIA (2017)

Preservative effects of Kaffir lime (*Citrus hystrix* DC.) leaves oleoresin incorporation on cassava starch-based edible coatings for refrigerated fresh beef. *International Food Research Journal* 24(4): 1464-1472.

Yoplac I, Vargas L, Robert P and Hidalgo A (2021) Characterization and antimicrobial activity of microencapsulated citral with dextrin by spray drying. *Heliyon* 7(4): 06737. <https://doi.org/10.1016/j.heliyon.2021.e06737>

Yoplac I, Hidalgo A and Vargas L (2022) Characterization, microstructure, and spectroscopic study of optimized sodium caseinate–sorbitol active biofilms with citral microencapsulate. *Polymer Bulletin* 80(5): 5447-5468. [https://doi.org/10.1007/s00289-](https://doi.org/10.1007/s00289-022-04345-5)

022-04345-5

Yoncheva K, Benbassat N, Zaharieva MM et al (2021) Improvement of the antimicrobial activity of oregano oil by encapsulation in chitosan–alginate nanoparticles. *Molecules* 26(22): 7017. <https://doi.org/10.3390/molecules26227017>

Yousefi M, Khorshidian N, Mortazavian AM and Khosravi-Darani K (2019) Preparation optimization and characterization of chitosan-tripolyphosphate microcapsules for the encapsulation of herbal galactagogue extract. *International Journal of Biological Macromolecules* 140: 920-928. <https://doi.org/10.1016/j.ijbiomac.2019.08.122>



# Postharvest conditions of *Capsicum annuum* and their effect on hot sauce added *Ananas comosus*

Condiciones postcosecha de *Capsicum annuum* y su efecto en la salsa picante añadida con *Ananas comosus*

<https://doi.org/10.15446/rfnam.v78n3.118619>

Andry Annabel Alvarez-Aspiazu<sup>1\*</sup>, Alicia Nicole Batallas-Terrero<sup>1</sup>, Jaime Fabián Vera-Chang<sup>1</sup>  
and Jorge Gustavo Díaz-Arreaga<sup>2</sup>

## ABSTRACT

### Keywords:

Acceptability  
Added value  
Physicochemical properties  
Pungency threshold  
Sensory profile

Postharvest handling of ingredients directly influences the sensory quality and stability of derived food products. This study aimed to evaluate the effect of the postharvest condition of chili pepper (*Capsicum annuum* L.) (fresh or dehydrated) and its proportion with pineapple (*Ananas comosus* L.) Merr.) on the physicochemical and sensory properties of a hot sauce. A completely randomized design with a factorial A×B arrangement (chili condition × pineapple percentage) was used, generating six treatments with three replications. Physicochemical variables were analyzed using ANOVA and Tukey's test ( $P \leq 0.05$ ), while sensory attributes were evaluated using the Kruskal-Wallis test. Treatments with dehydrated chili (T4–T6) showed higher pH, soluble solids content, and favorable sensory attributes such as color and flavor, with T4 (40% pineapple) standing out due to its high acceptability and lower pungency perception. In contrast, treatments with fresh chili (T1–T3) exhibited higher acidity, moisture, and pungency threshold, negatively affecting texture and overall perception. T6 reached the highest °Brix content (22.87), while T1 had the highest moisture (78.42%) and pungency (3.90). It is concluded that the use of dehydrated chili, especially in combination with 40–50% pineapple, significantly improves physicochemical and sensory parameters, enhancing product stability and consumer acceptance. These findings highlight the importance of postharvest handling in optimizing the formulation of value-added food products by balancing flavor, texture, and stability.

## RESUMEN

### Palabras clave:

Aceptabilidad  
Valor agregado  
Propiedades fisicoquímicas  
Umbral de picor  
Perfil sensorial

El manejo postcosecha de ingredientes influye directamente en la calidad sensorial y estabilidad de productos derivados. Este estudio tuvo como objetivo evaluar el efecto del estado postcosecha del ají (*Capsicum annuum* L.) (fresco o deshidratado) y su proporción con piña (*Ananas comosus* L.) Merr.) sobre las propiedades fisicoquímicas y sensoriales de una salsa picante. Se empleó un diseño completamente al azar con arreglo factorial A×B (estado del ají × porcentaje de piña), generando seis tratamientos con tres repeticiones. Las variables fisicoquímicas se analizaron mediante ANOVA y prueba de Tukey ( $P \leq 0,05$ ), y los atributos sensoriales con Kruskal-Wallis. Los tratamientos con ají deshidratado (T4–T6) presentaron mayor pH, contenido de sólidos solubles y atributos sensoriales favorables como color y sabor, destacando T4 (40% piña), con alta aceptabilidad y menor percepción de pungencia. En contraste, los tratamientos con ají fresco (T1–T3) exhibieron mayor acidez, humedad y umbral de pungencia, lo que afectó negativamente la textura y percepción global. T6 alcanzó el mayor contenido de °Brix (22,87), mientras que T1 mostró la mayor humedad (78,42%) y pungencia (3,90). Se concluye que el uso de ají deshidratado, especialmente combinado con 40–50% de piña, mejora significativamente los parámetros fisicoquímicos y sensoriales, favoreciendo la estabilidad y aceptación del producto. Esta evidencia resalta la importancia del manejo postcosecha para optimizar la formulación de alimentos con valor agregado, equilibrando sabor, textura y estabilidad.

<sup>1</sup>Facultad de Ciencias de la Industria y Producción, Universidad Técnica Estatal de Quevedo, Ecuador. [aalvareza@uteq.edu.ec](mailto:aalvareza@uteq.edu.ec) , [alicia.batallas2018@uteq.edu.ec](mailto:alicia.batallas2018@uteq.edu.ec) , [jverac@uteq.edu.ec](mailto:jverac@uteq.edu.ec) 

<sup>2</sup>Investigador Independiente, Quevedo, Ecuador. [jorge.diaz231994@gmail.com](mailto:jorge.diaz231994@gmail.com) 

\*Corresponding author

The chili pepper (*Capsicum annuum* (L.)) has been the subject of numerous studies in the food industry due to its capsaicin content (Gonçalves et al. 2024; Rezazadeh et al. 2021), an alkaloid responsible for its characteristic spiciness, a parameter that influences consumer acceptance of the product (Sunarmani et al. 2024). This compound has been crucial for the creation of various food products, such as sauces, stews, and dehydrated foods, which stand out for their unique sensory profiles (Hameed et al. 2022). In addition to providing spiciness, capsaicin has facilitated the incorporation of chili peppers into various culinary traditions, particularly in the preparation of hot sauces, an essential ingredient in many cuisines worldwide (Marikos 2024).

In Ecuador, the hot sauce industry represents a significant economic sector, with a production of 224 million kilograms in 2022, of which 6% was allocated to exports. These exports generated revenues of \$669 million, marking a 10% increase compared to the previous year (Chong and Parra 2019). Although it is not a staple food, hot sauce has become an essential complement to many traditional dishes, in addition to being a distinctive cultural element in various regions, driven by global trends (Pazos 2021).

One of the key factors in hot sauce production is the choice of the chili pepper's postharvest state, which is generally used fresh (Yin et al. 2021). However, studies have shown positive results when using dehydrated chili peppers, highlighting their enhanced sensory characteristics (Li et al. 2022).

The local hot sauce market is limited in terms of ingredients and formulations, which reduces the options available to consumers. To innovate and diversify production, it is essential to explore new alternatives that enrich flavor and expand the variety of products. The incorporation of tropical fruits, such as pineapple (*Ananas comosus* (L.

Merr.), represents a promising option. This fruit, widely cultivated in Ecuador (Abad and Pérez 2024), is rich in vitamin C, bromelain, and antioxidants, compounds that not only enhance the sensory qualities of hot sauce but also provide additional nutritional benefits (Ortega et al. 2021; Santos et al. 2021).

Considering the above and the fact that the sauce market in Ecuador is growing, where hot sauces play an important role, it is pertinent to carry out studies aimed at increasing the added value of chili bell pepper harvests and improving the competitiveness of the sector. Therefore, the aim of this research was to evaluate the effect of the post-harvest state of chili bell pepper (*Capsicum annuum* (L.)) (fresh or dehydrated) and its proportion with pineapple (*Ananas comosus* (L.) Merr.) on the physicochemical and sensory properties of a hot sauce.

## MATERIALS AND METHODS

### Location of the experimental site

The preparation of the treatments was carried out in the Unit Operations Laboratory. The physicochemical analysis was conducted in the Bromatology Laboratory, and the sensory analysis was performed with a group of students from the Faculty of Industry and Production Sciences (FCIP). These locations are within the La María campus of the Universidad Técnica Estatal de Quevedo (UTEQ), located at kilometer 7.5 of the Quevedo-El Empalme highway, in the San Felipe precinct, Mocache canton, Los Ríos province, at the geographic coordinates 01°04'56" S, 79°30'08" W.

### Data analysis

The data on physicochemical characteristics were subjected to analysis of variance. A Completely Randomized Design with a bifactorial AxB arrangement was applied, which involved the interaction between levels of factor A (Postharvest state of the chili pepper) and factor B (Pineapple inclusion percentage), as described in Table 1.

**Table 1.** Experimental factors and levels for chili sauce production.

Factors	Code	Levels
Postharvest state	A	a0: Fresh chili pepper a1: Dehydrated chili pepper
Pineapple inclusion percentage	b	b0: 40% pineapple b1: 45% pineapple b2: 50% pineapple



The interaction between factors resulted in six treatments (Table 2), each with three replications, forming a total of 18 experimental units. To determine statistical differences between treatments, Tukey's test ( $P \leq 0.05$ ) was applied using the InfoStat statistical software.

On the other hand, the sensory analysis data did not follow a normal distribution; therefore, the non-parametric Kruskal-Wallis test was used.

### Experiment management

#### Pineapple juice processing

The selection of pineapples (MD2 variety) followed

the criteria of Ganoza-Yupanqui et al. (2021), ensuring a soluble solids content between 12° and 15° Brix for an optimal balance of sweetness and acidity. The fruits were then washed with potable water to ensure product hygiene. After washing, the pineapples were peeled, cored, and chopped to facilitate processing. To enhance their sensory profile, the pieces were roasted, caramelizing their natural sugars and intensifying their flavor. Finally, the roasted pieces were blended until a homogeneous mixture was obtained, which was then filtered to separate the juice from the sediments. This process ensured a clean and high-quality base for the preparation of the treatments.

**Table 2.** Factorial arrangement with the proposed treatment combinations for the experimental design.

No.	Symbol	Description
T1	a0b0	Fresh chili + 40% pineapple
T2	a0b1	Fresh chili + 45% pineapple
T3	a0b2	Fresh chili + 50% pineapple
T4	a1b0	Dehydrated chili + 40% pineapple
T5	a1b1	Dehydrated chili + 45% pineapple
T6	a1b2	Dehydrated chili + 50% pineapple

#### Processing of spicy sauce with fresh and dried chili pepper

The chili peppers (Ratón variety) were thoroughly washed with potable water to remove impurities. The seeds and peduncles were then removed, ensuring the exclusive use of the pericarp and avoiding bitter flavors. For the treatments using fresh chili, the pericarps were blanched in hot water at 90 °C for 5 minutes, softening their texture

while preserving their color and flavor. They were then blended until a homogeneous paste was obtained and filtered to remove sediments and seed residues. In contrast, the chili intended for dry treatments was dehydrated at 80 °C for 5 hours, resulting in a fine powder. Finally, both the chili paste and powder were mixed with the filtered pineapple juice, along with spices and other ingredients, in the proportions established in Table 3.

**Table 3.** Formulation of chili sauce treatments with pineapple addition.

Ingredients	T1 (%)	T2 (%)	T3 (%)	T4 (%)	T5 (%)	T6 (%)
Pineapple	40	45	50	40	45	50
Fresh Chili	10	10	10	-	-	-
Dried Chili	-	-	-	1.6	1.6	1.6
Water	20	15	10	28.4	23.4	18.4
Vinegar	7	7	7	7	7	7
Salt	3	3	3	3	3	3
Sugar	6	6	6	6	6	6
Bell Pepper	2	2	2	2	2	2
Onion	7	7	7	7	7	7
Garlic	5	5	5	5	5	5

The mixtures obtained in the different formulations (treatments) were subjected to cooking at 90 °C for 15 minutes, allowing for complete flavor integration and achieving the desired consistency. Subsequently, the hot sauces were packaged in labeled glass jars, previously sterilized at 100 °C, ensuring their preservation. The jars were gradually cooled to 36 °C to stabilize the product before final storage at 4 °C, guaranteeing quality and extending shelf life.

### Evaluated variables

#### Physicochemical characteristics

##### pH determination

Ten grams of the sample were weighed into a beaker, and 100 mL of distilled water was added. The mixture was homogenized using a stirring rod, and the pH was measured by immersing the electrode of a previously calibrated pH-meter.

##### Volatile acidity (%)

Ten grams of the sample were weighed into an Erlenmeyer flask, followed by the addition of 50 mL of distilled water. The mixture was homogenized, and a burette was filled with 0.1 N NaOH. The electrode of the pH-meter was inserted into the diluted sample, and titration with NaOH was performed until a sudden change in the reading indicated the equivalence point. The calculation was performed using Equation 1.

$$\text{Volatile acidity}(\%) = \frac{v\text{NaOH} * N\text{NaOH} * \text{Meq}}{m} * 100 \quad (1)$$

Where v is the volume of NaOH consumed (mL), N is the normality of the NaOH solution, Meq is the molar mass expressed in g mol<sup>-1</sup> (98.079 for sulfuric acid), and m is the sample weight (g).

##### Soluble solids measurement (°Brix)

A sample was collected using a metal spoon and placed directly onto the measuring surface of the refractometer. By pressing the start button, the device automatically provided the reading, displaying the result as a percentage.

##### Moisture determination (%)

Crucibles were dried in an oven at 100 °C for 30 minutes and cooled in a desiccator for 15 minutes. They were

then weighed along with 1 g of the sample and placed in an oven at 100 °C for 24 hours. After an additional 15-minute cooling period, the final weight was recorded for moisture content calculation using Equation 2.

$$\text{Moisture determination}(\%) = \frac{m - (a - b)}{m} * 100 \quad (2)$$

Where m is the initial sample weight (g), a is the weight of the sample plus the crucible after drying, and b is the weight of the empty crucible.

##### Ash content determination (%)

The dried sample from the moisture analysis was placed in a muffle furnace at 500 °C for 4 hours. The samples were then cooled for 30 minutes and transferred to a desiccator for complete cooling over 15 minutes. The samples were weighed along with the crucible, and the data were recorded for calculation using Equation 3.

$$\text{Ash content determination}(\%) = \frac{W2 - W1}{W0} * 100 \quad (3)$$

Where W0 is the sample weight (g), W1 is the weight of the empty crucible, and W2 is the weight of the crucible plus the ashed sample.

##### Viscosity determination (cP)

The sample was placed in a beaker positioned beneath the viscometer rotor. The rotor needle was adjusted, and after pressing the start button, the equipment provided the result after 3 minutes.

##### Fat content analysis (%)

Three (3 g) of the sauce were weighed onto filter paper, which was then placed inside a thimble holder and covered with a thimble cover. This assembly was inserted into a Goldfish extractor, and 40 mL of petroleum ether was added to the beaker before securing it to the tube. The system was operated at 55 °C for 4 hours, after which the samples were transferred to solvent recovery beakers. Finally, they were placed in an oven at 100 °C for 2 hours, cooled in a desiccator, and weighed to record the data using Equation 4.

$$\text{Fat content}(\%) = \frac{W2 - W1}{W} * 100 \quad (4)$$

Where W is the sample weight (g), W1 is the weight of the empty beaker, and W2 is the weight of the beaker plus the extracted fat.

### Sensory analysis

A sensory evaluation was conducted with a panel of 20 students from the Food Science program at FCIP-UTEQ. Due to their academic background, they were semi-trained, ensuring an accurate evaluation. The samples were randomly coded and presented at room temperature. Each panelist received a standardized amount of each sample along with a spoon and a tasting sheet, which included different levels for color, aroma, flavor, texture, spiciness threshold, and overall acceptability. In a controlled environment, panelists assessed the spiciness level of the samples using a predefined scale and then submitted their individual evaluation sheets.

For the evaluation of color, aroma, flavor, and texture, a five-point hedonic scale was used. The color scale ranged from 1 = Orange, 2 = Intense Orange, 3 = Brick, 4 = Tile, to 5 = Butane. For aroma, the scale included 1 = Fruity (ripe fruits), 2 = Sweet, 3 = Slightly sweet, 4 = Not sweet, and 5 = Complex. The flavor descriptors were 1 = Pineapple, 2 = Chili, 3 = Garlic, 4 = Onion, and

5 = Vinegar. Texture was assessed using the following scale: 1 = Very viscous, 2 = Viscous, 3 = Neither viscous nor fluid, 4 = Very dense, and 5 = Dense.

Similarly, for spiciness threshold determination, a five-point hedonic scale was used to assess the panelists' perception of spiciness: 1 = Not spicy, 2 = Slightly spicy, 3 = Moderately spicy, 4 = Spicy, and 5 = Very spicy.

It is important to note that the selected panelists had no chili allergies and expressed a preference for consuming spicy foods. To evaluate acceptability, participants were asked to indicate which treatment they liked the most.

## RESULTS AND DISCUSSION

### Physicochemical characteristics

#### pH

Regarding the ANOVA analysis of the pH in the chili sauce, statistical differences were observed between treatments ( $P < 0.05$ ). The highest values were recorded in T4 (4.18) and T1 (4.17), with no significant differences between them, but both were statistically different from T3 (4.06), which had the lowest pH. T5 (4.14) did not show significant differences with T4, while T6 (4.08) differed from both but not from T2 (4.11), which presented an intermediate value (Figure 1).

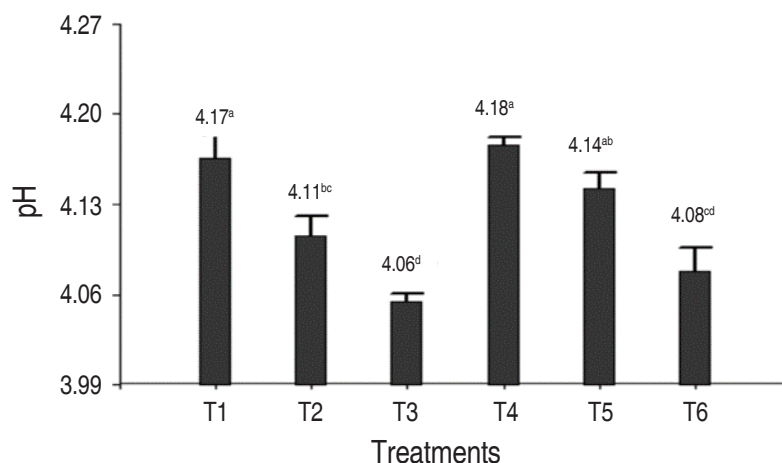


**Figure 1.** Effect of the postharvest condition of chili on the pH of a spicy sauce with added pineapple. T1: Fresh chili + 40% pineapple, T2: Fresh chili + 45% pineapple, T3: Fresh chili + 50% pineapple, T4: Dehydrated chili + 40% pineapple, T5: Dehydrated chili + 45% pineapple, and T6: Dehydrated chili + 50% pineapple.

The pH values obtained in this study are higher than those reported by Kammar-García et al. (2022), who found a pH of 3.60 in a chili sauce with tamarind, due to the high

acidity of tamarind. In comparison, pineapple juice has a less pronounced effect on pH (Trujillo 2021). On the other hand, the results of this research are similar to those of

Custodio and Fabian (2023), who reported a pH range of 4.07 to 4.43 in chili sauce with lima bean purée, indicating that the values found are within an acceptable range for this type of product.

### Volatile acidity (%)

Regarding the volatile acidity in chili sauce, statistical differences were observed between treatments ( $P < 0.05$ ).

The highest values were recorded in T3 (1.18%), T2 (1.18%), and T6 (1.17%), with no significant differences among them. In contrast, T4 showed the lowest volatile acidity (1.09%), differing significantly from the rest. Treatments T1 (1.12%) and T5 (1.12%) presented intermediate values, with no significant differences between them but differing from the other treatments (Figure 2).

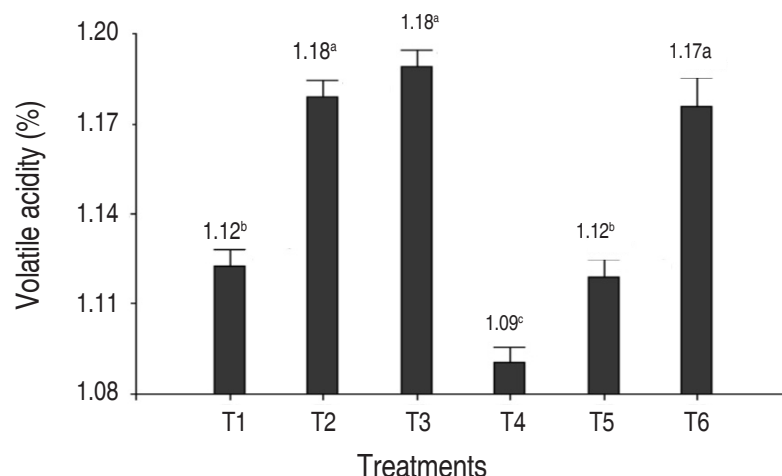


**Figure 2.** Effect of the postharvest state of chili in a spicy sauce with pineapple addition on volatile acidity. T1: Fresh chili + 40% pineapple, T2: Fresh chili + 45% pineapple, T3: Fresh chili + 50% pineapple, T4: Dehydrated chili + 40% pineapple, T5: Dehydrated chili + 45% pineapple, and T6: Dehydrated chili + 50% pineapple.

The volatile acidity values in this study were lower than those reported by Conforme (2019), who states that higher acidity contributes to the preservation of spicy sauces. Vílchez (2020) explains that dehydrated chili loses volatile compounds during thermal processing, which may reduce volatile acidity, while the addition of pineapple increases it due to its natural acids, aligning with the results obtained.

### Soluble solids (°Brix)

Regarding the soluble solids content (°Brix), statistical differences were observed between treatments ( $P < 0.05$ ). Treatment T6 presented the highest value (22.87 °Brix), significantly differing from the rest, followed by T3 (22.63 °Brix) and T5 (22.13 °Brix), which also showed significant differences between them. In contrast, treatments T1 (20.77 °Brix) and T4 (20.87 °Brix) recorded the lowest values, with no significant differences between them. Treatment T2 (21.87 °Brix) presented an intermediate value, differing from the other treatments (Figure 3).

Regarding soluble solids, Custodio and Fabian (2023) reported lower values (12 °Brix) compared to this study (20.77–22.87 °Brix), a difference attributed to the high solid content in pineapple juice. Additionally, Oña (2022) suggests that a maximum of 30 °Brix is optimal for consumer acceptance, confirming that the developed sauces meet this parameter.

### Ash content (%)

Regarding ash content, significant differences were observed between treatments ( $P < 0.05$ ). Treatments T3 (0.75%) and T6 (0.74%) showed the highest values, with no significant differences between them. Treatment T2 (0.67%) and T5 (0.66%) presented intermediate values and did not show significant differences between them, although they differed from the treatments with lower ash content. In contrast, treatments T1 (0.60%) and T4 (0.57%) recorded the lowest values, with no significant differences between them (Figure 4).

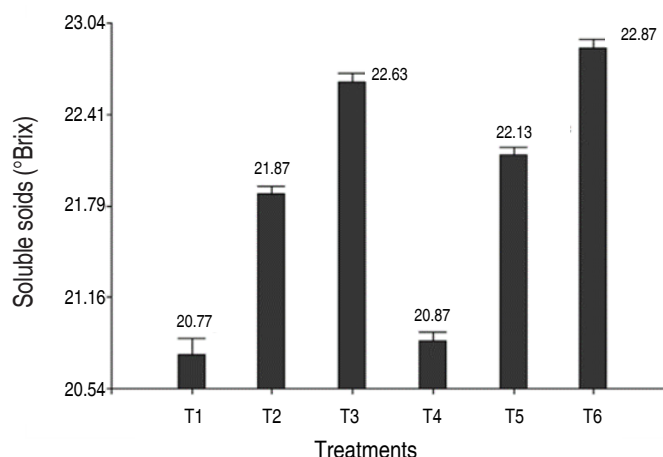


**Figure 3.** Effect of the Postharvest State of Chili in a Spicy Sauce with Pineapple Addition on Soluble Solids. T1: Fresh chili + 40% pineapple, T2: Fresh chili + 45% pineapple, T3: Fresh chili + 50% pineapple, T4: Dehydrated chili + 40% pineapple, T5: Dehydrated chili + 45% pineapple, and T6: Dehydrated chili + 50% pineapple.

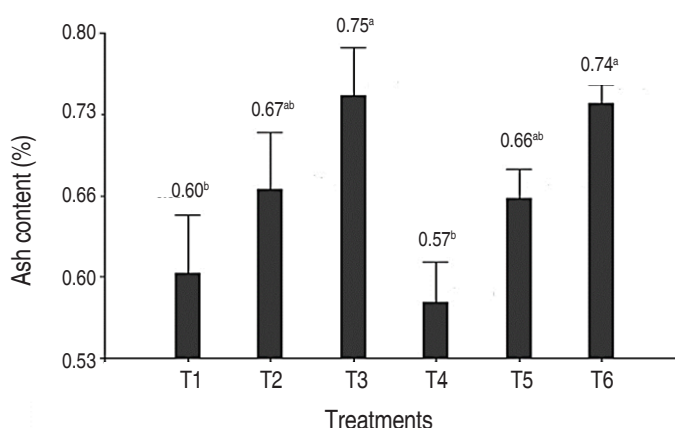


**Figure 4.** Effect of the Postharvest State of Chili in a Spicy Sauce with Pineapple Addition on Ash Content (%). T1: Fresh chili + 40% pineapple, T2: Fresh chili + 45% pineapple, T3: Fresh chili + 50% pineapple, T4: Dehydrated chili + 40% pineapple, T5: Dehydrated chili + 45% pineapple, and T6: Dehydrated chili + 50% pineapple.

The ash values obtained in this study were lower than those reported by Vélchez (2020), who recorded an average of 1.25% in sauces with pineapple pulp, indicating a lower mineral content in the evaluated formulations. More notably, Terry and Casusol (2018) found an ash content of 3.30%, significantly higher than the maximum of 0.75% obtained in this study, highlighting the variability in mineral composition depending on the ingredients and processes used.

#### Moisture content (%)

Regarding moisture content, statistical differences were observed between treatments ( $P < 0.05$ ). Treatment

T1 presented the highest value (78.42%), significantly differing from the treatments that included dehydrated chili. It was followed by T2 (77.68%) and T3 (77.15%), which showed no significant differences between them but differed from the treatments with lower moisture content. On the other hand, treatments T4 (75.35%), T5 (74.87%), and T6 (74.42%) recorded the lowest values, with T6 showing the lowest moisture content and significantly differing from the rest (Figure 5).

The moisture results in this study were lower than those reported by Terry and Casusol (2018), who recorded 90.4%, indicating that the formulation evaluated here has



a lower water content, likely due to the incorporation of ingredients with lower moisture levels. In contrast, another study reported a value of 73%, slightly lower than the lowest average obtained in this study (74.42%), though the difference is minimal.

### Viscosity (Cp)

Regarding viscosity (Cp), statistical differences were observed between treatments ( $P < 0.05$ ). Treatments T3 (5929.33 Cp) and T6 (5899.33 Cp) showed the highest values, with no significant differences between them,

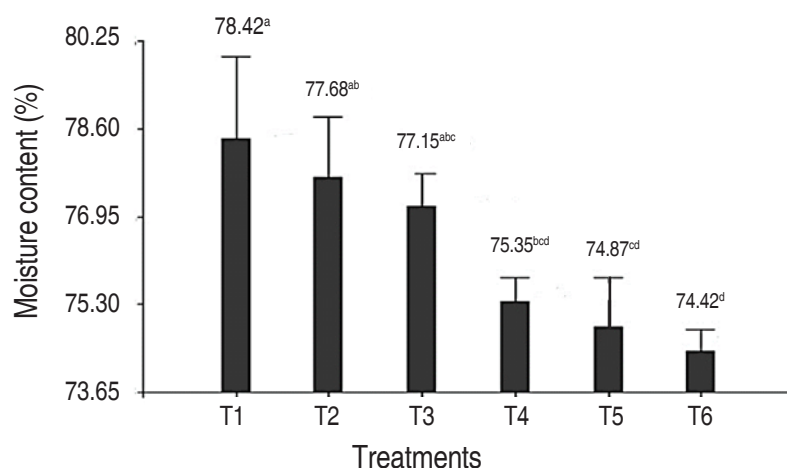


**Figure 5.** Effect of the postharvest state of chili in a spicy sauce with pineapple addition on moisture content (%). T1: Fresh chili + 40% pineapple, T2: Fresh chili + 45% pineapple, T3: Fresh chili + 50% pineapple, T4: Dehydrated chili + 40% pineapple, T5: Dehydrated chili + 45% pineapple, and T6: Dehydrated chili + 50% pineapple.

but differing from the other treatments. Meanwhile, treatments T2 (5286.00 Cp) and T5 (5277.67 Cp) presented intermediate values, with no significant differences between them, though they differed from the

treatments with lower viscosity. Finally, treatments T1 (4688.00 Cp) and T4 (4630.67 Cp) recorded the lowest values, with no significant differences between them (Figure 6).

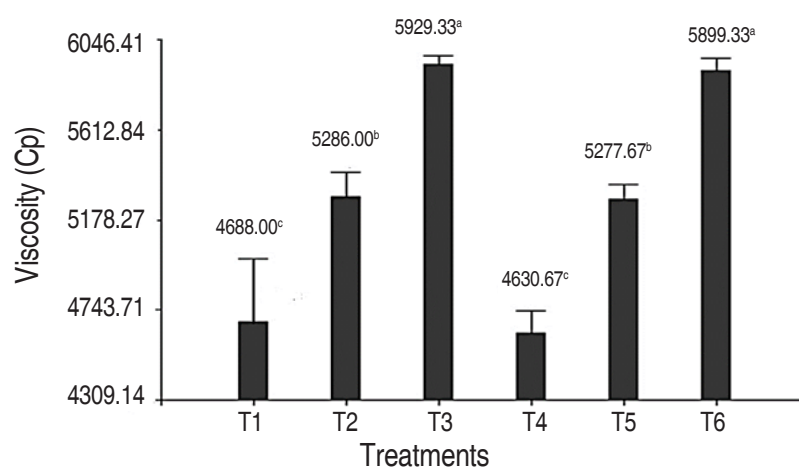


**Figure 6.** Effect of the postharvest state of chili in a spicy sauce with pineapple addition on viscosity (Cp). T1: Fresh chili + 40% pineapple, T2: Fresh chili + 45% pineapple, T3: Fresh chili + 50% pineapple, T4: Dehydrated chili + 40% pineapple, T5: Dehydrated chili + 45% pineapple, and T6: Dehydrated chili + 50% pineapple.

The viscosity results in this study indicate that the amount of pineapple significantly influences the texture of the sauce, as treatments with a higher pineapple content (T3 and T6) showed the highest viscosities. This aligns with the findings of Custodio and Fabian (2023), who reported an increase in viscosity when adding tamarind pulp, likely due to the presence of pectins and polysaccharides that form a denser and more cohesive structure in the mixture. According to Ganoza-Yupanqui et al. (2021), pectins act as gelling agents, which explains why a higher proportion of pineapple results in a thicker and less liquid sauce texture.

### Fat content (%)

Regarding fat content (%), statistical differences were observed between treatments ( $P < 0.05$ ). Treatment T3 (3.33%) presented the highest value. Treatments T2 (3.20%) and T6 (3.09%) showed intermediate values and did not present significant differences between them, although they differed from the others. Meanwhile, treatment T1 (2.80%) had a lower value than T2, T3, and T6 but was higher than T5 (2.61%) and T4 (2.40%). Notably, T4 recorded the lowest fat content and significantly differed from all other treatments (Figure 7).

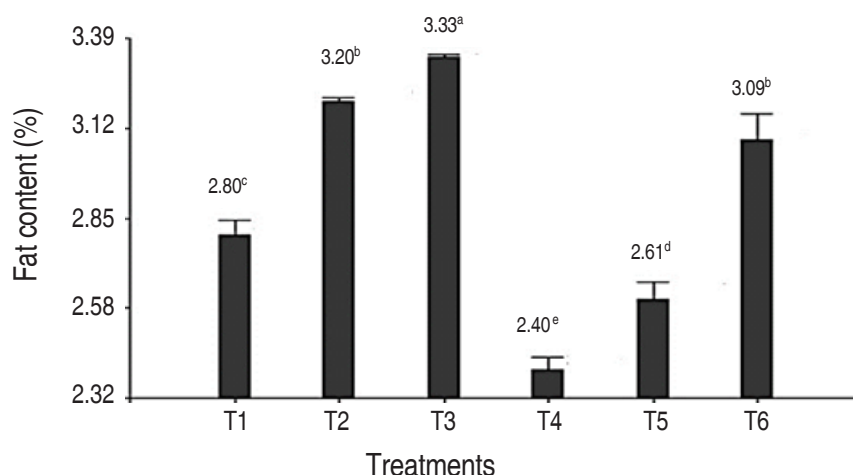


**Figure 7.** Effect of the postharvest state of chili in a spicy sauce with pineapple addition on fat content (%). T1: Fresh chili + 40% pineapple, T2: Fresh chili + 45% pineapple, T3: Fresh chili + 50% pineapple, T4: Dehydrated chili + 40% pineapple, T5: Dehydrated chili + 45% pineapple, and T6: Dehydrated chili + 50% pineapple.

The fat content results in this study align with the findings of Baldeón-Apaestegui and Hernández-Gorriti (2017), who explain that the dehydration process can reduce the fat percentage in chili composition.

### Sensory analysis

#### Color, aroma, flavor, and texture

Figure 8 shows that, in terms of color, treatment T4 stood out with the highest score (3.47), corresponding to a shade between “Tile” and “Butane.” T5 and T6 also exhibited high color values, associated with “Brick.” On the other hand, treatments with fresh chili, T1 (2.00), T2 (1.45), and T3 (1.20), showed lower shades, corresponding to “Intense Orange” and “Orange.”

Regarding aroma, T1 (2.20) and T4 (2.18) stood out with a “Sweet” scent, while T2 (1.53), T3 (1.33), and T6 (1.48) had

a “Fruity (ripe fruits)” aroma. T5 (1.77) was in an intermediate range, described as “Fruity” to “Sweet” (Figure 8). In terms of flavor, T4 led with a score of 2.65, described as “Garlic,” while the other treatments, including T1 (1.93), T2 (1.53), T3 (1.07), T5 (1.90), and T6 (1.83), remained within the “Chili” flavor range (Figure 8). For texture, T3 (3.10) and T2 (2.93) were preferred, categorized as “Neither viscous nor fluid,” while T4 received the lowest score (1.75), indicating a “Viscous” texture. T1 (2.32), T5 (2.07), and T6 (2.27) were described as “Very viscous” (Figure 8).

The results showed that the percentage of pineapple in the sauce directly influences the aroma, color, flavor, and texture perceived by the tasters. Regarding aroma, its increase was associated with a sweeter perception due to the presence of pineapple’s aromatic compounds, which mask the spicy aroma of chili (Contreras et al. 2015). In

terms of color, treatments with a higher pineapple content tended toward orange tones, explained by the natural

carotenoids in the fruit combined with chili pigments (Ulloa-Gómez et al. 2021).

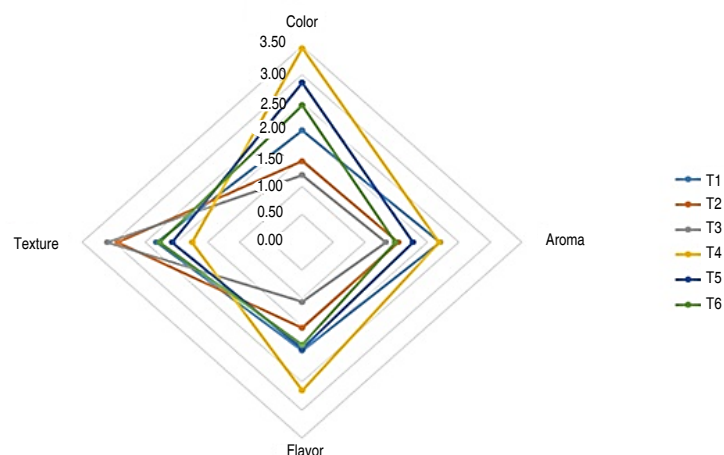


**Figure 8.** Sensory profile of each evaluated treatment. T1: Fresh chili + 40% pineapple, T2: Fresh chili + 45% pineapple, T3: Fresh chili + 50% pineapple, T4: Dehydrated chili + 40% pineapple, T5: Dehydrated chili + 45% pineapple, and T6: Dehydrated chili + 50% pineapple.

For flavor, pineapple contributed sweet and acidic notes that softened the intensity of the chili, a phenomenon also reported by Contreras et al. (2015). Regarding texture, a higher proportion of pineapple resulted in a denser perception, attributed to insoluble fiber that contributes to a firmer texture (Shiau et al. 2015). Finally, the type of chili used also influenced the sensory characteristics, as fresh chili was associated with a more intense flavor and a more viscous texture compared to dehydrated chili. This could be explained by the volatilization of compounds during dehydration and the loss of moisture, which reduces its ability to retain water in the sauce (Núñez et al. 2023).

### Spiciness threshold

Treatment T1 received the highest score for spiciness intensity, with a value of 3.90, categorized as “Spicy,” making it the sauce with the highest perceived heat. On the opposite end, treatment T6 had the lowest value, at 1.58, classified as “Mildly Spicy,” making it the least spicy sauce. The remaining treatments showed intermediate levels of spiciness, distributed as follows: T2 reached a value of 3.18 (“Moderately Spicy”); T3 obtained 2.88 (“Mildly Spicy”); T4 recorded 2.37 (“Mildly Spicy”); and T5 presented a value of 1.98 (“Mildly Spicy”) (Figure 9).

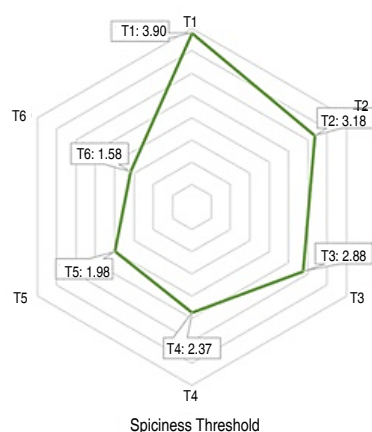


**Figure 9.** Spiciness threshold of each evaluated treatment. T1: Fresh chili + 40% pineapple, T2: Fresh chili + 45% pineapple, T3: Fresh chili + 50% pineapple, T4: Dehydrated chili + 40% pineapple, T5: Dehydrated chili + 45% pineapple, and T6: Dehydrated chili + 50% pineapple.

It was observed that a higher pineapple content in the sauce reduced the perception of spiciness, as its sweet and acidic compounds counteract the effect of capsaicin (Contreras et al. 2015). Additionally, dehydrated chili exhibited lower spiciness intensity compared to fresh chili, possibly due to the loss of volatile compounds during the dehydration process (Núñez et al. 2023).

### Acceptability

Treatment T4, composed of dehydrated chili and 40% pineapple, achieved the highest acceptance, with a preference of 8.00 panelists out of 20.00, reflecting a notable preference for this formulation. In contrast, the other treatments (T1, T2, T3, T5, and T6) recorded significantly lower acceptability levels.

### CONCLUSION

The formulation of hot sauces based on pineapple and different types of chili peppers, fresh and dried, showed that the combination of ingredients has a significant impact on the physicochemical and sensory properties of the product. In particular, formulation T4 (dehydrated chili + 40% pineapple) presented an optimum profile by reaching a pH of 4.18, soluble solids of 20.87 °Brix, and adequate levels of volatile acidity and fat content, parameters that flavor both the preservation and the sensory perception of the product. This same formulation obtained the highest score in the sensory tests, standing out in attributes such as color, aroma, and flavor, which positioned it as the most accepted by the panelists. These results confirm the technological and sensory feasibility of the T4 formulation, which stands out for its organoleptic balance and functional potential. In this context, it is recommended to develop complementary research focused on evaluating its shelf life, microbiological stability, and sensory behavior during storage, as well as its industrial feasibility for scaling and commercialization.

### ACKNOWLEDGMENTS

The authors thank the Universidad Técnica Estatal de Quevedo for providing access to its laboratories, infrastructure, and equipment, which made this research possible.

### CONFLICT OF INTERESTS

The authors declare no conflicts of interest.

### REFERENCES

- Abad Y and Pérez R (2024) Análisis de factibilidad de la exportación de piña desde Ecuador al mercado de Chile. *Revista Científica Mundo Recursivo* 7(2): 127–147. <https://atlantic.edu.ec/ojs/index.php/mundor/article/view/245/328>
- Baldeón-Apaestegui S and Hernández-Gorriti WR (2017) Identificación de la capsaicina y la deshidrocapsaicina en el extracto de oleoresina obtenido a partir del ají panca (*Capsicum chinense*). *Ingeniería Industrial* 35: 223–237. <https://doi.org/10.26439/ing.ind2017.n035.1803>
- Chong Delgado JS and Parra Valenzuela DF (2019) Propuesta para el desarrollo de una línea de salsas de ají artesanales en la ciudad de Guayaquil (Tesis de pregrado) Universidad de Guayaquil, Guayaquil, Ecuador. 88 p.
- Conforme G (2019) Efecto del tiempo de escaldado y fajilla termoformable sobre el pardeamiento de salsa picante del tomate de árbol (*Cyphomandra betacea* cav) (Tesis de posgrado) Escuela Superior Politécnica Agropecuaria de Manabí Manuel Félix López, Calcuta, Manabí, Ecuador. 49 p.
- Contreras EG, Acosta JM, Alvarado ZE, Jiménez ZJ, Obispo DM et al (2015) Nivel de preferencia de mermelada elaborada con rocoto (*Capsicum pubescens*) y piña (*Ananas comosus*). *Ciencia e Investigación* 18(2): 61–64. <https://doi.org/10.15381/ci.v18i2.13608>
- Custodio Comejo J del M and Fabian Zavaleta J (2023) Formulación y determinación del tiempo de vida útil de salsa picante con ají limo (*Capsicum Sinense* Jacq.) y puré de pallar (*Phaseolus lunatus* L.) (Tesis de pregrado), Universidad Nacional del Santa, Nuevo Chimbote, Perú. 284 p.
- Ganoza-Yupanqui ML, Muñoz-Acevedo A, Ybañez-Julca RO, Mantilla-Rodríguez E et al (2021) Potential antioxidant effect of fruit peels for human use from northern Peru, compared by 5 different methods. *Boletín Latinoamericano y Del Caribe de Plantas Medicinales y Aromáticas* 20(6): 611–637. <https://doi.org/10.37360/blacpma.21.20.6.44>
- Gonçalves MVS, Chandran D, Nelliaparambath L, Gokul AK and da Silva LE (2024) Chapter 13 – Applications of capsaicin in the food industry. pp 293–320. In: Swamy MK and Kumar A (eds.). *Capsaicinoids*. Springer Nature, Singapore. [https://doi.org/10.1007/978-981-99-7779-6\\_13](https://doi.org/10.1007/978-981-99-7779-6_13)
- Hameed A, Hayat A, Anwar MJ, Naz A and Khan MU (2022) Impact of different processing techniques on therapeutical potential and quality parameters of pepper. *International Journal of Food Science and Nutrition* 7(4): 151–158. <https://www.foodsciencejournal.com/archives/2022/vol7/issue4/7-4-83>
- Kammar-García A, Lazcano-Hernández M, López OV, Yañez-Bahena I et al (2022) Evaluación de las vías de deterioro de una salsa artesanal para su comercialización. *Revista Española de Nutrición Humana y Dietética* 26(4): 294–302. <https://doi.org/10.14306/renhyd.26.4.1713>
- Li X, Cheng X, Yang J, Wang X and Lü X (2022) Unraveling the difference in physicochemical properties, sensory, and volatile profiles of dry chili sauce and traditional fresh dry chili sauce fermented by *Lactobacillus plantarum* PC8 using electronic nose and HS-SPME-GC-MS. *Food Bioscience* 50: 102057. <https://doi.org/10.1016/j.fbio.2022.102057>
- Marikos C (2024) A history of sriracha: A global hot sauce made in America. *Arizona Journal of Interdisciplinary Studies* 10(1): 1–6.

Núñez D, Agualongo Sinchipa S, Callan Chela C and Gaibor Chávez J (2023) Deshidratación de diferentes variedades de ají para la obtención de polvo. *Bionatura* 8(4): 1–9.

Oña González PA (2022) Evaluación de una propuesta para la elaboración de una salsa fermentada picante tipo aderezo aplicando culantro de pozo (*Eryngium foetidum*) como potenciador de sabor (Tesis de pregrado) Universidad Agraria del Ecuador, Guayaquil, Ecuador. 49 p. <https://cia.uagraria.edu.ec/Archivos/O%C3%91A%20GONZ%C3%81LEZ%20PAUL%20ANDR%C3%89S.pdf>

Ortega Ibarra E, Hernández Ramírez G and Ortega Ibarra IH (2021) Composición nutricional y compuestos fitoquímicos de la piña (*Ananas comosus*) y su potencial emergente para el desarrollo de alimentos funcionales. *Boletín de Ciencias Agropecuarias Del ICAP* 7(14): 24–28. <https://doi.org/10.29057/icap.v7i14.7232>

Pazos Barrera J (2021) Elogio de las cocinas tradicionales del Ecuador 1ra ed). Pontificia Universidad Católica del Ecuador.

Rezazadeh A, Hamishehkar H, Ehsani A, Ghasempour Z and Moghaddas Kia E (2021) Applications of capsaicin in food industry: functionality, utilization and stabilization. *Critical Reviews in Food Science and Nutrition* 63(19): 4009–4025. <https://doi.org/10.1080/10408398.2021.1997904>

Santos DI, Martins CF, Amaral RA, Brito L, Saraiva JA et al (2021) Pineapple (*Ananas comosus* L.) by-products valorization: Novel bio ingredients for functional foods. *Molecules* 26(11): 3216. <https://doi.org/10.3390/molecules26113216>

Shiau, SY, Wu MY and Liu YL (2015) The effect of pineapple core

fiber on dough rheology and the quality of mantou. *Journal of Food and Drug Analysis* 23(3): 493–500. <https://doi.org/10.1016/j.jfda.2014.10.010>

Sunarmani, Agustinisari I and Setyadjit (2024) A study of the organoleptic and chemical characteristics of spiced shredded chili. *IOP Conference Series: Earth and Environmental Science* 1364(1): 012079.

Terry Calderón VM and Casusol Perea K (2018) Formulación de una salsa picante a base de pulpa de cocona (*Solanum sessiliflorum*), ají amarillo (*Capsicum baccatum*) y ají Charapita (*Capsicum chinense*). *Revista de Investigaciones de La Universidad Le Cordon Bleu* 5(1): 5–17. <https://doi.org/10.36955/RIULCB.2018v5n1.001>

Trujillo Orellana JE (2021) Evaluación de la capacidad antioxidante de extractos de la cáscara de piña (*Ananas comosus*), frente a un producto comercial (Tesis de pregrado), Universidad Politécnica Salesiana, Cuenca, Ecuador, 62 p.

Ulloa-Gómez L, Sáenz-Murillo MV, Castro-Chinchilla J and Ramírez-Sánchez M (2021) Temperaturas de acondicionamiento, poscosecha sobre el desarrollo de color de la epidermis y calidad interna de frutos de piña. *Agronomía Costarricense* 45(1): 103–114. <https://revistas.ucr.ac.cr/index.php/agrocost/article/view/45710/45728>

Vílchez Guadalupe ZY (2020) Comportamiento reológico de salsa picante de ají Charapita (*Capsicum frutescens*) con pulpa de piña (*Ananas comosus*), utilizando goma xantana (Tesis de pregrado), Universidad Nacional del Centro del Perú, Tarma, Perú. 128 p.

Yin M, Heng S, Rem S and Chin L (2021) Development of spicy sweet chili sauce. *Techno-Science Research Journal* 9(1): 48–54.



# Genetic variants of caseins and $\beta$ -lactoglobulin in Lucerna cattle and their association with milk quality

Variantes genéticas de caseínas y  $\beta$ -lactoglobulina en el ganado Lucerna y su asociación con la calidad de la leche

<https://doi.org/10.15446/rfnam.v78n3.114735>

Darwin Yovanny Hernández-Herrera<sup>1\*</sup>, Luis Gabriel González-Herrera<sup>2</sup> and Juan Carlos Rincón-Flórez<sup>1</sup>

## ABSTRACT

### Keywords:

Creole cattle  
Genetic linkage  
Haplotype frequencies  
Milk proteins



This study aimed to evaluate the variation in the genes *CSN1S1*, *CSN2*, *CSN1S2*, *CSN3* and *LGB* in the Lucerna breed (LUC). For this purpose, 94 LUC animals and 10 Hartón del Valle (HDV) animals were genotyped using the GGP™ Bovine 150 K chip, which contains four single-nucleotide polymorphisms (SNPs) in the *CSN1S1* gene, 14 in the *CSN2* gene, two in the *CSN1S2* gene, 12 in the *CSN3* gene and 11 in the *LGB* gene. Haplotypes and protein variants of  $\alpha_{s1}$ -CN,  $\beta$ -CN,  $\alpha_{s2}$ -CN,  $\kappa$ -CN and  $\beta$ -LG were reconstructed. Genotypic frequencies of the major variants were compared between sexes and generations. Hardy-Weinberg equilibrium,  $wF_{ST}$  and  $F_{IS}$  values were assessed for each of the SNPs. LD values and haplotype frequencies for the caseins were estimated and plotted. The *CSN1S1*\*B, *CSN2*\*A<sup>2</sup>, *CSN1S2*\*A, *CSN3*\*A and *LGB*\*B variants were the most frequent in both breeds. Genotype frequencies did not vary between sexes, and only the *CSN2*\*A<sup>2</sup>A<sup>2</sup> genotype varied between generations. Hardy-Weinberg equilibrium was maintained for all markers, except for one SNP in the *LGB* gene. The  $wF_{ST}$  values obtained were very low according to sex ( $wF_{ST}$ =0.0043) and generation ( $wF_{ST}$ =0.026). The  $F_{IT}$  value was -0.0086. Nineteen *CSN1S1*-*CSN2*-*CSN1S2*-*CSN3* haplotypes were found in LUC and eight in HDV with different frequencies. The genetic linkage between the casein genes was low. In conclusion, the genes studied are polymorphic, with a high frequency of variants related to milk production, quality and technological performance. These results can be used in assisted selection programs aimed at improving milk quality and processing traits.


## RESUMEN

### Palabras clave:

Ganado criollo  
Ligamiento genético  
Frecuencias haplotípicas  
Proteínas de la leche

El objetivo de esta investigación fue evaluar la variación en los genes *CSN1S1*, *CSN2*, *CSN1S2*, *CSN3* y *BLG* en la raza Lucerna (LUC). Para ello, 94 animales LUC y 10 animales Hartón del Valle (HDV) fueron genotipados usando el chip GGP™ Bovine 150 K, que tiene cuatro SNPs en el gen *CSN1S1*, 14 en el gen *CSN2*, dos en el gen *CSN1S2*, 12 en el gen *CSN3* y 11 en el gen *LGB*. A partir de los cuales fueron reconstruidos los haplotipos y variantes proteínicas de la  $\alpha_{s1}$ -CN,  $\beta$ -CN,  $\alpha_{s2}$ -CN,  $\kappa$ -CN y  $\beta$ -LG. Se compararon las frecuencias genotípicas de las variantes más importantes entre sexos y generaciones. Se evaluó el equilibrio de Hardy-Weinberg y los valores de  $wF_{ST}$  y  $F_{IS}$  para cada uno de los SNPs. Se estimaron y graficaron los valores de LD y las frecuencias haplotípicas para las caseínas. Las variantes *CSN1S1*\*B, *CSN2*\*A<sup>2</sup>, *CSN1S2*\*A, *CSN3*\*A y *BLG*\*B fueron las más frecuentes en ambas razas. Las frecuencias genotípicas no variaron entre sexos, y solo el genotipo *CSN2*\*A<sup>2</sup>A<sup>2</sup> varió entre generaciones. Todos los marcadores mostraron equilibrio de Hardy-Weinberg, excepto un SNP en el gen BLG. Los valores de  $wF_{ST}$  obtenidos fueron muy bajos por el sexo ( $wF_{ST}$ =0,0043) y generación ( $wF_{ST}$ =0,026). Mientras que, el valor de  $F_{IT}$  fue de -0,0086. Se encontraron 19 haplotipos *CSN1S1*-*CSN2*-*CSN1S2*-*CSN3* en LUC y ocho en HDV con frecuencias diferentes. El ligamiento genético fue bajo entre los genes de las caseínas. En conclusión, los genes evaluados son polimórficos y con alta frecuencia de las variantes relacionadas con mayor producción mejor calidad y rendimiento tecnológico de la leche. Estos resultados pueden ser utilizados en programas de selección asistida destinados a mejorar la calidad de la leche y los rasgos de procesado.

<sup>1</sup>Grupo de Investigación en Recursos Zoogenéticos, Facultad de Ciencias Agropecuarias, Universidad Nacional de Colombia Sede Palmira, Colombia. [dyhernandezh@unal.edu.co](mailto:dyhernandezh@unal.edu.co) , [jrcincon@unal.edu.co](mailto:jrcincon@unal.edu.co) 

<sup>2</sup>Grupo de investigación BIOGEM, Facultad de Ciencias Agrarias, Universidad Nacional de Colombia, Sede Medellín, Colombia. [luggonzalezhe@unal.edu.co](mailto:luggonzalezhe@unal.edu.co) 

\*Corresponding author:

The Lucerna cattle (LUC) is one of the two Colombian synthetic breeds, created in 1937 by crossbreeding the Hartón del Valle, Holstein and dairy Shorthorn breeds in proportions of 30, 30 and 40%, respectively (Giraldo et al. 2023). The creation of the breed was driven by the need for cattle to adapt to tropical environmental conditions, where hardiness, grazing ability, fertility, and longevity are essential (Molina et al. 2016). The LUC breed has an adult weight of 750-800 kg for males and 450-500 kg for females (Molina et al. 2016). Adjusted milk production at 305 days is reported to be  $2,425 \pm 0.514$  kg. This corresponds to an average of 0.15 kg per kg of cow per day of protein, 0.22 kg per cow per day of fat, and 0.59 kg per cow per day of total solids. Age at first calving and first calving interval averaged  $41.84 \pm 5.01$  months and  $12.84 \pm 1.65$  months, respectively. It has a low incidence of mastitis and a low somatic cell count (Rivera et al. 2019). In addition, studies show that it is minimally affected by ectoparasites, with  $7.1 \pm 1.06$  ticks per animal, and it maintains a low proviral load of bovine leukosis virus (Hernández-Herrera and Carrillo-González 2024). Currently, the breed is reported as not at risk according to the DAD-IS, and although its merits as a breed are clear, its use is not yet widespread in Colombia.

Milk is considered a high-value food from a nutritional perspective. Its composition varies within species due to environmental factors such as feed type, climate, lactation stage and milking interval, while breed and genetic composition are also determinants (Chessa et al. 2020). Essentially, the levels of  $\alpha_{s1}$ -CN,  $\beta$ -CN,  $\alpha_{s2}$ -CN and  $\kappa$ -CN kcaseins and the properties of the micelles they form influence the nutritional quality and technological performance of milk (Kay et al. 2021). These proteins are encoded by four genes (*CSN1S1*, *CSN2*, *CSN1S2* and *CSN3*) located in tandem on chromosome 6 between positions 85.4 and 85.7 Mb (ARS-UCD1.2 genome assembly). Variants in the *CSN1S1* gene are associated with an increase in casein and whey protein (Mohan et al. 2021); some alleles of the *CSN1S2* gene are associated with increased milk production (Ardicli et al. 2018); the \*A2 variant of the *CSN2* gene is associated with high yield and quality, as well as with a healthier product, since its digestion does not release the bioactive peptide  $\beta$ -casomorphin-7,

which is considered a risk factor for endocrine, nervous, and cardiovascular diseases (Kay et al. 2021); finally, the structural stability of micelles, and thus cheese quality, has been associated with variants in the *CSN3* gene (Poulsen et al. 2017; Zepeda-Batista et al. 2017). As for whey proteins, the *LAA* gene, which codes for  $\alpha$ -Lactalbumin ( $\alpha$ -LA) protein, is located on chromosome 5 at position 31.2 Mb.  $\beta$ -lactoglobulin ( $\beta$ -LG) is encoded by the *LGB* gene and is located on chromosome 11 at position 103.2 Mb (Sanchez et al. 2020).

In general, the genetic variation in these genes responds to changes in whey protein, shortening curdling time and thus affecting cheese yield (Čitek et al. 2023; Dantas et al. 2023; Kay et al. 2021). The genetic variation at these *loci* has been extensively studied in several dairy breeds worldwide (Sanchez et al. 2020; Chessa et al. 2020; Villalobos-Cortés et al. 2023), including the Colombian Holstein breed (Padilla-Doval et al. 2021) and the Colombian Creole breeds for the *CSN3*, *LAA* and *LGB* genes (Rosero et al. 2012; Hernández-Herrera et al. 2024). However, the genetic variations responsible for milk production and quality in the LUC breed have not yet been thoroughly studied. The new market for "A2 milk" has created a need for certification of production systems specializing in this type of milk, as well as the initiation of genetic selection programs based on molecular markers. This research was therefore carried out with the aim of determining the genetic variation in the genes *CSN1S1*, *CSN2*, *CSN1S2*, *CSN3* and *LGB* in the LUC breed and its linkage map, as an input to be used in the development of breeding programs.

## MATERIALS AND METHODS

The Reserva Natural El Hatíco provided 94 adult animals (20 males and 74 females) used in this study. Inclusion criteria were the lowest degree of relationships and clinical health. El Hatíco is located in the municipality of El Cerrito, (Valle del Cauca, Colombia). At an altitude of 1,000 meters above sea level (masl), with a mean annual temperature of 24 °C, 75% humidity and 750 mm of annual rainfall, corresponding to a tropical dry forest (bs-T), according to the Holdridge classification system (Molina et al. 2016). In addition, 10 animals of the Hartón del Valle (HDV) breed from the Agricultural Laboratory of

the Mario González Aranda farm belonging to Universidad Nacional de Colombia, Palmira Headquarters, were used as a reference population.

### DNA extraction

BD Vacutainer® tubes containing 7.2 mg EDTA were used to collect 3 mL of whole blood from the Coccygeal vein. Samples were transported to the Animal Genetics Laboratory of the Universidad Nacional de Colombia - Palmira for processing. Total DNA was extracted using the HigherPurity™ DNA Extraction and Purification Kit (Canvax®). The qualitative assessment of the DNA sample was conducted via electrophoresis on 0.8% agarose gels loaded with 6X BX/Loading Buffer (Canvax®), followed by staining employing GreenSafe DNA Gel Stain (Canvax®). To perform the quantitative analysis of the DNA, the Colibri spectrophotometer (Titertek Berthold Technologies GmbH & Co. KG) was utilized. DNA samples were dehydrated by sublimation in 1.5 mL conical tubes in a FreeZone freeze dryer. (Console FreeZone™ kit, Labconco™, Kansas City, MO, USA). Subsequently, the samples were dispatched to Neogen Genomics (<https://genomics.neogen.com/en>) for genotyping.

### Genotyping

Animals were genotyped using the GeneSeek® Genomic Profiler™ Bovine 150K chip (140,668 SNPs). This particular genotyping array contains more than 200 single-nucleotide polymorphisms in major genes that have been associated with genetic diseases. In relation to the milk protein genes, it has been determined that there are four SNPs in the *CSN1S1* gene, 14 in the *CSN2* gene, two in the *CSN1S2* gene, 12 in the *CSN3* gene and 11 in the *LGB* gene (Hernández-Herrera et al. 2024). The genetic variants in question manifest in a triplicate pattern across the chip, thereby facilitating the process of genotyping.

From the SNPs in each gene, it is possible to reconstruct the variants *\*B*, *\*C* and *\*D* of the  $\alpha_{S1}$ -CN protein; of the  $\beta$ -CN, the variants *\*A<sup>1</sup>*, *\*A<sup>2</sup>*, *\*B*, *\*H<sup>2</sup>* and *\*F*; the two SNPs in the *CSN1S2* gene allow to identify the variants *\*A* and *\*D* of the  $\alpha_{S2}$ -CN; in the  $\kappa$ -CN gene the variants *\*A*, *\*A<sup>1</sup>*, *\*B*, *\*I* and *\*H* can be distinguished, while in the *LGB* gene

the 11 genetic polymorphisms allow the reconstruction of the variants *\*A*, *\*B*, *\*C*, *\*D*, *\*E*, *\*F* and *\*H* of  $\beta$ -LG (Caroli et al. 2009; Sanchez et al. 2020; Hernández-Herrera et al. 2024).

### Analysis of data

The allele frequencies of the 43 SNPs were estimated. From these, protein variants were reconstructed (Chessa et al. 2020) for all genes in the LUC and HDV breeds. Using a GLM model with Poisson family, the interaction between the main genotypes (*\*BB*, *\*BC* and *\*CC* for the *CSN1S1* gene; *\*A<sup>1</sup>A<sup>1</sup>*, *\*A<sup>1</sup>A<sup>2</sup>* and *\*A<sup>2</sup>A<sup>2</sup>* for the *CSN2* gene; *\*AA*, *\*AD* and *\*DD* for the *CSN1S2* gene; *\*AA*, *\*AB* and *\*BB* for the *CSN3* gene and *\*AA*, *\*AB* and *\*BB* for the *LGB* gene) of each gene, sex and generation (generation 1: cattle born before 2010; generation 2: animals born between 2010 and 2015; generation 3: individuals born between 2016 and 2021) for the Lucerne breed only was explored, using R base (<http://www.r-project.org/>).

Deviations from Hardy-Weinberg equilibrium (HWE) and *wFST* values were quantified for each of the SNPs evaluated, using sex and generation as population structuring factors for casein. SNPs were pruned using sliding windows and a criterion  $r^2=0.2$ , and the LD value between them was estimated and plotted using the LD and LD plot functions, respectively, from the Gaston package see 1.5.9 (Dandine-Roulland and Perdry 2018) of R. Finally, the genotypes observed for each individual were combined, and the haplotypic frequencies of casein genotypes (*CSN1S1-CSN2-CSN1S2-CSN3*) were estimated by direct counting using R base (Chessa et al. 2020). These variants appear in triplicate within the chip, which ensures the genotyping process.

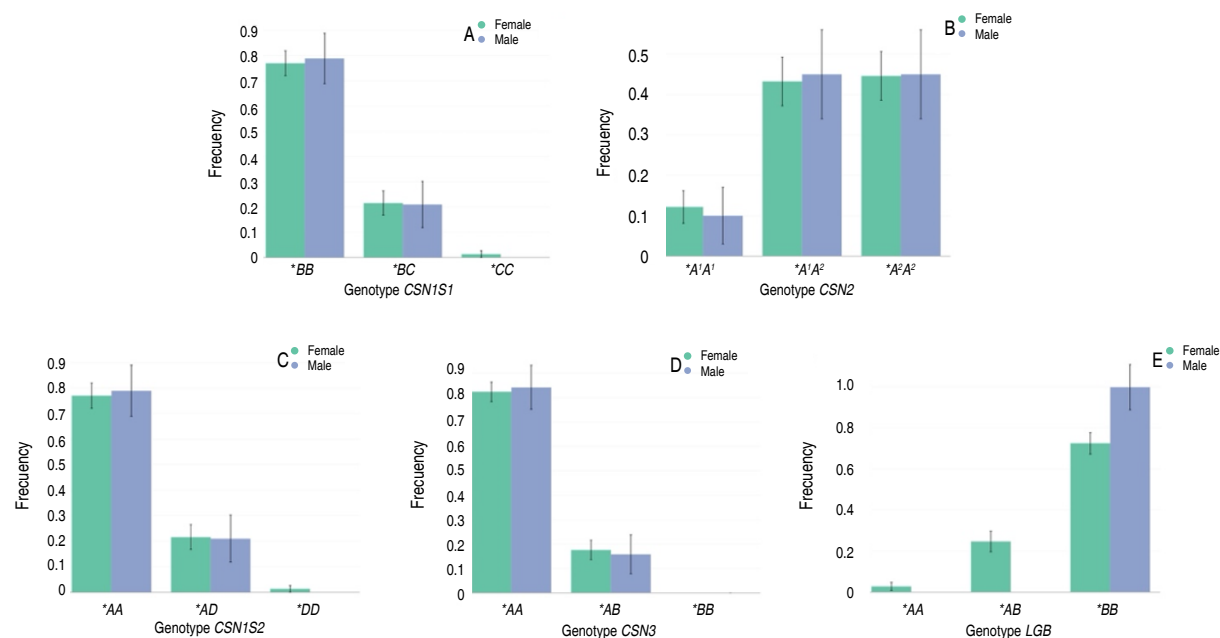
## RESULTS AND DISCUSSION

Of the four polymorphisms present in the *CSN1S1* gene, the SNPs rs433385179 and rs132656458 were monomorphic. This meant that only the *CSN1S1\*B* and *\*C* alleles were found in both breeds, with the former being the most common (Table 1). All SNPs were in HWE. Genotypic frequencies did not differ significantly between sexes (Figure 1A) or generations (Figure 2A).

**Table 1.** Allele frequencies of SNPs located in the *CSN1S1* gene and allele and genotypic frequencies of protein variants in the  $\alpha_{S1}$ -CN in the breeds studied.

SNP / Frequency	<i>CSN1S1</i> variant							
	*B				*C			
	LUC		HDV		LUC		HDV	
<i>CSN1S1_1</i>	-	-	-	-	-	-	-	-
Ala68Thr - 6:85418630	-	-	-	-	-	-	-	-
rs433385179	-	-	-	-	-	-	-	-
<i>CSN1S1_2</i>	T	A	T	A	-	-	-	-
Val91Asp - 6: 85420971	1.000	0.000	1.000	0.000	-	-	-	-
rs132656458	-	-	-	-	-	-	-	-
<i>CSN1S1_3</i>	G	A	G	A	-	-	-	-
31G>A - 6: 85428068	0.946	0.054	0.750	0.250	-	-	-	-
rs133474041	-	-	-	-	-	-	-	-
<i>alphaS1Casein26181</i>	-	-	-	-	A	G	A	G
Glu207Gly - 6:85427427	-	-	-	-	0.883	0.117	0.650	0.350
rs43703010	-	-	-	-	-	-	-	-
Allele frequency of the variant	0.882		0.650		0.118		0.350	
Genotypic frequency	LUC: BB=0.774 BC= 0.215 CC= 0.011				HDV: BB=0.400 BC= 0.500 CC= 0.101			

SNP: Single-nucleotide polymorphism, LUC: Lucerna breed, HDV: Hartón del Valle breed, A (Adenine), C (Cytokine), G (Guanine), and T (Thymine) represent allele frequencies found in each SPNs.

**Figure 1.** Genotypic frequencies of *CSN1S1* (A), *CSN2* (B), *CSN1S2* (C), *CSN3* (D), and *LGB* (E) genes by sex in the Lucerna breed.

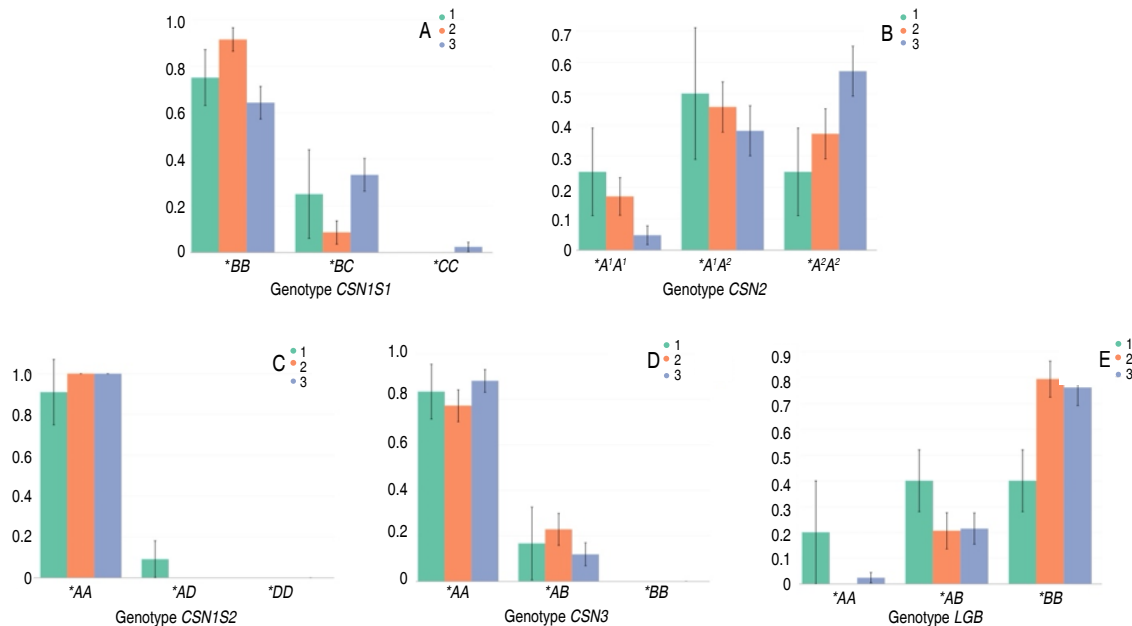


**Figure 2.** Genotypic frequencies of *CSN1S1* (A), *CSN2* (B), *CSN1S2* (C), *CSN3* (D), and *LGB* (E) genes by generation (generation 1: cattle born before 2010; generation 2: animals born between 2010 and 2015; generation 3: individuals born between 2016 and 2021) in the Lucerna breed.

Ten variants (\*A, \*B, \*C, \*D, \*E, \*F, \*G, \*H, \*I and \*J) are recognized in the  $\alpha_{s1}$ -CN protein (Meier et al. 2019), from which only three (\*B, \*C and \*D) can be reconstructed with the SNPs present in the GeneSeek® Genomic Profiler™ Bovine 150 K chip, despite the highly polymorphic nature of the gene (Ahmed et al. 2017), but this is explained by the breeds used to develop the chip. The *CSN1S1*\*B allele is reported to be the most frequent in several *Bos taurus* breeds, including Angler (1.0), Eringer (0.77), German Red Pied (0.93), German Yellow (1.0), Highland Cattle (1.0), Hinterwälder (0.93), Hungarian Grey Steppe (0.73), Jersey (0.68), Limpurger (1.0), Pinzgauer (0.74), Sarabi (0.54), Shorthorn (1.0) and Vorderwälder (0.87) (Gallinat et al. 2013). In the Holstein breed, the frequency of this allele is reported to be higher than 0.95 (Ardicli et al. 2018; Meier et al. 2019) and in the Simmental breed, 0.90 (Čítek et al. 2023). In the Colombian creole breed Blanco Orejinegro (BON), the frequency of the \*B allele reached 0.80 (Hernández-Herrera et al. 2024). On the other hand, in *Bos indicus* breeds, the *CSN1S1*\*C allele is the most common (Butana=0.66, Gir=0.50, Golpayegani=0.48, and Sistani=0.88) (Gallinat et al. 2013).

In the LUC breed, the \*BB genotype was the most common (0.774). In contrast, the \*BC genotype was the most frequent in the HDV breed (0.500) (Table 1). It has been reported that animals with the homozygous \*BB genotype have higher milk production and better milk quality, as it contains higher percentages of fat and protein (Ardicli et al. 2018; Mohan et al. 2021; Čítek et al. 2023).

Of the 14 SNPs evaluated in the *CSN2* gene, 11 were fixed in the LUC breed and 13 in the HDV breed. This meant the presence of \*A<sup>1</sup>, \*A<sup>2</sup>, \*B, and \*F variants of the  $\beta$ -CN protein in the LUC breed and only \*A<sup>1</sup> and \*A<sup>2</sup> variants in the HDV breed (Table 2) 15 variants (\*A<sup>1</sup>, \*A<sup>2</sup>, \*A<sup>3</sup>, \*B, \*C, \*D, \*E, \*F, \*G, \*H<sup>1</sup>, \*H<sup>2</sup>, \*I, \*J, \*K, and \*L) have been reported for this protein (Meier et al. 2019). The frequency of the reference allele for this gene (*CSN2*\*A<sup>1</sup>) was low, highlighting the high frequency of the *CSN2*\*A<sup>2</sup> variant in both breeds. This is in agreement with that reported for the breeds Eringer (0.54), German Yellow (0.52), Highland Cattle (0.81), Hinterwälder (0.79), Hungarian Grey Steppe (0.67), Jersey (0.63), Limpurger (0.77), Pinzgauer (0.65), Sarabi (0.65), Hinterwälder (0.79), Hungarian Grey Steppe (0.63), Limpurger (0.77), Pinzgauer (0.65), Sarabi (0.75)



and Shorthorn (0.57) (Gallinat et al. 2013), Holstein (0.55) and Jersey (0.73) (Chessa et al. 2020), Karan Fries (0.60) (Mohan et al. 2021) and in the BON breed (0.51) (Hernández-Herrera et al. 2024). However, this variant is more common in *B. indicus* breeds (Ahmed et al. 2017; Gallinat et al. 2013). The *CSN2*<sup>\*I</sup> allele has been reported at low frequency in the Black Pied (0.017) and Holstein (0.059) breeds from Germany (Meier et al. 2019), and, as reported in this study, the <sup>\*B</sup> and <sup>\*F</sup> alleles were found at low frequency in the BON breed (Hernández-Herrera et al. 2024). On the other hand, Padilla-Doval et al. (2021), who studied the Holstein breed in Colombia, reported that the <sup>\*B</sup> allele was the most common.

All SNPs analysed in the *CSN2* gene were in HWE. No differences in genotypic frequencies were found between the sexes (Figure 1B), but differences were found for the <sup>\*A</sup><sup>2</sup><sup>A</sup><sup>2</sup> genotype in the third generation ( $P < 0.05$ ), which

shows an increase in frequency with each generation (Figure 2B). The same trend of increase has been reported in the BON breed (Hernández-Herrera et al. 2024). The importance of the high frequency of this variant ( $\beta$ -*CN*<sup>\*A</sup><sup>2</sup>) is understood when it is considered that the intestinal digestion of milk protein releases the bioactive peptide  $\beta$ -casomorphin-7 in animals with the  $\beta$ -*CN*<sup>\*A</sup><sup>1</sup> genotype. This peptide has been implicated in the development of several diseases (Chessa et al. 2020; Villalobos-Cortés et al. 2023) and in the increase of both milk allergy and lactose intolerance (Muntean et al. 2022). In contrast, antithrombotic, antihypertensive, immunomodulatory, anticancer, and antimicrobial activities are recognized, as well as bioactive peptides resulting from protein digestion of the  $\beta$ -*CN*<sup>\*A</sup><sup>2</sup>, <sup>\*A</sup><sup>3</sup>, <sup>\*D</sup>, <sup>\*E</sup>, <sup>\*H</sup><sup>2</sup>, and <sup>\*I</sup> variants (Muntean et al. 2022). All of these variants have proline at position 67 of the protein instead of histidine (Caroli et al. 2009), producing what are known as A2-type milks.

**Table 2.** Allele frequencies of SNPs located in the *CSN2* gene and allele and genotypic frequencies of protein variants in the  $\beta$ -*CN* in the breeds studied.

SNP / frequency	CSN2 variant											
	*A¹				*A²		*B		*F		*H²	
	LUC		HDV		LUC	HDV	LUC	HDV	LUC	HDV	LUC	HDV
BCN_8491 Val247Ala - 6:85450908 rs715383373	T	C	T	C								
	1.000	0.000	1.000	0.000								
BCN_8463 6:85450976	C	T	C	T								
	1.000	0.000	1.000	0.000								
CSN2_2 His198Pro - 6:85451055 rs454083280	T	G	T	G								
	1.000	0.000	1.000	0.000								
CSN2_ X14711_8219 His156Gln - 6:85451180 rs43703012	C	A	C	A								
	1.000	0.000	1.000	0.000								
CSN2_5 Met93Leu - 6:85451236	G	T	G	T								
	1.000	0.000	1.000	0.000								
CSN2_6 Leu88Ile - 6:85451248	C	A	C	A								
	1.000	0.000	1.000	0.000								
CSN2_ X14711_8115 Gln72Glu - 6:85451284	C	G	C	G								
	1.000	0.000	1.000	0.000								
CSN2_8 Glu87Lys - 6:85452710 rs721259074	C	T	C	T								
	1.000	0.000	1.000	0.000								

Table 2

SNP / frequency	CSN2 variant									
	*A <sup>1</sup>		*A <sup>2</sup>		*B		*F		*H <sup>2</sup>	
	LUC	HDV	LUC	HDV	LUC	HDV	LUC	HDV	LUC	HDV
CSN2_	G	A	G	A						
X14711_6687										
Glu86Lys -										
6:85452713	1.000	0.000	1.000	0.000						
rs3423226649										
CSN2_	C	T	C	T						
X14711_6562										
Arg75Cys -										
6:85452837	1.000	0.000	1.000	0.000						
rs799602970										
CSN2_7			A	C	A	C				
His117Pro -										
6:85451298			0.335	0.665	0.300	0.700				
rs43703011										
CSN2_3					C	G	C	G		
Arg172Ser -										
6:85451132					0.979	0.021	1.000	0.000		
rs43703013										
CSN2_1							G	A	G	A
Pro202Leu -										
6:85451043							0.995	0.005	1.000	0.000
rs433954503										
CSN2_4									A	C
Met143Leu -										
6:85451221									1.000	0.000
rs109299401										
Allele frequency of the variant	0.314	0.300	0.665	0.700	0.016	0.000	0.005	0.000	0.000	0.000
Genotypic frequency	LUC: A <sup>1</sup> A <sup>1</sup> = 0.085 A <sup>1</sup> A <sup>2</sup> = 0.436 A <sup>1</sup> B=0.021 A <sup>2</sup> A <sup>2</sup> = 0.447 BF=0.011									
	HDV: A <sup>1</sup> A <sup>2</sup> = 0.600 A <sup>2</sup> A <sup>2</sup> = 0.400									

SNP: single-nucleotide polymorphism. LUC: Lucerna breed. HDV: Hartón del Valle breed. A (Adenine), C (Cytokine), G (Guanine), and T (Thymine) represent allele frequencies found in each SPNs.

There are at least 23 different brands of A2-type milk in markets around the world (Dantas et al. 2023). In Italy, for example, there has been selection for this allele since 1990, with a 10% increase by 2017 (Chessa et al. 2020). This research shows a significant increase in the  $A^2A^2$  genotype between generations 1 ( $\beta$ -CN $A^2A^2$ =0.25) and 3 ( $\beta$ -CN $A^2A^2$ =0.58). It is important to emphasize two points: first, the high frequency of this genotype in the LUC breed is likely due to its origin in the HDV breed; and second, there is no direct selection for this genotype in the herd under study. In addition, A2-type milk is not currently marketed in Colombia. Therefore, the increase in this genotype is likely due to the associated effects of this genotype, such as an increase in milk production, higher fat and protein

content, and better yield in curd production (Mohan et al. 2021). Demand for this type of product may increase in the country as consumer awareness of functional foods increases (Dantas et al. 2023).

Five variants are known in the  $\alpha_{s2}$ -CN protein, including  $A$ ,  $B$ ,  $C$ ,  $D$ , and  $E$  (Meier et al. 2019). However, the genotyping chip only has two SNPs (rs441966828 and rs463985801) in the *CSN1S2* gene that allow analysis of the  $A$  and  $D$  variants. In the HDV breed, the SNPs were monomorphic and only the SNP *CSN1S2\_2* varied in LUC (Table 3); therefore, the reference variant *CSN1S2* $A$  and the  $AA$  genotype were fixed in HDV and with a very high frequency in LUC.

**Table 3.** Allele frequencies of SNPs located in the *CSN1S2* gene and allele and genotypic frequencies of protein variants in the  $\alpha_{s2}$ -CN in the breeds studied.

SNP / Frequency	<i>CSN1S2</i> variant			
	<i>*A</i>		<i>*D</i>	
	LUC	HDV	LUC	HDV
<i>CSN2S2_1</i>	C	T	C	T
Ser68Phe - 6:85533780 rs441966828	1.000	0.000	1.000	0.000
<i>CSN1S2_2</i>			G	T
Glu74Asp - 6:85536434 rs463985801			0.995	0.005
Allele frequency of the variant	0.995	1.000	0.005	0.000
Genotypic frequency	LUC: AA=0.989 AD= 0.011			
	HDV: AA=1.000			

SNP: single-nucleotide polymorphism. LUC: Lucerna breed. HDV: Hartón del Valle breed. A (Adenine), C (Cytokine), G (Guanine), and T (Thymine) represent allele frequencies found in each SPNs.

These results are similar to those reported in the BON breed (*CSN1S2*\*A=0.997) (Hernández-Herrera et al. 2024) and in 20 other breeds studied (Gallinat et al. 2013; Ahmed et al. 2017; Meier et al. 2019). In contrast, the *\*D* allele has a high frequency (0.98) in the Holstein breed (Ardicli et al. 2018) and values between 2 and 10% in German breeds such as Angler, German Yellow, Hinterwälder, Limpurger, and Vorderwälder (Gallinat et al. 2013). In contrast, the *CSN1S2*\*E variant was only found in the Sarabi breed (0.02) (Gallinat et al. 2013) and the *CSN1S2*\*C variant in Angus with a frequency of 0.075. The positive effect of this gene on milk production and milk quality was attributed to the *\*AA* genotype (Gallinat et al. 2013). This research shows that there is no obvious selection in favor of the genotypes found in the *CSN1S2* gene, as the genotypic frequencies did not vary by sex (Figure 1C) or generation (Figure 2C) and were all in HWE.

The genotyping chip used detected 12 SNPs in the *CSN3* gene, five of which were fixed in the LUC strain and eight in the HDV strain. From these polymorphisms it is possible to reconstruct the *\*A*, *\*A'*, *\*B*, *\*E*, *\*H* and *\*I* variants of  $\kappa$ -CN of the 14 reported (*\*A*, *\*A'*, *\*B*, *\*B'*, *\*C*, *\*D*, *\*E*, *\*F'*, *\*F''*, *\*G'*, *\*G''*, *\*H*, *\*I* and *\*J*) (Caroliet a. 2009; Gallinat et al. 2013; Meier et al. 2019). In both breeds studied, the *\*A* variant of  $\kappa$ -CN had the highest frequency, followed by the  $\kappa$ -CN\**B* variant in LUC and by  $\kappa$ -CN\**I* in HDV (Table 4). The other distinguishable

alleles ( $\kappa$ -CN\**A'*, *\*E*, and *\*H*) showed a low frequency in LUC and were absent in HDV.

The frequency found for the *\*A* allele in the LUC breed is higher than what was reported in many breeds around the world, including Angler (0.55), Butana (0.47), Eringer (0.50), German Red Pied (0.71), German Yellow (0.45), Gir (0.07), Hinterwälder (0.75), Holstein (0.52), Hungarian Grey Steppe (0.55), Jersey (0.42), Karan Fries (0.62), Limpurger (0.80), Pinzgauer (0.59), Retinta (0.13), Sarabi (0.30), Shorthorn (0.60), Sistani (0.28) and Vorderwälder (0.78) (Gallinat et al. 2013; Ahmed et al. 2017; Meier et al. 2019; Chessa et al. 2020; Mohan et al. 2021); only slightly surpassed by Black Pied (0.83) (Meier et al. 2019). This gene has been studied in other breeds in Colombia. The frequency of the  $\kappa$ -CN\**A* variant has been reported as 0.68 in the BON breed (Hernández-Herrera et al. 2024), 0.68 in the HDV breed (Naranjo et al. 2007), and 0.80 in the Holstein breed (Padilla-Doval et al. 2021). In contrast, the  $\kappa$ -CN\**B* variant is reported at a high frequency in the Jersey breed (0.9) (Chessa et al. 2020), while the  $\kappa$ -CN\**H* variant is more common in *B. indicus* breeds such as Gir (0.5) and Sistani (0.5) (Gallinat et al. 2013).

The *\*BB* genotype was not found in the breeds studied, but the *\*AB* genotype was found (Table 4). Both genotypes are associated with higher milk production (Mahmoudi et al. 2020). In terms of quality, milk from animals with

SNP / Frequency	CSN3 variant																	
	*A			*A'			*E			*B			*H			*I		
	LUC	HDV	A	LUC	HDV	A	LUC	HDV	E	LUC	HDV	B	LUC	HDV	H	LUC	HDV	I
CSN3_AY380228_12690 Arg/His - 6:85656358	G	A	G	A														
	1.000	0.000	1.000	0.000														
CSN3_AY380228_12940 Thr= - 6:85656608	T	C	T	C														
	1.000	0.000	1.000	0.000														
CSN3_AY380228_12950 Arg164Ser - 6:85656618	C	A	C	A														
	1.000	0.000	1.000	0.000														
CSN3_AY380228_12951 Arg164His - 6:85656619	G	A	G	A														
	1.000	0.000	1.000	0.000														
CSN3_AY380228_13096 6:85656764	T	G	T	G														
	1.000	0.000	1.000	0.000														
CSN3_AY380228_13165 Ala235= - 6:85656833	A	G	A	G														
	0.910	0.090	0.800	0.200														
CSN3_AY380228_13111 Pro217= - 6:85656779	A			G			A			G			0.995			0.005		
	rs439304887			rs439304887			rs439304887			rs439304887			rs439304887			rs439304887		
CSN3_AY380228_13124 Ser222Gly - 6:5656792	A			G			A			G			0.995			0.005		
	rs43703017			rs43703017			rs43703017			rs43703017			rs43703017			rs43703017		
CSN3_AY380228_13068 Ile203Thr - 6:85656736	T			C			T			C			0.085			0.915		
	rs43703015			rs43703015			rs43703015			rs43703015			rs43703015			rs43703015		
CSN3_AY380228_13104_1 Ala215Asp - 6:85656772	A			C			A			C			0.888			0.112		
	rs43703016			rs43703016			rs43703016			rs43703016			rs43703016			rs43703016		
CSN3_AY380228_13065 Thr202Ile - 6:85656733	C			T			C			T			0.936			0.064		
	rs450402006			rs450402006			rs450402006			rs450402006			rs450402006			rs450402006		
CSN3_AY380228_12971 Ser171Ala - 6:85656639	T																	

SNP: single-nucleotide polymorphism. LUC: Lucerna breed. HDV: Hartón del Valle breed. A (Adenine), C (Cytokine), G (Guanine), and T (Thymine) represent allele frequencies found in each SPNs.

the  $\beta$ -LG\*AA genotype has a lower protein content ( $P<0.05$ ) (Mahmoudi et al. 2020). In contrast, milk from animals with genotype  $\beta$ -LG\*BB has higher protein, fat, calcium, and phosphorus content (Mahmoudi et al. 2020; Mohan et al. 2021). It also has a better fatty acid content and a higher yield in milk-to-cheese processing, understood by a higher structural stability of the micelles and a shorter coagulation time (Poulsen et al. 2017; Zepeda-Batista et al. 2017). IgE-binding epitopes common to the  $\kappa$ -CN\**A* and  $\kappa$ -CN\**E* variants are also known in the  $\kappa$ -CN, which could potentially be more allergenic than the  $\kappa$ -CN\**B* variant. However, bioactive peptides with antithrombotic, anti-inflammatory, and immune response modulating activity have also been described in this protein (Vargas-Bello-Pérez et al. 2019).

Due to the above-mentioned advantages of the *CSN3*\**B* variant, breeding programs have been initiated to increase its frequency. For example, in the Holstein breed in Italy, the frequency has increased from 0.18 to 0.35 in the last 17 years (Chessa et al. 2020). This does not seem to be the case in the LUC breed, where frequencies have not changed over time (Figure 2D), nor in the BON breed, where a tendency to decrease over time has been reported (Hernández-Herrera et al. 2024). None of the SNPs studied in the *CSN3* gene showed significant HWE deviations. The comparison of frequencies concerning sex in the LUC breed showed no differences (Figure 1D), contrary to those previously reported in the BON breed, where the  $\beta$ -LG\**B* variant is more frequent in females (Hernández-Herrera et al. 2024).

Using the  $\beta$ -LG\**B* allele as a reference, 11 variants ( $\beta$ -LG\**A*,  $\beta$ -LG\**C*,  $\beta$ -LG\**D*,  $\beta$ -LG\**E*,  $\beta$ -LG\**F*,  $\beta$ -LG\**G*,  $\beta$ -LG\**W*,  $\beta$ -LG\**I*,  $\beta$ -LG\**J*, and  $\beta$ -LG\**W*) have been reported (Caroli et al. 2009). The 11 SNPs included in the genotyping chip, located in the *LGB* gene, allowed the reconstruction of the variants  $\beta$ -LG\**A*,  $\beta$ -LG\**B*,  $\beta$ -LG\**D*,  $\beta$ -LG\**G*, and  $\beta$ -LG\**I* of  $\beta$ -LG, of which the last three showed low frequency in the LUC breed and absence in the HDV breed (Table 5). In both breeds, the  $\beta$ -LG\**B* allele of beta-lactoglobulin was the most common, followed by the  $\beta$ -LG\**A* allele. In the breeds Butana (0.46) (Ahmed et al. 2017), BON (0.67) (Hernández-Herrera et al. 2024), Holstein (0.70), and Simmental (0.59) (Čítek et al. 2023), the  $\beta$ -LG\**B* allele was the most frequent. In contrast, in a previous study, the  $\beta$ -LG\**A* variant was reported to be the most frequent in BON (0.51) (Rosero et al. 2012), Gyr and Jersey breeds (Gai et al. 2021).

Other reports suggest that animals with the  $\beta$ -LG\*AA genotype produce more milk. On the contrary, the  $\beta$ -LG\*BB genotype produces higher protein, fat, and shorter rennet formation time (Gai et al. 2021; Čítek et al. 2023). This genotype showed a frequency of around 30% in the breeds analyzed (Table 5). At least two interesting bioactive peptides (LQKW 58-61 and WYSLAMAASDI 19-29) have been reported in  $\beta$ -LG, which, through their antioxidant activity, reduce stress granule formation, scavenge 2,2'-azino-bis-acid radical cations, and increase myotube differentiation in skeletal muscle, resulting in an anti-aging effect (Kim et al. 2019; Čítek et al. 2023). However, these beneficial effects have not been associated with any particular genetic variant.

In this gene, the variant *LGB*\_X14710\_5263 (rs109625649) showed significant deviations from HWE. However, this did not imply differences in the genotype frequencies between sexes (Figure 1E) and between generations (Figure 2E), although the  $\beta$ -LG\*BB genotype was more common in males and the third generation. As mentioned above, there was no selection for this genotype in the herd studied, but it is possible that there was indirect selection due to the milk traits of these animals.

Regarding the population structure in the LUC breed, the *wFST* values obtained were low, considering all SNPs and as structuring factors sex (*wFST*=0.0043) and generation (*wFST*=0.026). In the BON breed, using the herd as a structuring factor, the reported *F<sub>ST</sub>* is 0.035, 0.003 by sex, and 0.001 by year (Hernández-Herrera et al. 2024). The *wFST* value for the variant associated with the  $\beta$ -CN\**A*<sup>2</sup> protein was 0.0512 ( $P<0.05$ ). While the estimated *F<sub>IT</sub>* value was -0.0086 ( $P>0.05$ ), which shows that there is no inbreeding, evaluated from the milk genes.

It has been proposed that, due to the physical proximity of the casein genes, they are more likely to be inherited as a linkage group rather than independently (Villalobos-Cortés et al. 2023). To test this, the 32 SNPs analyzed in caseins and the 11 SNPs in beta-lactoglobulin were pruned. Finally, 14 SNPs were informative in the casein genes and five in the *LGB* gene. Figures 3A and 3B show the heat maps of the LODs obtained. The highest LOD value was found between the SNPs *CSN3*\_AY380228\_13165



[illegible]

SNP: single-nucleotide polymorphism. LUC: Lucerna breed. HDV: Hartón del Valle breed. A (Adenine), C (Cytokine), G (Guanine), and T (Thymine) represent allele frequencies found in each SPNs.

( $\kappa$ -CN<sup>\*A</sup>) and CSN3\_AY380228\_13068 ( $\kappa$ -CN<sup>\*B</sup>), followed by another pair of SNPs also determining the <sup>\*A</sup> and <sup>\*B</sup> variants of the  $\kappa$ -CN gene (CSN3\_AY380228\_13165 and CSN3\_AY380228\_13104\_1) and the SNPs determining the  $\kappa$ -CN<sup>\*B</sup> variant (CSN3\_AY380228\_13068 and CSN3\_AY380228\_13104\_1). The CSN2S2\_1 SNPs, which determine the <sup>\*A</sup> variant of the  $\alpha_{S2}$ -CN gene, showed a high LOD value with the CSN3\_AY380228\_13165 variant, which determines the  $\kappa$ -CN<sup>\*A</sup> variant. Among the SNPs of the  $\beta$ -CN gene, the LOD values were low (LOD<0.07) and presented an average value between  $\kappa$ -CN and  $\beta$ -CN. The SNP CSN2\_7, which determines the most studied variant of  $\beta$ -CN (<sup>\*A2</sup>), did not show LOD values higher than 0.15 with other polymorphisms (Figure 3A). Then,

the SNP alphaS1Casein26181 of the  $\alpha_{S2}$ -CN<sup>\*C</sup> gene showed mean LD values with the SNP determining the <sup>\*B</sup> variant of the same gene, with the SNP CSN2S2\_1 determining the <sup>\*A</sup> variant of the  $\alpha_{S2}$ -CN gene, and the variant CSN3\_AY380228\_13065 coding for the <sup>\*H</sup> allele of the  $\kappa$ -CN. The linkage values between the informative SNPs of the LGB gene were low (LOD<0.03), except between LGB\_X14710\_3982 and LGB\_X14710\_5174 (LOD=0.50), which both determine the <sup>\*A</sup> allele of the  $\beta$ -LG (Figure 3B). These results show that the linkage between casein genes is low, and the highest linkage is found between SNPs of the same gene. A similar conclusion is presented by Hernández-Herrera et al. (2024) in BON cattle.

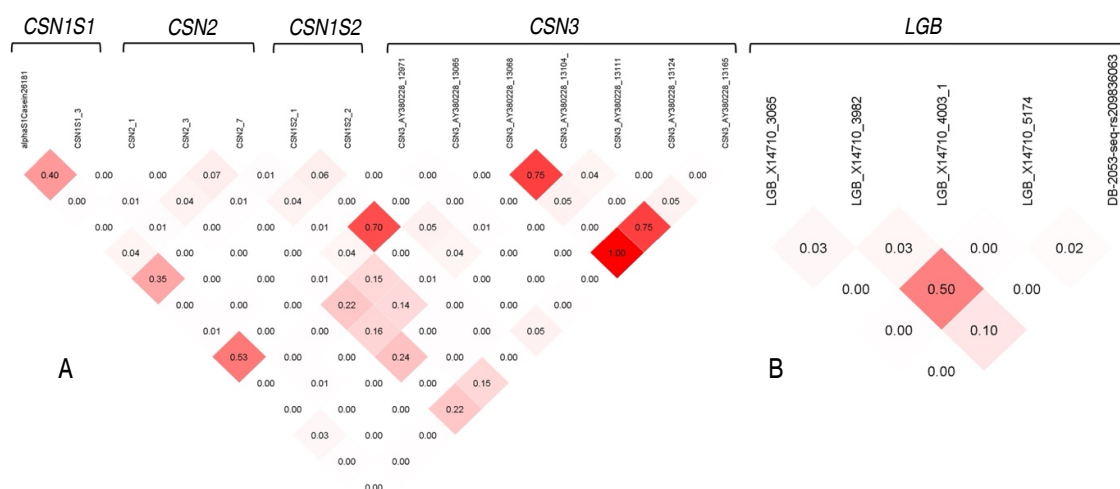


**Figure 3.** Linkage disequilibrium heat map of SNPs after pruning in the casein (A) and beta-lactoglobulin (B) genes in the Lucerne breed.

Twenty-two CSN1S1-CSN2-CSN1S2-CSN3 haplotypes were found, 19 in the LUC breed and eight in the HDV breed, of which five were shared between breeds and three were unique to the HDV (Table 6). Haplotype BB-A<sup>2</sup>A<sup>2</sup>-AA-AA had the highest frequency (0.312), followed by haplotypes BB-A<sup>1</sup>A<sup>2</sup>-AA-AA-AA (0.194) and BB-A<sup>1</sup>A<sup>2</sup>-AA-AB (0.118) in the LUC breed. The other haplotypes had frequencies of less than 6.5%. In the HDV breed, the most common haplotypes were BB-A<sup>1</sup>A<sup>2</sup>-AA-AA-AI and BC-A<sup>1</sup>A<sup>2</sup>-AA-AA-AB (0.2), which were rare in LUC. Coincidentally, the three most common haplotypes in the LUC breed were also common in the BON breed. In contrast, of the two most common haplotypes in the HDV breed, one was absent in BON, and the other had

a frequency below 5% (Hernández-Herrera et al. 2024). Using haplotypes reconstructed from CSN1S1-CSN2-CSN1S2-CSN3 alleles—rather than from genotypes as in the present study—84 haplotypes were identified in the Butana breed, with the most frequent being C-A2-A-A (0.156) (Ahmed et al. 2017). On the other hand, using only CSN2-CSN3 genes, the most common haplotype was A<sup>2</sup>-A in Holstein (0.474) and A<sup>2</sup>-B (0.646) in the Jersey breed (Chessa et al. 2020).

This research showed a low level of linkage between casein genes. Nevertheless, milk, being a composite of several proteins, could have synergistic relationships that affect its quality and technological performance. For

this reason, the effects of *CSN1S1-CSN2-CSN3* gene haplotypes on milk traits were studied. Thus, the most frequent haplotype *BB-A<sup>2</sup>A<sup>2</sup>-AA* (*CSN1S1-CSN2-CSN3*) in the LUC breed (31.2%) has contradictory reports. Perna et al. (2016) demonstrated that this haplotype is associated with low cheese yield when coagulation is induced by rennet. In contrast, when coagulation is induced by acidic methods, traits related to cheese

formation are significantly improved (Ketto et al. 2017). Similarly, the second most common haplotype in LUC (*BB-A<sup>1</sup>A<sup>2</sup>-AA*, 19.4%) was associated with better curdling time, better curdling structure, and higher cheese yield (Ketto et al. 2017). On the other hand, the *BB-A<sup>2</sup>A<sup>2</sup>-BB* haplotype was associated with higher milk protein and fat content and better rennet formation (Perna et al. 2016). This haplotype had a low frequency in the LUC breed.

**Table 6.** Haplotype frequencies of the *CSN1S1-CSN2-CSN1S2-CSN3* genes in the Lucerna and Hartón del Valle breeds.

No.	Haplotype <i>CSN1S1-CSN2-CSN1S2-CSN3</i>	LUC	HDV
1	<i>BB-A<sup>1</sup>A<sup>1</sup>-AA-AA</i>	0.043	-
2	<i>BB-A<sup>1</sup>A<sup>1</sup>-AA-AB</i>	0.022	-
3	<i>BB-A<sup>1</sup>A<sup>1</sup>-AD-AB</i>	0.011	-
4	<i>BB-A<sup>1</sup>A<sup>2</sup>-AA-AA</i>	0.194	-
5	<i>BB-A<sup>1</sup>A<sup>2</sup>-AA-AB</i>	0.118	-
6	<i>BB-A<sup>1</sup>A<sup>2</sup>-AA-AE</i>	0.011	-
7	<i>BB-A<sup>1</sup>A<sup>2</sup>-AA-AI</i>	0.022	0.200
8	<i>BB-A<sup>1</sup>B-AA-AB</i>	0.022	-
9	<i>BB-A<sup>2</sup>A<sup>2</sup>-AA-AA</i>	0.312	-
10	<i>BB-A<sup>2</sup>A<sup>2</sup>-AA-AB</i>	0.011	-
11	<i>BB-A<sup>2</sup>A<sup>2</sup>-AA-II</i>	-	0.100
12	<i>BB-BF-AA-AA</i>	0.011	-
13	<i>BC-A<sup>1</sup>A<sup>2</sup>-AA-A1B</i>	0.011	-
14	<i>BC-A<sup>1</sup>A<sup>2</sup>-AA-AA</i>	0.032	0.100
15	<i>BC-A<sup>1</sup>A<sup>2</sup>-AA-AB</i>	0.032	0.200
16	<i>BC-A<sup>1</sup>A<sup>2</sup>-AA-AH</i>	0.022	-
17	<i>BC-A<sup>2</sup>A<sup>2</sup>-AA-AA</i>	0.043	0.100
18	<i>BC-A<sup>2</sup>A<sup>2</sup>-AA-AB</i>	0.011	0.100
19	<i>BC-A<sup>2</sup>A<sup>2</sup>-AA-AH</i>	0.065	-
20	<i>BC-A<sup>2</sup>A<sup>2</sup>-AA-AI</i>	-	0.100
21	<i>CC-A<sup>2</sup>A<sup>2</sup>-AA-AB</i>	-	0.100
22	<i>CC-A<sup>2</sup>A<sup>2</sup>-AA-AH</i>	0.011	-

LUC: Lucerna breed. HDV: Hartón del Valle breed.

Finally, these results justify the efforts made by private and public bodies to conserve Colombian Creole breeds and to promote the development of current conservation programs into genetic breeding programs, not only to promote the use of adapted breeds, but also as breeds capable of producing high-quality milk.

## CONCLUSION

Only 46 and 23% of the SNPs evaluated were found to be polymorphic in the LUC and HDV breeds, respectively. Nevertheless, it was possible to reconstruct the most significant variants (*CSN1S1\*B*,  $\beta$ -*CN\*A<sup>2</sup>*,  $\kappa$ -*CN\*B*, and  $\beta$ -*LG\*B*) from the perspective

of their association with milk production, nutritional quality, and technological performance. These variants exhibited high frequency in both breeds, with minor variations attributable to the limited number of HDV animals utilized and the geographical origin of the LUC breed in HDV. The linkage found between single-nucleotide polymorphisms located in the same gene was high. In contrast, the linkage between the casein genes was found to be low, suggesting that they are independently inherited. The high frequency of these favorable alleles in the Lucerna population—despite the absence of targeted selection—suggests a strategic opportunity to incorporate this information into genetic selection programs aimed at improving both productive efficiency and milk compositional and technological quality. Furthermore, the low genetic linkage among the loci studied suggests that independent selection for each gene is feasible, enabling greater genetic gain without constraints imposed by linkage disequilibrium. This genetic characterization provides a foundation for implementing marker-assisted selection (MAS), advancing towards genomic selection, and promoting the broader use of the Lucerna breed not only for its tropical adaptability but also for its potential to produce high-quality milk.

## ACKNOWLEDGMENTS

The authors would like to thank the Reserva Natural El Hatico for facilitating all the processes necessary to carry out this research.

## ETHICAL CONSIDERATIONS

All processes within the experimental analysis were carried out in accordance with the guidelines proposed in 'The international guiding principles for biomedical research involving animals' (CIMOS and ICLAS 2012).

## CONFLICT OF INTERESTS

The authors declare no competing interests.

## REFERENCES

Ahmed A, Rahmatalla S, Bortfeldt R et al (2017) Milk protein polymorphisms and casein haplotypes in Butana cattle. *Journal of Applied Genetics* 58(2): 261-271. <https://doi.org/10.1007/s13353-016-0381-2>

Ardicli S, Soyudal B, Samli H et al (2018) Effect of *STAT1*, *OLR1*, *CSN1S1*, *CSN1S2*, and *DGAT1* genes on milk yield and composition traits of Holstein breed. *Revista Brasileira de Zootecnia*

47: e20170247. <https://doi.org/10.1590/rbz4720170247>

Caroli AM, Chessa S and Erhardt GJ (2009) Invited review: Milk protein polymorphisms in cattle: Effect on animal breeding and human nutrition. *Journal of Dairy Science* 92(11): 5335-5352. <https://doi.org/10.3168/jds.2009-2461>

Chessa S, Gattolin S, Cremonesi P et al (2020) The effect of selection on casein genetic polymorphisms and haplotypes in Italian Holstein cattle. *Italian Journal of Animal Science* 19(1): 833-839. <https://doi.org/10.1080/1828051X.2020.1802356>

Čítek J, Samková E, Brzákova M et al (2023) *CSN1S1* and *LALBA* polymorphisms and other factors influencing yield, composition, somatic cell score, and technological properties of cow's milk. *Animals* 13(13): 2079. <https://doi.org/10.3390/ani13132079>

Dandine-Roulland C and Perdry H (2018) Genome-Wide data manipulation, association analysis and heritability estimates in R with gaston 1.5. *Human Heredity* 83(1): 1-29.

Dantas A, Kumar H, Prudencio E et al (2023) An approach on detection, quantification, technological properties, and trends market of A2 cow milk. *Food Research International* 167: 112690. <https://doi.org/10.1016/j.foodres.2023.112690>

Gai N, Uniacke-Lowe T, O'Regan J et al (2021) Effect of protein genotypes on physicochemical properties and protein functionality of bovine milk: A review. *Foods* 10(10): 2409. <https://doi.org/10.3390/foods10102409>

Gallinat JL, Qanbari S, Drögemüller C et al (2013) DNA-Based identification of novel bovine casein gene variants. *Journal of Dairy Science* 96(1): 699-709. <https://doi.org/10.3168/jds.2012-5908>

Giraldo N, Viveros A, Rincón J and González-Herrera L (2023) Curva de primera lactancia en ganado bovino con diferente proporción Lucerna y su relación con factores ambientales asociados a la producción de leche. *Livestock Research for Rural Development* 35(Article # 1).

Hernández-Herrera D and Carrillo-González D (2024) Association of BoLA-DRB3 Alleles with the Progression of Bovine Leukosis in the Lucerna Breed. *Tropical Animal Science Journal* 47(4): 417-425. <https://doi.org/10.5398/tasj.2024.47.4.417>

Hernández-Herrera DY, Rincón-Flórez JC and Pulido-Hoyos MN (2024) Milk protein polymorphisms and casein haplotypes in Blanco Orejinegro cattle of Colombia. *Revista de Ciências Agroveterinárias* 23(1): 117-129. <https://doi.org/10.5965/223811712312024117>

Kay S, Delgado S, Mittal J et al (2021) Beneficial effects of milk having A2  $\beta$ -Casein protein: Myth or reality?. *The Journal of Nutrition* 151(5): 1061-1072. <https://doi.org/10.1093/jn/nxaa454>

Ketto I, Knutsen T, Øyaas J et al (2017) Effects of milk protein polymorphism and composition, casein micelle size and salt distribution on the milk coagulation properties in Norwegian Red cattle. *International Dairy Journal* 70: 55-64. <https://doi.org/10.1016/j.idairyj.2016.10.010>

Kim Y, Kim J, Cheon S et al (2019) Alpha-casein and beta-lactoglobulin from cow milk exhibit antioxidant activity: A plausible link to antiaging effects. *Journal of Food Science* 84(11): 3083-3090. <https://doi.org/10.1111/1750-3841.14812>

Mahmoudi P, Rostamzadeh J, Rashidi A et al (2020) A meta-analysis on association between *CSN3* gene variants and milk yield and composition in cattle. *Animal Genetics* 51(3): 369-381. <https://doi.org/10.1111/age.12922>

Meier S, Korkuć P, Arends D and Brockmann G (2019) DNA

sequence variants and protein haplotypes of casein genes in German Black Pied cattle (DSN). *Frontiers in Genetics* 10. <https://doi.org/10.3389/fgene.2019.01129>

Mohan G, Kumar A, Khan S et al (2021) Casein (CSN) gene variants and parity affect the milk protein traits in crossbred (*Bos taurus* x *Bos indicus*) cows in sub-tropical climate. *Tropical Animal Health and Production* 53(2): 289. <https://doi.org/10.1007/s11250-021-02736-w>

Molina I, Angarita E, Mayorga O et al (2016) Effect of *Leucaena leucocephala* on methane production of Lucerna heifers fed a diet based on *Cynodon plectostachyus*. *Livestock Science* 185: 24-29. <https://doi.org/10.1016/j.livsci.2016.01.009>

Muntean I, Bocsan I, Wiest L et al (2022) Predictive factors for oral immune modulation in cow milk allergy. *Nutrients* 14(3): 494. <https://doi.org/10.3390/nu14030494>

Naranjo J, Posso A, Cárdenas H and Muñoz J (2007) Detección de variantes alélicas de la kappa-caseína en bovinos Hartón del Valle». *Acta Agronómica* 56 (1): 43-48. [https://revistas.unal.edu.co/index.php/acta\\_agronomica/article/view/568](https://revistas.unal.edu.co/index.php/acta_agronomica/article/view/568)

Padilla-Doval J, Zambrano-Arteaga JC, Echeverri-Zuluaga JJ and López-Herrera A (2021) Análisis genético de cinco polimorfismos de nucleótido simple de caseínas lácteas obtenidos con chips genómicos en ganado Holstein de Antioquia, Colombia. *Revista de la Facultad de Medicina Veterinaria y de Zootecnia* 68 (2): 137-149 <https://doi.org/10.15446/rfmvz.v68n2.98026>

Perna A, Intaglietta I, Gambacorta E and Simonetti A (2016) The influence of casein haplotype on quality, coagulation, and yield traits of milk from Italian Holstein cows. *Journal of Dairy Science* 99(5): 3288-3294. <https://doi.org/10.3168/jds.2015-10463>

Poulsen N, Gregersen V, Maciel G et al (2017) Novel genetic

variation associated to *CSN3* strongly affects rennet-induced milk coagulation. *International Dairy Journal* 71: 122-30. <https://doi.org/10.1016/j.idairyj.2017.03.012>

Rivera J, Chará J, Murgueitio E and Molina J (2019) Feeding leucaena to dairy cows in intensive silvopastoral systems in Colombia and Mexico. *Tropical Grasslands* 7(4): 370-374. [https://doi.org/10.17138/tgft\(7\)370-374](https://doi.org/10.17138/tgft(7)370-374)

Rosero J, Álvarez L, Muñoz J et al (2012) Allelic frequency of the kappa-casein gene in colombian and creole cattle breeds. *Revista Colombiana de Ciencias Pecuarias* 25(2): 173-182. <https://doi.org/10.17533/udea.rccp.324744>

Sanchez M, Fritz S, Patry C et al (2020) Frequencies of milk protein variants and haplotypes estimated from genotypes of more than 1 million bulls and cows of 12 French cattle breeds. *Journal of Dairy Science* 103(10): 9124-9141. <https://doi.org/10.3168/jds.2020-18492>

Vargas-Bello-Pérez E, Márquez-Hernández R and Hernández-Castellano L (2019) Bioactive peptides from milk: animal determinants and their implications in human health. *Journal of Dairy Research* 86(2): 136-144. <https://doi.org/10.1017/S0022029919000384>

Villalobos-Cortés A, Rodríguez G, Castillo H and Franco S (2023) Characterization of casein variants in the Guaymi and Guabala breeds through a low-density chip arrangement. *Journal of Applied Animal Research* 51 (1): 69-73. <https://doi.org/10.1080/09712119.2022.2154216>

Zepeda-Batista J, Saavedra-Jiménez L, Ruíz-Flores A et al (2017) Potential influence of  $\kappa$ -casein and  $\beta$ -lactoglobulin genes in genetic association studies of milk quality traits. *Asian-Australasian Journal of Animal Sciences* 30(12): 1684-1688. <https://pubmed.ncbi.nlm.nih.gov/28728383/>





# Effect of antibiotic residues from subclinical mastitis on $\beta$ -lactoglobulin concentration in bovine and goat milk

Efecto de los residuos de antibióticos por mastitis subclínica sobre la concentración de  $\beta$ -lactoglobulina en leche bovina y caprina

<https://doi.org/10.15446/rfnam.v78n3.119097>

Yamile Jiménez Alfonso<sup>1\*</sup> and Luis Edgar Tarazona-Manrique<sup>2</sup>

## ABSTRACT

### Keywords:

Animal health  
Food quality  
HPLC  
Milk proteins  
Veterinary drug residues


$\beta$ -Lactoglobulin ( $\beta$ -LG) is an important milk protein, accounting for approximately 10% of total milk protein and 50–60% of whey proteins. Its concentration can vary depending on the species and several factors, including the use of antibiotics in the treatment of conditions such as subclinical mastitis. If withdrawal periods are not properly observed, antibiotic residues may remain in the milk, compromising its quality and posing risks to consumers. This study evaluated the effect of antibiotic residues from the treatment of subclinical mastitis on the concentration of  $\beta$ -LG in milk from cattle (*Bos taurus*) and goats (*Capra hircus*) on farms located in Paipa, Boyacá (Colombia). Twelve milk samples were collected from Simhol and Jerhol cattle and from Saanen and Alpina goats that tested positive for subclinical mastitis using the CMT. Samples were collected before and 24 hours after treatment with beta-lactams and tetracyclines.  $\beta$ -LG concentration was quantified by reverse-phase high-performance liquid chromatography (RP-HPLC), and the data were analyzed using a linear model under a 2×2 factorial design with the following factors: antibiotic residues (present-absent) and species (cow-goat). A significant reduction of 0.43 g L<sup>-1</sup> ( $P < 0.05$ ) in  $\beta$ -LG concentration was observed in association with the presence of antibiotic residues, with no interaction with species. These results are exploratory and suggest a possible negative impact of antibiotics on the functional and nutritional quality of milk, potentially related to protein carbonylation processes.


## RESUMEN

### Palabras clave:

Sanidad animal  
Calidad alimentaria  
HPLC  
Proteínas de la leche  
Residuos de medicamentos veterinarios

La  $\beta$ -Lactoglobulina ( $\beta$ -LG) es una proteína importante de la leche, representando aproximadamente el 10% del total proteico y entre el 50-60% de las proteínas del suero. Su concentración puede variar según la especie y diversos factores, como el uso de antibióticos en el tratamiento de enfermedades como la mastitis subclínica, los cuales, si no se respetan los tiempos de retiro, pueden dejar residuos en la leche que podrían comprometer su calidad composicional e inocuidad, representando un riesgo para el consumidor final. Este estudio evaluó el efecto de los residuos de antibióticos en el tratamiento de mastitis subclínica sobre la concentración de  $\beta$ -LG en leche de bovinos (*Bos taurus*) y caprinos (*Capra hircus*), en fincas ubicadas en Paipa, Boyacá (Colombia). Se recolectaron 12 muestras de leche de bovinos Simhol y Jerhol y caprinos Saanen y Alpina, positivos para esta afección mediante CMT. Las muestras se tomaron antes y 24 horas después del tratamiento con betalactámicos y tetraciclinas. La  $\beta$ -LG se cuantificó por medio de cromatografía líquida de alta resolución en fase reversa (RP-HPLC), y los datos se analizaron mediante un modelo lineal bajo un diseño factorial 2×2 con los factores: residuos antibióticos (presencia-ausencia) y especie (vaca-cabra). Se observó una reducción significativa de 0,43 g L<sup>-1</sup> ( $P < 0,05$ ) en la concentración de  $\beta$ -LG asociada a la presencia de residuos antibióticos, sin interacción con la especie. Estos resultados constituyen hallazgos exploratorios que sugieren un posible impacto negativo de los antibióticos sobre la calidad funcional y nutricional de la leche, posiblemente relacionado con procesos de carbonilación proteica.

<sup>1</sup>Grupo de investigación en Estudios Micro y Macro Ambientales (MICRAM) - Grupo de Investigación en Sanidad y Producción Animal del Trópico Alto Colombiano (GIPATRACOL), Maestría en Ciencias Biológicas, Universidad Pedagógica y Tecnológica de Colombia, Sede Tunja, Colombia. [yamile.jimenez@uptc.edu.co](mailto:yamile.jimenez@uptc.edu.co) 

<sup>2</sup>Grupo de Investigación en Ciencias Veterinarias (GINCIVET), Programa de Medicina Veterinaria y Zootecnia, Universidad Internacional del Trópico Americano-UNITROPICO. Yopal, Colombia. [ltarazonam@unal.edu.co](mailto:ltarazonam@unal.edu.co) 

\*Corresponding author

Milk and its derivatives from bovine and goat sources are important sources of dietary energy and essential nutrients, including calcium, magnesium, selenium, riboflavin, vitamin B12, and pantothenic acid. These nutrients contribute to strengthening the skeletal system, supporting muscle regeneration, and regulating immune function (FAO 2024). Among the main whey proteins,  $\beta$ -lactoglobulin ( $\beta$ -LG) is predominant in the milk of most mammals except guinea pigs, rabbits, rodents, and humans and has therefore been associated with allergenic potential in infants, causing symptoms that may manifest in the skin, respiratory system, and digestive tract (Giannetti et al. 2021).

$\beta$ -LG is the main whey protein, representing about 10% of total milk protein and 50–60% of whey proteins. It is a globular protein from the lipocalin family, typically found in dimeric form with a molecular weight of 36 kDa and composed of 162 amino acids (Kontopidis et al. 2002). In cattle, 11 variants of  $\beta$ -LG have been identified, with isoforms A and B being the most common. These differ by two amino acid substitutions. Compared to bovine  $\beta$ -LG, caprine  $\beta$ -LG shows eight amino acid sequence differences, though without significant alterations to its tertiary structure (Crowther et al. 2018). It is synthesized in mammary gland epithelial cells from blood precursors and fulfills important functions, including transporting hydrophobic molecules via three binding sites, regulating phosphorus metabolism in the mammary gland, and contributing to the transfer of passive immunity to newborns (Varlamova and Zaripov 2020).

The concentration of  $\beta$ -LG varies by species, ranging from approximately 2–4 g L<sup>-1</sup> in cattle and averaging 3.02 g L<sup>-1</sup> in goats (Gołębiowski et al. 2020). Beyond its biological roles,  $\beta$ -LG exhibits antioxidant properties and functional characteristics valuable to agribusiness, such as gelling, foaming, emulsifying, and flavor-binding capacities (Madureira et al. 2007). However, its metabolic function can be altered by environmental conditions—mainly milk pH, protein and ion concentrations, and temperature—which may affect its chemical structure, transport capacity, and synthesis (Varlamova and Zaripov 2020). Additionally, this protein has demonstrated the ability to bind various ligands *in vitro* such as steroids, fatty acids, retinoids, vitamin D, and cholesterol, making it a potential carrier for various types of ligands, including drugs (Kontopidis et al. 2002).

Furthermore, the quality of this protein can be influenced by several factors, including the use of antibiotics to treat diseases such as mastitis (Beltrán et al. 2013). In Colombia, mastitis is estimated to cause losses of up to USD 25,000 per affected farm annually (SIC 2021). Antimicrobial drugs are used for the treatment and prevention of this condition, and they may be administered either parenterally or locally (Beltrán et al. 2013). However, irrational use poses a serious problem due to its implications for public health, milk processing, and product quality (Tarazona-Manrique et al. 2024). Among the most commonly used pharmacological groups are  $\beta$ -lactams and tetracyclines (Sachi et al. 2019). Studies indicate that tetracyclines bind near Trp19 within a hydrophobic domain of  $\beta$ -LG (Mukherjee et al. 2018), although there is no clear evidence of a specific binding site for  $\beta$ -lactams on this protein.

Regarding regulation, European Regulation No. 853/2004 establishes that milk intended for human consumption must not contain antibiotic residues exceeding the maximum residue limits (MRLs) set forth in Commission Regulation (EU) No. 37/2010 and the Codex Alimentarius, which includes MRLs and risk management recommendations (RGRs) for veterinary drug residues in food, as outlined in its 2023 version. This legislation sets the MRL for tetracyclines and  $\beta$ -lactams (cephalosporins) at 100  $\mu$ g kg<sup>-1</sup> (FAO and WHO 2023). In Colombia, Resolution 1382 of 2013 establishes MRLs for veterinary drugs in foods of animal origin intended for human consumption (Ministerio de Salud y Protección Social 2013).

Recent studies have shown that the presence of antibiotic residues affects both the quality and quantity of milk's nutritional components, mainly whey proteins with special emphasis on  $\beta$ -LG, by inducing carbonylation of certain amino acid residues, which promotes protein degradation (Marrugo-Padilla et al. 2022). Additionally,  $\beta$ -LG has been shown to spontaneously and moderately bind to certain veterinary drugs such as amoxicillin (Habibian-Dehkordi et al. 2022) and levamisole (Ghasemi et al. 2024), which are administered parenterally. This highlights the potential for milk contamination by these compounds, directly related to the protein's concentration, posing a public health concern.

In Colombia, no studies have been reported that evaluate the impact of antibiotic residues from the treatment of subclinical mastitis on  $\beta$ -lactoglobulin ( $\beta$ -LG) concentration

in bovine and goat milk. This gap underscores the need to further investigate interactions between milk proteins and antimicrobials commonly used in dairy production, due to their potential impact on compositional quality and product safety. Within this context, the present pilot study aimed to evaluate the effect of  $\beta$ -lactam and tetracycline antibiotic residues on  $\beta$ -LG concentration in dairy cattle milk, 24 hours after drug administration in milk of bovine and goat origin, produced on farms located in the municipality of Paipa, Department of Boyacá, Colombia.

## MATERIALS AND METHODS

### Study area and period

The study was conducted in the municipality of Paipa, Department of Boyacá (Colombia), during July 2024, which corresponds to the rainy season. The area is situated at an average altitude of 2,525 meters above sea level (masl), with an average annual temperature of 13 °C, approximately 80% relative humidity, and an annual rainfall of 944 mm. Paipa is characterized by significant agricultural activity, particularly traditional dairy farming of both cattle and goats (Acuña et al. 2022).

### Animals included in the study- experimental units

The sample size was determined based on the exploratory nature of the study and the project's budgetary constraints. Inclusion criteria included: diagnosis of subclinical mastitis at the time of sampling, absence of prior pharmacological treatments, representation of common dairy breeds in the region (Simhol and Jerhol in cattle, Alpina and Saanen in goats), and producer consent for animal participation. Additional data collected for each animal included age, lactation stage, daily milk production, and number of calvings. The study involved four cattle: two Simhol cows, aged 6 and 7 years, each with four calvings and daily milk production (DMP) of 14 L and 10 L, respectively. At the time of sampling, both cows were in the second third of lactation, and their production was evaluated based on a standardized 305-day lactation period. Also included were two Jerhol cows, aged 5 and 7 years, with three and four calvings, and DMPs of 18 L and 15 L, respectively—also in the second third of lactation. Additionally, two goats were analyzed: the first, an Alpine breed, was 3 years old, with two parturitions and a daily milk production of 3 L, in the first third of lactation (standardized at 240 days); the second, a Saanen breed, was two years old,

with one parturition and a daily production of 2 L, also in the first third of lactation.

### Sample collection

Animals were evaluated for the presence of mastitis using the California Mastitis Test (CMT), employing reagent provided by California Animal Health, following this protocol: the first stream of milk was discarded, and approximately 5 mL of milk was collected in the corresponding wells of the paddle. An equal volume of commercial reagent was added to each well. A gentle circular motion was applied on a horizontal plane for 20 seconds to mix the reagent with the milk. The results were collected and interpreted as follows: 0 (negative or no thickening of the sample), Trace (slight thickening that disappeared with circular motion), 1 or + (marked thickening with no tendency to form a gel), 2 or ++ (immediate thickening with slight gel formation), or 3 or +++ (gel formation with the mixture's surface raised). This evaluation reflects the inflammatory response based on the viscosity of the gel formed when the reagent interacts with the milk (Mendoza et al. 2017). The Alpine goat (individual 1) showed an initial CMT result of 2; the Saanen goat (individual 2), a result of 1; the Simhol cows (individuals 3 and 4), both had a score of 2; and the Jerhol cows (individuals 5 and 6) presented scores of 2 and 1, respectively. A first sample collection was then carried out, followed by the application of experimental treatments. Individuals 2, 3, and 5 were administered oxytetracycline 20% (tetracycline) parenterally, while individuals 1, 4, and 6 received intramammary treatment with Cobactan LC, containing 2.5% cefquinome sulfate (a  $\beta$ -lactam). Twenty-four hours later, a second round of sample collection was performed to assess the early-stage effect of antibiotic administration on protein concentration. The sampling procedure began with teat washing using a soap solution, followed by rinsing with sterile water and drying with sterile gauze. Teats were then disinfected with an iodine solution. Once asepsis was completed, 500 mL of milk was collected in sterilized glass jars, drawing equal amounts from the four teats in cows and two teats in goats. Samples were stored at 4 °C until they were transferred to the BIOPOLAB laboratory in Bogotá for analysis by Reverse-Phase High-Performance Liquid Chromatography (RP-HPLC). A total of twelve samples were collected and analyzed in duplicate.

### Chromatographic conditions

The concentration of  $\beta$ -LG was determined using RP-HPLC based on a protocol developed by the BIOPOLAB laboratory, adapted from the method described by Ding et al. (2011). This methodology enabled efficient separation and accurate quantification of the protein under optimized conditions for the milk matrices analyzed. The equipment used was a Thermo Dionex Ultimate 3000 UHPLC system. Separation was performed using a ZORBAX Eclipse XDBC18 analytical column (4.6×150 mm, 5  $\mu$ m film thickness). Linear gradient elution was conducted as outlined in Table 1, at a flow rate of 0.8 mL min<sup>-1</sup>, using two solvents: Solvent A (acetonitrile with 0.1% trifluoroacetic acid [TFA]) and Solvent B (HPLC-grade water with 0.1% TFA). Each sample analysis lasted 42 minutes. The column was maintained at 30 °C, and detection was carried out at

220 nm using a diode array detector (DAD), with results expressed in milliabsorbance units (mAU). The injection volume was 50  $\mu$ L. For calibration, a  $\beta$ -lactoglobulin protein standard (90% purity, Sigma-Aldrich) was used to generate a calibration curve. The resulting chromatogram displayed a stable retention time and a symmetrical peak, demonstrating the sensitivity and reliability of the method for protein quantification (Figure 1).

**Table 1.** Gradient elution time.

Time (min)	Phase A%	Phase B%
0	33	67
30	45	55
42	33	67

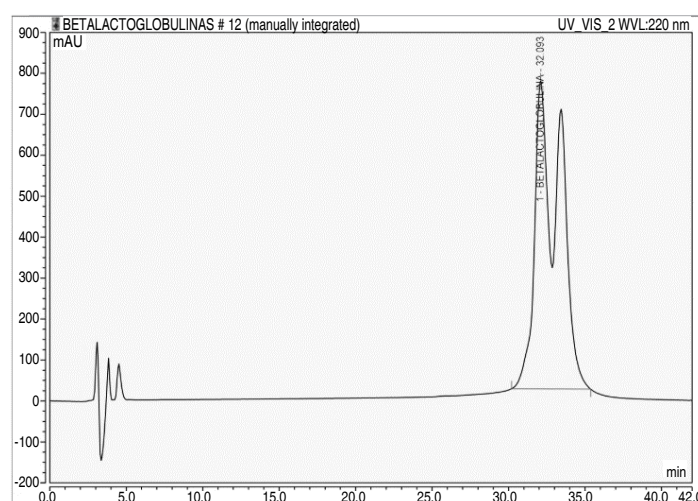


**Figure 1.** Chromatogram of the protein standard  $\beta$ -Lactoglobulin at 90% purity from Sigma-Aldrich.

### Sample treatments

Two milliliters of milk sample were diluted with 14 mL of Type 1 water in a test tube. The pH of the samples was adjusted to 4.3 by adding 200  $\mu$ L of acetic acid solution (10%, v/v), followed by 200  $\mu$ L of 1 M sodium acetate solution. The volume was then brought to 20 mL with Type 1 water. The sample was centrifuged at 3,000 rpm and 20 °C for 10 minutes. The volume of the supernatant (SN) was recorded (approximately 18.5 mL). The resulting precipitate was acidified with 1 mM sodium acetate buffer (pH=4.3) to match the SN volume, allowed to precipitate again, and centrifuged under the same conditions. The

second SN was discarded, and 620  $\mu$ L of phosphate buffer was added to the resulting precipitate. The mixture was dissolved in an ultrasonic bath. The final solutions were prepared using 50 mM phosphate buffer (pH=6.8) and a mixture of Mobile Phase A and Mobile Phase B (70:30). All aliquots were filtered through a 0.22  $\mu$ m nylon filter before being injected into the equipment. To bring the results within the linear working range of the calibration curve, a dilution factor of 2 was applied. From the beginning, the standards were dissolved in 50 mM phosphate buffer solution at pH=6.8. The reported values correspond to the total concentration of  $\beta$ -lactoglobulins in the samples,



accounting for aliquots, dilutions, and other calculations, and are expressed in  $\text{g L}^{-1}$ .

### Statistical analysis

To analyze the concentration of  $\beta$ -LG in bovine and goat milk as a function of the presence or absence of antibiotic residues, statistical tests were conducted to verify the normality of the data, followed by fitting a one-factor variance model with two levels. First, the data distribution was evaluated using the Shapiro-Wilk normality test. Once normality was confirmed, a linear model (Equation 1) was fitted to compare the  $\beta$ -LG concentration between samples with and without antibiotic residues.

$$y_{ij} = \mu + \tau_i + \varepsilon_{ij} \quad (1)$$

Where  $y_{ij}$  is the concentration of  $\beta$ -LG,  $\mu$  is the overall mean concentration of  $\beta$ -LG,  $\tau_i$  is the effect of antibiotic residues, and  $\varepsilon_{ij}$  is the random error of the model.

In additional analysis, a 2x2 factorial experimental design was applied to study the interaction between two factors: species (bovine or goat) and the presence and absence of antibiotic residues, as shown in Equation 2.

$$y_{ijk} = \mu + \alpha_i + \beta_j + (\alpha\beta)_{ij} + \varepsilon_{ijk} \quad (2)$$

Where  $y_{ijk}$  is the concentration of  $\beta$ -LG for the k-th replicate of the i-th level of the species and the j-th level of antibiotic residue,  $\mu$  is the overall mean  $\beta$ -LG concentration,  $\alpha_i$  is the main effect of the i-th level of the "species" factor (bovine or goat),  $\beta_j$  is the main effect of the j-th level of the "antibiotic residues" factor (presence or absence),  $(\alpha\beta)_{ij}$  is the interaction effect between the i-th level of the "species" factor and the j-th level of the "antibiotic residues" factor and  $\varepsilon_{ijk}$  is the random error of the model.

This design allowed the evaluation of the main effects of each factor, as well as their potential interaction on  $\beta$ -LG concentration. As in the previous analysis, the normality of the residuals and homoscedasticity were verified to ensure the validity of the results. Comparisons of the effects of the factors on  $\beta$ -LG concentration were carried out using ANOVA, with a significance level of 0.05 to determine whether significant differences existed between groups. All analyses were performed using the RStudio statistical software.

## RESULTS AND DISCUSSION

### Effect of antibiotic residues on $\beta$ -LG protein concentration.

This study evaluated the effect of antibiotic treatments administered for subclinical mastitis on the concentration of  $\beta$ -lactoglobulin ( $\beta$ -LG) in bovine and goat milk, to identify possible alterations associated with the presence of antimicrobial residues. Table 2 presents  $\beta$ -LG concentration values, expressed in  $\text{g L}^{-1}$ , from milk samples analyzed in duplicate. The samples were classified by species, breed, sampling time (before and 24 h after antibiotic administration), and presence of residues. The antibiotic treatments included 20% oxytetracycline administered parenterally and cefquinome (Cobactan LC 2.5%) administered intramammarily. This dataset allows for the observation of changes in  $\beta$ -LG concentrations following recent antibiotic exposure and provides insights into potential differences between species and breeds. Although the sample size ( $n=12$ ) is limited, the design of this pilot study using repeated measures allows for a preliminary estimation of intra-animal variability in  $\beta$ -LG concentration and detection of potential changes due to antibiotic administration, both parenteral and intramammary. Pilot studies of this kind are commonly employed to assess biological variability and analytical feasibility prior to the design of confirmatory studies with larger, statistically powered sample sizes (Stevenson 2021).

The concentration of  $\beta$ -LG protein was compared between samples with and without antibiotic residues from the  $\beta$ -lactam and tetracycline families. A linear model was applied using the presence or absence of antibiotic residues as a single factor. The model showed that the average  $\beta$ -LG protein concentration in the absence of antibiotic residues across both bovine and goat samples was  $3.97 \text{ g L}^{-1}$ . In contrast, in the presence of these antibiotic residues, the concentration decreased by an average of  $0.473 \text{ g L}^{-1}$ . The model yielded an R-squared value of 0.507, indicating that 50.79% of the variability in  $\beta$ -LG concentration is explained by the presence of antibiotic residues ( $P<0.05$ ). This result suggests a statistically significant and substantial effect of antibiotic residues on  $\beta$ -LG protein concentration, as illustrated in Figure 2.

**Table 2.** Concentration of  $\beta$ -lactoglobulin ( $\beta$ -LG) in bovine and goat milk samples according to species, breed, sampling time, and presence of antibiotic residues.

Sample	Individual	Species	Breed	Timing (h)	Antibiotic residues	Treatment	$\beta$ -LG (g L <sup>-1</sup> )	Duplicate (g L <sup>-1</sup> )
1	1	Goat	Alpine	Before	Absence	—	3.96	4.01
2	1	Goat	Alpine	24 after	Presence	Cobactan at 2.5% LC	3.69	3.67
3	2	Goat	Saanen	Before	Absence	—	3.98	3.98
4	2	Goat	Saanen	24 after	Presence	Oxytetracycline at 20%	3.73	3.72
5	3	Cow	Simhol	Before	Absence	—	3.74	3.74
6	3	Cow	Simhol	24 after	Presence	Oxytetracycline at 20%	3.12	3.13
7	4	Cow	Simhol	Before	Absence	—	3.67	3.72
8	4	Cow	Simhol	24 after	Presence	Cobactan at 2.5% LC	3.23	3.19
9	5	Cow	Jerhol	Before	Absence	—	4.27	4.25
10	5	Cow	Jerhol	24 after	Presence	Oxytetracycline at 20%	3.62	3.66
11	6	Cow	Jerhol	Before	Absence	—	4.25	4.24
12	6	Cow	Jerhol	24 after	Presence	Cobactan at 2.5% LC	3.64	3.65

Figure 2 illustrates the reduction in  $\beta$ -LG protein concentration in samples containing antibiotic residues. The central line for each group represents the mean  $\beta$ -LG concentration. In the absence of antibiotic residues, the mean concentration is approximately 4.0 g L<sup>-1</sup>, with a data dispersion ranging from 3.6 to 4.2 g L<sup>-1</sup>, indicating greater

variability. In contrast, in the presence of antibiotic residues, the mean concentration decreases to approximately 3.5 g L<sup>-1</sup>, with a narrower dispersion ranging from 3.2 to 3.7 g L<sup>-1</sup>. This pattern highlights not only a reduction in protein concentration but also reduced variability in the presence of antibiotic residues.

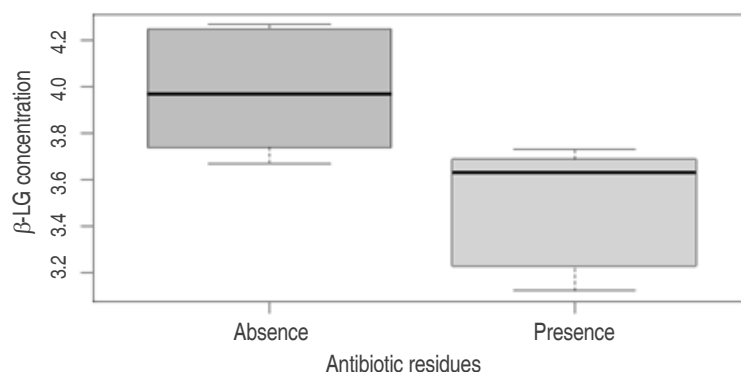


**Figure 2.**  $\beta$ -LG protein concentration as a function of the presence or absence of antibiotic residues.

### Effect of the interaction between species and antibiotic residues on $\beta$ -LG protein concentration

The factorial experimental design, which considered the factors of species (cow and goat) and antibiotic residue presence (present or absent), revealed that milk from bovine sources had a slightly higher  $\beta$ -LG protein concentration by  $0.0125 \text{ g L}^{-1}$  compared to goat milk. However, this difference was not statistically significant ( $P>0.05$ ). When holding species constant, the presence of antibiotic residues resulted in a decrease of  $0.26 \text{ g L}^{-1}$  in  $\beta$ -LG protein concentration, regardless of the route of antibiotic

administration. Regarding the interaction effect between species and antibiotic residues, a further decrease of  $0.320 \text{ g L}^{-1}$  in protein concentration was observed. However, this interaction was also not statistically significant ( $P>0.05$ ), indicating that the effect of antibiotic residues on  $\beta$ -LG concentration does not significantly depend on the species. Overall, the model explains 60.33% of the variability in  $\beta$ -LG concentration, with a marginal level of significance ( $P=0.05$ ), suggesting that while the model captures a substantial portion of the variation, its predictive power remains limited. These findings are illustrated in Figure 3.

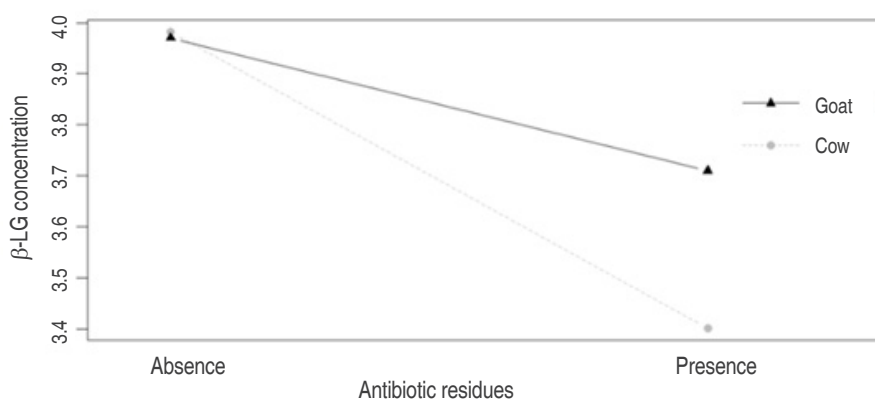


**Figure 3.** Protein concentration as a function of species and antibiotic residues.

These results are, to the best of current knowledge, the first of their kind reported from an investigation conducted in Colombia. Statistically, it was determined that species is not a factor influencing  $\beta$ -LG protein concentration in the context of subclinical mastitis, unlike the presence of antibiotic residues, which does appear to have an effect. This outcome is likely due to the reported similarity between intra- and interspecies protein isoforms (Crowther et al. 2018; Varlamova and Zaripov 2020). These findings may suggest that drugs belonging to the family of  $\beta$ -lactam and tetracycline antibiotics may alter  $\beta$ -LG protein concentration, likely due to their ability to promote carbonylation of milk proteins. This process leads to a loss of solubility and induces oxidative damage by generating stable carbonyl groups on amino acid side chains (Alviz-Amador et al. 2019), ultimately affecting  $\beta$ -lactoglobulin levels in both bovine and goat milk.

These effects have been previously documented. Marrugo-Padilla et al. (2020) evaluated the oxidative damage induced on caseins and whey proteins from a

binary mixture of four tetracyclines and three pyrethroids. Their findings demonstrated a significant reduction in protein stability and integrity, attributed to carbonylation. Later, in an *in vitro* study, Marrugo-Padilla et al. (2022) investigated the carbonylation of caseins and whey proteins induced by tetracyclines at concentrations equivalent to maximum residue limits (MRLs). They observed irreversible carbonylation in most samples, resulting in a marked loss of solubility and a decrease in the gastric and intestinal digestibility of  $\beta$ -LG, thereby compromising its nutritional quality.

Similarly, Marquez et al. (2021) confirmed that both tetracycline and  $\beta$ -lactam residues at MRL concentrations can promote *in vitro* carbonylation in chicken breast proteins. In a follow-up study, Márquez et al. (2022) demonstrated that higher drug concentrations lead to greater oxidative effects on various meat proteins, including sarcoplasmic, myofibrillar, and insoluble proteins. These results support the hypothesis that antibiotic residues in biological matrices such as milk and meat induce

post-translational modifications in proteins via oxidative stress, with carbonylation serving as a key biomarker of this process. Importantly, these alterations not only compromise the functional properties of milk, such as solubility and digestibility, but may also have implications for human health. Recent studies have suggested that the consumption of oxidatively modified proteins is associated with the development of metabolic disorders, intestinal inflammation, and even carcinogenic processes (Muñoz et al. 2018; Estévez and Luna 2017). Consequently, adhering to antibiotic withdrawal periods is essential to allow for the gradual recovery of protein synthesis in the mammary gland, the restoration of a normal milk protein profile, and the prevention of human exposure to antibiotic residues (Mestorino et al. 2008).

Regarding pharmacokinetics, tetracyclines typically reach peak blood concentration within 6–8 hours, while  $\beta$ -lactams reach their maximum concentration approximately 12–18 hours after parenteral administration (Paredes 2010). This pharmacological behavior facilitates their significant excretion into milk and likely explains the observed reduction in  $\beta$ -LG concentration at the time of the second sampling (24 hours post-administration). Therefore, it is necessary to evaluate the effects of these drugs on  $\beta$ -LG concentration throughout the entire duration of their therapeutic use. Monitoring protein concentration dynamics across the complete administration and withdrawal timeline of each antibiotic will provide deeper insights into their physiological impacts on milk composition and the safety prescription period of each drug, as well as any potential residual effects that may persist days after cessation of administration.

It has been shown that  $\beta$ -LG concentration increases in animals suffering from mastitis of microbial origin, as  $\beta$ -LG possesses antimicrobial properties that may support the recovery process (Chaneton et al. 2011). Therefore, a decrease in its concentration following antibiotic administration could have implications for the animal's recovery and its ability to respond to subsequent infections that lead to mastitis.

Further research in this area is essential to translate findings into practical applications in the field. Identifying potential alterations in the concentration of biologically significant milk proteins such as  $\beta$ -LG within the context

of drug use to treat mastitis-causing microorganisms can guide the rational use of veterinary pharmaceuticals and ensure the production of high-quality dairy products.

## CONCLUSION

This study determined that the presence of antibiotic residues from the  $\beta$ -lactam and tetracycline families, used in the treatment of subclinical mastitis, has a statistically significant impact on the concentration of  $\beta$ -LG protein, reducing its average content by 0.473 g L<sup>-1</sup>. No statistically significant differences were observed in  $\beta$ -LG concentration between the two species evaluated (cow and goat). Regardless of the specific drug administered,  $\beta$ -LG levels showed a significant decrease 24 hours after parenteral administration. These findings reinforce the critical importance of strictly adhering to the withdrawal periods established for each antibiotic. Compliance ensures that residue levels in milk remain below the maximum permissible limits (MRLs), in accordance with current food safety regulations. This protects public health and helps preserve the compositional and functional quality of milk.

The results presented here represent the first data of this kind reported in Colombia, underscoring the relevance and pioneering nature of this research within the national scientific landscape. To enhance the precision and reliability of future studies, it is recommended that sample sizes be increased. Furthermore, the use of advanced analytical techniques such as mass spectrometry should be implemented to enable accurate quantification of antibiotic residues in milk. Lastly, proteomic analyses, docking studies, and molecular simulations are suggested to characterize the potential conformational and functional changes of the  $\beta$ -LG protein in the presence of  $\beta$ -lactam and tetracycline residues. Such analyses may help identify critical binding regions and clarify the biochemical consequences of these drug-protein interactions.

## ACKNOWLEDGMENTS

The authors would like to express their gratitude to the Universidad Pedagógica y Tecnológica de Colombia (UPTC) for the financial support provided through Call VIE 05 of 2023 – Support for Research Projects (Thesis or Degree Work) for Master's or Doctoral programs in research. This support was essential to the successful development of this study.

## CONFLICT OF INTERESTS

The authors declare that there are no conflicts of interest associated with this study.

## REFERENCES

- Acuña OY, Acuña BO, Cobo EA, Pinzón LC and Albesinano LE (2022) Producción láctea y quesera, municipio de Paipa en el contexto de la “seguridad alimentaria”. *Sociedad y Economía* 47: 1-23. <https://doi.org/10.25100/sye.v0i47.11382>
- Alviz-Amador A, Galindo-Murillo R, Pineda-Alemán R and Pérez-González H (2019) 4-HNE carbonylation induces local conformational changes on bovine serum albumin and thioredoxin. A molecular dynamics study. *Journal of Molecular Graphics & Modelling* 86: 298–307. <https://doi.org/10.1016/j.jmgm.2018.11.001>
- Beltrán MC, Romero T, Althaus RL and Molina MP (2013) Evaluation of the Charm maximum residue limit  $\beta$ -lactam and tetracycline test for the detection of antibiotics in ewe and goat milk. *Journal of Dairy Science* 96(5): 2737–2745. <https://doi.org/10.3168/jds.2012-6044>
- Chaneton L, Pérez Sáez J and Bussmann L (2011) Antimicrobial activity of bovine  $\beta$ -lactoglobulin against mastitis-causing bacteria. *Journal of Dairy Science* 94: 138–145. <https://doi.org/10.3168/jds.2010-3319>
- Crowther JM, Allison JR, Smolenski GA, Hodgkinson AJ, Jameson GB and Dobson R (2018) The self-association and thermal denaturation of caprine and bovine  $\beta$ -lactoglobulin. *European biophysics journal* 47: 739–750. <https://doi.org/10.1007/s00249-018-1300-8>
- Ding X, Yang Y, Zhao S et al (2011) Analysis of  $\alpha$ -lactalbumin,  $\beta$ -lactoglobulin A and B in whey protein powder, colostrum, raw milk, and infant formula by CE and LC. *Dairy Science & Technology* 91: 213–225. <https://doi.org/10.1007/s13594-011-0006-9>
- Estévez M and Luna C (2017) Dietary protein oxidation: A silent threat to human health? *Critical Reviews in Food Science and Nutrition* 57: 3781–3793. <https://doi.org/10.1080/10408398.2016.1165182>
- FAO – Food and Agriculture Organization of the United Nations (2024) Composición de la leche. Organización de las Naciones Unidas para la Alimentación y la Agricultura. <https://www.fao.org/dairy-production-products/products/milk-composition/es>
- FAO - Food and Agriculture Organization of the United Nations and WHO - World Health Organization (2023) Codex Alimentarius: Norma general para los contaminantes y las toxinas presentes en los alimentos y piensos (1993). <https://www.fao.org/fao-who-codexalimentarius/codex-texts/list-standards/en/>
- Ghasemi M, Habibian S and Farhadian S (2024) Change in thermal stability and molecular structure characteristics of whey protein beta-lactoglobulin upon the interaction with levamisole hydrochloride. *Food Chemistry* 431: 137073. <https://doi.org/10.1016/j.foodchem.2023.137073>
- Giannetti A, Toschi G, Ricci G, Miniaci A, Di Palma E and Pession A (2021) Cow's milk protein allergy as a model of food allergies. *Nutrients* 13: 1525. <https://doi.org/10.3390/nu13051525>
- Golebiowski A, Pomastowski P, Rodzik A, Król-Górniak A et al (2020) Isolation and self-association studies of beta-lactoglobulin. *International Journal of Molecular Sciences* 21:9711. <https://doi.org/10.3390/ijms21249711>
- Habibian-Dehkordi S, Farhadian S, Ghasemi M and Evini M (2022) Insight into the binding behavior, structure, and thermal stability properties of  $\beta$ -lactoglobulin/Amoxicillin complex in a neutral environment. *Food Hydrocolloids* 133: 107830. <https://doi.org/10.1016/j.foodhyd.2022.107830>
- Kontopidis G, Holt C and Sawyer L (2002) The ligand-binding site of bovine beta-lactoglobulin: evidence for a function?. *Journal of Molecular Biology* 318: 1043–1055. [https://doi.org/10.1016/S0022-2836\(02\)00017-7](https://doi.org/10.1016/S0022-2836(02)00017-7)
- Madureira AR, Pereira CI, Gomes AM, Pintado ME and Xavier Malcata F (2007) Bovine whey proteins – Overview on their main biological properties. *Food Research International* 40: 1197–1211. <https://doi.org/10.1016/j.foodres.2007.07.005>
- Marquez J, Padilla AM, Cuadro DM and Cavallo ER (2021) Residues of tetracyclines and  $\beta$ -lactams antibiotics induce carbonylation of chicken breast. *F1000Research* 10: 575. <https://doi.org/10.12688/f1000research.53863.1>
- Márquez Lázaro JP, Mora L, Méndez Cuadro D, Rodríguez Cavallo E and Toldrá F (2022) *In vitro* oxidation promoted by sarafloxacin antibiotic residues on myosin and chicken meat proteins. *Journal of Food Composition and Analysis* 111: 104622. <https://doi.org/10.1016/j.jfca.2022.104622>
- Marrugo-Padilla A, Méndez-Cuadro D and Rodríguez-Cavallo E (2022) Tetracycline residues induce carbonylation of milk proteins and alter their solubility and digestibility. *International Dairy Journal* 125: 105226. <https://doi.org/10.1016/j.idairyj.2021.105226>
- Marrugo-Padilla A, Méndez-Cuadro D and Rodríguez-Cavallo E (2020) Combined tetracycline and pyrethroid residues increases protein carbonylation in bovine milk. *International Dairy Journal* 107: 104708. <https://doi.org/10.1016/j.idairyj.2020.104708>
- Mendoza JA, Vera YA and Peña LC (2017) Prevalencia de mastitis subclínica, microorganismos asociados y factores de riesgo identificados en hatos de la provincia de Pamplona, Norte de Santander. *Revista de la Facultad de Medicina Veterinaria y de Zootecnia* 64(2): 11-24. <https://doi.org/10.15446/rfmvz.v64n2.67209>
- Mestorino ON, Lucas MF, Daniele MR and Errecalde JO (2008) Perfil de eliminación en leche de la asociación cefalexina-neomicina tras su administración por vía intramamaria. *Revista del Colegio de Veterinarios de la Provincia de Buenos Aires* 42: 31–35. <http://sedici.unlp.edu.ar/handle/10915/152241>
- Ministerio de Salud y Protección Social (2013) Resolución 1382 de 2013: Por la cual se establecen los límites máximos para residuos de medicamentos veterinarios en los alimentos de origen animal, destinados al consumo humano (Diario Oficial No. 48.779).
- Mukherjee M, Saha Sardar P, Roy P et al (2018) Antenna effect and phosphorescence spectra to find the location of drug tetracycline in bovine  $\beta$ -lactoglobulin A. *JBIC Journal of Biological Inorganic Chemistry* 23: 917–927. <https://doi.org/10.1007/s00775-018-1591-3>
- Muñoz S, Méndez L, Dasilva G, Torres JL et al (2018) Targeting hepatic protein carbonylation and oxidative stress occurring on diet-induced metabolic diseases through the supplementation with fish oils. *Marine Drugs* 16: 353. <https://doi.org/10.3390/md16100353>
- Paredes V (2010) Farmacología veterinaria (Tomo II, 1ra ed.). Editorial Universidad Nacional Agraria.
- Sachi S, Ferdous J, Sikder M and Hussani S (2019) Antibiotic residues in milk: Past, present, and future. *Journal of Advanced Veterinary and Animal Research* 6: 315. <https://doi.org/10.5455/javar.2019.f350>
- SIC - Superintendencia de Industria y Comercio (2021) Pérdidas en la industria láctea por los bajos controles de mastitis. <https://www.sic.gov.co/>



Stevenson MA (2021) Sample size estimation in veterinary epidemiologic research. *Frontiers in Veterinary Science* 7: 539573. <https://doi.org/10.3389/fvets.2020.539573>

Tarazona-Manrique LE, Vargas-Abella JC and Andrade-Becerra RJ (2024) Antibiotic resistance profile of Coagulase-negative staphylococci species isolated from subclinical mastitis in Colombian dairy herds.

*Revista de Investigación Veterinaria del Perú (RIVEP)*, 35: e29246. <http://doi.org/10.15381/rivep.v35i5.29246>

Varlamova EG and Zaripov OG (2020) Beta-lactoglobulin-nutrition allergen and nanotransporter of different nature ligands therapy with therapeutic action. *Research in Veterinary Science* 133: 17–25. <https://doi.org/10.1016/j.rvsc.2020.08.014>

---

# Root colonization of tamarind tree (*Tamarindus indica* L.) and occurrence of arbuscular mycorrhizal fungi in soils – Sopetrán, Antioquia

Colonización de raíces de tamarindo (*Tamarindus indica* L.) y ocurrencia de hongos micorrízicos arbusculares en los suelos – Sopetrán, Antioquia

<https://doi.org/10.15446/rfnam.v78n3.113960>

Sandra Muriel Ruiz<sup>1\*</sup>, Valentina Restrepo-Cossio<sup>1</sup>, Estefanía Martínez Olier<sup>1</sup> and Marcelo Betancur Agudelo<sup>2</sup>

## ABSTRACT

### Keywords:

AMF diversity  
Native agroecosystems  
Rhizosphere  
Soil microorganisms  
Symbiotic associations  
Tropical dry forest


The tamarind tree (*Tamarindus indica* L.) is a multipurpose species, primarily used in the food and medical industries, cultivated by traditional growers who do not employ a fertilization process in their crop fields. In Colombia, few studies have related the presence of this plant in low-fertility soils to the colonization of arbuscular mycorrhizal (AM) fungi. This study aims to know the AMF associated with the rhizosphere of tamarind trees in the tropical dry forest from the Western Antioquia region, and to establish the AMF colonization of the roots. For this purpose, samples of the rhizosphere and roots from a production plot were taken, spores were extracted and morphotype identification was made, and after slide mounting, the spores were described under the microscope based on their morphological characteristics and identified using specialized identification keys. In the previously decolorized and dyed roots, the fungi colonization was determined, distinguishing hyphae, arbuscules and vesicles presence. Fifteen species of AMF were described, 53% of them belonging to the Glomeraceae family and 20% to the Acaulosporaceae family. The mycorrhizal colonization was observed in 50% of samples, hyphae were found in 39%, arbuscules in 31%, and vesicles in 14%. This record is higher than other reports on *T. indica*, which may indicate the importance of this symbiosis for the plant in traditional production systems studied.


## RESUMEN

### Palabras clave:

Diversidad de HMA  
Agroecosistemas nativos  
Rizosfera  
Microorganismos del suelo  
Asociaciones simbióticas  
Bosque seco tropical

El tamarindo (*Tamarindus indica* L.) es una especie multipropósito, usada principalmente con fines alimenticios y medicinales, cultivada por productores tradicionales, quienes no realizan fertilización del cultivo. En Colombia hay pocos estudios que relacionen la presencia de estas plantas en suelos de baja fertilidad natural y la colonización por hongos micorrízicos arbusculares (HMA). Este trabajo tuvo como objetivo conocer los HMA asociados a la rizosfera de árboles de *T. indica*, en el bosque seco tropical del occidente cercano de Antioquia y establecer la colonización de HMA de las raíces. Para ello se tomaron muestras de rizosfera y raíces de un lote en producción, se hizo extracción de esporas para su separación por morfotipo, luego del montaje las esporas fueron descritas en sus características morfológicas en microscopio y determinadas con claves especializadas. En las raíces previamente decoloradas y teñidas se determinó la colonización por los hongos, discriminando la presencia de hifas, arbuscúlos y vesículas. Se describieron 15 especies de HMA, un 53% de ellas pertenecientes a Glomeraceae y 20% a Acaulosporaceae. La colonización micorrícica encontrada fue de 50%, en el 39% de las muestras se hallaron hifas, en el 31% arbuscúlos y en el 14% vesículas. Este registro es mayor a otros reportes en *T. indica*, esto puede ser indicativo de la importancia de esta simbiosis para la planta en los sistemas de producción tradicionales estudiados.

<sup>1</sup>Politécnico Colombiano Jaime Isaza Cadavid, Medellín, Colombia. [sbmuriel@elpoli.edu.co](mailto:sbmuriel@elpoli.edu.co) , [valentinacossio22@gmail.com](mailto:valentinacossio22@gmail.com) , [korzolier@gmail.com](mailto:korzolier@gmail.com) 

<sup>2</sup>Universidad de Caldas, Manizales, Colombia. [marcelo.betancur@ucaldas.edu.co](mailto:marcelo.betancur@ucaldas.edu.co) 

\*Corresponding author

**T***amarindus indica* L. is a species from the monotypic genus *Tamarindus* (subfamily Detarioideae, family Fabaceae) (LPWG 2017), native from tropical Africa (Van der Stege et al. 2011), cultivated in tropical and subtropical regions of the world (Kareem et al. 2023). The tamarind is a long-lived tree that can reach heights of up to 30 meters and produce fruit for up to 200 years (Bahru et al. 2014; Ndiaye et al. 2022). It is considered a multipurpose species, as all its parts are usable. In Western Africa, the tree is attributed to up to 250 different uses, making it an essential resource for the survival of many people (Van der Stege et al. 2011). These uses span a wide array of categories, including—but not limited to—food, medicine, spirituality, ethnoveterinary applications, industrial uses, human and animal welfare (e.g., relief from heat and radiation), and wood utilization, either as an energy source or for cabinetmaking (Muriel et al. 2021; Zeleke 2022). Studies on its chemical composition underscore tamarind's nutritional value due to its content of amino acids, vitamins, proteins, minerals, and bioactive compounds, particularly its high concentration of tartaric acid (Bhadoriya et al. 2011).

In Colombia, tamarind is cultivated in the departments of Antioquia and Atlántico (Agronet 2021); however, production remains secondary and is characterized by low levels of technification. The western region of Antioquia, located within the tropical dry forest (T-df) ecosystem, has traditionally been a tamarind-producing area. There the trees can be in silvopastoral systems, like trees scattered through paths, pasturelands, vegetable patches, and backyards in urban houses that are seldom harvested or managed (Álvarez et al. 2015). The fruit is the most used part of the plant in the production of sweets, sauces and juices, which are offered to the region's tourists (Álvarez et al. 2015). This constitutes the main economic support to the individuals dedicated to the manufacture and selling of tamarind sweets. Nonetheless, increasing land demand for other uses has led to the falling of tamarind trees, resulting in a local demand for the fruit that exceeds its supply. This situation highlights the need to promote and expand its cultivation.

The tamarind tree is well adapted to semi-arid tropical regions and is capable of withstanding drought conditions. It can grow in a wide variety of soils; however, it thrives best in deep, well-drained soils that are slightly acidic or saline

(Bhadoriya et al. 2011). Although there are no studies about the appropriate soil features for the tamarind farming, it has been reported to establish relationships with mycorrhizal fungi and nitrifying bacteria (Parrotta 2000; Bourou et al. 2010); therefore, it is expected that soils with a significant presence of organic matter, could offer the right setting to foster the development of plants. Within the important organisms for crop nutrition, the arbuscular mycorrhizal fungi (AMF) can benefit their host, mainly by increasing the absorption of water and soil nutrients, such as phosphate ions which are relatively still, due to the fungus mycelium capacity to grow beyond the phosphorus depletion zone and to develop rapidly around the root (Smith and Read 2008; Rini et al. 2020). Moreover, the AMF protects the plant from soil pathogens, from stress conditions and provides regulation of hydric interactions.

Regarding *Tamarindus indica*, few studies link the role of AMF with the presence of trees in low fertility soils. In one of these studies, Bourou et al. (2010) characterized the diversity of AMF associated with the tamarind rhizosphere in three agroecological zones in Senegal, finding species of the genera *Acaulospora*, *Glomus* and *Scutellospora* and a higher mycorrhization in soils under poor conditions or exposed to drought. AMF studies have been carried out mostly in India and Africa; in Colombia, there is only one study that has been documented about the case of AMF associated with *Tamarindus indica* cultivations (Arcos 2015), in which it is pointed out the presence of 10 morphotypes, from which 40% corresponded to *Acaulospora* and 30% to *Glomus*. Understanding the role of this symbiosis in the establishment of new crop plants is important, as it may facilitate the growth of tamarind seedlings (Waddar and Lakshman 2010; Kareem et al. 2023). In consequence, this study aimed to identify the AMF associated with the tamarind trees' rhizosphere, and to determine their root colonization.

## MATERIALS AND METHODS

### Study site

The study was carried out in a *T. indica* L. productive lot from Los Comunes farm, located in 'El Llano de Montaña' village in the municipality of Sopetrán (Antioquia, Colombia, coordinates 06°29'44.6" N 75°45'55.2" W). The climatic conditions of the location were consistent with tropical dry forest according to Holdridge (1987), with an average temperature of 27.6 – 29 °C, annual precipitation of

1,097 mm and 73.2% humidity (Álvarez et al. 2015). In the study, tamarind trees were about 40 years old, under a traditional silvopastoral cropping system, with periodic irrigation, since to rainless periods take place in the tropical dry forest. Plants were not fertilized, and minimal management activity was carried out. In a physicochemical

soil analysis conducted before starting fieldwork, it was established that the soil had a clay loam texture, with a pH of 6.2%, organic material content of 8.8% and 15 mg kg<sup>-1</sup> of P content (Table 1). In addition, the soil was rich in organic matter, with a high salt content and a medium level of phosphorus, which are conditions for growing tamarind trees.

**Table 1.** Los Comunes farm physicochemical soil analysis (El Llano de Montaña village, Sopetrán municipality).

Variable	Units	Value	Interpretation
Sand	%	34	Soil class: Clayey
Clay	%	24	
Silt	%	42	
pH	-	6.2	Slightly acidic
O.M.	%	8.8	High
Al	cmolc kg <sup>-1</sup>	0	-
Ca	cmolc kg <sup>-1</sup>	16.4	High
Mg	cmolc kg <sup>-1</sup>	9.9	High
K	cmolc kg <sup>-1</sup>	2.55	Medium
Na	cmolc kg <sup>-1</sup>	0.14	Low
CECe	cmolc kg <sup>-1</sup>	28.99	High
P	mg kg <sup>-1</sup>	15	Medium
S	mg kg <sup>-1</sup>	1.6	Low
Fe	mg kg <sup>-1</sup>	30	Medium
Mn	mg kg <sup>-1</sup>	5	Medium
Cu	mg kg <sup>-1</sup>	4	High
Zn	mg kg <sup>-1</sup>	3	High
B	mg kg <sup>-1</sup>	0.2	Medium

O.M.: Organic matter; CECe: Effective cation exchange capacity.

### Field sampling

To extract spores and perform morphological identification of arbuscular mycorrhizal fungi (AMF), soil samples were collected from the rhizosphere of seven trees at a depth of 20 cm. To determine the percentage of AMF colonization, the thinnest tertiary roots from five trees were gathered. The sampling was completely random. Then, samples were stored and refrigerated at 4 °C and then taken to the laboratory for post-processing.

### Spore extraction and AMF slide mounting

First, spores were extracted through humid sieving and sucrose gradient centrifugation (Gerdemann and Nicolson 1963). Then, spores were separated using a

light microscope and according to size, shape, color and hyphae accessory characteristics. Next, spores were mounted on microscope slides with PVLG (Polyvinyl-lactoglycerol) mixed with Melzer (1:1 v/v). Finally, slides were stored at 35 °C for 3-4 days for fixation (Stürmer and Siqueira 2011).

### Determination of morphotypes

Spore phenotypes were compared with original studies available in Glomeromycota-PHYLOGENY (<http://www.amf-phylogeny.com/>) and online references of species' descriptions from the International Collection of Arbuscular Mycorrhizal Fungi - INVAM from the West Virginia University, USA (<https://invam.wvu.edu>) and the Department of Plant

Protection of the Agricultural University of Szczecin, Poland (<http://www.zor.zut.edu.pl/Glomeromycota/index.html>). Correct names of the species were verified by Index Fungorum (<http://www.indexfungorum.org/>).

### Analysis of AMF species richness

Species richness was calculated as the number of AMF species identified from field samples and trap culture. The frequency of occurrence (F) was calculated by the equation  $F = (J_i/K) \times 100$ , where F is the frequency of species I,  $J_i$  is the number of samples in which the species was detected, and K is the total number of samples. Species frequency was classified as dominant ( $85\% \leq FO \leq 100\%$ ), very common ( $50\% \leq FO < 85\%$ ), common ( $30\% \leq FO < 50\%$ ) and rare ( $FO < 30\%$ ), according to Zhang et al. (2004).

### Determination of AMF colonization

The root staining and discoloration method described by Koske and Gemma (1989) was used. Since *T. indica* roots are characterized as being woody and reddish, the method was adapted and roots were submerged for 1 hour in 20% of KOH at 90 °C, 20 minutes in 1% hypochlorite, and 5 minutes in 10% of HCL. Lastly, roots were immersed in 0.05% trypan blue to stain internal tissues, as well as AMF vesicles and arbuscules present inside the tree roots. The percentage of colonization was determined in samples

taken from five trees, through the microscope slide intersection method, using one slide per sample (McGonigle et al. 1990). In this method, roots were aligned parallel to the long axis of the slide and observed at 200x magnification. The number of intersections was examined by counting arbuscules, vesicles and hyphae. This procedure was repeated in 12 visual fields of root simples from each tree.

## RESULTS AND DISCUSSION

A total of 15 AMF species associated with tamarind (*Tamarindus indica*) crop soils were identified and are listed with their abundances in Table 2. Of the species found, 53% belonged to the Glomeraceae family, 20% to the Acaulosporaceae, and 13% to the Diversisporaceae. In terms of genus-level diversity, *Glomus* was the most abundant, representing 33% of the identified species, followed by *Acaulospora*, *Diversispora*, and *Rhizophagus*, each accounting for 13% of the total species (Figure 1). The average percentage of colonized trees was of 50%, and regarding the observed structures in the microscope's visual field, 39% were found with hyphae, 31% with arbuscules and 14% with vesicles (Figure 2). On the other hand, the present investigation found that in the roots of *T. indica* evaluated, there were other structures corresponding to dark septate endophytes, which are also part of the rhizosphere.

**Table 2.** Occurrence frequency and global frequency (F%) of arbuscular mycorrhizal fungus species in soil around of trees of *Tamarindus indica* trees in the municipality of Sopetrán.

ID	Family	Species	Size / diameter spore (µm)	Characteristics & INVAM spore color	Frequency of occurrence	F (%)
a	Acaulosporaceae	<i>Acaulospora aff. delicata</i>	100	Globose spore, color (0-10/40-0 melon color)	R	14.29
b	Acaulosporaceae	<i>Acaulospora aff. denticulata cf.</i>	58 to 60	Globose spore, color (0-20/80-0 RGB orange color)	C	42.86
c	Acaulosporaceae	<i>Entrophospora aff. infrequens</i>	120 to 130	Globose spore to subglobose, color (0-10/40-0 melon color)	R	14.29
d	Claroideoglomeraceae	<i>Claroideoglomus aff. etunicatum</i>	110 to 140	Globose spore to ovoid, color (0-40/100-10 orange color)	MC	71.43
e	Diversisporaceae	<i>Diversispora sp1 cf.</i>	90	Globose spore to subglobose, color (0-0/20-0 light yellow color)	R	14.29
f	Diversisporaceae	<i>Diversispora sp2 cf.</i>	70	Globose spore to subglobose, color (0-0/50-0 pale orange color)	R	14.29



Table 2

ID	Family	Species	Size / diameter spore (µm)	Characteristics & INVAM spore color	Frequency of occurrence	F (%)
g	Glomeraceae	<i>Funnelliformis geosporum</i>	130 to 140	Globose spore to ovoid, color (0-10/20-10 yellow color)	R	14.29
h	Glomeraceae	<i>Glomus</i> aff. <i>macrocarpum</i>	120	Globose spore to subglobose, color (0-60/70-10 mid orange color)	R	28.57
i	Glomeraceae	<i>Glomus glomerulatum</i>	56	Globose spore to subglobose, color (20-20/40-0 persian orange color)	MC	57.14
j	Glomeraceae	<i>Glomus rubiforme</i>	40 to 50	Ovoid spore to subglobose, color (0-30/70-10 mandarin color)	C	42.86
k	Glomeraceae	<i>Glomus</i> sp1	150	Globose spore, (20/100-0 yellow color)	D	85.71
l	Glomeraceae	<i>Glomus</i> sp2 aff. <i>badium</i>	80	Globose spore to ovoid, color (0-40/50-10 ochre color)	R	28.57
m	Glomeraceae	<i>Rhizophagus</i> aff. <i>clarus</i>	50 to 71	Globose spore to ovoid, color (0-10/30-10 melon color)	MC	57.14
n	Glomeraceae	<i>Rhizophagus</i> sp1.	70	Globose spore to subglobose, color (0-30/70-10 mandarin color)	R	14.29
o	Paraglomeraceae	<i>Paraglomus</i> aff. <i>occultum</i>	70	Globose spore to avoid, color (0-0/10-0 light yellow color)	R	14.29

D = dominant ( $85\% \leq FO \leq 100\%$ ), VC = very common ( $50\% \leq FO < 85\%$ ), C = common ( $30\% \leq FO < 50\%$ ), R = rare ( $FO < 30\%$ ) (Zhang et al. 2004).

Bourou et al. (2010) documented to AMF colonization ranging from 3.9 to 11% of the roots of *T. indica* trees, with higher colonization rates in trees established on soils under poor conditions and subjected to drought. In the present study, the colonization percentage found was significantly greater (50%) than that reported by Arcos (2015), who also assessed trees from the same region as those evaluated in this study and found 12% of colonization. Some authors report that differences in the colonization percentage may be influenced by a series of environmental and functional factors such as host, regional location, temperatures, rain and the availability of nutrients to soils (Smith and Read 2008). It is possible that the tamarind crops particular conditions in this case, such as medium phosphorous content, limited availability of water, high competence with unwanted plants and the absence of other farming practices, set out an environment in which some AMF are adapted to tolerate stress conditions, in the sense suggested by Chagnon

et al. (2013). Different mechanisms have been proposed to explain physiological, molecular and morphological changes in symbiotic plants when overcoming the effects of water stress. These mechanisms explain how the plants survive and maintain vigorous growth under the aforementioned conditions (Abdelmalik et al. 2020; Cheng et al. 2021). Jiménez (2019) demonstrated that tamarind seedlings inoculated with *Glomus* commercial had a greater amount of dry matter in roots and aerial parts than non-inoculated seedlings, as well as a faster recovery when seedlings were attacked by leaf-cutting ants.

In this study, a higher percentage of the genus *Glomus* associated with tamarind was found, while Arcos (2015) found a higher presence of *Acaulospora*. These two genera are abundant in tropical soil (Peña-Venegas et al. 2007; Cofré et al. 2019). Additionally, they contain species that have been reported to be associated with plants exposed to episodes of drought (Lenoir et al. 2016; Bahadur et al. 2019).

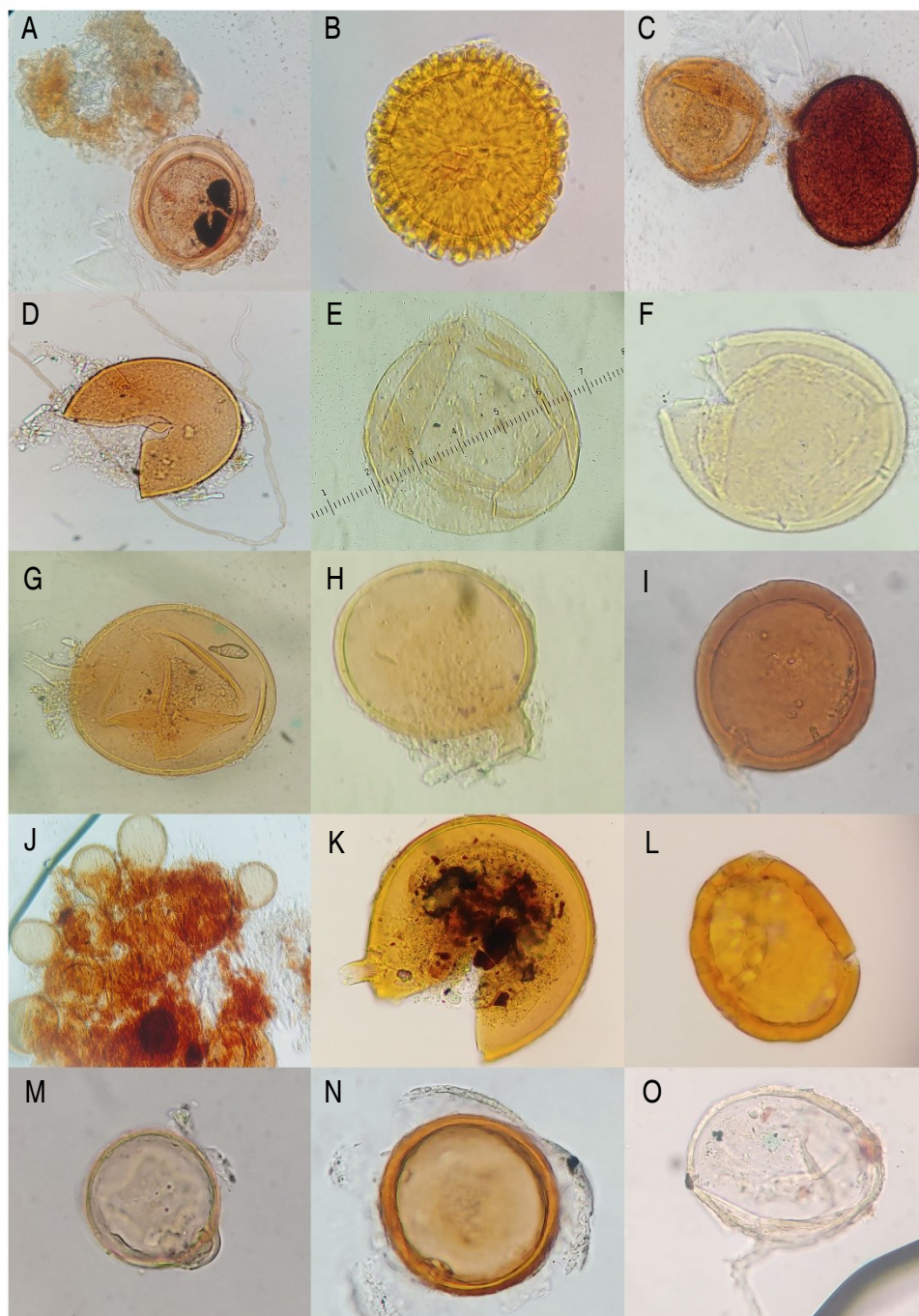


**Figure 1.** *Tamarindus indica* spore diversity in Sopetrán municipality, Antioquia - Colombia. **A.** *Acaulospora* aff. *delicata*, **B.** *Acaulospora* aff. *denticulata* cf., **C.** *Entrophospora* aff. *Infrequens*, **D.** *Claroideoglossum* aff. *etunicatum* cf., **E.** *Diversispora* sp1 cf., **F.** *Diversispora* sp2 cf., **G.** *Funneliformis* geosporum, **H.** *Glomus* aff. *macrocarpum*, **I.** *Glomus* glomerulatum, **J.** *Glomus* rubiforme, **K.** *Glomus* sp1, **L.** *Glomus* sp2 aff. *badium*, **M.** *Rhizophagus* aff. *clarus*, **N.** *Rhizophagus* sp1 and **O.** *Paraglossum* aff. *occultum*.

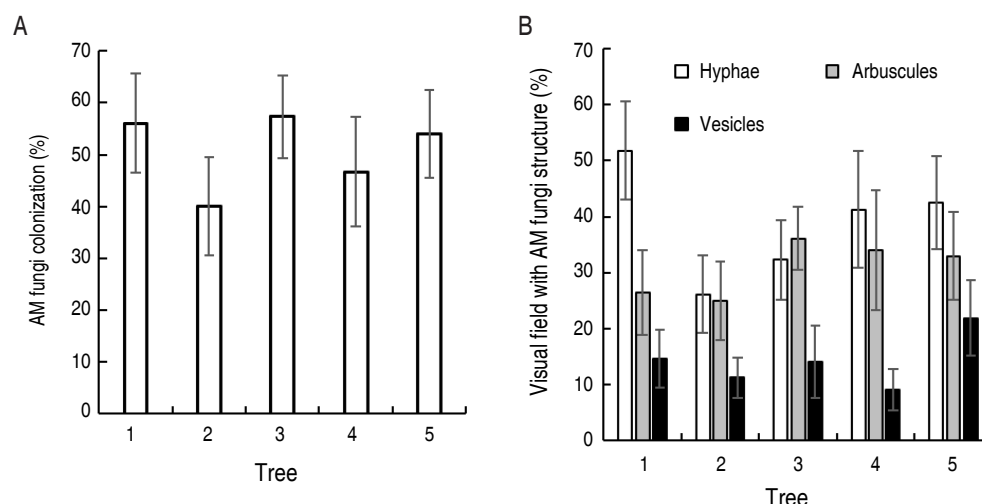


**Figure 2.** Tamarind roots colonized by AM fungi. **A.** Colonization and **B.** Microscope visual field with AMF presence.

## CONCLUSION

*Tamarindus indica* is a species that establishes symbiotic connections with a great variety of AM fungi, specifically those from the genera *Glomus* and *Acaulospora* in the tropical dry forest of Western Antioquia. The percentage of AMF colonization highlights its importance to tamarind plants in an environment prone to recurring drought. Future research could focus on defining mycorrhizal dependence, exploring its interaction with nitrifying bacteria and confirming the species identity through molecular techniques.

## CONFLICT OF INTEREST

The authors express that they do not have any conflict of interest.

## REFERENCES

- Abdelmalik A, Alsharani T, Al-Qarawi AA, Ahmed A and Aref I (2020) Response of growth and drought tolerance of *Acacia seyal* Del. seedlings to arbuscular mycorrhizal fungi. *Plant, Soil and Environment* 66: 264-271. <https://doi.org/10.17221/206/2020-PSE>
- Agronet- Red de información y comunicación del sector agropecuario colombiano (2021) Reporte: Área, Producción y Rendimiento Nacional por Cultivo. <https://www.agronet.gov.co/estadistica/paginas/home.aspx?cod=1>
- Álvarez VM, Muriel SB and Osorio N (2015) Plantas asociadas al turismo y los sistemas tradicionales de manejo en el occidente cercano antioqueño (Colombia). *Ambiente y Desarrollo* 19: 67-82. <https://doi.org/10.11144/Javeriana.ayd19-37.pats>
- Arcos D (2015) Evaluación de hongos formadores de micorriza arbuscular (HMA), en cuatro especies vegetales promisorias, en el Departamento de Antioquia. (Tesis de pregrado) Politécnico Colombiano

Jaime Isaza Cadavid. Medellín, Colombia. 88 p.

Bahadur A, Batool A, Nasir F, Jiang S et al (2019) Mechanistic insights into arbuscular mycorrhizal fungi-mediated drought stress tolerance in plants. *International Journal of Molecular Sciences* 20: 4199. <https://doi.org/10.3390/ijms20174199>

Bahru T, Eshete A, Mulatu Y, Kebede Y, Tadesse W et al (2014) Effect of provenances on seed germination, early survival and growth performance of *Tamarindus indica* L. in Ethiopia: A key multipurpose species. *Advances in Science and Engineering: An International Journal (MSEJ)* 1: 1-8.

Bhadoriya SS, Ganeshpurkar A, Narwaria J, Rai G and Jain AP (2011) *Tamarindus indica*: Extent of explored potential. *Pharmacognosy Review* 5: 73-81. <https://doi.org/10.4103/0973-7847.79102>

Bourou S, Ndiaye F, Diouf M, Diop T and Damme PV (2010) Tamarind (*Tamarindus indica* L.) parkland mycorrhizal potential within three agro-ecological zones of Senegal. *Fruits* 65: 377-385. <https://doi.org/10.1051/fruits/2010032>

Chagnon P, Bradley R, Maherali H and Klironomos J (2013) A trait-based framework to understand life history of mycorrhizal fungi. *Trends in Plant Science* 18: 484-491. <http://doi.org/10.1016/j.tplants.2013.05.001>

Cheng S, Zou YN, Kuča K, Hashem A, Abd\_Allah EF and Wu QS (2021) Elucidating the mechanisms underlying enhanced drought tolerance in plants mediated by arbuscular mycorrhizal fungi. *Frontiers in Microbiology*, 12, 809473. <https://doi.org/10.3389/fmicb.2021.809473>

Cofré MN, Soteras F, Iglesias MR, Velázquez S, Abarca C et al (2019) Biodiversity of arbuscular mycorrhizal fungi in South America: A review. Pp. 49-72- In: Pagano MC and Lugo MA (eds.). *Mycorrhizal Fungi in South America*. Springer, Berlin.

Gerdemann JW and Nicolson TH (1963) Spores of mycorrhizal Endogone species extracted from soil by wet sieving and decanting. *Transactions of The British Mycological Society* 46: 235-244. [https://doi.org/10.1016/S0007-1536\(63\)80079-0](https://doi.org/10.1016/S0007-1536(63)80079-0)

Holdridge LR (1987) *Ecología basada en zonas de vida*. Agroamérica. Costa Rica.

Jiménez JP (2019) *Crecimiento y desarrollo de plántulas de*

tamarindo (*Tamarindus indica* L.) y zapote (*Matisia cordata* Bonpl.) asociadas a hongos arbusculares. (Tesis de pregrado) Politécnico Colombiano Jaime Isaza Cadavid. Medellín, Colombia. 51 p.

Kareem AA, Ogunwande OA, Olaitan OA and Oyelowo OJ (2023) Influence of arbuscular mycorrhiza on the growth potential of *Tamarindus indica* L. seedlings. Journal of the Cameroon Academy of Sciences 19: 141-148. <https://doi.org/10.4314/jcas.v19i2.3>

Koske RE and Gemma JN (1989) A modified procedure for staining roots to detect VA mycorrhizas. Mycological Research 92: 486-488. [https://doi.org/10.1016/S0953-7562\(89\)80195-9](https://doi.org/10.1016/S0953-7562(89)80195-9)

Lenoir I, Fontaine J and Sahraoui AL (2016) Arbuscular mycorrhizal fungal responses to abiotic stresses: A review. Phytochemistry 123: 4-15. <https://doi.org/10.1016/j.phytochem.2016.01.002>

McGonigle TP, Miller MH, Evans DG, Fairchild GL and Swan JA (1990) A new method which gives an objective measure of colonization of roots by vesicular—arbuscular mycorrhizal fungi. New Phytologist 115: 495-501. <https://doi.org/10.1111/j.1469-8137.1990.tb00476.x>

Muriel SB, Vélez LD, Álvarez - Osorio VM, Aguilar M, Correa C, Gómez A and Arias E (2021) Las plantas promisorias y los sistemas tradicionales de producción del bosque seco tropical en el occidente cercano antioqueño. Editorial Universidad Nacional de Colombia. 70 p. ISBN 978-958-794-707-6

Ndiate In, Qun CL and Nkoh JN (2022) Importance of soil amendments with biochar and/or Arbuscular Mycorrhizal fungi to mitigate aluminum toxicity in tamarind (*Tamarindus indica* L.) on an acidic soil: A greenhouse study. Heliyon 8: E09009. <https://doi.org/10.1016/j.heliyon.2022.e09009>

Parrotta JA (2000) *Tamarindus indica* L. Tamarindo. pp. 519-523. In: Native and Exotic Trees of Puerto Rico and the Caribbean Islands. Francis JK and Lowe CA (eds.). U.S. Department of Agriculture, Forest Service, International Institute of Tropical. Rio Piedras.

Peña-Venegas CP, Cardona GI, Arguelles JH and Arcos AL

(2007) Micorrizas arbusculares del sur de la amazonia colombiana y su relación con algunos factores fisicoquímicos y biológicos del suelo. Acta Amazónica 37: 327-336. <https://doi.org/10.1590/S0044-59672007000300003>

Rini MV, Susilowati E, Riniarti M and Lukman I (2020) Application of *Glomus* sp. and a mix of *Glomus* sp. with *Gigaspora* sp. in improving the Agarwood (*Aquilaria malaccensis* Lamk.) seedling growth in Ultisol soil. Earth and Environmental Science 449: 012004. <https://doi.org/10.1088/1755-1315/449/1/012004>

Smith SE and Read DJ (2008) Mycorrhizal symbiosis. Third edition. Academic Press, London.

Stürmer SL and Siqueira JO (2011) Species richness and spore abundance of arbuscular mycorrhizal fungi across distinct land uses in Western Brazilian Amazon. Mycorrhiza 21: 255-267. <https://doi.org/10.1007/s00572-010-0330-6>

LPWG - The Legume Phylogeny Working Group (2017) <https://www.legumedata.org/working-groups/phylogenetics/>

Van der Stege C, Prehler S, Hartl A and Reinhard C (2011) Tamarind (*Tamarindus indica* L.) in the traditional West African diet: not just a famine food. Fruits 66: 171-185. <https://doi.org/10.1051/fruits/2011025>

Waddar KH and Lakshman HC (2010) Effect of AM fungi on seedlings of *Tamarindus indica* L. and *Azadirachta indica* Juss for integrated nursery stock. International Journal of Plant Protection 3: 248-252.

Zelege AG (2022) Underutilized non timber forest products in Ethiopia; socioeconomic, status and yield potential (Doctoral dissertation), Universidad de Valladolid. Valladolid, España.

Zhang Y, Guo L-D and Liu R-J (2004) Survey of arbuscular mycorrhizal fungi in deforested and natural forest land in the subtropical region of Dujiangyan, southwest China. Plant and Soil 261:257-263. <https://doi.org/10.1023/B:PLSO.0000035572.15098.f6>



# Woody Plant Medium optimizes *in vitro* germination and development of *Calycophyllum spruceanum*

Woody Plant Medium optimiza la germinación y el desarrollo de *Calycophyllum spruceanum* *in vitro*

<https://doi.org/10.15446/rfnam.v78n3.119370>

Antony Cristhian Gonzales-Alvarado<sup>1,2\*</sup>, Nilda Hilario-Román<sup>3</sup>, Jorge Manuel Revilla-Chávez<sup>4</sup>,  
Cristian Richard Saico Cope<sup>5</sup> and Jorge Arturo Mori-Vásquez<sup>1</sup>

## ABSTRACT

**Keywords:**

Agar  
Capirona  
Culture media  
Environmental restoration  
Rubiaceae


Climate change and biodiversity loss pose critical threats to ecosystems, making reforestation with native species an attractive mitigation strategy. However, seedling production systems need to be optimized. This study aimed to evaluate the effect of different culture media and concentrations on the germination and *in vitro* morphological development of *Calycophyllum spruceanum*. A completely randomized design with five treatments was used: 100% Murashige and Skoog (MS), 50% MS, 100% Woody Plant Medium (WPM), 50% WPM, and a control treatment (agar), with seven replicates per treatment. Germination parameters were evaluated for 21 days, and morphological development at 70 days. The main results showed that WPM and agar obtained the highest germination percentages (73.33 and 75.24%, respectively) and germination rate (2.02 and 2.32 seeds per day, respectively), while WPM stood out in terms of final germination time. In morphological development, WPM recorded the highest values for number of leaves (8.18), nodes (5.25), plant height (16.83 cm), and fresh and dry biomass (147.27 and 16.07 mg), compared to the other treatments. In addition, principal component analysis showed that WPM was associated with germination and development variables, with significant correlations. In conclusion, the WPM medium optimized germination and promoted the development of healthy and homogeneous seedlings, positioning it as an efficient alternative for propagation, ecological restoration, and native species conservation programs.

## RESUMEN

**Palabras clave:**

Agar  
Capirona  
Medio de cultivo  
Restauración ambiental  
Rubiaceae

El cambio climático y la pérdida de biodiversidad representan amenazas críticas para los ecosistemas, por lo que la reforestación con especies nativas surge como una alternativa mitigadora. Sin embargo, se requiere optimizar los sistemas de producción de plántulas. El objetivo de este estudio fue evaluar el efecto de diferentes medios de cultivo y concentraciones en la germinación y el desarrollo morfológico *in vitro* de *Calycophyllum spruceanum*. Se utilizó un diseño completamente al azar con cinco tratamientos: 100% Murashige and Skoog (MS), 50% MS, 100% WPM, 50% WPM y un tratamiento control (agar), con siete repeticiones por tratamiento. Se evaluaron parámetros de germinación durante 21 días y desarrollo morfológico a los 70 días. Los principales resultados demostraron que WPM y agar obtuvieron los mayores porcentajes de germinación (73,33 y 75,24%), índice de velocidad de germinación (2,02 y 2,32 semillas por día), mientras en el tiempo de germinación final, el WPM destacó. En el desarrollo morfológico, WPM registró los valores más altos de número de hojas (8,18), nodos (5,25), altura de planta (16,83 cm) y biomasa fresca y seca (147,27 y 16,07 mg), en comparación con los demás tratamientos. Además, el análisis de componentes principales mostró que WPM se asoció a las variables de germinación y desarrollo, con correlaciones significativas. En conclusión, el medio WPM optimizó la germinación y favoreció el desarrollo de plántulas saludables y homogéneas, lo que lo posiciona como una alternativa eficiente para programas de propagación, restauración ecológica y conservación de especies nativas.

<sup>1</sup>Facultad de Ciencias Forestales y Ambientales, Escuela Profesional de Ingeniería Forestal, Universidad Nacional de Ucayali, Carretera Federico Basadre km 6.200, Pucallpa, Ucayali, Perú. [jorge\\_mori@unu.edu.pe](mailto:jorge_mori@unu.edu.pe) 

<sup>2</sup>Centro de Ciências Naturais y Humanas, Universidade Federal do ABC, São Bernardo do Campo, São Paulo, Brasil. [antony.gonzales@ufabc.edu.br](mailto:antony.gonzales@ufabc.edu.br) 

<sup>3</sup>Facultad de Ciencias Agropecuarias, Escuela de Formación Profesional de Agronomía, Universidad Nacional Daniel Alcides Carrión, Chanchamayo, Junín, Perú. [nhilario@undac.edu.pe](mailto:nhilario@undac.edu.pe) 

<sup>4</sup>Instituto de Investigaciones de la Amazonia Peruana, Dirección Regional de Ucayali, Yarina Cocha, Perú. [jrevilla@iiap.gob.pe](mailto:jrevilla@iiap.gob.pe) 

<sup>5</sup>Facultad de Ciencias, Universidad Nacional Agraria La Molina, Lima, Perú. [cristian.saico3@gmail.com](mailto:cristian.saico3@gmail.com) 

\*Corresponding author



Current global challenges, such as climate change and biodiversity loss, pose critical threats to ecosystems (Blankinship 2024). Given this situation, ecosystem restoration has emerged as a key strategy to mitigate these effects (Zhang et al. 2024). Among the most effective strategies, reforestation plays a central role by facilitating the recovery of degraded areas, promoting land-use neutrality, and improving ecological functionality through the balancing of ecosystem services (Das et al. 2020). A crucial component of successful reforestation initiatives is the incorporation of native species with high ecological value, as these species contribute significantly to soil rehabilitation, biodiversity conservation, and climate change mitigation (da Silva et al. 2024). *Calycophyllum spruceanum* (Rubiaceae), a native tree species of the Amazon Basin found in Peru, Brazil, Colombia, and Ecuador, is notable for its rapid growth, adaptability to degraded and flood-prone soils, and high-quality wood (Saldaña et al. 2022). These characteristics make it a suitable candidate for reforestation and ecosystem restoration programs, particularly in areas severely impacted by degradation. Furthermore, the increasing interest in this species, driven by both its ecological and commercial value, highlights the importance of optimizing its propagation to meet market demand without compromising biodiversity (Santos et al. 2016).

Within this framework, plant tissue culture techniques have gained attention as a biotechnological tool for the rapid and large-scale propagation of plant species. These techniques offer advantages such as space-efficient multiplication, improved pathogen control, and enhanced nutrient management, ensuring the production of healthy and uniform seedlings, an essential aspect for effective ecological restoration and commercial cultivation (Indacochea et al. 2018).

Although several studies have explored the ecological and silvicultural aspects of *C. spruceanum* (Guerra-Arévalo et al. 2024), biotechnological research has primarily focused on its pharmacological, biochemical, and genomic properties (Saldaña et al. 2022). Tissue culture studies; however, remain limited, with only two investigations addressing *in vitro* establishment and callus induction (Olivas 2014; Figueiredo et al. 2014).

Given the fundamental role of culture media in germination and seedling development, it is essential to identify formulations that optimize germination rates and promote the development of genetically and phytosanitarily sound, uniform seedlings. To date, no studies have examined the influence of culture media on the germination and morphological development of *C. spruceanum*, which is crucial for enhancing the efficiency and quality of seedling production in support of reforestation efforts. According to Sudheer et al. (2022), culture media significantly influence plant growth by supplying essential nutrients, providing structural support, and maintaining optimal conditions for morphological development. Previous *in vitro* studies on *C. spruceanum* have employed Murashige and Skoog (MS) medium (Olivas 2014; Figueiredo et al. 2014). However, recent findings suggest that Woody Plant Medium (WPM) may offer superior outcomes in terms of germination and development (Gonzales-Alvarado et al. 2024). WPM has been reported to enhance shoot proliferation, rooting, and overall growth in species such as *Durio dulcis* and *Guazuma crinita*, outperforming conventional media under *in vitro* conditions (Hardarani et al. 2023; Gonzales-Alvarado et al. 2024). Based on this evidence, it is hypothesized that the WPM culture medium will result in higher germination rates and improved morphological development in *C. spruceanum* compared to other commonly used media. This study aims to evaluate the effect of different culture media and concentrations on the germination and *in vitro* morphological development of *C. spruceanum*, to maximize seedling productivity, quality, and uniformity. The findings will contribute to the scientific understanding of this species' biology and support its application in reforestation and genetic improvement programs. In this way, the research seeks to provide innovative and sustainable solutions to face global challenges, promoting the recovery of degraded areas and strengthening conservation efforts.

## MATERIALS AND METHODS

### Plant material and sterilization

The experiment was conducted at the Plant Tissue Culture Laboratory of the National University of Ucayali, located in Pucallpa, Peru. As plant material, seeds of *Calycophyllum spruceanum*, which were acquired in commercial seed markets, were used. Seed sterilization was performed in a laminar flow chamber. The seeds were immersed in a

Benlate® solution (30 g L<sup>-1</sup>) for 30 minutes. Subsequently, they were immersed in 70% alcohol and immediately treated with 1% sodium hypochlorite (NaClO), adding three drops of Tween® 20. The solution was kept in constant agitation for 10 minutes. Finally, the seeds were rinsed five times with sterilized distilled water to ensure the elimination of residues.

### Culture media, treatments, and variables

For *in vitro* germination, Murashige and Skoog (MS) and Woody Plant Medium (WPM) at different concentrations were used as base culture medium. Agar alone was used as a control. The experiment consisted of five treatments: T1: 100% MS, T2: 50% MS, T3: 100% WPM, T4: 50% WPM, and T5: control (agar only). Additionally, in each of the treatments, 6.5 g L<sup>-1</sup> of agar (PhytoTech®), 30 g L<sup>-1</sup> of sucrose, and pH was adjusted to 5.8. However, for the control (T5), only 30 g L<sup>-1</sup> sucrose was added, and the pH was adjusted to 5.8, because it already contained agar.

Each treatment consisted of seven replicates, and five flasks (13 cm height and 6 cm mouth) were used in each replicate. Each flask contained 45 mL of medium, which were autoclaved at 121 °C and 1.1 atm for 20 min. Subsequently, the flasks were cooled and three seeds per flask were inoculated, being 105 seeds per treatment, which were placed randomly. The flasks were incubated at a temperature of 23±2 °C, with a relative humidity of 80% and a photoperiod of 16 hours.

The variables related to germination, such as germination percentage (G), germination speed index (GSI), germination initiation day (GID), final day of germination (FDG), germination energy (GE), germination energy period (GEP), germination energy period percentage (% GEP) were evaluated for 21 days after *in vitro* inoculation (Bewley and Black 1994). Equation 1 was used for the germination percentage G (%):

$$G(\%) = \frac{\sum n_i}{N} \times 100 \quad (1)$$

Where,  $\sum n_i$  is the total number of germinated seeds and N is the total number of inoculated seeds. The germination speed index (GSI) was calculated using Equation 2:

$$GSI = \frac{G_1}{N_1} + \frac{G_2}{N_2} + \dots + \frac{G_n}{N_n} \quad (2)$$

Where G<sub>1</sub>, G<sub>2</sub>, ... G<sub>n</sub> refer to the number of germinated seeds and N<sub>1</sub>, N<sub>2</sub>, ... N<sub>n</sub>, to the number of days after *in vitro* inoculation. Germination energy (GE) was determined using Equation 3:

$$GE = \frac{G_n}{N} \times 100 \quad (3)$$

Where G<sub>n</sub> is the number of seeds germinated in a given day period (seven days), and N is the total number of inoculated seeds. The germination energy period (GEP) was used through Equation 4:

$$GEP = \frac{PG}{N} \times 100 \quad (4)$$

Where PG is the number of seeds where the highest percentage of non-accumulated germination occurs and N is the total number of inoculated seeds.

The morphological development variables, such as plant height (PH), number of nodes (NN), number of leaves (LN), fresh biomass (FB), and dry biomass (DB), were analyzed 70 days after inoculation. To determine the fresh biomass, all seedlings from each treatment were used, cleaned, and weighed on a digital analytical balance accurate to 0.1 mg. Subsequently, the same seedlings were dried in an oven at 70 °C for 72 hours to determine the total dry biomass (Gonzales-Alvarado and Cardoso 2024).

### Experimental design and statistical analysis

The experiment was carried out using a completely randomized design. For all variables evaluated, the assumptions of normality were verified using the Shapiro-Wilk test and homogeneity of variances using the Levene test. When these assumptions were not met, the Kruskal-Wallis nonparametric test was applied.

The variables associated with germination and morphological development complied with the assumptions of normality and homoscedasticity, and were therefore subjected to an analysis of variance (ANOVA). In cases where significant differences were found, Tukey's test of means was used with a significance level of 5% ( $\alpha=0.05$ ). However, the variable number of nodes (NN) did not meet the assumptions, so it was analyzed using the Kruskal-Wallis nonparametric test. To analyze the seed germination percentage as a function of the treatments, a second-degree polynomial regression was applied.

In addition, principal component analysis (PCA) was performed, including all the variables analyzed, using the ggplot2 function and confidence ellipses (level=0.95) in the biplot (Wickham 2016). For the correlation analysis between variables, Spearman's correlation coefficient was used by corplot, considering  $-0.6 \leq P \leq 0.6$ , as strong correlation (Wei et al. 2024). All statistical analyses were performed using R Studio software, version 4.3.2.

## RESULTS AND DISCUSSION

### Effect of culture media on *in vitro* germination parameters of *Calycophyllum spruceanum*

The germination behavior (G) of *C. spruceanum* shows a trend of progressive increase, stabilizing around 15 to 18 days after *in vitro* inoculation (Figure 1). The mathematical

models fitted to the data correspond to quadratic equations with high coefficients of determination ( $R^2 > 0.94$ ), indicating an adequate representation of germination behavior in each treatment.

It is observed that the culture medium significantly influences germination, with notable differences in the germination rate and the final percentage reached. The treatment with agar (T5) presents the most negative quadratic coefficient ( $-0.3613x^2$ ), suggesting a faster initial germination, but with an earlier stabilization. In contrast, the WPM and 50% WPM treatments (T3 and T4) show a more sustained germination rate over time, reaching higher values compared to the MS and 50% MS treatments (T1 and T2).

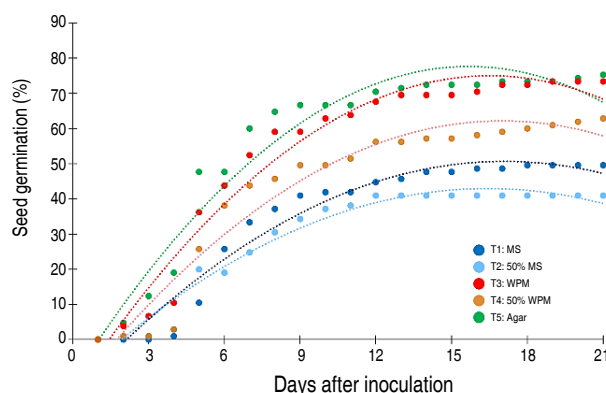


**Figure 1.** Germination percentage of *C. spruceanum* during 21 days post-inoculation in different culture media. **T1:**  $y = -0.2262x^2 + 7.7312x - 15.946$ .  $R^2 = 0.9474$ , **T2:**  $y = -0.2041x^2 + 6.7035x - 12.13$ .  $R^2 = 0.961$ , **T3:**  $y = -0.33x^2 + 10.899x - 15.022$ .  $R^2 = 0.9598$ , **T4:**  $y = -0.2668x^2 + 9.0709x - 14.946$ .  $R^2 = 0.9413$ , and **T5:**  $y = -0.3613x^2 + 11.339x - 11.335$ .  $R^2 = 0.9449$ .

Germination is a fundamental aspect for proper management in plant development (Gonzales-Alvarado et al. 2022). Germination of *C. spruceanum* was influenced by the type of culture medium and its concentration. The use of agar and Woody Plant Medium (WPM) resulted in the highest germination percentages within 21 days, reaching 75.24 and 73.33%, respectively (Table 1 and Figure 1). Similar results were reported by Gonzales-Alvarado et al. (2024) and Marwein and Vijayan (2024), who observed that 100% agar and WPM enhanced the germination of *Guazuma crinita* and *Adinandra griffithii*, respectively. In contrast, Guerra-Arévalo et al. (2024) evaluated organic substrates for the germination of *C. spruceanum* and achieved 62.3% germination. When compared with these previous results, the application of agar and WPM in the

present study increased the germination percentage by 17.7 and 20.77%, respectively. According to Pereira (2023), agar is a polysaccharide derived from algae that does not provide nutrients to plants and facilitates seed hydration, activating metabolic pathways that lead to the synthesis of proteins and enzymes essential for germination. In the present study, no statistically significant differences were found between agar (T5) and WPM (T3) regarding germination performance in *C. spruceanum* (Table 1). This result can be attributed to the early developmental stages of the embryo, during which external nutrients are not essential, as the embryo utilizes seed reserves to generate energy and the necessary chemical compounds for development (Meneses et al. 2022). According to Gonzales-Alvarado et al. (2022), they also emphasized the

importance of medium composition in seed germination. For instance, Kirillov et al. (2024) reported that MS medium enhanced germination in *Aflautunia ulmifolia*, achieving over 50% germination compared to other media. However, in the present study, WPM promoted higher germination percentages than MS treatments. This effect may be associated with the lower concentrations of nitrogen, potassium, and ions in WPM, as well as its reduced ammonium content—approximately 25% lower than that of MS medium (Munthali et al. 2022).

Regarding the germination speed index. (GSI) and germination energy (GE), agar (T5) and WPM (T3) produced the highest values, with GSI reaching 2.32 and 2.02 seeds per day, and GE values of 60 and 52.38%, respectively. Germination was initiated at two days post-inoculation in all treatments except T1 (MS). Furthermore, during the Germination Energy Period (GEP), T1 (MS) exhibited the slowest response, reaching GE at six days with only 15.24%, the lowest value recorded (Table 1). In contrast, T5 and T3 presented GEP values of 28.57 and 25.71%, respectively.

**Table 1.** Effect of culture medium on *in vitro* germination parameters (mean ± standard error) of *C. spruceanum*.

Culture medium	(%)	GSI (seeds per day)	GID	FDG	GE (%) (7 days)	GEP (days)	GEP (%)
T1: MS	49.52±2.46 <sup>BC</sup>	1.10±0.07 <sup>C</sup>	4	16	33.33±4.11 <sup>BC</sup>	6	15.24
T2: 50% MS	40.95±5.13 <sup>C</sup>	1.03±0.15 <sup>C</sup>	2	12	24.76±4.04 <sup>C</sup>	5	17.14
T3: WPM	73.33±4.11 <sup>A</sup>	2.02±0.21 <sup>AB</sup>	2	19	52.38±3.97 <sup>A</sup>	5	25.71
T4: 50% WPM	62.86±5.22 <sup>AB</sup>	1.50±0.10 <sup>BC</sup>	2	21	43.81±4.08 <sup>AB</sup>	5	22.86
T5: Agar	75.24±2.80 <sup>A</sup>	2.32±0.11 <sup>A</sup>	2	21	60±5.25 <sup>A</sup>	5	28.57
CV	18	22.7			26.64		

Different capital letters indicate significant differences between treatments according to the Tukey test at the 5% significance level. G: germination percentage, GSI: germination speed index, GID: germination initiation day, FDG: final day of germination, GE: germination energy, GEP: germination energy period, and GEP (%): percentage of germination energy period.

On the Final Day of Germination (FDG), WPM completed the germination process in 19 days, while agar did so in 21 days. These results support the hypothesis that WPM enhances germination. The favorable outcomes observed with agar can be attributed to its stable surface, which supports seed germination and seedling development, despite its lack of nutrients. In contrast, WPM, characterized by lower salt concentrations (Delgado-Paredes et al. 2023), did not negatively impact germination parameters such as G, GSI, GID, GE, GEP, and GEP (%), indicating no phytotoxic effects on *C. spruceanum*. Conversely, the high salt concentration in MS medium appeared to limit the development of these germination parameters *in vitro* (Cabral-Miramontes et al. 2022).

**Effect of culture media on the morphological development and biomass of *Calycophyllum spruceanum***

The results of morphological development showed significant differences in all the variables analyzed (Figure 2). Initial plant development encompassed key morphological parameters that influenced subsequent

growth and adaptation to different cultivation conditions. Understanding these parameters contributed to the efficient production of seedlings and optimized propagation under *in vitro* conditions the efficient production of seedlings and optimizes their propagation in *in vitro* systems.

The application of Woody Plant Medium (WPM) significantly enhanced the morphological development of *C. spruceanum*, yielding the highest values for number of leaves (LN), number of nodes (NN), and plant height (PH), with averages of 8.18 leaves per plant, 5.25 nodes per plant, and 16.83 cm in height, respectively (Figure 2). Similar results were reported by Marwein et al. (2024), Lima et al. (2024), and Meneses et al. (2022), in which WPM demonstrated superior efficiency compared to other culture media, promoting the morphological development of *in vitro* seedlings of *Rhododendron inaequale* Hutch, *Vismia japurensis*, and *Vaccinium floribundum*, respectively. According to Krasnoperova and Bukharina (2020), indicated that WPM enhances both plant survival and development, supporting the hypothesis that this medium optimizes the morphological development of *Calycophyllum spruceanum*.

To date, no previous studies have evaluated this specific aspect, suggesting that the present findings may contribute to the large-scale propagation of the species with

improved morphological traits, suitable for meeting market demand in ecological restoration programs and industrial applications.

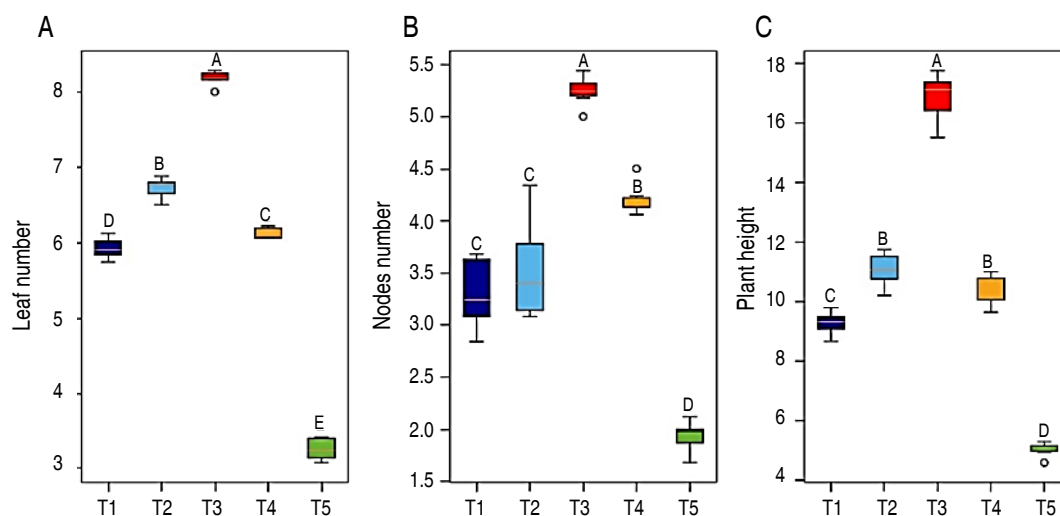


**Figure 2.** Effect of culture media on *in vitro* morphological development of *C. spruceanum*. **A.** number of leaves (LN). **B.** number of nodes (NN), and **C.** plant height (PH). T1: MS; T2: 50% MS; T3: WPM; T4: 50% WPM; and T5: Agar. Different letters indicate significant differences between treatments according to Tukey's test at 5% significance level.

According to Stachevski et al. (2013), WPM has 50% of the ionic strength of Murashige and Skoog (MS) medium, as well as higher levels of sulfur (S) and lower concentrations of ammonium ( $\text{NH}_4^+$ ) and nitrate ( $\text{NO}_3^-$ ), which reduce the risk of ionic toxicity and improve the adaptability of woody species. Additionally, its balanced composition of macro- and micronutrients, including adjusted concentrations of nitrogen, phosphorus, and potassium, was essential for regulating plant metabolic functions (Delgado-Paredes et al. 2023). Previous studies on *C. spruceanum* under *in vitro* conditions employed MS medium for bud establishment and callus induction, with promising results (Olivas 2014; Figueiredo et al. 2014), obtaining promising results. The findings of the present study indicated that WPM represents a more effective alternative for enhancing morphological development and could complement previous efforts in tissue culture research on this species.

After 70 days of *in vitro* cultivation of *C. spruceanum*, T3 (WPM) exhibited the highest mean number of leaves (8.18 leaves per plant) and the greatest leaf area. These characteristics are associated with increased survival during the post-*in vitro* acclimatization phase and contribute to more efficient seedling production in

a shorter period (Valladares and Niinemets 2008). In contrast, plants under treatment T5 (agar) displayed yellowish leaves with visible signs of stress, likely due to the absence of nutrients in the culture medium (Figure 3). These observations highlight the need for further studies on nutrient accumulation in plant tissues to complement the present findings. Similar results were reported by Gonzales-Alvarado et al. (2022) in *Guazuma crinita*, where plants cultured in phytogel for four months exhibited leaf yellowing and other stress-related symptoms.

Regarding the production of fresh biomass (FB) and dry biomass (DB), it was identified that WPM allowed obtaining the highest values, with 147.27 and 16.07 mg per plant, respectively (Table 2), significantly surpassing the other treatments. The results support the hypothesis that the use of WPM optimizes germination, morphological development, and accumulation of biomass in *C. spruceanum*. In contrast, the agar-only treatment showed a marked limitation in growth, which could be attributed to the deficiency of essential nutrients, since agar alone does not provide the necessary compounds for proper plant development. This had



a negative impact on the physiology of the seedlings, which showed an evident yellowing, as illustrated in Figure 3, possibly due to nutritional deficiencies and alterations in chlorophyll synthesis.

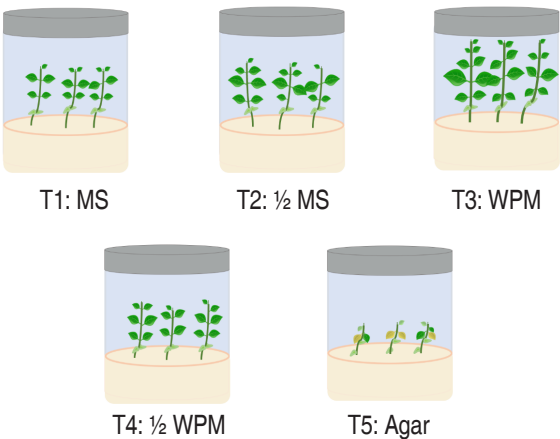


**Figure 3.** Morphological characteristics of *C. spruceanum* at 70 days post-inoculation *in vitro*.

**Table 2.** Effect of culture media on biomass of *C. spruceanum*.

Culture medium	FB (mg per plant)	DB (mg per plant)
T1: MS	90.26±0.29 <sup>B</sup>	10.67±0.05 <sup>B</sup>
T2: 50% MS	91.24±0.41 <sup>B</sup>	10.76±0.08 <sup>B</sup>
T3: WPM	147.27±0.30 <sup>A</sup>	16.07±0.08 <sup>A</sup>
T4: 50% WPM	90.49±0.48 <sup>B</sup>	10.51±0.10 <sup>B</sup>
T5: Agar	54.36±0.15 <sup>C</sup>	6.43±0.08 <sup>C</sup>
CV	0.96	2

Different letters indicate significant differences between treatments according to Tukey's test at 5% significance level. **FB**: fresh biomass, and **DB**: dry biomass.

The use of WPM in *C. spruceanum* not only optimizes production times but also yields plants with enhanced morphological characteristics, which is essential for large-scale propagation. From an applied perspective, the methodology implemented in this study has the potential to substantially support the mass production of seedlings, thereby facilitating supply for reforestation programs and the restoration of degraded ecosystems. However, it is important to consider that establishing seeds under controlled and aseptic conditions—such as in specific *in vitro* culture media—may entail higher operational and logistical costs compared to direct sowing in field substrates. Nonetheless, this initial investment is justified by the production of healthy, uniform seedlings

with a greater likelihood of survival, which represents a significant advantage for projects requiring high-quality plant material. *In vitro* propagation of *C. spruceanum*, therefore, is recommended as an innovative strategy to promote environmental sustainability and ensure the availability of this species for conservation and forest development initiatives. Furthermore, the findings regarding the application of WPM provide a robust foundation for future research in the *in vitro* culture of *C. spruceanum*, including studies on micropropagation, genetic transformation, and molecular biology. This approach may also prove valuable for research focused on the extraction of bioactive compounds of pharmacological and industrial relevance, enabling the efficient production of high-value secondary metabolites.

### Main component analysis and correlation of germination parameters, morphological development, and biomass of *Calycophyllum spruceanum*

The main component analysis (PCA) and correlation of germination parameters and morphological development yielded relevant insights. In the PCA, treatments with agar (T5) and WPM (T3) were grouped and associated with germination percentage (G), germination speed index (GSI), and germination energy (GE) (Figure 4A). However, in the analysis of morphological development, these treatments showed clear differentiation. The WPM treatment (T3) exhibited stronger associations with leaf number (LN), number of nodes (NN), plant height (PH), fresh biomass (FB), and dry biomass (DB) (Figure 5A).

Correlation analysis revealed positive associations within both germination and morphological development parameters (Figure 4B and Figure 5B). Among the germination parameters, correlation coefficients exceeded 0.87, with the strongest observed between GSI and germination percentage (G), at 0.93 (Figure 4B). To date, this is the first *in vitro* study to report such correlations in *C. spruceanum*, emphasizing the importance of further investigations into its germination processes. Additional research should focus on optimizing germination under *ex vitro* conditions to enhance propagation efficiency. Moreover, the inclusion of other germination-related parameters is recommended to refine and improve alternative propagation protocols for both natural and controlled environments.

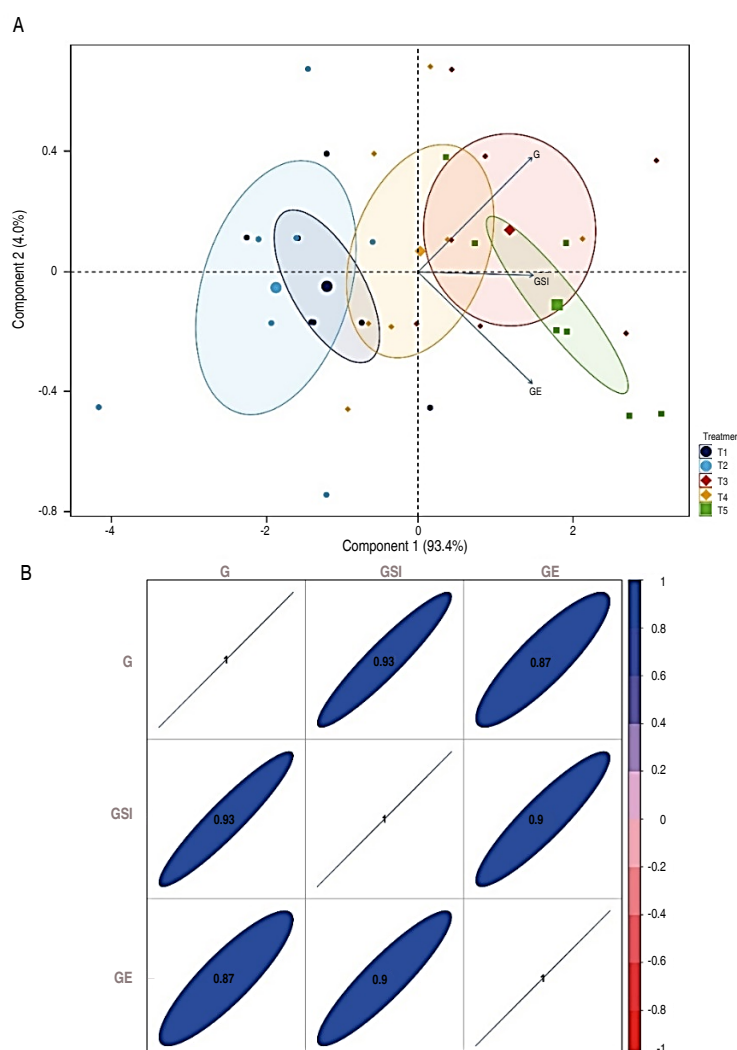


**Figure 4.** A: Main component analysis of germination parameters of *C. spruceanum*, and B: Correlation analysis between germination variables of *C. spruceanum*. G: germination percentage, GSI: germination speed index, and GE: germination energy.

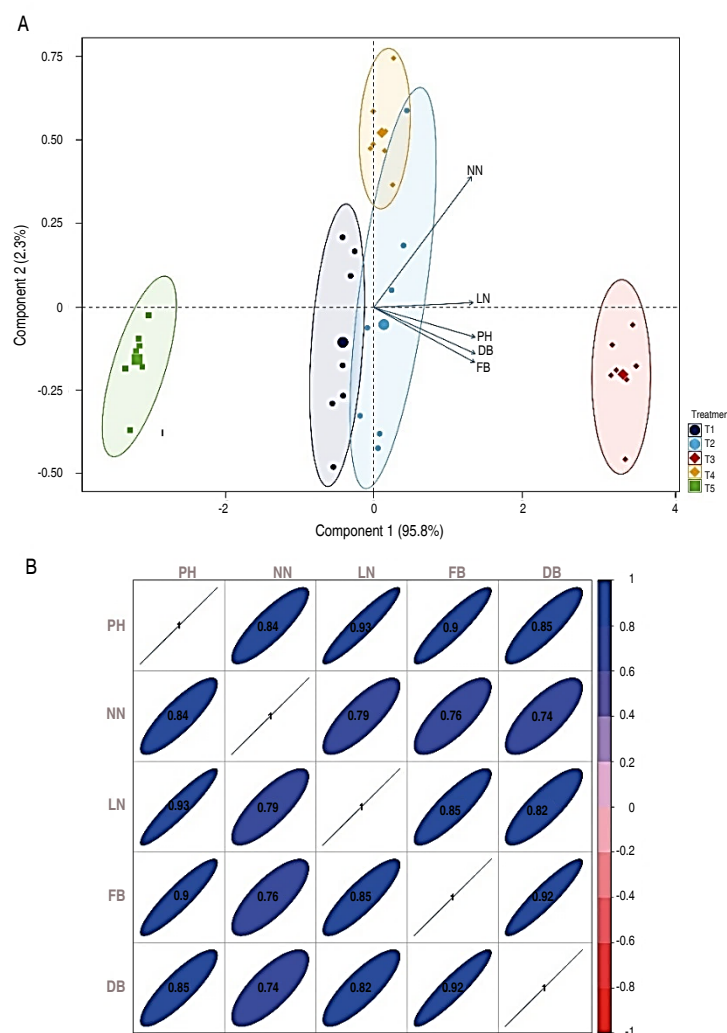


**Figure 5. A:** Main component analysis of morphological development and biomass of *C. spruceanum*, and **B:** Correlation analysis of morphological development and biomass variables of *C. spruceanum*. **PH:** plant height, **NN:** number of nodes, **LN:** number of leaves, **FB:** fresh biomass, and **DB:** dry biomass.

Regarding morphological development, the correlations of plant height (PH), number of nodes (NN), and number of leaves (LN) were greater than 0.84, suggesting a strong association between these growth factors. The highest correlations were recorded between fresh biomass (FB) and dry biomass (DB), with a value of 0.92, confirming that better morphological development contributes directly to higher biomass accumulation. Similar results were reported by Gonzales-Alvarado et al. (2024) and Mori-Vásquez et al. (2024) in *Guazuma crinita* and *Simarouba amara*, respectively, where strong correlations were evidenced between fresh and dry biomass, as well as between plant height and biomass. These results reinforce the

present findings and confirm the interdependence between morphological traits and biomass production.

The outcomes of this study underscore the necessity for further investigations into the responses of *C. spruceanum* under various growth conditions. It is particularly important to evaluate root system interactions, assess physicochemical parameters such as pH, electrical conductivity (EC), and the accumulation of macro and micronutrients. Additionally, future research should explore the influence of biochemical components in the culture media on chlorophyll content and the expression of growth- and development-related genes under *in vitro* conditions. Integrating genetic, physiological,

and molecular approaches would facilitate more accurate correlations between morphological responses and molecular regulation in this species. Such insights could significantly enhance propagation protocols and improve the efficiency of *C. spruceanum* seedling production for both commercial use and conservation or ecological restoration programs.

## CONCLUSION

This study demonstrated that culture media and their different concentrations directly influence germination parameters and *in vitro* morphological development. In particular, Woody Plant Medium (WPM) significantly optimized both germination and morphogenetic development of *C. spruceanum*, promoting the production of healthy and uniform seedlings. These results highlight the importance of selecting an appropriate culture medium and its concentrations to obtain high-quality and uniform plants, which is essential for supporting ecological restoration and native species conservation programs. Furthermore, these observations underscore the need for additional studies on nutrient accumulation in plant tissues to complement the findings obtained. It should be noted that this is the first report comparing different culture media for *C. spruceanum*. Further research on this and other species of ecological interest is recommended to strengthen conservation and restoration strategies for degraded ecosystems.

## ACKNOWLEDGMENTS

We thank the collaborators who participated in the field and laboratory phases, contributing significantly to the development of this research. Finally, we acknowledge the valuable suggestions of the anonymous reviewers that allowed us to substantially improve the manuscript.

## CONFLICT OF INTERESTS

The authors declare that there is no conflict of interest of any kind in the preparation and publication of the manuscript.

## REFERENCES

Bewley JD and Black M (1994) Seeds. Physiology of development and germination. Second edition. Springer, New York. 445 p. <https://doi.org/10.1007/978-1-4899-1002-8>

Blankinship LA, Gillaspie S and Aboul-Enein BH (2024) Highlighting the importance of biodiversity conservation through the Holy Qur'an. *Conservation Biology* 39: e14309. <https://doi.org/10.1111/cobi.14309>

Cabral-Miramontes JP, Chávez-Simental JA, Pulido-Díaz C et al (2022) *In vitro* propagation of apple tree from mature zygotic embryos. *Revista Mexicana de Ciencias Agrícolas* 13(4): 603–616. <https://doi.org/10.29312/remexca.v13i4.2164>

da Silva YKR, Martins GC, Guedes RS et al (2024) Native plant species as an alternative to rehabilitate iron ore waste piles in Carajás Mineral Province, Brazil. *Communications in Soil Science and Plant Analysis* 55(11): 1579–1592. <https://doi.org/10.1080/00103624.2024.2321934>

Das J, Jha S and Goyal MK (2020) On the relationship of climatic and monsoon teleconnections with monthly precipitation over meteorologically homogenous regions in India: Wavelet and global coherence approaches. *Atmospheric Research* 238: 104889. <https://doi.org/10.1016/j.atmosres.2020.104889>

Delgado-Paredes GE, Vásquez-Díaz C, Esquerre-Ibañez B et al (2023) Germinación de semillas, micropropagación y conservación de germoplasma *in vitro* de *Cedrela odorata* (Meliaceae) en el norte del Perú. *Bosque (Valdivia)* 44(1): 97–109. <https://doi.org/10.4067/s0717-92002023000100097>

Figueiredo FDA, Vale PAA, Mesquita AGG et al (2014) *In vitro* micropropagation and callus induction of Mulateiro (*Calycophyllum spruceanum*) seeds collected from the Amazon Basin. *The International Journal of Science and Technology* 2(3): 1–3.

Gonzales-Alvarado AC, Mori-Vásquez JA, Tuisima Coral LL et al (2022) Influencia de la desinfección, medios de cultivo y fitohormonas en el desarrollo morfogénico *in vitro* de germoplasma de *Guazuma crinita* Mart. *Folia Amazónica* 31(1): 57–66. <https://doi.org/10.24841/fa.v31i1.572>

Gonzales-Alvarado AC and Cardoso JC (2024) Development, chlorophyll content, and nutrient accumulation in *in vitro* shoots of *Melaleuca alternifolia* under light wavelengths and 6-BAP. *Plants* 13(20): 2842. <https://doi.org/10.3390/plants13202842>

Gonzales-Alvarado AC, Tuanama Pinchi RR, Arévalo-Salles CC et al (2024) Respuesta germinativa y desarrollo fisiológico *in vitro* de *Guazuma crinita* Mart. a partir de semillas sexuales. *Acta Agronómica* 71(1): 16–24.

Guerra-Arévalo WF, Cercado-Delgado JR, Espinoza-García HF et al (2024) Emergence, growth, and quality of *Calycophyllum spruceanum* plants produced in different containers and substrates. *Agrosystems, Geosciences and Environment* 8: e70002. <https://doi.org/10.1002/agg2.70002>

Hardarani N, Zahra SN, Wahdah R et al (2023) Respon Eksplan Buku Durian Lahung (*Durio dulcis*) terhadap konsentrasi BAP (Benzil Amino Purin) pada media WPM (Woody Plant Medium). *Daun: Jurnal Ilmiah Pertanian dan Kehutanan* 10(2): 235–247. <https://doi.org/10.33084/daun.v10i2.6091>

Indacochea B, Parrales J, Hernández A et al (2018) Evaluación de medios de cultivo *in vitro* para especies forestales nativas en peligro de extinción en Ecuador. *Agronomía Costarricense* 42(1). <https://doi.org/10.15517/rac.v42i1.32203>

Kirillov V, Pathak A, Patel SR et al (2024) An efficient micropropagation protocol for an endangered tree species *Aflatunia ulmifolia* (Franch.) Vassilcz. *In vitro Cellular and Developmental Biology - Plant* 60: 28–38. <https://doi.org/10.1007/s11627-023-10392-y>

Krasnoperova V and Bukharina I (2020) The study into the method of culture *in vitro* as a method of vegetative propagation of

coniferous trees. Russian Agricultural Sciences 46:19–22. <https://doi.org/10.3103/S1068367420010061>

Lima LM, Silva WL, Souza JC et al (2024) *In vitro* cultivation of *Vismia japurensis*: Isolation of the new anthrone 1,8,10-trihydroxy-3,10-dimethyl-9(10H)-anthracenone. Anais da Academia Brasileira de Ciências 96: e20230456. <https://doi.org/10.1590/0001-3765202420230456>

Marwein D, Vijayan D and Asosii AM (2024) Optimized *in vitro* propagation, acclimatization and reintroduction of endemic *Rhododendron inaequale* Hutch. from northeast India. Asian Journal of Biotechnology and Bioresource Technology 10(3): 51–59. <https://doi.org/10.9734/ajb2t/2024/v10i3211>

Marwein D and Vijayan D (2024) Influence of culture media and growth hormones on *in vitro* propagation of *Adinandra griffithii* Dyer., a critically endangered and endemic plant from northeast India. Vegetos 38: 1047–1054. <https://doi.org/10.1007/s42535-024-00900-9>

Meneses LS, Morillo LE and Vásquez-Castillo W (2022) *In vitro* propagation of *Vaccinium floribundum* Kunth from seeds: Promissory technology for mortiño accelerated production. Canadian Journal of Plant Science 102(1): 216–224. <https://doi.org/10.1139/cjps-2020-0290>

Mori-Vásquez JA, Panduro Tenazoa NM, Muñoz Fernandez VJ et al (2024) Efecto de la desinfección, el desarrollo foliar y las fitohormonas en la inducción de callos de *Simarouba amara* Aubl. Ciencia y Tecnología Agropecuaria 25(3): e3662. [https://doi.org/10.21930/rcta.vol25\\_num3\\_art:3662](https://doi.org/10.21930/rcta.vol25_num3_art:3662)

Munthali C, Kinoshita R, Onishi K et al (2022) A model nutrition control system in potato tissue culture and its influence on plant elemental composition. Plants 11(20): 2718. <https://doi.org/10.3390/plants11202718>

Olivas OO (2014) Desinfección de yemas axilares para su establecimiento *in vitro* de la capirona (*Calycophyllum spruceanum* Benth.). [Tesis de pregrado, Universidad Nacional Agraria de la Selva]. Repositorio Institucional UNAS.

Pereira L (2023) Chapter 3 - Algal polysaccharides. In Dominguez H, Pereira L, Kraan S (eds) Functional ingredients from algae for

foods and nutraceuticals (Second edition). Woodhead Publishing, pp 151–212. <https://doi.org/10.1016/B978-0-323-98819-3.00015-8>

Saldaña CL, Rodríguez-Grados P, Chávez-Galarza JC et al (2022) Unlocking the complete chloroplast genome of a native tree species from the Amazon Basin, Capirona (*Calycophyllum spruceanum*, Rubiaceae), and its comparative analysis with other Ixoroideae species. Genes 13(1): 113. <https://doi.org/10.3390/genes13010113>

Santos AB, Ribeiro-Oliveira JP and Carvalho CM (2016) Sobre a botânica, a etnofarmacologia e a química de *Calycophyllum spruceanum* (Benth.) Hook. f. ex K. Schum. Revista Brasileira de Plantas Mediciniais 18(1 suppl 1): 383–389. [https://doi.org/10.1590/1983-084X/15\\_152](https://doi.org/10.1590/1983-084X/15_152)

Stachevski TW, Franciscon L and Degenhardt-Goldbach J (2013) Efeito do meio de cultura na calogênese *in vitro* a partir de folhas de erva-mate. Pesquisa Florestal Brasileira 33: 339–342. <https://doi.org/10.4336/2013.pfb.33.75.441>

Sudheer WN, Praveen N, Al-Khayri JM et al (2022) Chapter 3 - Role of plant tissue culture medium components. In Rai AC, Kumar A, Modi A, Singh M (eds) Advances in plant tissue culture. Academic Press, pp 51–83. <https://doi.org/10.1016/B978-0-323-90795-8.00012-6>

Valladares F and Niinemets Ü (2008) Shade tolerance, a key plant feature of complex nature and consequences. Annual Review of Ecology, Evolution, and Systematics 39(1): 237–257. <https://doi.org/10.1146/annurev.ecolsys.39.110707.173506>

Wei T, Simko V, Levy M et al (2024) corrrplot: Visualization of a Correlation Matrix (Version 0.95) [Software]. <https://cran.r-project.org/web/packages/corrrplot/index.html>

Wickham H (2016) Programming with ggplot2. In Wickham H (ed) Ggplot2: Elegant Graphics for Data Analysis. Springer International Publishing, pp 241–253. [https://doi.org/10.1007/978-3-319-24277-4\\_12](https://doi.org/10.1007/978-3-319-24277-4_12)

Zhang H, Lee CKF, Law YK et al (2024) Integrating both restoration and regeneration potentials into the real-world forest restoration planning. SSRN. <https://doi.org/10.2139/ssrn.4752980>





## ÍNDICE DE AUTORES

- Akinrinola Tajudeen Bamidele.** Response of *Corchorus olitorius* L. to cocoa pod husk powder and urea fertilizer. Vol. 78(3): 11213-11225. 2025.
- Aldas Morejon Jhonnatan Placido.** Gluten-free cookies made with white carrot (*Arracacia xanthorrhiza* Bancr) and rice (*Oryza sativa*) flour. Vol. 78(3): 11285-11291. 2025.
- Alvarado Moran Milena Mayerli.** Gluten-free cookies made with white carrot (*Arracacia xanthorrhiza* Bancr) and rice (*Oryza sativa*) flour. Vol. 78(3): 11285-11291. 2025.
- Alvarez-Aspiazu Andry Annabel.** Postharvest conditions of *Capsicum annuum* and their effect on hot sauce added *Ananas comosus*. Vol. 78(3): 11307-11318. 2025.
- Aponjolosun Miracle Oluwaseyi.** Response of *Corchorus olitorius* L. to cocoa pod husk powder and urea fertilizer. Vol. 78(3): 11213-11225. 2025.
- Batallas-Terrero Alicia Nicole.** Postharvest conditions of *Capsicum annuum* and their effect on hot sauce added *Ananas comosus*. Vol. 78(3): 11307-11318. 2025.
- Benbelkacem Abdelkader.** Multi-trait selection of bread wheat (*Triticum aestivum* L.) genotypes under semi-arid conditions in Algeria. Vol. 78(3): 11191-11201. 2025.
- Bendezu-Granda Lia Loan.** *In vitro* propagation of sweet cucumber (*Solanum muricatum* Ait): Effects of auxins and cytokinins. Vol. 78(3): 11239-11246. 2025.
- Betancur Agudelo Marcelo.** Root colonization of tamarind tree (*Tamarindus indica* L.) and occurrence of arbuscular mycorrhizal fungi in soils – Sopetrán, Antioquia. Vol. 78(3): 11345-11352. 2025.
- Bolaños Martínez Freddy.** Tomato (*Solanum lycopersicum* L.) leaf disease detection using computer vision. Vol. 78(3): 11203-11212. 2025.
- Cavichioi Bruno Mussoi.** Non-destructive estimation of leaf area in hairy fleabane (*Conyza bonariensis*). Vol. 78(3): 11247-11254. 2025.
- Contreras Gómez Alix Estela Yusara.** Global trends in sustainable cocoa (*Theobroma cacao* L.) production: A bibliometric analysis (2019–2025). Vol. 78(3): 11267-11284. 2025.
- Dawiteratika Corilia.** Efficacy of *Tithonia diversifolia* and NPK fertilizers on papaya seedling growth in marginal soils. Vol. 78(3): 11227-11238. 2025.
- Díaz-Arreaga Jorge Gustavo.** Postharvest conditions of *Capsicum annuum* and their effect on hot sauce added *Ananas comosus*. Vol. 78(3): 11307-11318. 2025.
- Djenadi Chafika.** Multi-trait selection of bread wheat (*Triticum aestivum* L.) genotypes under semi-arid conditions in Algeria. Vol. 78(3): 11191-11201. 2025.
- Duarte Junior Ary José.** Non-destructive estimation of leaf area in hairy fleabane (*Conyza bonariensis*). Vol. 78(3): 11247-11254. 2025.
- Fagbola Olajire.** Response of *Corchorus olitorius* L. to cocoa pod husk powder and urea fertilizer. Vol. 78(3): 11213-11225. 2025.
- Gomez-Fuentes Graciela.** *In vitro* propagation of sweet cucumber (*Solanum muricatum* Ait): Effects of auxins and cytokinins. Vol. 78(3): 11239-11246. 2025.
- Gonzales-Alvarado Antony Cristhian.** Woody Plant Medium optimizes *in vitro* germination and development of *Calycophyllum spruceanum*. Vol. 78(3): 11353-11363. 2025.
- González-Herrera Luis Gabriel.** Genetic variants of caseins and  $\beta$ -lactoglobulin in Lucerna cattle and their association with milk quality. Vol. 78(3): 11319-11333. 2025.
- Guapi Álava Gina Mariuxi.** Gluten-free cookies made with white carrot (*Arracacia xanthorrhiza* Bancr) and rice (*Oryza sativa*) flour. Vol. 78(3): 11285-11291. 2025.
- Guerrón Troya Vicente Alberto.** Gluten-free cookies made with white carrot (*Arracacia xanthorrhiza* Bancr) and rice (*Oryza sativa*) flour. Vol. 78(3): 11285-11291. 2025.
- Hernández-Herrera Darwin Yovanny.** Genetic variants of caseins and  $\beta$ -lactoglobulin in Lucerna cattle and their association with milk quality. Vol. 78(3): 11319-11333. 2025.
- Hilario-Román Nilda.** Woody Plant Medium optimizes *in vitro* germination and development of *Calycophyllum spruceanum*. Vol. 78(3): 11353-11363. 2025.
- Jiménez Alfonso Yamile.** Effect of antibiotic residues from subclinical mastitis on  $\beta$ -lactoglobulin concentration in bovine and goat milk. Vol. 78(3): 11335-11344. 2025.
- Ladoui Khaoula Khadidja.** Multi-trait selection of bread wheat (*Triticum aestivum* L.) genotypes under semi-arid conditions in Algeria. Vol. 78(3): 11191-11201. 2025.
- Leães Glaucio Pacheco.** Non-destructive estimation of leaf area in hairy fleabane (*Conyza bonariensis*). Vol. 78(3): 11247-11254. 2025.
- Long Do Minh.** Assessment of physical properties and biological activity of chitosan beads with *Citrus hystrix* essential oil. Vol. 78(3): 11293-11305. 2025.
- Lucas Tilio Adan.** Non-destructive estimation of leaf area in hairy fleabane (*Conyza bonariensis*). Vol. 78(3): 11247-11254. 2025.
- Macedo Mariana.** Non-destructive estimation of leaf area in hairy fleabane (*Conyza bonariensis*). Vol. 78(3): 11247-11254. 2025.

- 
- Martínez Castro Víctor Manuel.** Hydrogen production by dark fermentation from by-products of coffee wet processing and other organic wastes. Vol. 78(3): 11255-11266. 2025.
- Martínez Olier Estefanía.** Root colonization of tamarind tree in (*Tamarindus indica* L.) and occurrence of arbuscular mycorrhizal fungi in soils –Sopetrán, Antioquia. Vol. 78(3): 11345-11352. 2025.
- Mefti Mohammed.** Multi-trait selection of bread wheat (*Triticum aestivum* L.) genotypes under semi-arid conditions in Algeria. Vol. 78(3): 11191-11201. 2025.
- Moreno Cárdenas Edilson León.** Hydrogen production by dark fermentation from by-products of coffee wet processing and other organic wastes. Vol. 78(3): 11255-11266. 2025.
- Mori-Vásquez Jorge Arturo.** Woody Plant Medium optimizes *in vitro* germination and development of *Calycophyllum spruceanum*. Vol. 78(3): 11353-11363. 2025.
- Muriel Ruiz Sandra.** Root colonization of tamarind tree (*Tamarindus indica* L.) and occurrence of arbuscular mycorrhizal fungi in soils – Sopetrán, Antioquia. Vol. 78(3): 11345-11352. 2025.
- Mutamima Anisa.** Efficacy of *Tithonia diversifolia* and NPK fertilizers on papaya seedling growth in marginal soils. Vol. 78(3): 11227-11238. 2025.
- Nurmadani Rizki.** Efficacy of *Tithonia diversifolia* and NPK fertilizers on papaya seedling growth in marginal soils. Vol. 78(3): 11227-11238. 2025.
- Olivera-Soto Julio A.** *In vitro* propagation of sweet cucumber (*Solanum muricatum* Ait): Effects of auxins and cytokinins. Vol. 78(3): 11239-11246. 2025.
- Ouakkal Meriem.** Multi-trait selection of bread wheat (*Triticum aestivum* L.) genotypes under semi-arid conditions in Algeria. Vol. 78(3): 11191-11201. 2025.
- Palacio Betancur Sebastian.** Tomato (*Solanum lycopersicum* L.) leaf disease detection using computer vision. Vol. 78(3): 11203-11212. 2025.
- Quiñones Navia Iván Andrés.** Hydrogen production by dark fermentation from by-products of coffee wet processing and other organic wastes. Vol. 78(3): 11255-11266. 2025.
- Quoc Le Pham Tan.** Assessment of physical properties and biological activity of chitosan beads with *Citrus hystrix* essential oil. Vol. 78(3): 11293-11305. 2025.
- Restrepo-Cossio Valentina.** Root colonization of tamarind tree (*Tamarindus indica* L.) and occurrence of arbuscular mycorrhizal fungi in soils – Sopetrán, Antioquia. Vol. 78(3): 11345-11352. 2025.
- Revilla Escobar Karol Yannela.** Gluten-free cookies made with white carrot (*Arracacia xanthorrhiza* Bancr) and rice (*Oryza sativa*) flour. Vol. 78(3): 11285-11291. 2025.
- Revilla-Chávez Jorge Manuel.** Woody Plant Medium optimizes *in vitro* germination and development of *Calycophyllum spruceanum*. Vol. 78(3): 11353-11363. 2025.
- Rincón-Flórez Juan Carlos.** Genetic variants of caseins and  $\beta$ -lactoglobulin in Lucerna cattle and their association with milk quality. Vol. 78(3): 11319-11333. 2025.
- Rizal Muhammad.** Efficacy of *Tithonia diversifolia* and NPK fertilizers on papaya seedling growth in marginal soils. Vol. 78(3): 11227-11238. 2025.
- Rodríguez Villamizar Mary Yaneth.** Global trends in sustainable cocoa (*Theobroma cacao* L.) production: A bibliometric analysis (2019–2025). Vol. 78(3): 11267-11284. 2025.
- Saico Ccope Cristian Richard.** Woody Plant Medium optimizes *in vitro* germination and development of *Calycophyllum spruceanum*. Vol. 78(3): 11353-11363. 2025.
- Sanabria Ospino Alfredo Enrique.** Global trends in sustainable cocoa (*Theobroma cacao* L.) production: A bibliometric analysis (2019–2025). Vol. 78(3): 11267-11284. 2025.
- Sanchez-Quispe Luz.** *In vitro* propagation of sweet cucumber (*Solanum muricatum* Ait): Effects of auxins and cytokinins. Vol. 78(3): 11239-11246. 2025.
- Tarazona-Manrique Luis Edgar.** Effect of antibiotic residues from subclinical mastitis on  $\beta$ -lactoglobulin concentration in bovine and goat milk. Vol. 78(3): 11335-11344. 2025.
- Tumpe-Jaquehua Alvaro.** *In vitro* propagation of sweet cucumber (*Solanum muricatum* Ait): Effects of auxins and cytokinins. Vol. 78(3): 11239-11246. 2025.
- Uhlmann Lilian Osmari.** Non-destructive estimation of leaf area in hairy fleabane (*Conyza bonariensis*). Vol. 78(3): 11247-11254. 2025.
- Ulgum André da Rosa.** Non-destructive estimation of leaf area in hairy fleabane (*Conyza bonariensis*). Vol. 78(3): 11247-11254. 2025.
- Vera-Chang Jaime Fabián.** Postharvest conditions of *Capsicum annuum* and their effect on hot sauce added *Ananas comosus*. Vol. 78(3): 11307-11318. 2025.
- Vicente-Vega Maria.** *In vitro* propagation of sweet cucumber (*Solanum muricatum* Ait): Effects of auxins and cytokinins. Vol. 78(3): 11239-11246. 2025.
- Yahiaoui Samia.** Multi-trait selection of bread wheat (*Triticum aestivum* L.) genotypes under semi-arid conditions in Algeria. Vol. 78(3): 11191-11201. 2025.
-